ANAEROBIC DIGESTION AND PRETREATMENT TECHNIQUES THAT ENHANCE THE DIGESTIBILITY OF LIGNOCELLULOSIC BIOMASS

A Dissertation

by

OPEYEMI ADEKUNMI OLOKEDE

Submitted to the Graduate and Professional School of
Texas A&M University
in partial fulfillment of the requirements for the degree of

DOCTOR OF PHILOSOPHY

Chair of Committee,	Mark T. Holtzapple
Committee Members,	Mahmoud El-Halwagi
	Ahmad Hilaly
	Zivko Nikolov
Head of Department,	Arul Jayaraman

August 2022

Major Subject: Chemical Engineering

ABSTRACT

To improve biological digestibility, lignocellulose was pretreated by shock, alkali, and combinations thereof. Shock is most effective when it precedes alkaline pretreatment, presumably because it opens the biomass structure and enhances diffusion of pretreatment chemicals. Lignocellulose digestibility from calcium hydroxide treatment improves significantly with oxygen addition. In contrast, sodium hydroxide is a more potent alkali, and thereby eliminates the need for oxygen to enhance pretreatment. For animal feed, $Ca(OH)_2$ treatment is recommended because residual calcium ions are valuable nutrients. However, for methane-arrested, anaerobic digestion (MAAD), NaOH treatment is preferred because sodium is a better buffer. The effect of shock is most pronounced when the no-shock control employed the same soaking-and-drying procedure as the shock treatment.

MAAD is a more accurate assessment technique when lignocellulose is employed in the carboxylate platform, a promising approach that utilizes nearly all biomass components. Using recommended pretreatment conditions identified from a previous study, three corn stover pretreatments were compared using MAAD: (1) shock-only, (2) NaOH-only, and (3) shock + NaOH. Air-dried sewage sludge was used as nutrient source. At 100 g/L initial substrate concentration, compared to untreated corn stover, shock-only decreased conversion (amount of biomass digested) by 14%, NaOH-only increased conversion by 82%, and shock + NaOH increased conversion by 104%.

To sustainably produce carboxylic acids, paper and chicken manure were co-digested through semi-continuous countercurrent (MAAD) using a mixed culture of marine microorganisms grown at mesophilic conditions (40 °C). During the digestion, anion-exchange resin (Amberlite IRA-67) adsorption was applied to simultaneously recover inhibitory acid products from the digestion medium. The adsorption efficiency was enhanced by supplying CO_2 during *in-situ* adsorption. Compared with stand-alone digestion (control), integrating adsorption with MAAD significantly increased biomass conversion and acid yield by 2.28 and 2.09 times, respectively.

The effects of frozen (fresh), air-dried, and baked nutrients (chicken manure, sewage sludge) on MAAD was studied. Continuum particle distribution (CPDM) maps show the impact of liquid residence time (LRT) and volatile solids loading rate (VSLR) on conversion and product concentration. Baked chicken manure reduced conversion and acid concentration, which suggests that oven-drying damages nutrients. At high VSLR, air-dried nutrients have higher acid concentrations than fresh nutrients, but conversion is low; thus, fresh nutrients are preferred. At the same conditions, fresh chicken manure and sewage sludge have similar acid concentration; however, sewage sludge yields a larger proportion of caproic acid.

Most biomass sources require expensive pretreatment to remove lignin, a component that makes biomass less reactive. However, prickly pear cladodes have low lignin content and high sugar content. Batch MAADs of prickly pear cladodes were performed and CPDM maps were generated. With a product yield of ~50% and biomass conversion of ~70%, prickly pear performed better than previously studied

lignocellulosic feedstocks. At 100 g solids/L liquid, the CPDM map predicts that high acid concentrations (93 g/L) and conversions (93%) are obtained at VSLR of 6 g/(L_{liq}·day) and LRT of 35 days. The high sugar content and low lignin content of prickly pear makes it a suitable feedstock for the carboxylate platform.

DEDICATION

To my father, who always pushed me to pursue diligence in academics.

To my stepmother, who radically transformed my life by her love and patience.

To my family, who always believed in me from the very beginning.

To my wife, who stood by me during my entire doctoral program, encouraging me in my highest and lowest moments.

To my church family, who showered me with prayers and words of encouragement.

To my creator for his favor and mercy in all my endeavors.

ACKNOWLEDGEMENTS

Words cannot describe my gratitude to my advisor, Dr. Mark T. Holtzapple, for his guidance and support. His eternal optimism despite our lack of funding and damages from the winter storm was an inspiration for me to soldier on. I would also like to thank my committee members Dr. Mahmoud El-Halwagi, Dr. Zivko Nikolov, and Dr. Ahmad Hilaly for their help and support throughout my doctoral program.

I am thankful to my fellow graduate students and lab members, Nathan Kamphuis, Chao Liang, Haoran Wu, Huang Ju, Simon Schiele, Shenchun Hsu and Kejia Liu for their assistance and companionship. I am also thankful to the undergrad researchers who provided the necessary labor force to finish this study. A special thanks to Tennille Faber, Drew Marks, Sarah English, Jessica Leung, Hunter Donathen, Miranda Barrow, Christopher Ainsworth, Jessica Robertson, Aidan Broyles, Agnes Morah, Dylan Cantu, Isa Duong, Joshua Gruener, Katherine Burcham, Sarah Hulgan, Irene Johnson, Ammarah Junaid, Lucas Kretzschmar, Emily Parvino, Daniel Peel, Trevor Way, Jacob Zubrod, Kelsea Bird, Elise Helms, Matthew Magno, Christine Park, Varun Patel, Tiffany Zhang, Matthew Cochran, Toan Van.

I would also like to convey my thanks to Ashley Henley and Terah Cooper for their friendship and advice during my program. I am grateful to my family and friends for their enduring love and support throughout this journey. Finally, I am thankful to my wife, Natalie Olokede, who was my unwavering pillar of support.

CONTRIBUTORS AND FUNDING SOURCES

Contributors

This work was supervised by a dissertation committee consisting of Drs. Mark Holtzapple, Mahmoud El-Halwagi, Ahmad Hilaly of the Department of Chemical Engineering and Zivko Nikolov of the Department of Biological and Agricultural Engineering. The experimental data used in the dissertation was completed by the student in collaboration with Huang Ju, Simon Schiele, Haoran Wu, Kejia Liu, and Shenchun Hsu.

Funding Sources

This work was supported by Dr. Mark Holtzapple's funding.

NOMENCLATURE

MAAD	Methane-Arrested Anaerobic Digestion
Aceq	Acetate Acid Equivalents
CPDM	Continuum Particle Distribution Model
NAVS	Non-acid Volatile solids
VSLR	Volatile Solids Loading Rate
LRT	Liquid Residence Time
ISPR	In-situ Product Removal
MSCO	Multi-Staged Countercurrent Operation
Formic acid	Methanoic acid
Acetic acid	Ethanoic acid
Propionic acid	Propanoic acid
Butyric acid	Butanoic acid
Valeric acid	Pentanoic acid
Caproic acid	Hexanoic acid
Enanthic acid	Heptanoic acid
Caprylic acid	Octanoic acid

TABLE OF CONTENTS

Page

LIST OF FIGURES

Page

LIST OF TABLES

1. INTRODUCTION

In 2020, fossil fuels accounted for 73% of total U.S. energy consumption, whereas renewables accounted for only 11%.[1] Fossil fuel consumption increases environmental pollution and produces greenhouse gases that cause global warming.[2] There are many carbon-neutral sources of electricity (e.g., wind, solar, hydro, nuclear); however, biofuels are the only practical option for liquid transportation fuels. Currently, liquid biofuels are produced primarily from foods, such as grains and sugarcane.[3] U.S. bioethanol is produced from corn grain, which is rich in easily hydrolyzed starch. Even though global demand for bioethanol has more than quadrupled in the last two decades, replacing fossil fuels with bioethanol is not feasible for the following reasons: high production costs, limited availability of crops, and competition with food.[4]

To produce liquid fuels, lignocellulose is a more reliable feedstock that does not compete with food, is inexpensive, and can be supplied in large quantities.[5] Currently, lignocellulose is the fourth largest energy source after coal, petroleum, and natural gas. Producing biofuels from abundant lignocellulose is a feasible route for mitigating greenhouse emissions and increasing energy security.[6] Large percentages of lignocellulosic agricultural residues are wasted and could be repurposed as feedstock for biofuels. For example, corn stover accounts for 43% of U.S. agricultural residues, yet only ~6% is collected and used.[7]

Lignocellulose can be converted to liquid biofuels by the thermochemical, sugar, and carboxylate platforms. The *thermochemical platform* uses gasification and pyrolysis,

but is inefficient and has low yields.[8,9] The *sugar platform* uses extracellular enzymes to convert polysaccharides into monosaccharides that are anaerobic digestion. The requirement for sterile operating conditions makes this approach expensive. Furthermore, many biomass components (e.g., pectin, protein) are not used. The *carboxylate platform* anaerobically digests nearly all biomass components (except lignin and ash) to short- and medium-chain carboxylates, which are subsequently chemically converted to fuels and chemicals.[10,11]

The carboxylate platform is an example of consolidated bioprocessing (CBP) where enzyme production, hydrolysis, and anaerobic digestion are integrated in a single process step.[12] Via consolidation, CBP reduces processing cost and meanwhile increases hydrolysis rates.[13] In this anaerobic process, all metabolic products are carboxylic acids.[14] Because no sterility is required, a mixed culture of microorganisms is introduced as inoculum. Instead of using expensive enzymes, the carboxylate platform utilizes indigenous enzymes produced by a mixed culture of microorganisms. The use of mixed cultures improves the robustness and vitality of the process. It also increases the variability of feedstocks that can be used in this consolidated bioprocess. Because this microbial consortium can utilize nearly all biomass components (Figure 1-1), it has sometimes been described as "the big mouth."[15,16] Sugar polymers are saccharified and converted to carboxylic acids. Proteins are either consumed for cell growth or converted to carboxylic acids. This indiscriminate utilization of biomass components contributes to the high yields observed in this platform. After anaerobic digestion, well-developed gasification technology converts lignin residue into hydrogen.[8]

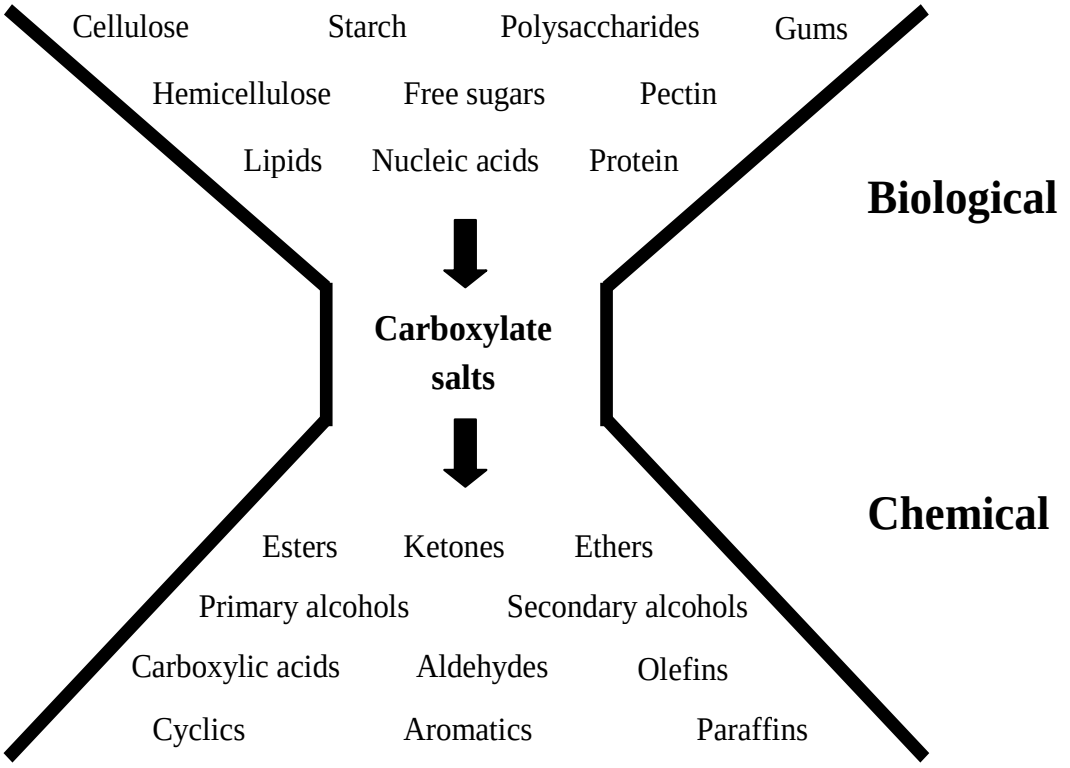

Figure 1-1. Carboxylate salts are key intermediates from biomass in the carboxylate platform.

The MixAlco® process is an example of the carboxylate platform developed in Dr. Mark Holtzapple's laboratory at Texas A&M University (Figure 1-2).[17] In this process, pretreatment exposes the cellulose within the biomass and methane-arrested anaerobic digestion (MAAD) decomposes the biomass into carboxylate salts. These salts are then concentrated by dewatering, chemically converted to ketones, hydrogenated to alcohols and oligomerized to hydrocarbons (e.g., gasoline, jet fuel). To increase the amount of carboxylate salts available for the downstream processes, the carboxylate platform must be enhanced to fully utilize lignocellulosic biomass. There are three key processes to be investigated: pretreatment, MAAD, and product recovery.

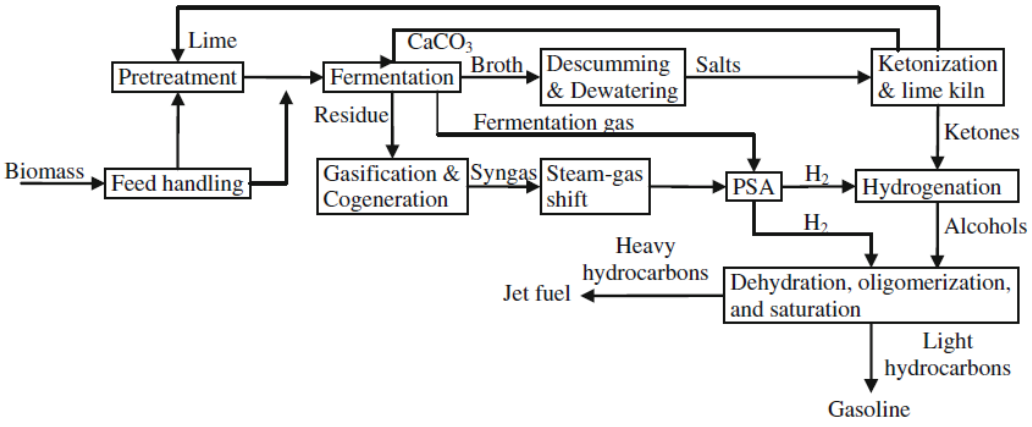

Figure 1-2. Block diagram of the MixAlco™ process.

1.1. Pretreatment

Herbaceous lignocellulose is composed primarily of 40–50% cellulose (glucose polymer), 25–35% hemicellulose (sugar heteropolymer), 15–20% lignin (non-digestible phenyl-propene compound), plus smaller amounts of oils, minerals, soluble sugars, and other components.[15] Cellulose and hemicellulose are the primary sources of digestible sugars. Enzymatic hydrolysis of these carbohydrate polymers is hindered by the presence of lignin, which imparts strength and resists against pests and microbes.[18] Lignin binds cellulose and hemicellulose together, creating a composite matrix that is difficult to penetrate using chemicals, enzymes, or microorganisms.[19] To fully convert lignocellulose into biofuels, pretreatment is necessary (Figure 1-3).[20]

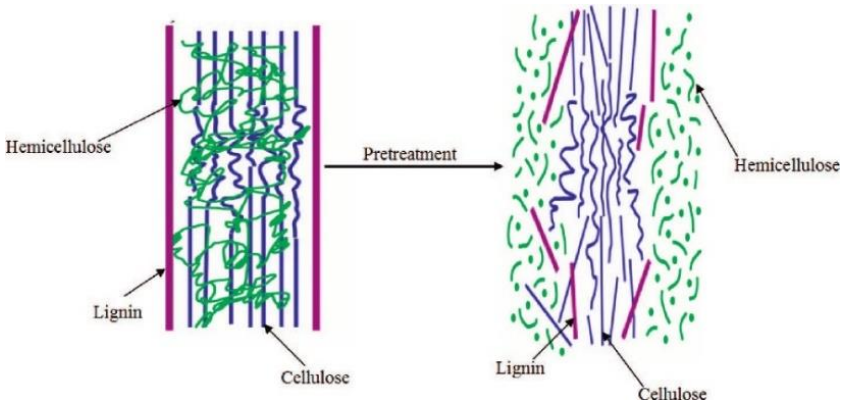

Figure 1-3. Schematic of lignocellulosic biomass structure.

Pretreatment removes some of the impediments that limit enzymatic digestibility, such as high lignin content,[19] low accessible surface area,[21] acetyl groups on hemicellulose,[18] and high cellulose crystallinity.[22] In lignocellulose-to-biofuel conversion, pretreatment can be the most expensive step; however, it has the potential to increase yields dramatically, which lowers overall costs.[20] After pretreatment increases cellulose accessibility, anaerobic digestion or saccharification must be performed to convert the biomass into carboxylic acids or ethanol.

1.2. Meethane-Arrested Anaerobic Digestion (MAAD)

In anaerobic digestion, biomass undergoes hydrolysis, acidogenesis, and acetogenesis (Figure 1-4).[23] This biological pathway is ubiquitous and has been used in sewage treatment plants to digest organic waste into methane and carbon dioxide. Because methane has a low commercial value, methanogenesis is constrained by adding a methane inhibitor; thus, products that should have been transformed to methane accumulate as carboxylic acids. Because the digester pH is neutral, carboxylic acids are present as their corresponding salts.

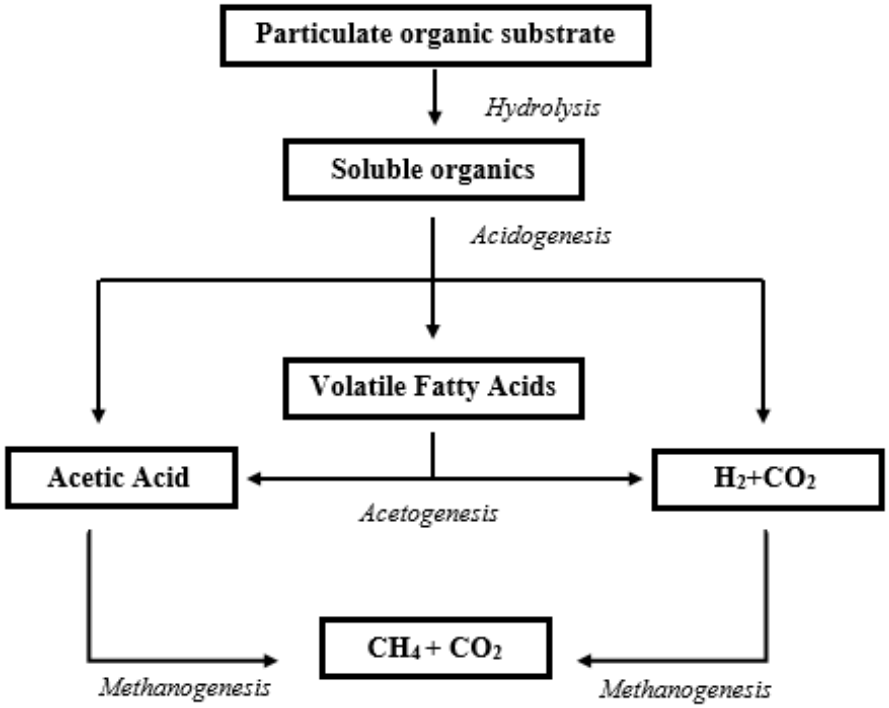

Figure 1-4. Anaerobic digestion process.

This biological pathway is ubiquitous and has been used in sewage treatment plants to digest organic waste into methane and carbon dioxide. Because methane has a low commercial value, methanogenesis is constrained by adding a methane inhibitor; thus, products that should have been transformed to methane accumulate as carboxylic acids. Because the digester pH is neutral, carboxylic acids are present as their corresponding salts.

As batch MAAD progresses, the biomass becomes less reactive and product inhibition reduced MAAD performance. Countercurrent MAAD (Figure 1-5) was developed to solve the disadvantages of batch MAAD. It has higher conversions, lower

product inhibition, and produces higher product yields.[24] Furthermore, it allows microorganisms to contact biomass at lower acid concentrations, unlike in batch MAAD, where higher concentrations of carboxylic acids inhibit MAAD microorganisms.[25] The challenge with countercurrent MAAD is the required labor and long operation duration, typical months, whereas batch MAAD takes a relatively shorter time to reach completion. To address this issue, the Continuum Particle Distribution Model (CPDM) is used to predict continuous countercurrent MAAD data from batch MAAD data.

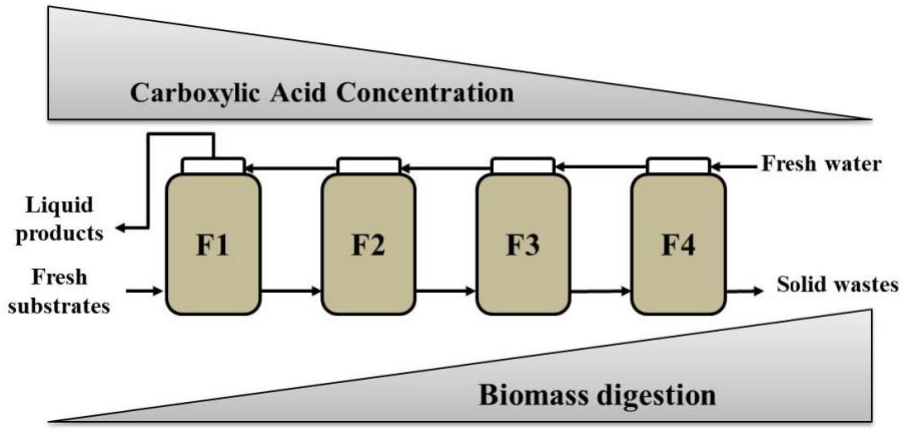

Figure 1-5. Four-stage countercurrent methane-arrested anaerobic digestion (MAAD).

CPDM is a technique developed by Loescher and Ross that has been extensively utilized to predict the performance of countercurrent MAAD.[26,27] A *continuum particle* is defined as a gram of solid in the initial unreacted state.[26,27] In this study, it represents one gram of non-acid volatile solids (NAVS). Based on one set of batch MAAD data, this method can determine conversions and product concentrations of consolidated bioprocessing at a range of volatile solids loading rates (VSLR) and liquid residence times (LRT). The CPDM method reduces labor by predicting the optimal countercurrent

MAAD condition through mathematical modeling. Countercurrent MAAD is performed with only one set of VSLR and LRT and requires three to four months to reach steady state. Obtaining data for a wide range of operating conditions would require many years of experiments, which is inherently impractical. However, CPDM overcomes this problem by mathematically simulating the performance of multiple operating conditions.[28]

1.3. Product Recovery

In the carboxylate platform, product recovery is usually performed after MAAD is completed. However, *in-situ* product removal (ISPR) has the potential for mitigating product inhibition in MAAD process. ISPR is a type of process intensification that enhances performance by simultaneously separating inhibitory products from the digestion broth.[29,30] Methods for separating carboxylates from digestion broth include precipitation, adsorption, liquid-liquid extraction, electrodialysis, nanofiltration, and reverse osmosis.[31] Among these techniques, adsorption with ion-exchange resins is popular at both laboratory and industrial scales. Compared to other techniques, the main advantages of adsorption include the relative simplicity of implementation, the ease of the auxiliary phase removal, and the wide range of commercially available adsorbents.[31–33] Many anaerobic digestion studies have been conducted to study the effects of ISPR with anion-exchange resins. For example, lactic acid productivity increased 1.3-fold in a homolactic anaerobic digestion with *in-situ* acid removal using a weak-base anion-exchange resin (Amberlite IRA-67).[34] Also, in batch MAAD, extracting carboxylates using IRA-67 significantly improves acid yield and substrate conversion.[35]

By investigating pretreatment, MAAD and product recovery, several improvements can be made to the carboxylate platform. These improvements are necessary to fully harness the energy hidden within lignocellulosic feedstocks.

The aims of this study are the following:

- Assess corn stover pretreatment using enzymatic hydrolysis
- Assess corn stover pretreatment using methane-arrested anaerobic digestion (MAAD)
- Assess nutrients on MAAD in the carboxylate platform
- Optimize carboxylic acid production from semi-continuous MAAD of cellulosic substrates by *in-situ* product removal with anion-exchange resin
- Co-treat lignocellulosic biomass
- Investigate MAAD of microalgae biomass
- Investigate MAAD of prickly pear cactus biomass.

2. ASSESSMENT OF SHOCK PRETREATMENT AND ALKALI PRETREATMENT ON CORN STOVER USING ENZYMATIC HYDROLYSIS*

2.1. Introduction

In 2019, fossil fuels accounted for 80% of total U.S. energy consumption whereas renewables accounted for only 11%.[1] Fossil fuel consumption increases environmental pollution and produces greenhouse gases that cause global warming.[2] There are many carbon-neutral sources of electricity (e.g., wind, solar, hydro, nuclear); however, biofuels are the only practical option for liquid transportation fuels. Currently, liquid biofuels are produced primarily from foods, such as grain and sugar.[3] U.S. bioethanol is produced from corn grain, which is rich in easily hydrolyzed starch. Even though global demand for bioethanol has more than quadrupled in the last two decades, replacing fossil fuels with bioethanol is not feasible for the following reasons: high production costs, limited availability of crops, and competition with food.[4]

To produce liquid fuels, lignocellulose is a more reliable feedstock that does not compete with food, is inexpensive, and can be supplied in large quantities.[5] Currently, lignocellulose is the fourth largest energy source after coal, petroleum, and natural gas. Producing biofuels from abundant lignocellulose is a feasible route for mitigating greenhouse emissions and increasing energy security.[6] A large percentage of

*Reprinted with permission from "Assessment of shock pretreatment and alkali pretreatment on corn stover using enzymatic hydrolysis" by Opeyemi Olokede, Shen-chun Hsu, Simon Shiele, Huang Ju, Mark Holtzapple, 2021. *Biotechnology Progress*, Volume 38, Issue 1, Copyright 2021 by American Institute of Chemical Engineers.

lignocellulosic agricultural residues are wasted and could be repurposed as feedstock for biofuels. For example, corn stover accounts for 43% of U.S. agricultural residues, yet only ~6% is collected and used.[7]

Lignocellulose can be converted to liquid biofuels by the thermochemical, sugar, and carboxylate platforms. The *thermochemical platform* is inefficient and has low yields.[8,9] The *sugar platform* uses extracellular enzymes to convert polysaccharides into monosaccharides that are fermented. The requirement for enzymes and sterile operating conditions makes this approach expensive. Furthermore, many biomass components (e.g., pectin, protein) are not used. The *carboxylate platform* ferments nearly all biomass components (except lignin and ash) to short- and medium-chain carboxylates, which are subsequently chemically converted to fuels and chemicals.[10,11] The MixAlco™ process is an example of the carboxylate platform and uses methane-arrested anaerobic digestion (MAAD) without requiring extracellular enzymes or sterile operating conditions. Using indigenous enzymes, it ferments a wide range of biomass feedstocks, including municipal solid waste, agricultural residues, sewage sludge, and manure. Compared to other options, the carboxylate platform has low costs and high yields.[8]

Herbaceous lignocellulose is composed primarily of 40–50% cellulose (glucose polymer), 25–35% hemicellulose (sugar heteropolymer), 15–20% lignin (non-fermentable phenyl-propene compound), plus smaller amounts of oils, minerals, soluble sugars, and other components.[15] Cellulose and hemicellulose are the primary sources of fermentable sugars. Enzymatic hydrolysis of these carbohydrate polymers is hindered by the presence of lignin, which imparts strength and resists against pests and microbes.[18]

Lignin binds cellulose and hemicellulose together, creating a composite matrix that is difficult to penetrate using chemicals, enzymes, or microorganisms.[19] To fully convert lignocellulose into biofuels, pretreatment is necessary.

Pretreatment removes some of the impediments that limit enzymatic digestibility, such as high lignin content,[19] low accessible surface area,[21] acetyl groups on hemicellulose, [18] and high cellulose crystallinity.[22] In lignocellulose-to-biofuel conversion, pretreatment can be the most expensive step; however, it has the potential to increase yields dramatically, which lowers overall costs.[20]

Broadly, pretreatment methods can be classified as physical, chemical, or both.[36] Acid pretreatment requires aggressive temperatures and pressures. Although effective, it is expensive, and it degrades sugars. Furthermore, concentrated acids are toxic, hazardous, and corrosive thereby requiring expensive corrosion-resistant materials. In contrast, alkaline pretreatments can be performed at low temperatures and pressures. Compared to acid pretreatment, alkaline pretreatment causes less sugar degradation. Acceptable alkaline pretreatment agents include hydroxides of ammonium, calcium, potassium, and sodium.[18,20] Alkaline pretreatment with $Ca(OH)_2$ – oxidative lime pretreatment (OLP) and submerged lime pretreatment (SLP) – effectively and economically removes lignin and preserves vital sugars.[11,37] Alkaline pretreatment with NaOH causes biomass to swell, which increases internal surface area, decreases polymerization, reduces crystallinity, and breaks down lignin structure.[19]

Among mechanical pretreatments, shock pretreatment is a novel method that uses a detonation wave to mechanically disrupt the microscopic structure without damaging

the macroscopic integrity of the biomass particle[38,39] The final shock pressure is 18 times greater than the initial pressure of explosive gas.[40] It is estimated to cost <$5/ton.[41] Combining shock and lime pretreatments improves enzymatic digestibility of lignocellulose.[11,38,39,42,43]

In previous studies on the MixAlco™ process, alkaline OLP and SLP were neutralized by bubbling carbon dioxide through the liquid slurry. Calcium carbonate has low solubility in water, so an excess amount of calcium carbonate can be added to the fermenter. As acids are released during the MAAD, calcium carbonate dissolves and self-buffers to about pH 5.8, thus eliminating the need for a pH controller.[44] Calcium carbonate is inexpensive and easily calcined to lime using conventional kiln technology; thus, lime is easily recovered and recycled. Despite these advantages, because calcium carbonate is not able to maintain neutral pH, it negatively impacts acid production as shown in Figure 2-1.[41]

To avoid inefficiencies associated with switching cations in the MixAlco™ process, it is more economical to use the same cation in the pretreatment as in the MAAD buffer. Among the most effective cations (Figure 2-1), sodium is an excellent choice because it is less expensive than potassium.[41] Using NaOH for pretreatment leads to the use of $NaHCO_3$ to buffer the MAAD. High-temperature sodium hydroxide pretreatment reduces the process time to a few minutes.[45] Sodium hydroxide is moderately priced and is widely used in the paper industry for delignification processes.[46] For the carboxylate platform, NaOH pretreatment is preferred because the presence of sodium ions improves MAAD performance (Figure 2-1).

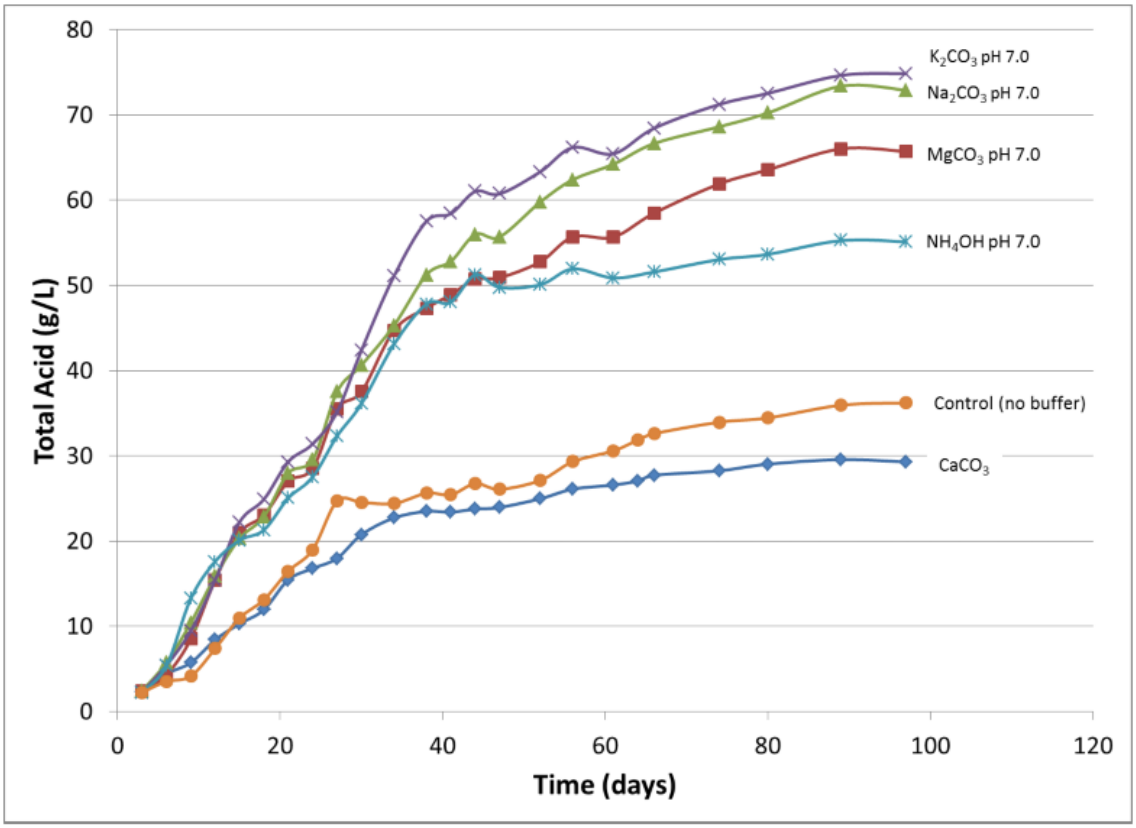

Figure 2-1. Effect of buffers which were titrated as needed on total acid production in mixed-acid batch fermentation.

Lignocellulose pretreatment can be used to enhance the digestibility of ruminant feeds.[38] In their daily diets, non-lactating beef cattle require 12 times more calcium than sodium (Table 2-1). Lactating beef cows require higher amounts of sodium in their diets (probably due to the transfer of sodium to the milk) ranging from 0.1% (Table 2-1) to 0.22% recommended by the US National Research Council.[47,48] Nonetheless, lactating cows require 7 times more calcium than sodium. For animal feeds, $Ca(OH)_2$ pretreatment is preferred because less washing is required to remove residual ions.

Table 2-1. Mineral requirements for the maintenance of cattle. Each number is a percentage of daily dry matter intake. The calcium requirements were calculated under the assumption that animals consume 2% of their body weight as dry matter.

	Calcium (%)	Sodium (%)
Non-lactating beef cattle	0.81	0.06–0.08
Lactating beef cow	1.59	0.1

This chapter reports the efficacy of the following corn stover pretreatment methods: shock, lime, sodium hydroxide, shock with lime, and shock with sodium hydroxide. The following experimental variables are investigated: choice of alkali, temperature, time, oxygen pressure, and shock pressure. In this chapter, pretreatment efficacy is quantified using enzymatic hydrolysis. This study was performed with Shenchun Hsu, Huang Ju and Simon Schiele. In Chapter 3, digestibility is assessed using MAAD employed in the MixAlco^{TM} process.

2.2. Materials and Methods

2.2.1. Alkaline Pretreatment

Corn stover was pretreated using both calcium hydroxide $Ca(OH)_2$ and sodium hydroxide NaOH. The procedure was adapted from Falls.[49] Alkaline pretreatment was performed in 304 stainless steel pipe reactors (12.7-cm long, 3.8-cm internal diameter) with 3.8-cm 304 stainless steel caps. Corn stover, which was harvested in 2012, was milled using a large Champion mill to ~1 cm uniform particle size.[40] Corn stover (7 g, dry basis) and a mixture of alkali and water were mixed in each reactor ensuring a 5 g dry biomass/100 g slurry. To prevent leakage, the reactor was sealed using Teflon tape.

The reactor was preheated in a hot-water bath for 10 min. In some cases, oxygen was added through a flexible hose attached to a cylinder containing pure oxygen (Praxair Distribution, Inc., Bryan, TX); the reactor pressure was 6.89 bar (abs).[50] To achieve constant stirring, the reactor was attached to a swing arm located within a preheated temperature-controlled oven (Figure 2-2).[49] After the desired reaction time, the reactor was removed from the oven and cooled in a cold-water bath. Pressure was relieved by using a wrench to open the reactor slightly for about 5 minutes. To neutralize the biomass slurry in the reactor, hydrochloric acid was added to the opened reactor. Fisherbrand™ laboratory grade plastic pH strips were used to confirm neutralization. The reactor contents were dumped over a #80 sieve to separate the soluble fraction from the solid residue. The solid residue was washed with 12 L of water to remove any $CaCl_2$ or NaCl formed during the neutralization of the alkali. For some experiments, only the solid residue was collected for storage or hydrolysis. In other experiments, both the filtrate and the residue were collected for storage or hydrolysis in 1-L plastic centrifuge bottles (Thermo Scientific, Nalgene, Rochester, NY). To compare on an equal basis, the loading for NaOH or $Ca(OH)_2$ was quantified based on the hydroxide group (g OH^-/100 g dry biomass).

2.2.2. Shock Pretreatment

To mechanically disrupt the microscopic biomass structure, corn stover was shock pretreated using shock waves generated by detonating explosive gas ($H_2 + O_2$) [42]. The 2-L shock tube was filled with a biomass slurry (5% biomass loading) and sealed with an impact wrench. A stoichiometric mixture of hydrogen and oxygen was added to

the shock-tube to a specific initial filling pressure and ignited with a glow plug. To optimize the shock pressure, the initial fill pressure was varied. The shock-treated corn stover was collected using a #80 sieve. The moist biomass was air dried at room temperature and stored in Ziploc bags.

2.2.3. Enzymatic Hydrolysis

The enzymatic hydrolysis procedure closely follows the NREL procedure with a few modifications.[51] For each sample, 1-L HDPE bottles (Nalgene centrifuge bottles, Fisher catalog # 05-562-26) were used as enzymatic hydrolysis reactors. To ensure proper mixing, the reactors rotated at 120 rpm in a roller incubator maintained at 50^{o}C.

2.2.4. Substrate

Raw (untreated) and pretreated corn stover were used as substrates. The dry biomass loading was 5% of the reactor volume. Prior to enzymatic hydrolysis, the raw (untreated) corn stover samples were analyzed for composition using the standard NREL procedure.[52] The mass fraction of glucan and xylan in the corn stover used in this study was 0.360 and 0.222, respectively.[53]

2.2.5. Enzymes

Enzymatic hydrolysis was performed using Novozymes Cellic CTec3 and Novozymes Cellic HTec3. The respective protein contents of CTec3 and HTec3 were determined to be 326 mg protein/mL and 243 mg protein/mL using Pierce^{TM} BCA protein assay.[39,54,55] CTec3 is effective for the hydrolysis of cellulose whereas HTec3 is effective for the hydrolysis of hemicellulose. Simultaneous conversion of cellulose and hemicellulose improves xylose and glucose yields; the combined effect increases the

hydrolysis rate by disentangling lignocellulose biomass.[54] For both HTec3 and CTec3, the individual enzyme loadings were 2 mg protein/g dry biomass loaded into the enzymatic hydrolysis reactor. This low enzyme loading was chosen to amplify the pretreatment effects.[41,49]

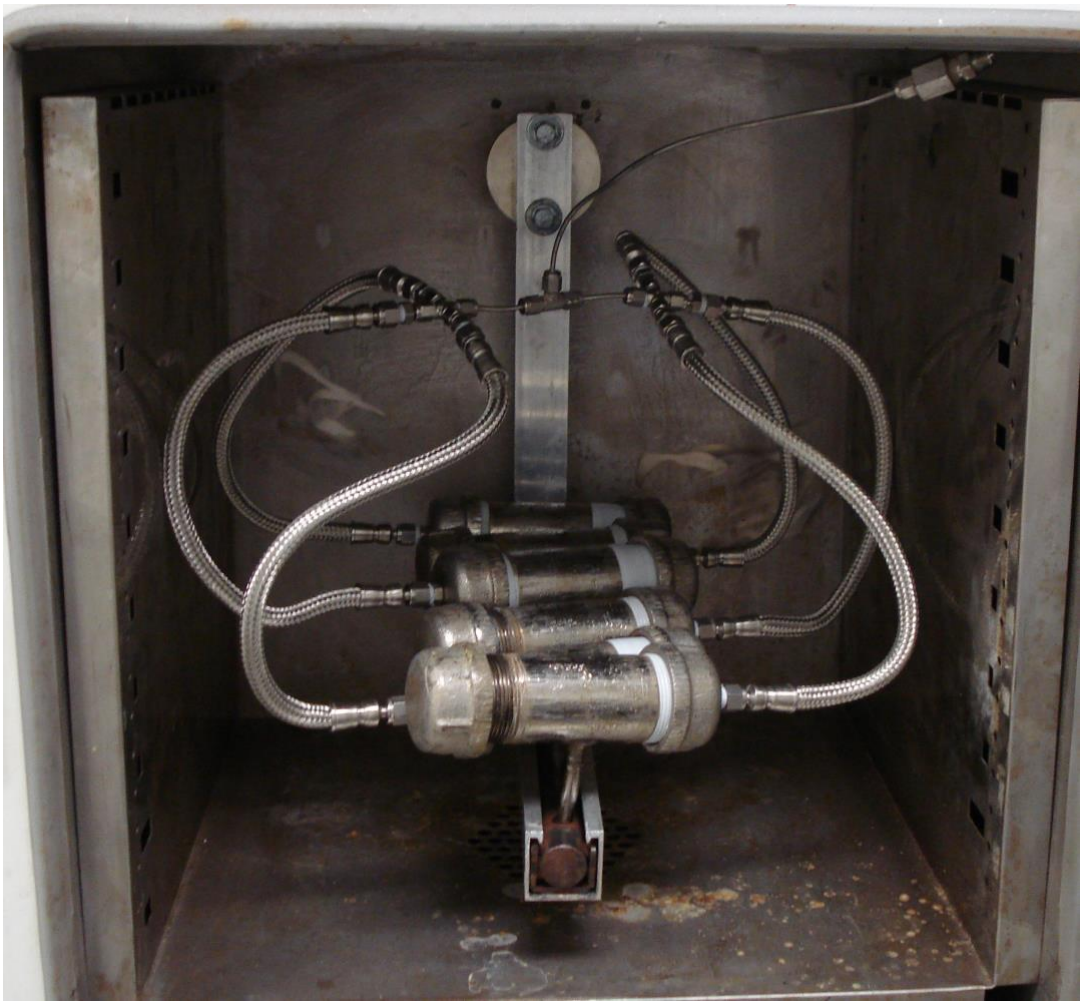

Figure 2-2. Stainless steel pipe reactor attached to swing arm in a temperature-controlled oven.

2.2.6. Citrate Buffer

Citrate buffer (0.1 M) was used to adjust the pH of the biomass slurry to maintain optimal enzyme performance; it comprised 50% of the slurry in each reactor, the other half is comprised of enzymes, antibiotics, biomass, and deionized water. The desired pH range is 4.75–5.25 and 4.80–5.20 for cellulase CTec3 and hemicellulase HTec3, respectively.[56,57] The citrate buffer was prepared by mixing trisodium citrate dihydrate (99%, ACROS Organics), citric acid monohydrate (99.5%, ACROS Organics), and deionized water.

2.2.7. Antibiotics

Because of the fragile nature of enzymes, an antibiotic cocktail was required to prevent the growth of contaminating microorganisms. A cocktail of tetracycline (crystalline powder, Alfa Aesar) and cycloheximide (95%, ACROS Organics) was prepared. Both tetracycline and cycloheximide serve as a protein biosynthesis inhibitors and antibiotics. Tetracycline was dissolved in an aqueous solution (70% ethanol or 553 g ethanol/L) to form a 10 g tetracycline/L solution. Cycloheximide was dissolved into deionized water to produce a 10 g cycloheximide/L solution. Tetracycline (80 μL) and cycloheximide (60 μL) where added per 1 mL of slurry.

2.2.8. Hydrolysis of Filtrate Samples

Filtrates collected after alkaline pretreatment were adjusted to a pH range of 5–6. The same buffer containing antibiotics and enzymes (as previously described) was added in a 1:1 ratio to the volume of each filtrate sample in 1-L HDPE bottles. The bottles were placed in an incubator at 120 rpm and 50°C for 5 days.

2.2.9. Digestibility

Digestibility is defined as the percentage of sugars present in the raw biomass that are released during hydrolysis for 5 days at a slurry concentration of 5 wt. % biomass. Because glucan and xylan are hydrolyzed to glucose and xylose during enzymatic hydrolysis, the mass increases because of the water of hydrolysis. The correction factors of 1.111 for glucan and 1.136 for xylan account for this increase in mass.[40] Digestibility of the pretreated solid residue is defined as

$$D_{\text{solid}} = \frac{m_{\text{product}}}{m_{\text{digestible BM}}} \quad (2\text{-}1)$$

where m_{product} is the mass of glucose and xylose produced during enzymatic hydrolysis and $m_{\text{digestible BM}}$ is the mass of the equivalent glucose and xylose present in the raw biomass

$$m_{\text{product}} = \left(c_{\text{glucose}} + c_{\text{xylose}}\right) * V_{\text{reactor}} \quad (2\text{-}2)$$

where c_{glucose} (g/L) and c_{xylose} (g/L) are the concentrations of glucose and xylose measured by high-performance liquid chromatography (HPLC, Agilent Infinity) equipped with a refractive index detector, autosampler, a pair of de-ashing guard columns (Bio-Rad Micro-Guard de-ashing cartridges, 30 mm × 4.6 mm), and a carbohydrate analysis column (Aminex® HPX-87P column, 300 mm × 7.8 mm). The mobile phase was HPLC-grade water with a flow rate of 0.6 mL/min, column temperature of 85°C and an assay time of 21 minutes per sample.

In some of the studies reported herein, the enzymatic digestibility (D) is based on sugars released from enzymatic digestion of both the solid residue (D_{solid}) and filtrate (D_{filtrate}):

$$D = D_{\mathrm{solid}} + D_{\mathrm{filtratre}} = \frac{(m_{\mathrm{product}})_{\mathrm{solid}} + (m_{\mathrm{product}})_{\mathrm{filtrate}}}{m_{\mathrm{digestible\ BM}}} \quad (2\text{-}3)$$

During each treatment, biomass may be lost through the sieve and may dissolve into the liquid phase. Pretreatment yield (Y_{pre}) accounts for the mass loss from both shock (Y_{shock}) and alkali (Y_{alkali}) treatments:

$$Y_{\mathrm{pre}} = Y_{\mathrm{shock}} \cdot Y_{\mathrm{alkali}} = \left(\frac{m_{\mathrm{shocked}} + m_{\mathrm{MC,1}}}{m^0_{\mathrm{shock}}}\right) \cdot \left(\frac{m_{\mathrm{chem}} + m_{\mathrm{MC,2}}}{m^0_{\mathrm{NaOH}}}\right) \quad (2\text{-}4)$$

where m^0_{shock} and m^0_{NaOH} are the dry weight of pre-shock biomass (100 g in this study) and biomass before alkaline treatment (7 g in this study), respectively. Moreover, m_{shocked} is the dry weight of post-shock corn stover. The dry weight of post-alkaline-treated corn stover (m_{chem}) is used for subsequent enzymatic hydrolysis, whereas $m_{\mathrm{MC,1}}$ and $m_{\mathrm{MC,2}}$ are the dry weights of the samples used to measure moisture content after shock and alkali treatments, respectively.

When glucan and xylan are hydrolyzed into glucose and xylose, the mass increases from the water of hydrolysis. The correction factors ACC and ACX are 1.111 and 1.136, respectively.

$$m_{\mathrm{digestible\ BM}} = \left(x^0_{\mathrm{glucan}} \cdot \mathrm{ACC} + x^0_{\mathrm{xylan}} \cdot \mathrm{ACX}\right) \cdot \frac{m_{\mathrm{chem}}}{Y_{\mathrm{pre}}} \quad (2\text{-}5)$$

where x^0_{glucan} and x^0_{xylan} are the mass fractions of glucan and xylan in raw corn stover reported by Bond as 0.360 and 0.222, respectively.[42]

2.2.10. Statistical Analysis

All experimental results were the average of values obtained from running the experiments in triplicate. Microsoft Excel was used to calculate average digestibility values, standard deviations, two-sample t-tests assuming unequal variances, and Tukey's mean separation tests. Two-sample t-tests assuming unequal variances, at a significance level of 0.05, were performed on paired data points between treatments. An asterisk was placed above data points that differed significantly between treatments. Tukey's mean separation test, at a significance level of 0.05, was performed to compare all the data points across treatments and between treatments. Statically significant difference was indicated using letters (a, b, c, ab, etc.) located beside data points. Treatments not sharing a common letter differed significantly. Stated differently, treatments that share a common letter are statistically similar.

2.3. Results and Discussion

Multiple experiments were performed with varying pretreatment conditions as displayed in Table 2-2. For some experiments, only the biomass residue recovered from the alkaline pretreatment step was enzymatically hydrolyzed, which accords with oxidative lime procedure in previous studies.[49] In other experiments, both the biomass residue and the filtrate were enzymatically hydrolyzed.

2.3.1. Residue and Filtrate

At aggressive alkaline pretreatment conditions, over 10% of the digested sugars are dissolved in the filtrate of both alkalis (Figure 2-3). This result suggests that biomass dissolved in the alkaline slurry must be included because it significantly increases

enzymatic digestibility. Most of the residue-only experiments were repeated with residue + filtrate. Because the conclusions from the residue-only and residue + filtrate experiments were consistent with each other, this implies that a uniform portion of pretreated biomass always dissolved into the alkali slurry.

Table 2-2. Comprehensive list of experimental variables.

Figure	Shock-gun initial filling pressure (bar)	Shock Control	Alkali Used	Alkali concentration (g OH^-/100 g dry BM)	Pressurized oxygen (bar)	Temp (^oC)	Duration (min)	Use of Filtrate
3-3	N/A	N/A	Var	10	20.68	100	90	Y
3-4	N/A	N/A	NaOH	8	10.34	100	Var	Y
3-5	N/A	N/A	Var	Var	N/A	100	60	N
3-6	N/A	N/A	Var	Var	N/A	50	60	Y
3-7	N/A	N/A	NaOH	8	10.34	Var	60	N
3-8	5.52	N/A	NaOH	4	N/A	Var	60	Y
3-9	N/A	N/A	NaOH	8	10.34	100	Var	N
3-10	N/A	N/A	NaOH	8	N/A	50	Var	N
3-11	N/A	N/A	NaOH	8	Var	100	60	N
3-12	N/A	N/A	NaOH	8	Var	100	60	Y
3-13	6.89	A	NaOH	Var	10.34	100	60	N
3-14	6.89	A	NaOH	Var	N/A	100	60	Y
3-15	5.52	A	NaOH	Var	N/A	50	60	Y
3-16	6.89	B	NaOH	Var	N/A	100	60	Y
3-17	Var	N/A	NaOH	4	N/A	50	60	Y

Control A is raw corn stover subjected to alkaline treatment directly.
Control B is raw corn stover wetted and dried (as in shock treatment) and then is subjected to alkaline treatment.

Figure 2-4 shows that throughout the duration of the alkali treatment, the portion of sugars from the filtrate are significant and should be included in the total digestibility. From this figure, we also observe that the sugars dissolved into the filtrate seems to increase with time. Without the filtrate, it is easy to conclude that digestibility does not

change significantly after 40 minutes. But with the inclusion of the filtrate, a more complete estimate of the digestibility is acquired.

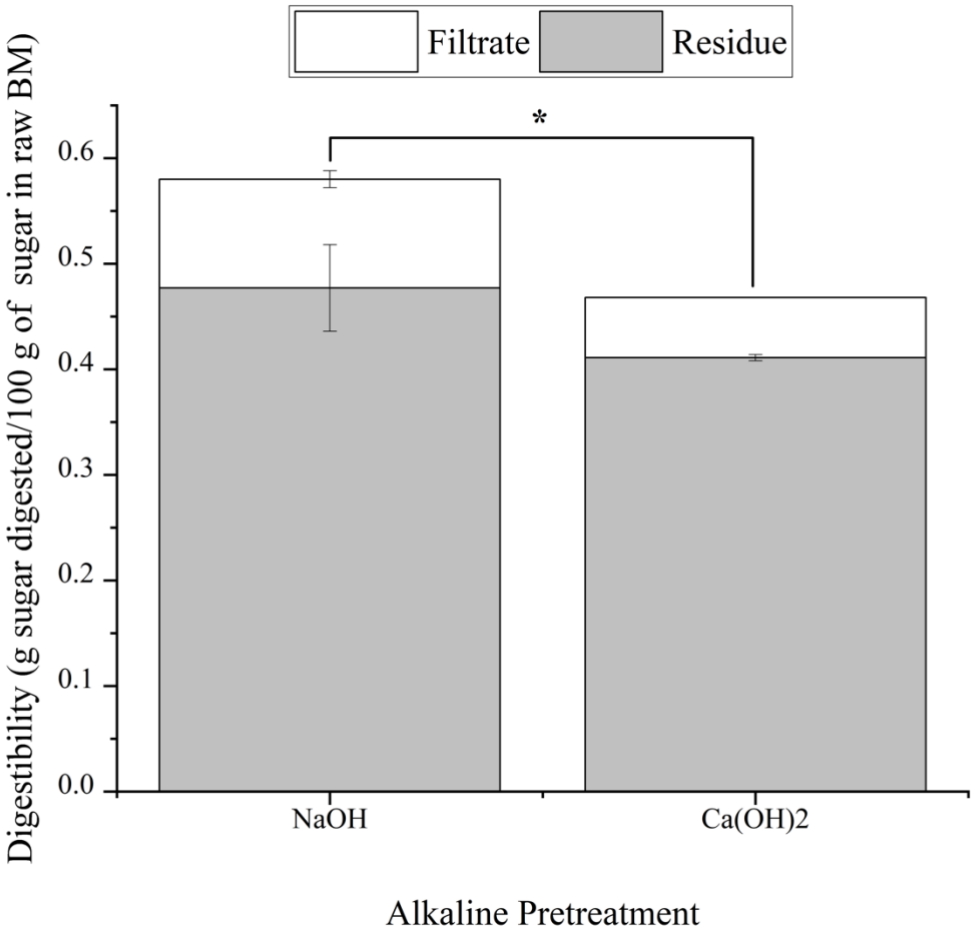

Figure 2-3. Effect of alkali choice on sugar dissolution and digestibility. (Other conditions: No shock treatment, 10 g OH^-/100 g dry biomass, 20.68 bar of pressurized oxygen, 100°C, 90 min.)

2.3.2. Choice of Alkalis

The use of NaOH, rather than $Ca(OH)_2$, resulted in significantly higher digestibility at high hydroxide concentrations and temperature (Figures 2-3 and 2-5). For

both alkalis, the sugar yield peaked at 8 g OH^-/100 g dry biomass (Figure 2-5) implying that increasing the hydroxide concentration beyond this point provides little to no benefit.

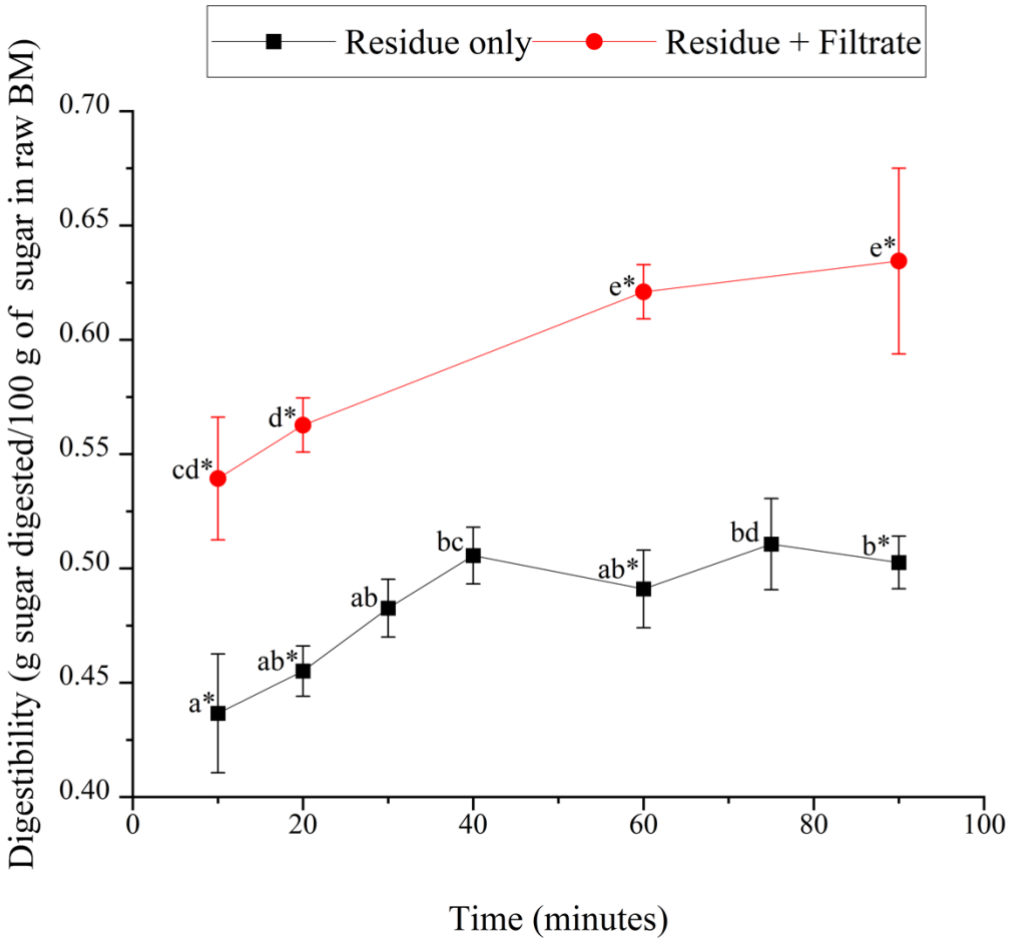

Figure 2-4. Effect of time on the dissolution of digested sugars. (Other conditions: No shock treatment, NaOH, 8 g OH^-/100 g dry biomass, 10.34 bar of pressurized oxygen, 100°C.)

NaOH, which is more soluble in water than $Ca(OH)_2$, acts quickly on the biomass fiber and immediately initiates pretreatment. In contrast, $Ca(OH)_2$ dissolves gradually as time passes hence requiring a longer duration to pretreat the biomass.

Figures 2-5 and 2-6 show the supremacy of NaOH over $Ca(OH)_2$ at a loading >4 g OH^- /100 g dry biomass; however, at this value and below, both alkaline agents perform similarly.

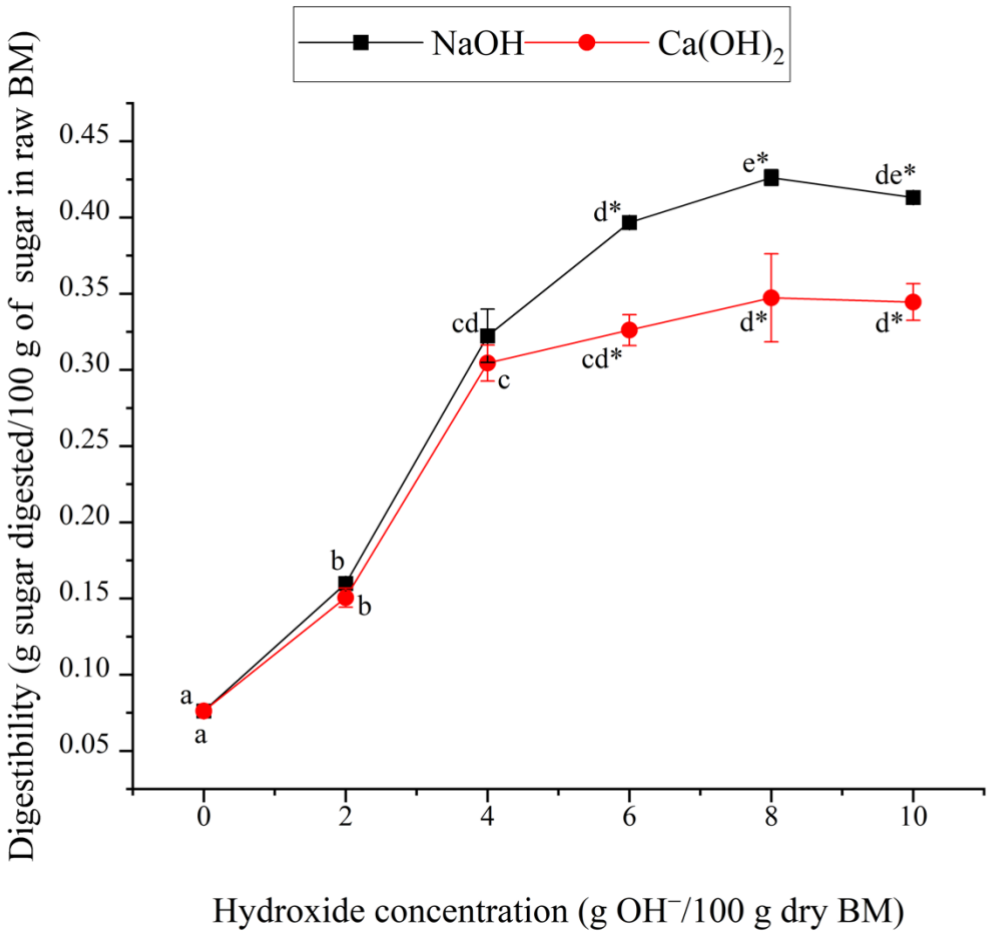

Figure 2-5. Effect of hydroxide concentration on digestibility. (Other conditions: No shock treatment, 100ºC, 60 min, filtrate not included in enzymatic hydrolysis.)

In fact, at one condition shown in Figure 2-6 (3 g OH^-/100 g dry biomass), $Ca(OH)_2$ had a slightly higher yield (25.7%) compared to NaOH (21.8%). In an industrial setting, after alkali pretreatment, the aqueous slurry can be recycled for

additional pretreatments.[58] Alternatively, the slurry can also be neutralized with carbon dioxide and fermented along with the biomass to produce valuable mixed acids.

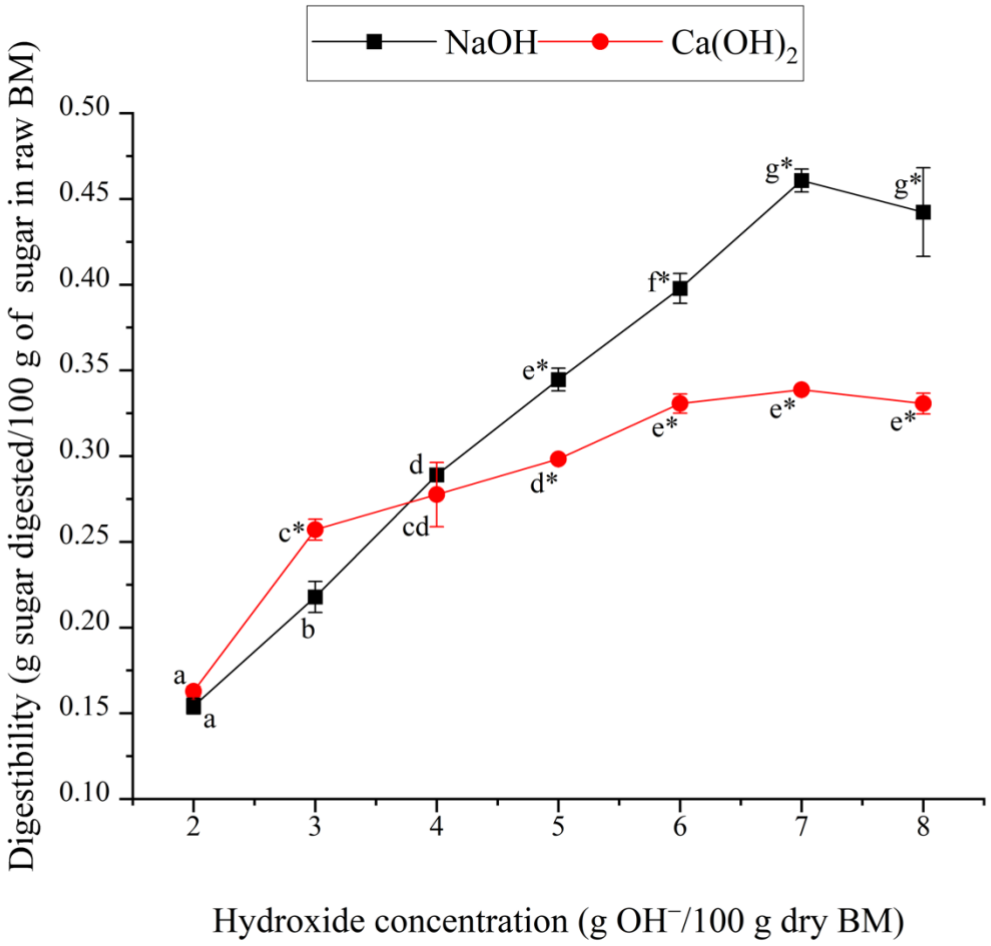

Figure 2-6. Effect of alkali choice and alkali concentration on digestibility. (Other conditions: No shock treatment, 10 g OH^-/100 g dry biomass, 50ºC, 60 min, filtrate included in enzymatic hydrolysis.)

2.3.3. Temperature

Increasing temperature increases digestibility; however, the sharp increase plateaus at approximately 100°C, where the digestibility stops increasing (Figures 2-7 and 2-8).

When temperature is >140°C, Figure 2-7 (8 g OH^-/100 g dry biomass) shows digestibility reduces sharply, whereas in Figure 2-8 (4 g OH^-/100 g dry biomass) there is only a slight drop in digestibility. These results occur because the higher OH^- loading is more aggressive and degrades sugars at the high temperatures.

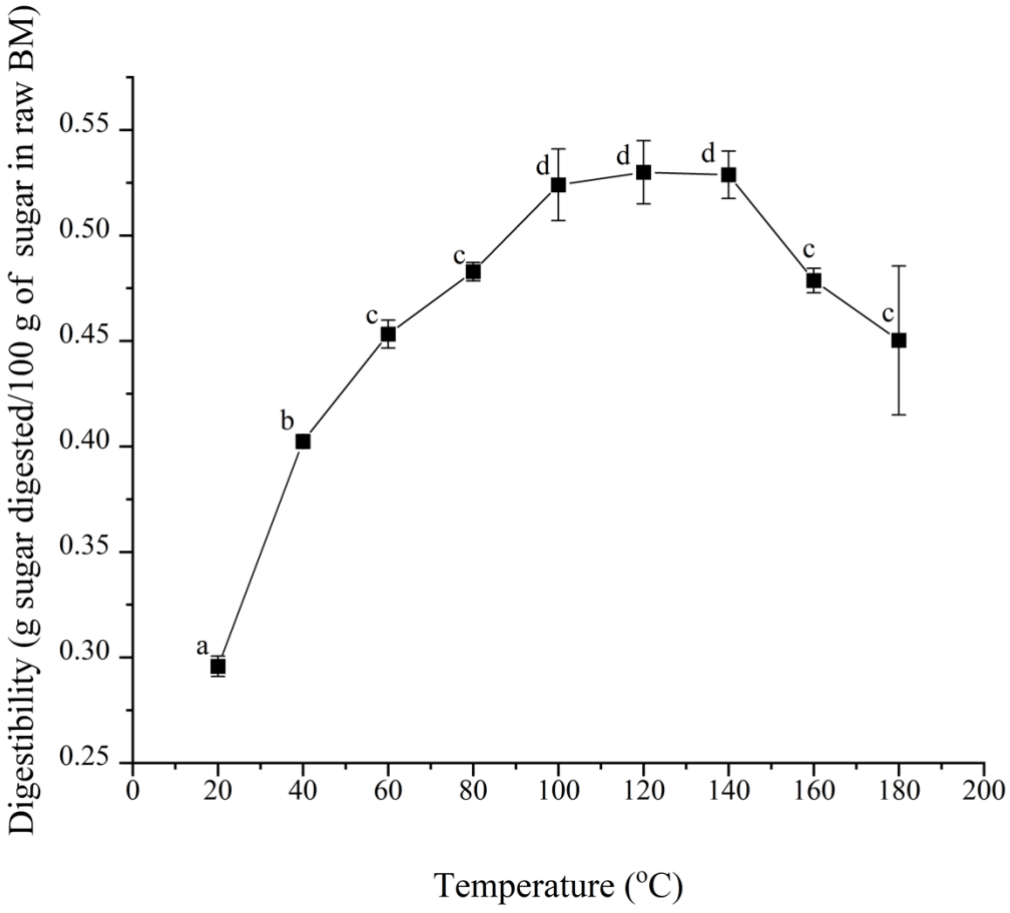

Figure 2-7. Effects of temperature on digestibility. (Other conditions: No shock treatment, NaOH, 8 g OH^-/100 g dry biomass, 10.34 bar of pressurized oxygen, 60 min, filtrate not included in enzymatic hydrolysis.)

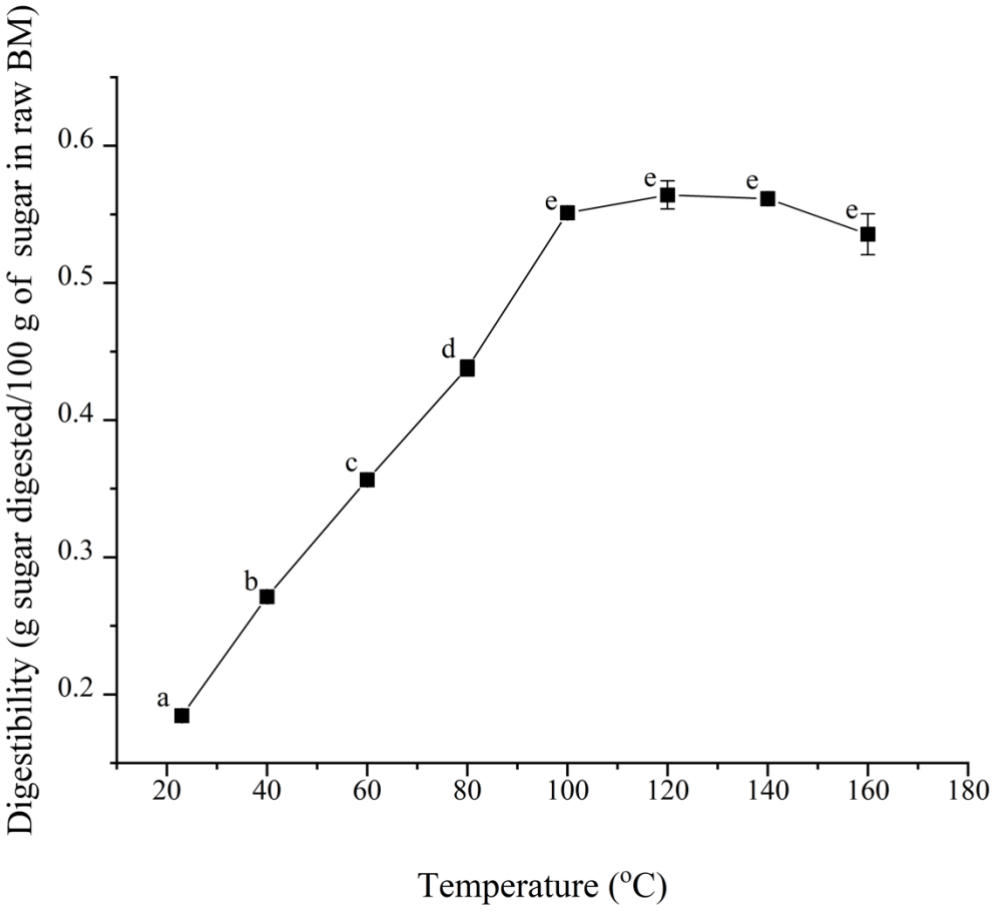

Figure 2-8. Effects of temperature on digestibility. (Other conditions: 5.52 bar shock treatment, NaOH, 4 g OH^-/100 g dry biomass, 60 min, filtrate included in enzymatic hydrolysis.)

2.3.4. Time

At 100°C and 8 g OH^-/100 g dry BM, NaOH pretreatment for only 40 min resulted in 50% of the sugars being hydrolyzed (Figure 2-9). When dissolved sugars in the pretreatment filtrate are included, a sugar yield of 62.3% was observed after 60 min of NaOH pretreatment at 100°C (Figure 2-4). At these aggressive conditions, no significant

increase in digestibility was observed after 60 minutes. Therefore, for aggressive NaOH pretreatment, the recommended treatment time is 1 h.

At 50°C, it requires 48 h for the digestibility to stop increasing with time (Figure 2-10); therefore, when milder pretreatment conditions are implemented, longer durations are required.

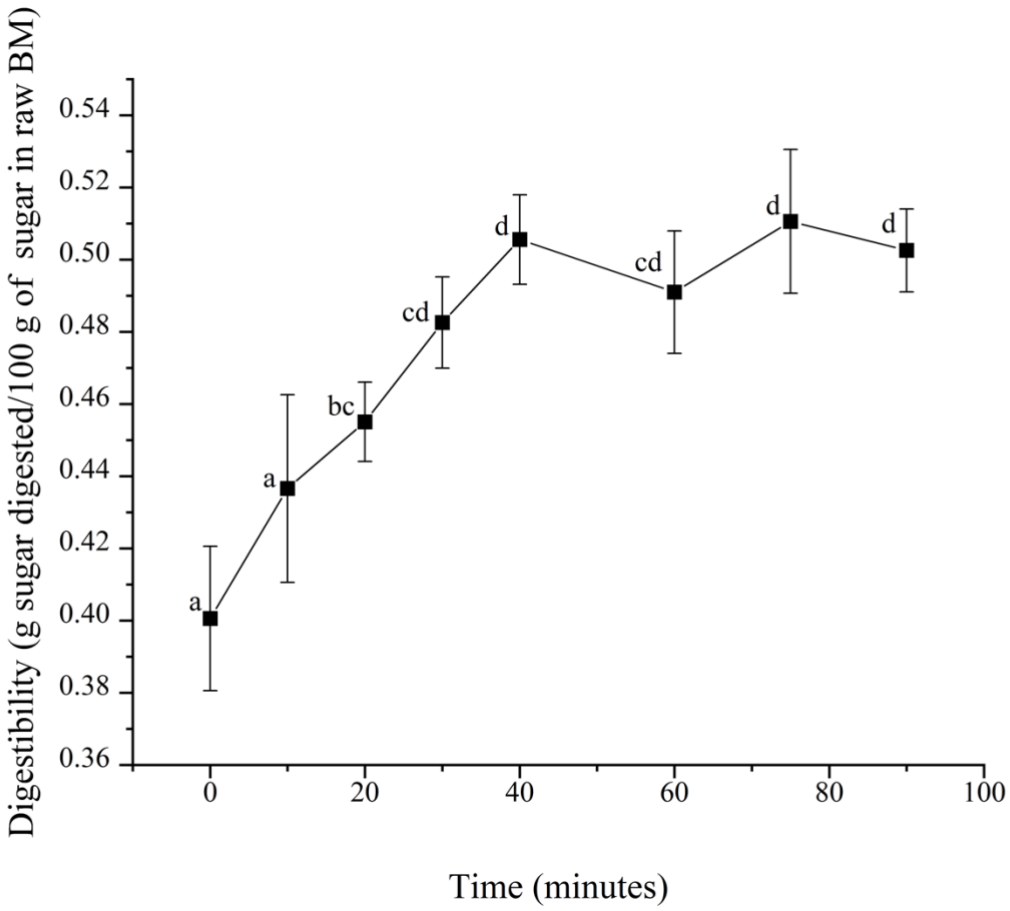

Figure 2-9. Effect of treatment time on digestibility. (Other conditions: No shock treatment, NaOH, 8 g OH^-/100 g dry biomass,10.34 bar of pressurized oxygen, 100°C, filtrate not included in enzymatic hydrolysis.)

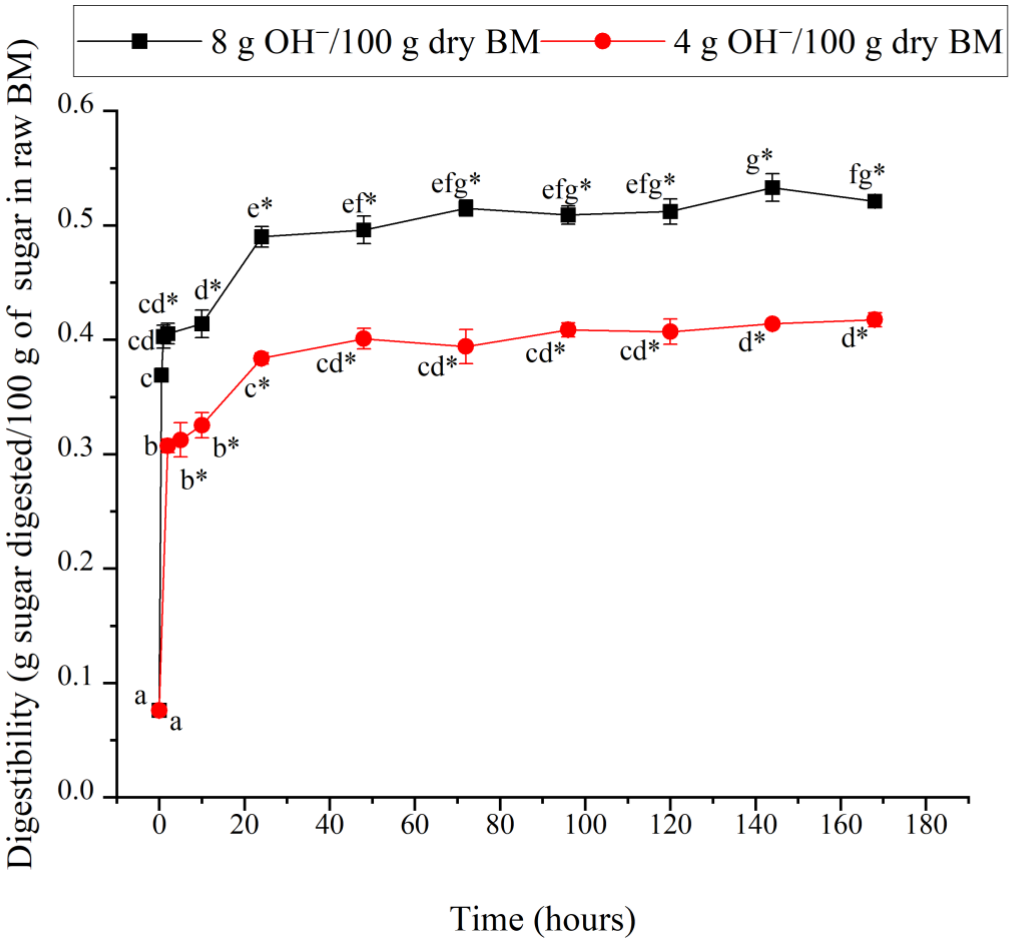

Figure 2-10. Effect of time on digestibility. (Other conditions: No shock treatment, NaOH, 50ºC, filtrate not included in enzymatic hydrolysis.)

2.3.5. Oxygen Pressure

Aggressive NaOH pretreatment, performed at high temperature and high hydroxide concentration, was not affected by elevated oxygen pressure in the reactors (Figure 2-11). This is a contrast to $Ca(OH)_2$ pretreatment, in which previous studies showed oxygen improves digestibility.[7,38,50,54,59] This low effect of oxygen on NaOH pretreatment was observed with and without the inclusion of hydrolyzed filtrate (Figure

2-12). These results show that in NaOH pretreatments, pressurized oxygen does not benefit enzymatic digestibility.

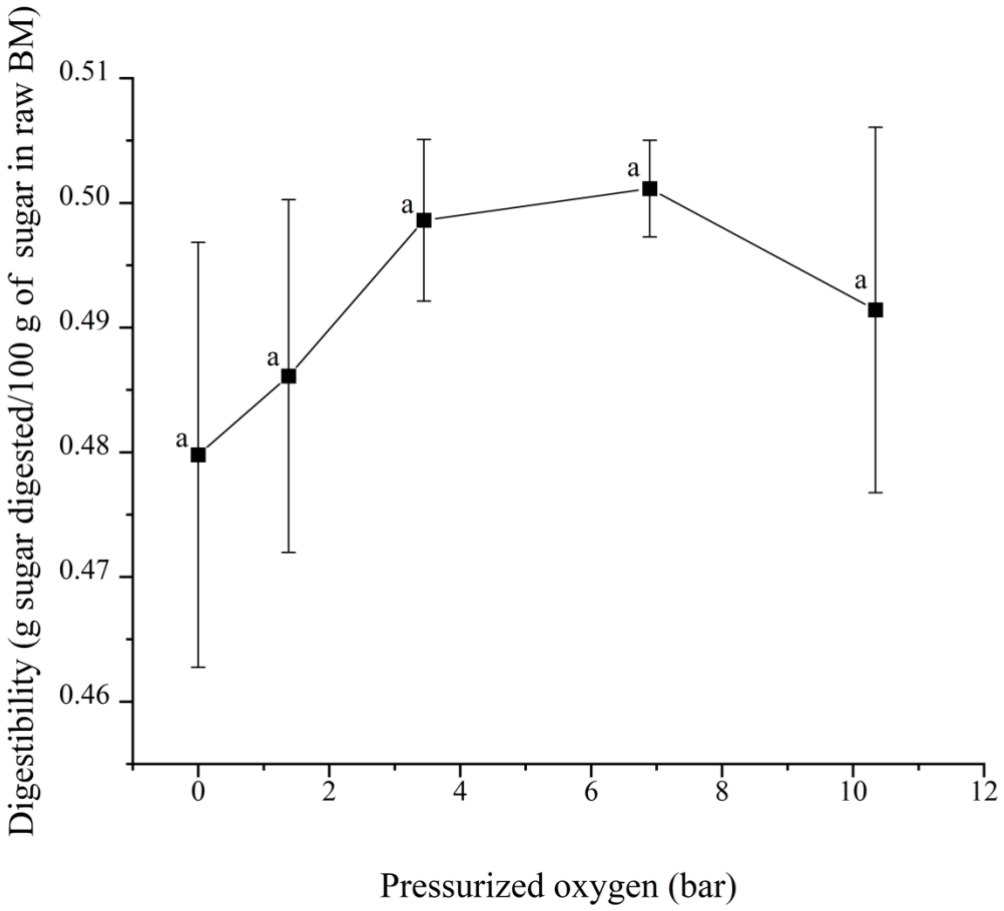

Figure 2-11. Effect of pressurized oxygen on digestibility. (Other conditions: No shock treatment, NaOH, 8 g OH^-/100 g of dry biomass, 100°C, 60 min, filtrate not included in enzymatic hydrolysis.)

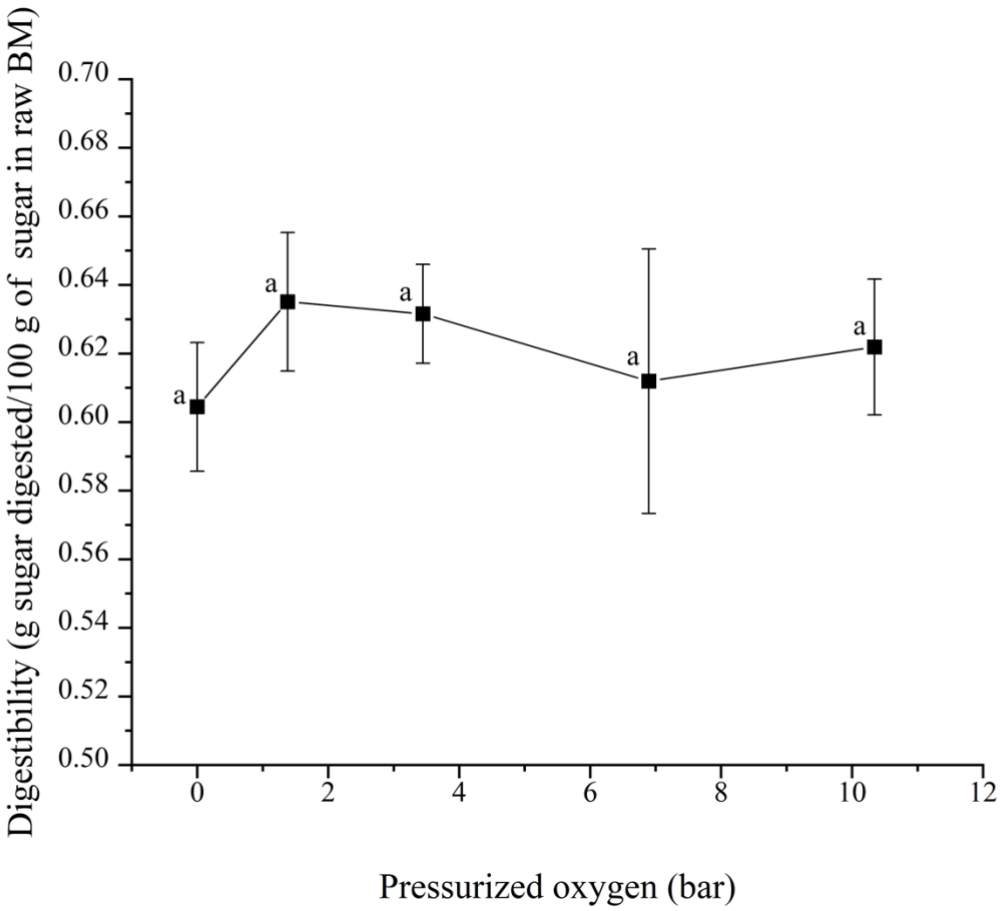

Figure 2-12. Effect of pressurized oxygen on digestibility. (Other conditions: No shock treatment, NaOH, 8 g OH^-/100 g of dry biomass, 100°C, 60 min, filtrate included in enzymatic hydrolysis.)

2.3.6. Shock Pretreatment Configuration and OH^- Loading

The purpose of Section 2.3.6 is to determine the efficacy of shock treatment when combined with NaOH pretreatment. In this section, NaOH treatment plus shock was compared to Control A (NaOH-treated raw corn stover). To combine shock treatment with NaOH treatment, one must come first. Figure 2-13 shows the effect from no shock, post shock, and pre shock. Post shock (i.e., NaOH treatment followed by

shock) has no benefit. Pre shock (i.e., shocking followed by NaOH treatment) improves the digestibility at low hydroxide loadings but has no benefit at high loadings (Figure 2-13). At 100°C, pre shock with NaOH treatment of 3 g OH^-/100 g of biomass yielded 49% of digested sugars vs. 42% without shock (Figure 2-14). Presumably, pre shock enhances alkaline pretreatment by opening the biomass structure and thereby improves diffusion of hydroxide. At 100°C and low hydroxide concentrations, shock pretreatment improves sugar yields, but not at higher hydroxide concentrations (Figure 2-14). In contrast, at 50°C the digestibility was enhanced by shock treatment at some hydroxide concentrations (Figure 2-15).

Bond[40,41] reports electron micrographs of raw corn stover, submerged lime pretreated (SLP) corn stover, and SLP + shock corn stover, but observed little substantial differences; thus, the changes in biomass structure are below the resolution of electron microscopes. To overcome this problem, future studies will employ enzyme adsorption isotherms to measure the accessible surface area of the biomass.[60] The enzymes will serve as appropriate probes in the biomass structure and thereby shed more light on the effects of shock treatment.

To the naked eye, there are no visible differences between shocked and unshocked biomass. The fact that the gross structure is unaffected by shock treatment makes it ideal for animal feed because the coarse particles have sufficient ruminal residence time to ensure they digest. In contrast, physical treatments that yield small particles (e.g., ball milling) are not suitable for animal feed because the small particles escape from the rumen before digesting.

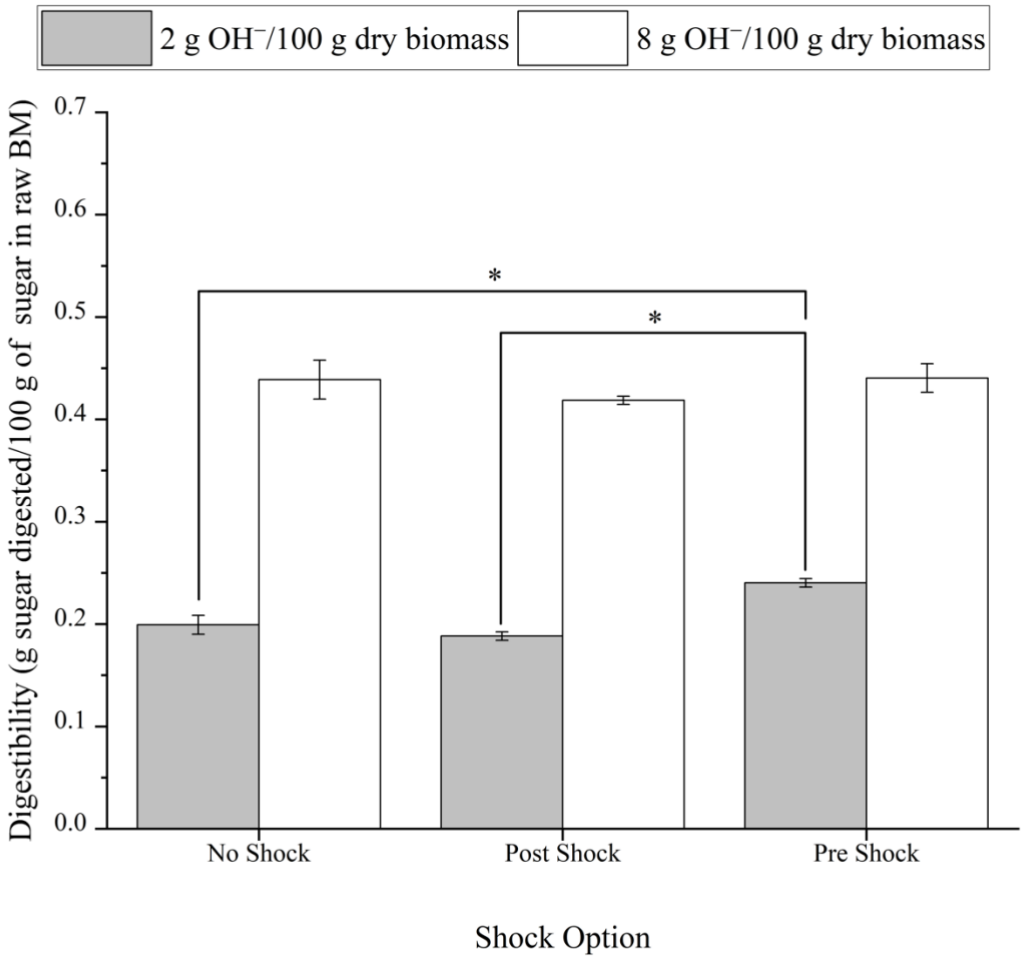

Figure 2-13. Effect of pretreatment configuration on digestibility. (Other conditions: 6.89 bar shock treatment, Control A, NaOH, 10.34 bar of pressurized oxygen, 100ºC, 60 min, filtrate not included in enzymatic hydrolysis.)

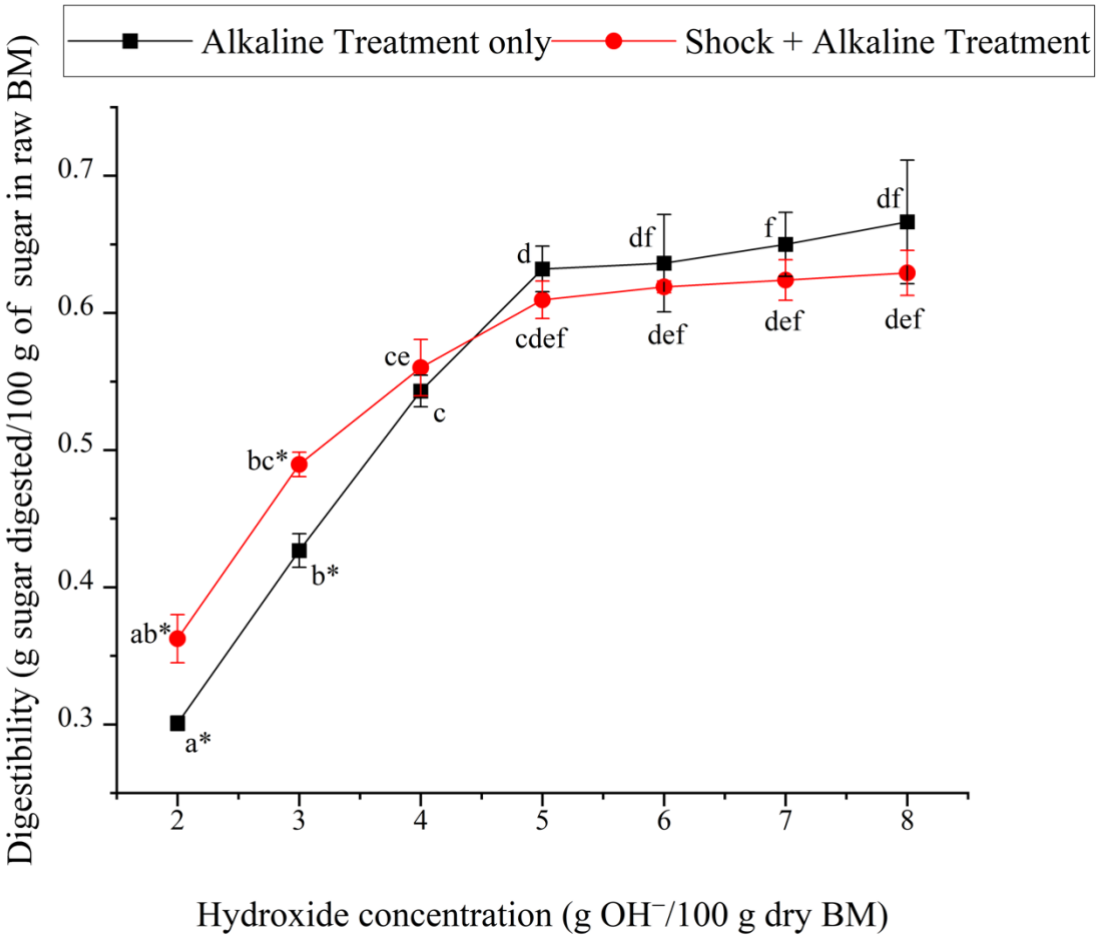

Figure 2-14. Effect of shock treatment and hydroxide concentration on digestibility. (Other conditions: 6.89 bar shock treatment, Control A, NaOH, 100°C, 60 min, filtrate included in enzymatic hydrolysis.)

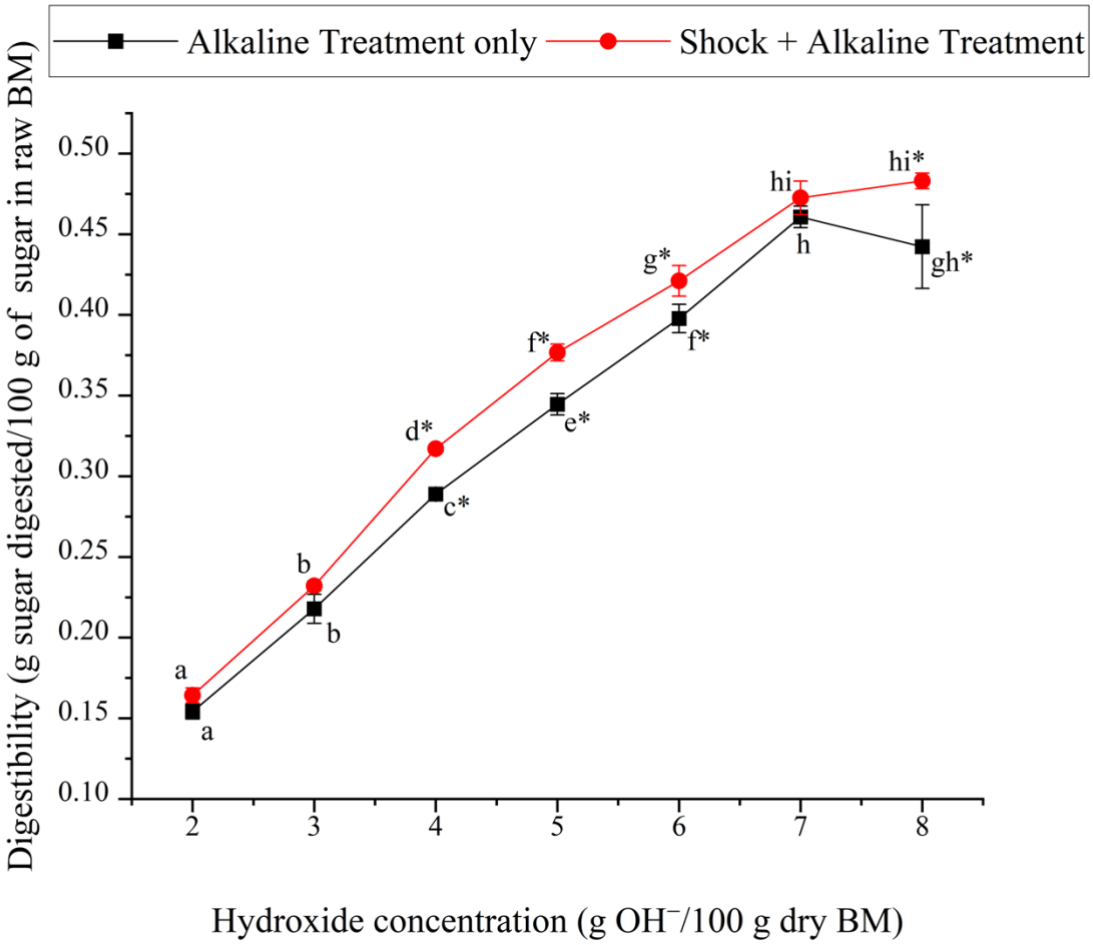

Figure 2-15. Effect of shock treatment digestibility. (Other conditions: 5.52 bar shock treatment, Control A, NaOH, 50ºC, 60 min, filtrate included in enzymatic hydrolysis.)

2.3.7. Redefining the Control Experiment

To ensure the pressure wave distributes evenly to the biomass, shock pretreatment is implemented in an aqueous slurry of biomass. To perform accurate mass balances after shock treatment, it was subsequently dried. In Figures 2-13–2-15, the control experiment – described as Control A in Table 2-2 – uses raw corn stover subjected to alkaline treatment directly. Control A did not account for the soaking and drying that the corn stover receives during shock pretreatment.

To determine the impact of this soaking-and-drying process, studies were performed in which the control biomass – described as Control B in Table 2-2 – was soaked and dried, but not shocked, and subsequently was treated with alkali. The Control B biomass used in "no-shock" experiments was soaked in water for a few minutes and then removed and air dried, the same soak-and-dry procedure used in the shock experiments. Then, this "no-shock" biomass was treated with NaOH. This new procedure creates a fair comparison between shock and no-shock experiments because shock is the only difference between the experimental treatment and the control.

Figure 2-16 shows the impact of implementing this small change in the control. Unlike in Figure 2-15, the benefit of shock pretreatment is uniform in Figure 2-16. Furthermore, the impact of shock pretreatment is much greater. Switching from Control A to Control B revealed that shock pretreatment improved digestibility when combined with both mild and aggressive NaOH pretreatment conditions. These results show that wetting and drying negatively influences the digestibility of corn stover and can confound the interpretation of shock vs. no shock data.

According to Falls et al., shock treatment alone causes a slight increase in cellulose crystallinity and has a negative impact on enzymatic digestibility.[38,43] However, previous studies have shown that combining shock treatment with oxidative lime pretreatment greatly increases biomass digestibility.[38,39,43] Falls et al. hypothesized that even though shock slightly increases crystallinity, this negative effect is countered from the disruption of the lignin/hemicellulose matrix surrounding cellulose, providing greater access for enzymes.[43] From the results of Control A and Control B, an alternative

explanation is that the negative impact from shock-only treatment simply reflects the negative impact from wetting and drying, and not the shock itself. According to Weimer et al., wetting cellulose even at room temperature can increase crystallinity.[61] Thus, the slight increase in crystallinity from shock treatment – and its negative effects on digestibility – may have resulted from wetting-drying rather than shock itself.

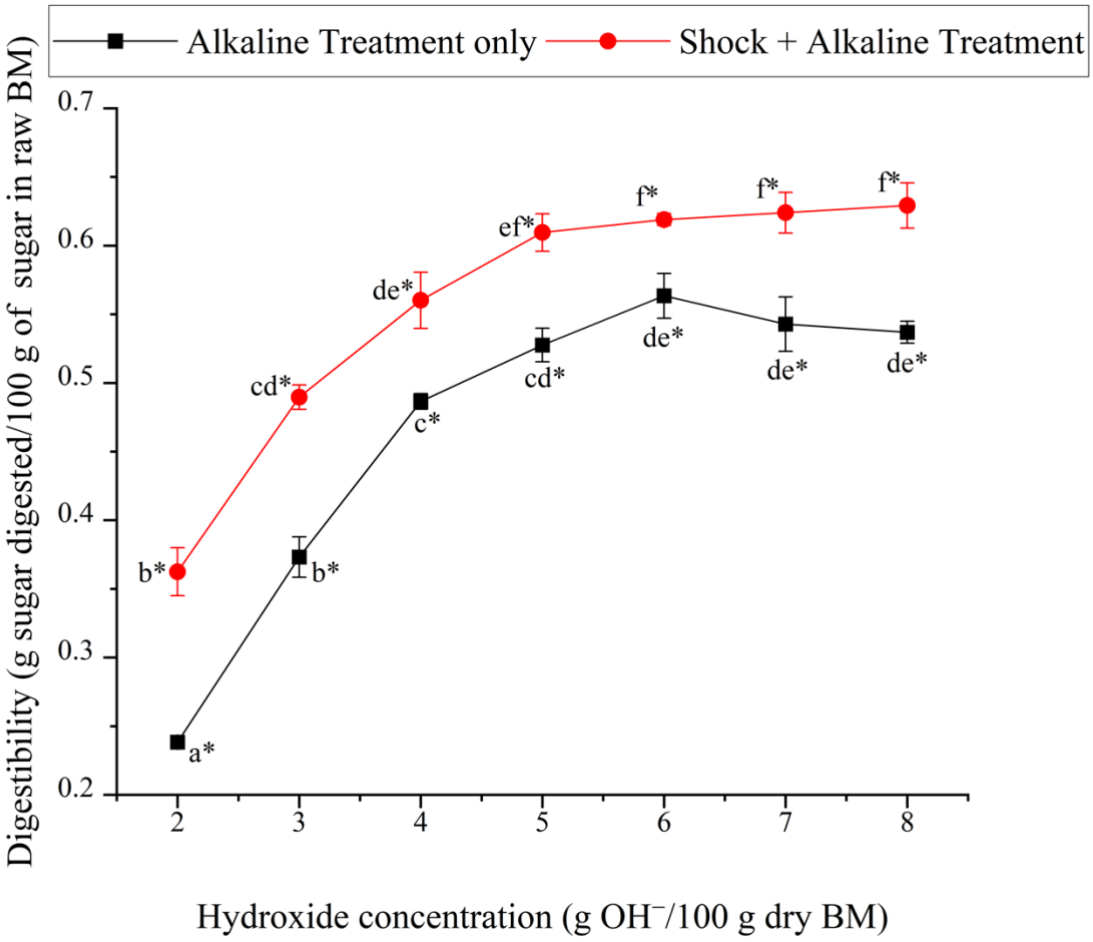

Figure 2-16. Effect of shock treatment and hydroxide concentration on digestibility. (Other conditions: 6.89 bar shock treatment, Control B, NaOH, 100°C, 60 min, filtrate included in enzymatic hydrolysis.)

In the laboratory, the intermediate drying step was only performed to ensure more accurate mass balances. In contrast, in an industrial setting, shock would be immediately followed by alkaline treatment without drying the intermediate material and would avoid the resulting negative impact on digestibility. The benefits of shock shown in Figure 2-16 are more likely to represent an industrial process. Because shock treatment is inexpensive (about $5/ton), it might reduce the overall cost by reducing the severity (temperature, alkali loading, time) of the chemical pretreatment.[41]

2.3.8. Shock Pretreatment Pressure

Previously, during shock pretreatments, the default initial pressure of the H_2/O_2 mixture was 6.89 bar (abs) (100 psia). To determine if lower pressures are effective, and hence reduce costs, experiments were performed with initial pressure ranges between 4.14 to 6.89 bar (abs). Figure 2-17 shows the recommended initial loading pressure is around 5.52 bar (abs) (80 psia), because it resulted in similar biomass digestibility as 6.89 bar (abs). Pressures lower than 5.52 bar (abs) were less effective. Implementing this change to the shock pretreatment process reduces the quantity of gases used during each shock detonation, and reduces the final pressure, both of which reduce costs. According to Bond, the peak shock pressure after detonation is 18 times the initial loading pressure;[40] therefore, reducing the initial loading pressure to 5.52 bar (abs) (80 psia) produces a peak shock pressure of 99.3 bar (abs) (1440 psia).

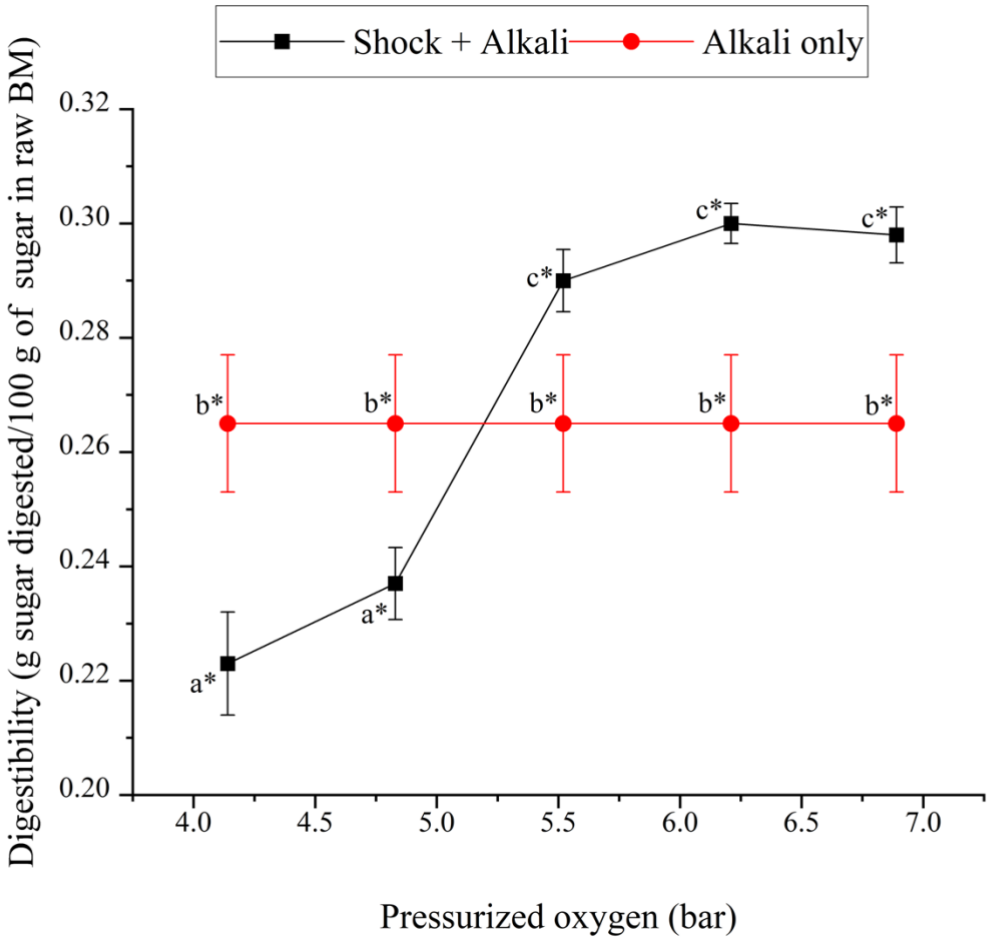

Figure 2-17. Effect of shock tube initial loading pressure. (Other conditions: NaOH, 4 g OH^-/100 g of dry biomass, 50°C, 60 min, filtrate included in enzymatic hydrolysis.)

For industrial applications, pretreatment must be economically feasible. Sodium hydroxide is a major expense, so it is worthwhile to employ processing conditions that reduce alkali loading. Furthermore, low temperatures are attractive because of reduced energy requirements and because low-cost plastic vessels can be employed. Therefore, corn stover treated under 4 g OH^-/100 g dry BM at 50°C for 1 h incorporated with shock treatment (5.52 bar (abs) initial pressure) was chosen as the biomass substrate used in

experiments that assess digestibility using MAAD, as would be employed in the MixAlco™ process.

2.4. Conclusion

This research study has the following conclusions:

- Alkaline pretreatment dissolves a significant portion of the biomass into the pretreatment filtrate. To accurately determine the efficacy of alkaline pretreatment, the sugars dissolved into the filtrate must be hydrolyzed and included as part of the product.
- At low hydroxide loadings (<4 g OH^-/100 g dry BM), NaOH and $Ca(OH)_2$ perform similarly. Above this threshold, NaOH is superior.
- Treating with $Ca(OH)_2$ is best suited for animal feed. The residual calcium ions are beneficial nutrients; therefore, less washing is required after biomass pretreatment.
- Treating with NaOH is best suited for the carboxylate platform because the presence of sodium ions improves MAAD performance.
- In $Ca(OH)_2$ treatments, oxygen is known to be beneficial. In contrast, NaOH pretreatments showed no significant benefit from pressurized oxygen.
- NaOH is so potent that it requires much shorter durations to pretreat biomass than does $Ca(OH)_2$.
- Increasing alkaline pretreatment temperature improves digestibility below 100°C, but digestibility increases modestly above that.

- Shock treatment “amplifies” alkaline treatment by opening the biomass structure to improve diffusion of alkali into the biomass structure. For this reason, shock treatment is most effective when performed prior to alkaline pretreatment.
- The recommended initial loading pressure for shock treatment is 5.52 bar (abs) (80 psia).
- The benefit of shock treatment is more pronounced with Control B, which removed only one variable (shock) while keeping all other variables (wet-dry, NaOH treatment) the same.
- Future laboratory experiments should eliminate the drying step after shock treatment, which would better represent an industrial process.
- An economical pretreatment should minimize the cost of energy and chemicals. These objectives are met using the following recommended conditions: shock pretreatment performed prior to NaOH pretreatment, initial H_2/O_2 pressure of 5.52 bar (abs), NaOH treatment using 4 g OH^-/100 g dry BM without pressurized oxygen at 50°C for 1 h.

These recommended conditions will be used to treat biomass employed in MAAD suitable for the MixAlco® process, which will be reported in Chapter 3.

3. ASSESSMENT OF CORN STOVER PRETREATED WITH SHOCK AND ALKALI USING METHANE-ARRESTED ANAEROBIC DIGESTION (MAAD)*

3.1. Introduction

Annually, 51 billion tons of greenhouse gases are added to the atmosphere.[62] Continued release of carbon dioxide from combusting fossil fuels will accentuate the impacts of climate change. To address climate change – and improve energy security – researchers have spent decades developing biofuels.[63] Because it is abundant and inexpensive, lignocellulose is a viable feedstock for biofuels.[5] According to the U.S. Department of Energy, the estimated annual amount of lignocellulose from U.S. forest and agricultural resources is 1.3 billion tons.[64] Corn stover, which is underutilized, is an abundant lignocellulosic feedstock that could supply 24 million tons/yr to the biofuel industry.[65]

Lignocellulose is composed of cellulose, hemicellulose, lignin, and other organic materials. Cellulose and hemicellulose can be biochemically converted to liquid fuels; however, lignin prevents access to these polysaccharides. To overcome this barrier, multiple pretreatments have been investigated such as alkali, acid, ammonia, shock, and many others.[11,49,66–68]

---

*Reprinted with permission from "Assessment of corn stover pretreated with shock and alkali using methane-arrested anaerobic digestion" by Opeyemi Olokede, Shen-chun Hsu, Huang Ju, Elise Helms, Aidan Broyles, Mark Holtzapple, 2022. *Biotechnology Progress*, e3257, Copyright 2022 by American Institute of Chemical Engineers.

Currently, a popular method for converting pretreated lignocellulose to biofuels is the sugar platform, which enzymatically hydrolyzes polysaccharides into monosaccharides that are fermented to ethanol, or other products. Because it can rapidly produce near-theoretical product yields, the sugar platform is attractive.[69] Unfortunately, it underutilizes numerous biomass components (e.g., pectin and protein), and requires expensive sterile operating conditions. The carboxylate platform was developed as an alternative to the sugar platform. This platform uses indigenous enzymes present in a microbial community to convert biomass to carboxylic acids, which subsequently are chemically converted to fuels and industrial chemicals.[19] In traditional anaerobic digestion, carboxylic acids would be lost to methane and carbon dioxide. In the carboxylate platform, to prevent this loss, an inhibitor is added, hence the term *methane-arrested anaerobic digestion* (MAAD).

MAAD is an example of consolidated bioprocessing where enzyme production, lignocellulose hydrolysis, and anaerobic digestion are integrated into a single process step, thereby reducing process costs and increasing hydrolysis rates.[12, 13] In MAAD, nearly all metabolic products are neutral salts of carboxylic acids (C2 to C8).[14] Because no sterility is required, a mixed culture of microorganisms performs the fermentation. Instead of adding exogenous enzymes, the MAAD microbial consortium produces a wide spectrum of indigenous enzymes well matched to the feedstock. During MAAD, biomass undergoes the first three steps of conventional anaerobic digestion: hydrolysis, acidogenesis, and acetogenesis (Figure 1-4).[23] However, in MAAD, the fourth step – methanogenesis – is inhibited; thus, products that would have been fermented to low-

value methane and carbon dioxide accumulate as high-value carboxylic acids. Because the digester pH is neutral, carboxylic acids are present as their corresponding carboxylate salts.

Mixed cultures improve the robustness, vitality, and variety of feedstocks that can be used in consolidated bioprocessing. Except for lignin, the MAAD microbial consortium can utilize nearly all biomass components (Figure 1-1),[16] which contributes to the high yields obtained by the carboxylate platform. After anaerobic digestion is complete, well-developed gasification technologies can convert undigested lignin-rich residues into hydrogen and process heat.[8] The hydrogen can be used to upgrade the carboxylate intermediates to hydrocarbon fuels, or it can be fed to the fermentor as a reducing agent.[70]

In a previous study, shock and alkaline pretreatment conditions were assessed using extracellular enzymes.[71] Enzymatic hydrolysis is rapid and precise, and therefore useful for screening multiple pretreatment conditions. However, extracellular enzymes are employed in the sugar platform, which has numerous industrial challenges elucidated earlier. The carboxylate platform has the potential to overcome these challenges, so the ultimate selection of a pretreatment process must be verified with MAAD. Although pretreatment assessment with MAAD is slow, it is more accurate when determining the best pretreatment for the carboxylate platform.

As batch MAAD progresses, the reaction slows because biomass becomes less reactive, and products inhibit the microorganisms. Countercurrent MAAD (Figure 1-5) was developed to overcome these challenges resulting in higher conversions and higher

product concentrations.[24] Fresh substrate enters Fermentor F1, where the high biomass reactivity allows for high product concentrations. Fresh water enters Fermentor F4, where the low product concentration compensates for the low biomass reactivity and thereby allows for high conversions.[25] The challenge with countercurrent MAAD is the labor and long operation duration – typical 3 to 5 months – required to achieve a single steady-state condition. In contrast, batch MAAD takes a relatively shorter time – typically 1 month – to reach completion. To address this situation, the continuum particle distribution model uses batch data to predict continuous countercurrent data within 4–20%.[11,72,73]

Continuum particle distribution modeling was developed by Loescher et al., and has been utilized extensively to predict the performance of countercurrent MAAD.[11,26,27,72,73] A *continuum particle* is defined as one gram of solids in the initial unreacted state.[26,27] In this study, it represents one gram of non-acid volatile solids (NAVS). From one set of batch MAAD data, this method predicts conversions and product concentrations of countercurrent fermentation over a wide range of volatile solids loading rates and liquid residence times. Through mathematical modeling, continuum particle distribution modeling creates a "map" that allows design engineers to select the best operating conditions to achieve a target conversion and product concentration.[28]

Using extracellular enzymes, previous experiments on corn stover surveyed numerous pretreatment approaches where parameters were systematically varied to determine operating conditions that maximize digestibility.[71] From these enzymatic

studies, the following two-step pretreatment process is recommended: (1) **shock treatment** of an aqueous slurry of raw corn stover with headspace containing stoichiometric mixture of hydrogen and oxygen, initial pressure 5.52 bar (abs), followed by detonation; and (2) **NaOH treatment** using 4 g OH^-/100 g dry biomass maintained at 50°C for 1 h. At this moderate sodium hydroxide concentration, shock treatment is presumed to enhance enzymatic digestion by creating microscopic fissures that improve diffusion of alkali into the biomass structure. At high sodium hydroxide concentrations, the alkali is powerful enough that shock treatment is not beneficial.[71]

MAAD requires sources of energy and nutrients. In a four-stage countercurrent fermentation, Rughoonundun et al. studied the co-digestion of sugarcane bagasse (energy source) and sewage sludge (nutrient source).[74] She produced 60.8 g/L total acid, the highest product concentration ever recorded from countercurrent fermentation of lignocellulose in the carboxylate platform. In this chapter, corn stover was co-digested with air-dried sewage sludge as the nutrient source. To create the continuum particle distribution model "maps," the following corn stover conditions were evaluated: (1) raw, (2) shock-only, (3) NaOH-only, and (4) shock + NaOH. This study was performed with Shenchun Hsu and Huang Ju.

3.2. Material and Methods

3.2.1. Substrate

This study used unwashed, Champion-milled, field corn stover harvested in 2012. To maintain constant moisture content, it was stored in a steel barrel. The carbon-to-nitrogen ratio (C-N ratio) was measured by the Soil, Water and Forage Testing

Laboratory at Texas A&M University (College Station, Texas). The test was based on a combustion method using an Elementa Variomax CN.[75] The C-N ratio was reported as 69.2 g carbon/g nitrogen (41.5wt% total carbon and 0.6 wt% total nitrogen).

Sewage sludge was collected from the Carter Creek Wastewater Treatment plant (College Station, Texas). Wastewater was collected in 1-gallon buckets and then transferred into 1-L polypropylene bottles (Nalgene®). The bottles were centrifuged at 4000 rpm (3040 × *g*) for 10 min. The supernatant was discarded. The black sediment was fan dried at room temperature for 48 h. The C-N ratio of sewage sludge was reported as 6.20 g carbon/g nitrogen (33.7 wt% total carbon and 5.43 wt% total nitrogen). Smith and Holtzapple recommended an optimal C-N ratio of 13.0 to 25.0 carbon/g nitrogen.[76] Therefore, the substrate used in this study was a combination of 70 wt% corn stover and 30 wt% sewage sludge, with a combined C-N ratio of 19.1 g carbon/g nitrogen. This study is comprised of four different pretreatments of corn stover according to the following codes: (1) **R** – raw, (2) **S** – shock-only, (3) **N** – NaOH-only, (4) **SN** – shock + NaOH.

3.2.2. Digester Configuration

Substrates were digested in 1-L polypropylene centrifuge bottles, which were sealed using rubber stoppers to prevent leaks and allow convenient venting of gases (Figure 3-1).[26] The rubber stoppers had a glass septum and two 0.25-in stainless steel bars in the middle. The metal bars facilitated mixing as the bottles rotated in the rolling incubator (Wheaton Modular Cell Production Roller Apparatus). The digesters rotated

horizontally at 4 rpm and at 40°C. Every rubber stopper, glass septum, metal bar, and bottle were autoclaved before use.

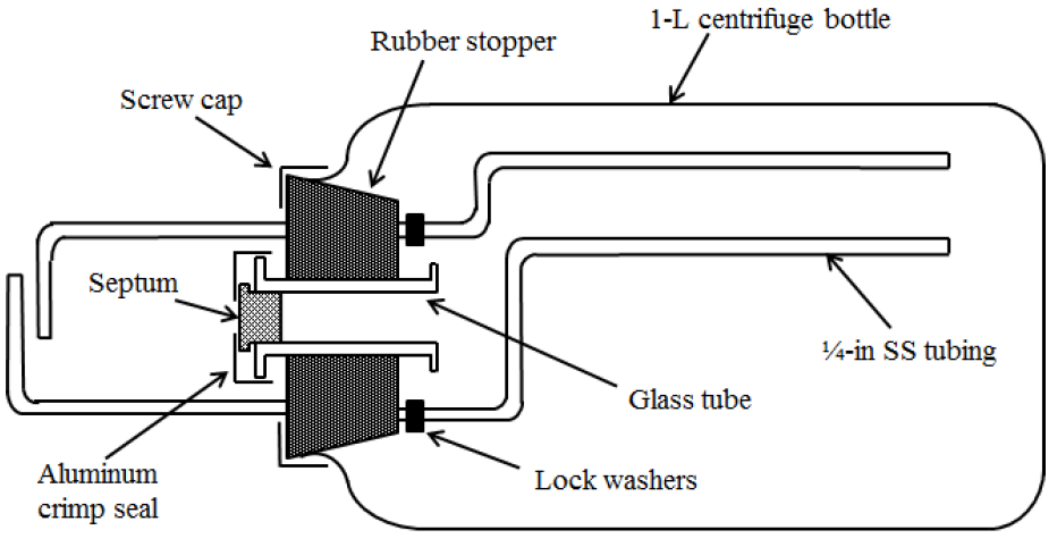

Figure 3-1. Schematic of digester

3.2.3. Anaerobic Digestion Media

De-oxygenated water was used to ensure the digesters remained anaerobic. The de-oxygenated water was prepared by boiling distilled water for 10 min and allowing it to cool to room temperature. Afterwards, for every 1 L of water, 0.275 g of cysteine hydrochloride and 0.275 g of sodium sulfide was added to the boiled water. The solution was stirred using a magnetic stirrer until all chemicals were fully dissolved. Iodoform was used to prevent methanogenesis. Iodoform (CHI_3) was prepared in a solution containing 20 g inhibitor/L 190-proof ethanol. Because iodoform is sensitive to light, temperature, and air, the solution was stored in a tinted bottle wrapped with foil at 4°C. Every 48 h, 60 µL of iodoform solution was added to each digester.

3.2.4. Inoculum

The inoculum was a mixed culture of marine microorganisms collected from plant-rich beaches in Galveston, TX. Half-meter-deep shoreline pits were dug from which sediment was collected and stored in 1-L polypropylene bottles filled with deoxygenated water. At this depth, the sediment color was observed to change from yellow/brown sand to dark gray/black, thus signifying high microbial activity. The sediment was stored at 4^{o}C to keep the microbes inactive until use. Before inoculation, sediment samples were shaken vigorously, and settled for at least 3 h. The supernatant was used to inoculate each batch digester. Inoculum accounted for 12.5% of the digester working volume.

To acclimate the mixed-microbial cultures, inoculum adaptation was performed with the same conditions (such as substrate, nutrients, pH, buffer, and temperature) used in the batch digesters. Substrate – composed of 30 wt% air-dried sewage sludge and 70 wt% corn stover – was placed in 1-L polypropylene bottles at a concentration of 50 g dry substrate/L. Deoxygenated water and supernatant (50 mL) from the inoculum were added to each digester. $NaHCO_3$ was added periodically to maintain neutral pH. To prevent methanogenesis, iodoform solution (60 µL) was added every 2 d to each digester. Prior to taking data, adaptation was performed for 2–3 weeks.

3.2.5. Pretreatment of Corn Stover

The NaOH pretreatment experiments are described in a previous study.[71] Details for shock treatment are described in detail in previous studies.[41–43] In this study, corn stover was pretreated using the recommended two-step process from a previous study: (1) **shock treatment** of an aqueous slurry of raw corn stover with headspace containing stoichiometric mixture of hydrogen and oxygen, initial pressure 5.52 bar (abs), followed by detonation of explosive gas (H_2 + O_2) with a glow plug; and (2) **NaOH treatment** using 4 g OH^-/100 g dry biomass maintained at 50°C for 1 h.[71]

Shock treatment is estimated to cost $5/ton,[41] which is much smaller than conventional chemical pretreatments estimated to cost about $45/ton.[77] To maintain consistency in methodology across multiple pretreatment studies, the loading for NaOH was quantified based on the hydroxide group (g OH^-/100 g dry biomass) according to Equation 3-1.

$$W\left(\frac{\text{g NaOH}}{\text{100 g dry biomass}}\right) = [\text{OH}]^- \left(\frac{\text{g OH}^-}{\text{100 g dry biomass}}\right) \cdot \frac{1}{M_{OH^-}} \left(\frac{\text{mol OH}^-}{\text{g OH}^-}\right) \cdot \frac{1}{v_{NaOH}} \left(\frac{\text{mol NaOH}}{\text{mol OH}^-}\right) \cdot M_{NaOH} \left(\frac{\text{g NaOH}}{\text{mol NaOH}}\right) \quad (3\text{-}1)$$

where $[\text{OH}]^-$ is the hydroxide loading, W is the NaOH loading required for the pretreatment, v_{NaOH} is the number of dissociable hydroxide groups per mole of caustic (e.g., v_{NaOH} = 1 for NaOH), and M_{NaOH} = 40 and M_{OH^-} = 17 are molecular weights of NaOH and hydroxide group, respectively.

In this study, the hydroxide loading is 4 g OH^-/100 g dry biomass, or 9.4 g NaOH/100 g dry biomass (Equation 3-1). At a cost of $300/ton NaOH, if the alkali is not

recycled, it contributes $28/ton dry biomass.[78] To lower this cost, in an industrial setting, NaOH can be recycled and reused after pretreatment.[58] After alkaline pretreatment, using a gas distributor to adjust pH, CO_2 was sparged into the pretreatment slurry, which formed sodium bicarbonate, the desired buffer for anaerobic digestion. The final pH was adjusted to 6.5–7.5, which is favorable for MAAD.

3.2.6. Methane-Arrested Anaerobic Digestion (MAAD)

Calculated amounts of substrate, digestion media, inoculum, buffer, and iodoform were added into each batch digester (Table 3-1 and 3-2). The digesters were then purged with nitrogen, capped, and placed in the incubator. Every 2 d, the digesters were removed from the incubator, and the amount of biogas was measured. The amount of gas produced by the anaerobic digestion is a crude measure of digestion activity and acid production. Then the digesters were centrifuged at 4000 rpm (3040 × *g*) for 10 min and the supernatant was decanted into a beaker.

Liquid samples (1 mL) were collected from the supernatant for carboxylic acid analysis. The pH of each digester was measured using an Oakton™ handheld pH meter and adjusted to neutrality by adding $NaHCO_3$. Finally, the supernatant was returned to each digester, and 60 µL of iodoform solutions (20 g CHI_3/L 200-proof ethanol) was added into each digester followed by nitrogen purging. The digesters were homogenized by vigorous shaking and returned to the incubator. After the anaerobic digestion was terminated, to analyze moisture and ash contents, solid samples were acquired from the group consisting of 100 g dry substrate/L. Digestion performance was calculated for each group.

Table 3-1. Initial loadings of each digester for **R** and **S**

	Label	Substrate Concentration (g/L)	Working volume (mL)	Inoculum (mL)	Dry corn stover (g)	Dry Sewage (g)	Carboxylic acids (g/L)	D.O. water (mL)
R	20-R	20	200	25	2.8	1.2	0	175
	40-R	40	200	25	5.6	2.4	0	175
	70-R	70	200	25	9.8	4.2	0	175
	100-R	100	200	25	14	6	0	175
	100^{+}-R	100	200	25	14	6	20	171.1
S	20-S	20	200	25	2.8	1.2	0	175
	40-S	40	200	25	5.6	2.4	0	175
	70-S	70	200	25	9.8	4.2	0	175
	100-S	100	200	25	14	6	0	175
	100^{+}-S	100	200	25	14	6	20	171.1

(Note: D.O. water stands for de-oxygenated water, and the densities of acetic acid, propionic acid, and butyric are 1.05, 0.99, and 0.96 g/cm^3. For the D.O. water required for 100^{+} group: $171.1 = 200 - 25 - 0.2 \cdot \left(\frac{16}{1.05} + \frac{1}{0.99} + \frac{3}{0.96}\right)$).

Table 3-2. NaOH pretreatment parameters and initial loadings of digesters for **N** and **SN**

	Label	Substrate Conc. (g/L)	Dry corn stover (g)	Total reaction weight (g)	20 g/L NaOH (mL)	Distilled water (mL)	Working Volume (mL)	Inoculum (mL)	Dry Sewage (g)	Total Acid Conc (g/L)	D.O. water (mL)
N	20-N	20	2.8	28	13.2	11.8	200	25	1.2	0	147
	40-N	40	5.6	56	26.4	23.6	200	25	2.4	0	119
	70-N	70	9.8	98	46.1	41.4	200	25	4.2	0	77
	100-N	100	14	140	65.9	59.1	200	25	6	0	35
	100^{+}-N	100	14	140	65.9	59.1	200	25	6	20	31.1
SN	20-SN	20	2.8	28	13.2	11.7	200	25	1.2	0	147
	40-SN	40	5.6	56	26.4	23.4	200	25	2.4	0	119
	70-SN	70	9.8	98	46.1	41	200	25	4.2	0	77
	100-SN	100	14	140	65.9	58.6	200	25	6	0	35
	100^{+}-SN	100	14	140	65.9	58.6	200	25	6	20	31.1

(Note: D.O. water stands for de-oxygenated water, and the density of 20 g/L NaOH solution is approximate at 1 g/cm^3. The total reaction weight is the sum of biomass (wet), NaOH solution, and D.I. water. The densities of acetic acid, propionic acid, and butyric are 1.05, 0.99, and 0.96 g/cm^3. For the D.O. water required for 100^{+} group: $31.1 = 200 - 25 - 140 - 0.2 \cdot \left(\frac{16}{1.05} + \frac{1}{0.99} + \frac{3}{0.96}\right)$).

3.2.7. Analytical Methods

Biogas was measured by inserting a needle into the digester septum. This needle was connected to an inverted glass graduated cylinder containing 300 g/L calcium chloride solution, which prevents carbon dioxide absorption and microbial growth.[79] To determine methane inhibitor efficacy, gas samples were taken randomly from different digesters and analyzed for N_2, CO_2, CH_4, and H_2. The biogas was analyzed by manually injecting a 30-mL gas sample into an Agilent 6890 Series chromatograph with a thermal conductivity detector (TCD) and a 4.6-m-long, 2.1-mm-ID stainless steel packed column (60/80 Carboxen100, Supelco 1-2390). The inlet temperature was 230°C, the oven temperature was 200°C, and the detector temperature was 200°C. The total run time was 20 min, and helium was the carrier gas.

Supernatant samples were analyzed using an Agilent 6890 Series chromatograph with an automatic liquid sampler (Agilent 7683 series), a flame ionization detector (FID), and a DB-FFAP capillary column (30 mm × 0.320 mm).[80] Moisture and ash contents were determined as previously described.[24] Moisture content (MC) is defined as the amount of moisture vaporized from wet samples after baking at 105^{o}C for 24 h. Ash content (AC) is defined as the residue after heating the dried samples in a furnace at 550^{o}C for 24 h. To accurately account for volatile acids, 30 mg $Ca(OH)_2$/(g sample) was added to liquid samples before drying to ensure all volatile acids were converted to salts.

3.2.8. Measuring MAAD Performance

Non-acid volatile solid (NAVS) is used to characterize the mass of substrate added to the digester. NAVS excludes acids initially present in the feedstock, and is

calculated as the difference between the mass of volatile solids (VS) and carboxylic acids present in the feedstock.

$$\text{NAVS} = [(1 - \text{MC}) \times (1 - \text{AC}) \times \text{Total biomass (g)}] - \text{(g total carboxylic acid)} \quad (3\text{-}2)$$

where MC is the fraction of moisture in wet biomass and AC is the fraction of ash in dry biomass.

To express the acid mixture as a single acid concentration, Aceq (acetic acid equivalent) is used. It equates the reducing potential of a carboxylic acid mixture to an energy-equivalent mass of acetic acid.[81] On a mole basis, Aceq is calculated as follows:

$$\alpha\ (\text{mol/L}) = 1.00 \times \text{acetic (mol/L)} + 1.75 \times \text{propionic (mol/L)} + 2.50 \times \text{butyric (mol/L)} + 3.25 \times \text{valeric (mol/L)} + 4.00 \times \text{caproic (mol/L)} + 4.75 \times \text{heptanoic (mol/L)} + 5.50 \times \text{octanoic (mol/L)} \quad (3\text{-}3)$$

Aceq can be converted to a mass basis by multiplying by the molecular weight of acetic acid.

$$\text{Aceq}\left(\frac{\text{g}}{\text{L}}\right) = 60.05\left(\frac{\text{g}}{\text{mol}}\right) \times \alpha\left(\frac{\text{mol}}{\text{L}}\right) \quad (3\text{-}4)$$

MAAD performance is measured by parameters such as conversion, selectivity, and yield. *Conversion* is a measure of the amount of substrate digested during the process. *Yield* is a measure of the amount of carboxylic acid produced from the substrate. *Selectivity* is a measure of the amount of digested substrate that is directly converted to carboxylic acids instead of being used for other cell functions. The data collected at the beginning and end of digestion were used to calculate these parameters. The MAAD parameters are defined as follows:

$$\text{Conversion} = \frac{\text{NAVS}_{\text{digested}}(\text{g})}{\text{NAVS}_{\text{fed}}(\text{g})} \quad (3\text{-}5)$$

$$\text{Yield} = \frac{\text{Total carboxylic acids produced (g)}}{\text{NAVS}_{\text{fed}}(\text{g})} \quad (3\text{-}6)$$

$$\text{Selectivity} = \frac{\text{Total carboxylic acids produced (g)}}{\text{NAVS}_{\text{digested}}(\text{g})} \quad (3\text{-}7)$$

$$\text{NAVS}_{\text{digested}} = \text{NAVS}_{\text{fed}} - \text{NAVS}_{\text{remaining}} \quad (3\text{-}8)$$

$$\text{NAVS}_{\text{remaining}} = \text{VS}_{\text{liquid}} + \text{VS}_{\text{solid}} - \text{Total acid in digester} \quad (3\text{-}9)$$

$$\text{NAVS}_{\text{fed}} = \text{VS}_{\text{corn stover}} + \text{VS}_{\text{sewage sludge}} + \text{VS}_{\text{urea}} - \text{Initial acids present} \quad (3\text{-}10)$$

3.2.9. Continuum Particle Distribution Model

To construct the continuum particle distribution model map, five different substrate loadings in the batch experiments were conducted: 20, 40, 70, 100, and 100+ g dry substrate/L liquid.[11] The 100+ group has the same substrate concentration as 100 g/L, but part of the digestion media is supplemented with 20 g mixed acids/L (16 g acetic acid/L, 1 g propionic acid/L, 3 g butyric acid/L). The added acids accentuate inhibition, which provides additional information to the model. To increase the pH to neutrality prior to inoculation, additional buffer was added to the 100+ g/L digester. To increase accuracy, each batch experiment was performed in triplicate.

The acetate equivalents from the five groups were fit to the following empirical equation.

$$\text{Aceq}(t) = a + \frac{bt}{1+ct} \quad (3\text{-}11)$$

where *t* is the time in days, and *a*, *b*, and *c* are empirical constants determined by the least-square method. The reaction rate was determined by differentiating Aceq(*t*) (Equation 3-11).

$$r = \frac{\mathrm{d}(\mathrm{Aceq}(t))}{\mathrm{d}t} = \frac{b}{(1+ct)^2} \quad (3\text{-}12)$$

The specific reaction rate ($\hat{r}$), which is the reaction rate per particle, was calculated by dividing the reaction rate (r) by initial substrate concentration (S_0) in each fermentor. The initial substrate concentration was calculated by dividing the mass of initial substrate (g volatile solid) by the working volume of the fermentor.

$$\hat{r} = \frac{r}{S_o} \quad (3\text{-}13)$$

For each group, the conversion x(t) was calculated through the following equation.

$$x(t) = \frac{\mathrm{Aceq}(t) - \mathrm{Aceq}(0)}{S_o \cdot \sigma} \quad (3\text{-}14)$$

where σ is selectivity (g Aceq produced/g VS digested). Selectivity σ is assumed constant throughout all substrate concentrations and is derived from selectivity s (g total acids produced/g VS digested) and φ, the ratio of total grams of carboxylic acid produced to total grams of Aceq.

$$\sigma = \frac{s}{\varphi} \quad (3\text{-}15)$$

The measured values of $x(t)$, Aceq(t), and φ were fit to Equation 3-16 where e, f, g, and h are empirical constants determined by the least square method.

$$\hat{r}_{pred} = \frac{e(1-x)^f}{1+g(\varphi \cdot Aceq)^h} \quad (3\text{-}16)$$

For each set of batch experiments, Equation 3-16 and the corresponding set of fitted empirical constants (e, f, g, and h) were used in a MATLAB program to simulate four-stage countercurrent fermentation with different volatile solids loading rates (VSLR) and liquid retention times (LRT). The MATLAB program produced an array of predicted

values of carboxylic acid concentration and conversion for the countercurrent fermentation at various VSLR and LRT values. These values were then used to plot the "map" displaying acid concentration exiting F1 (*y*-axis) and conversion exiting F4 (*x*-axis) for various VSLR and LRT values.

3.2.10. Statistical Analyses

The nonlinear regression for the model was performed using Microsoft Excel Solver. The one-way analysis of variance (ANOVA) followed by t-test was performed at the 0.05 level using Microsoft Excel Data Analysis. Tukey-Kramer HSD tests was performed to compare multiple means at a significance level of 0.05 using JMP® software. An asterisk was placed between data points that differed significantly. All error bars were reported using the estimated standard deviation values.

3.3. Results and Discussion

3.3.1. Total Acid Production

Because methane production was inhibited, for both untreated and pretreated corn stover, production of total acids was used to estimate the extent of digestion. **S** had no impact on total acid production (Figure 3-2). At 40 and 100 g/L, **N** produced significantly higher acids than **S** and **R** (Figures 3-2b, 3-2d). Sodium hydroxide is an effective alkali for pretreating lignocellulosic biomass rendering it more digestible. At substrate concentrations 20, 70, and 100 g/L, **SN** produces significantly higher total acids than the other batches (Figures 3-2a, 3-2c, 3-2d). In fact, at 100 g/L, **SN** produced ~92% more acids than **N**, and ~109% more acids than **R** (Figure 3-2c). At substrate concentration 100+ g/L, similar amounts of acids were produced from the different

feedstocks (Figure 3-2e). Product inhibition completely masked the effects of pretreatment.

Figure 3-3 displays the total acid produced during the batch MAAD as a function of time. After 10 d of anaerobic digestion, **SN** outperforms all the other batches at all substrate concentrations, except 100+ g/L. At all substrate concentrations, **S** performed slightly worse than raw corn stover. During the first 30 d, the impact of product inhibition was more pronounced for **R**. **S** performed worse than **R** (Figure 3-3). Shock treatment is known to increase biomass crystallinity,[38,43] but it is unknown whether this occurs from shock itself, or the soaking-and-drying process associated with the laboratory-scale shock treatment.[71] Further investigation is required.

3.3.2. Carboxylic Acid Composition

Figure 3-4 displays the carboxylic acid composition. At 20 and 100+ g/L, acetic acid was the predominant product. Low substrate concentration (20 g/L) and high product concentration (100+ g/L) had less chain elongation. At 40, 70, and 100 g/L substrate concentrations, acid compositions were similar. In all digesters, acetic, propionic, and *n*-butyric acids accounted for over 50% of acids produced. During primary anaerobic digestion – which occurs after hydrolysis – short-chain carboxylic acids are the main products of undefined mixed cultures.[10] For example, using 40% corn stover and 60% swine manure, Chan et al. reported 55–70% wt% acetic acid.[82] At 100 g/L, **S** produced the highest amounts of valeric, caproic, and enanthic acids amounting to ~45% of total acids.

Although shock pretreatment had little impact on total acid production, it influenced chain elongation of acetic and propionic acids to higher acids, which occurs through interspecies hydrogen transfer.[83] **R** and **S** produced more medium-chain acids than **N** and **SN**. Although NaOH treatment improves total acids produced, it reduced chain elongation. Across all feedstocks, very little caprylic acid was produced.

3.3.3. Acetate Equivalent

Figures 3-5–3-9 illustrate the Aceq concentrations for each substrate concentration in each batch digester. The concentration profile shows the accumulative amount of Aceq during digestion. Generally, higher substrate concentrations produce greater Aceq. Compared to **R**, **S** had slightly less Aceq, as was discussed previously. In contrast, compared to **R**, **N** had significantly higher acid production. Moreover, at 70 and 100 g/L, **SN** produced even more acid than **N**. In lignocellulose, sodium hydroxide treatment reduces crystallinity and degree of polymerization.[84]

Although shock treatment increases biomass crystallinity, presumably it creates micro-fractures that increase the internal surface area accessible to microorganisms. These effects compensated for the increased crystallinity, making it easier for NaOH to penetrate the biomass. Consequently, shock treatment combined with NaOH pretreatment results in greater acid production than using NaOH alone. At 100+ g/L, product inhibition was significant. Compared to the other groups, only **SN** had slightly higher Aceq concentration, and **R** and **N** shared similar Aceq concentrations. Within the first 25 d, **S** had Aceq concentrations that were significantly lower than all other groups.

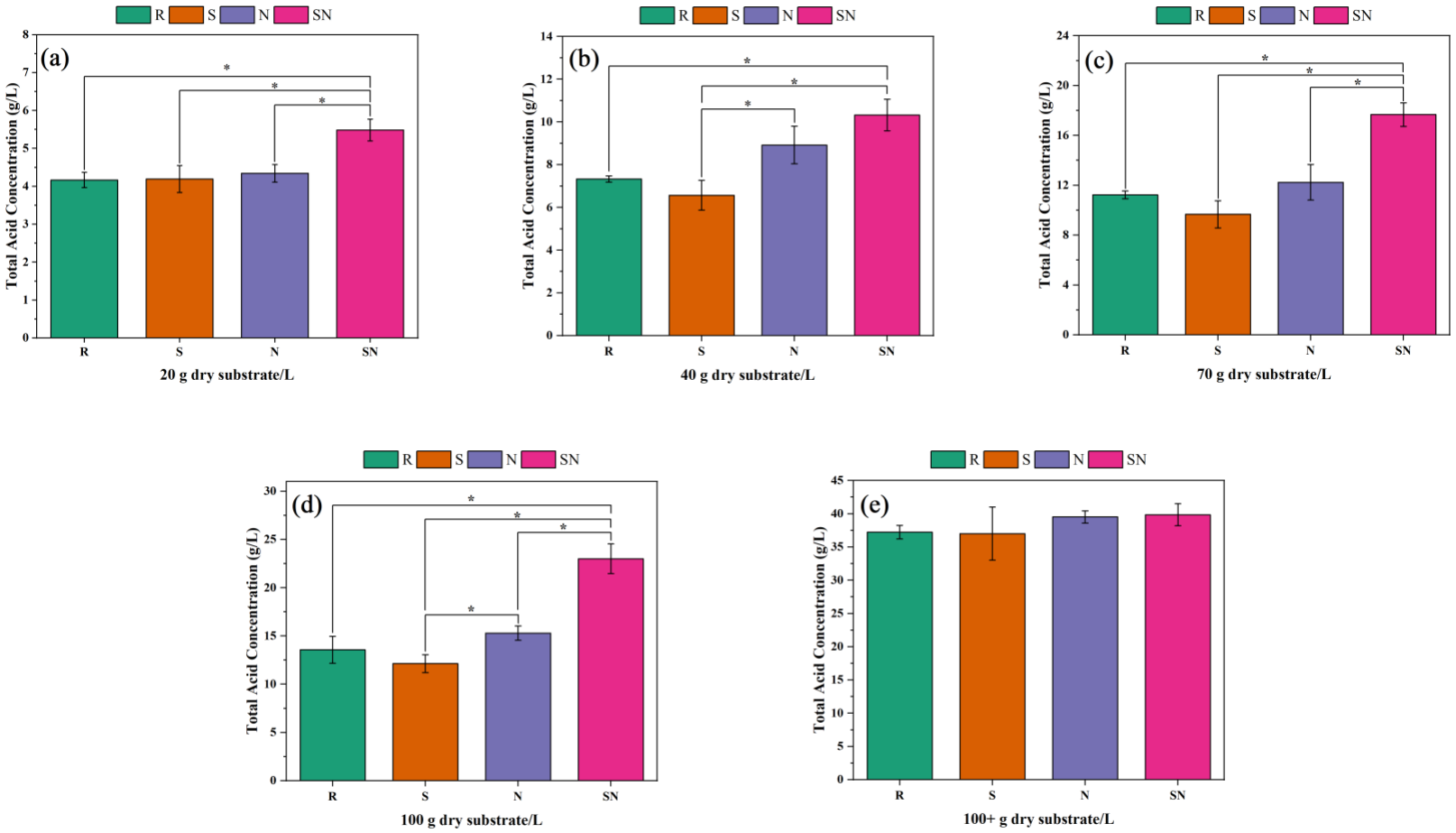

Figure 3-2. Total carboxylic acids produced.

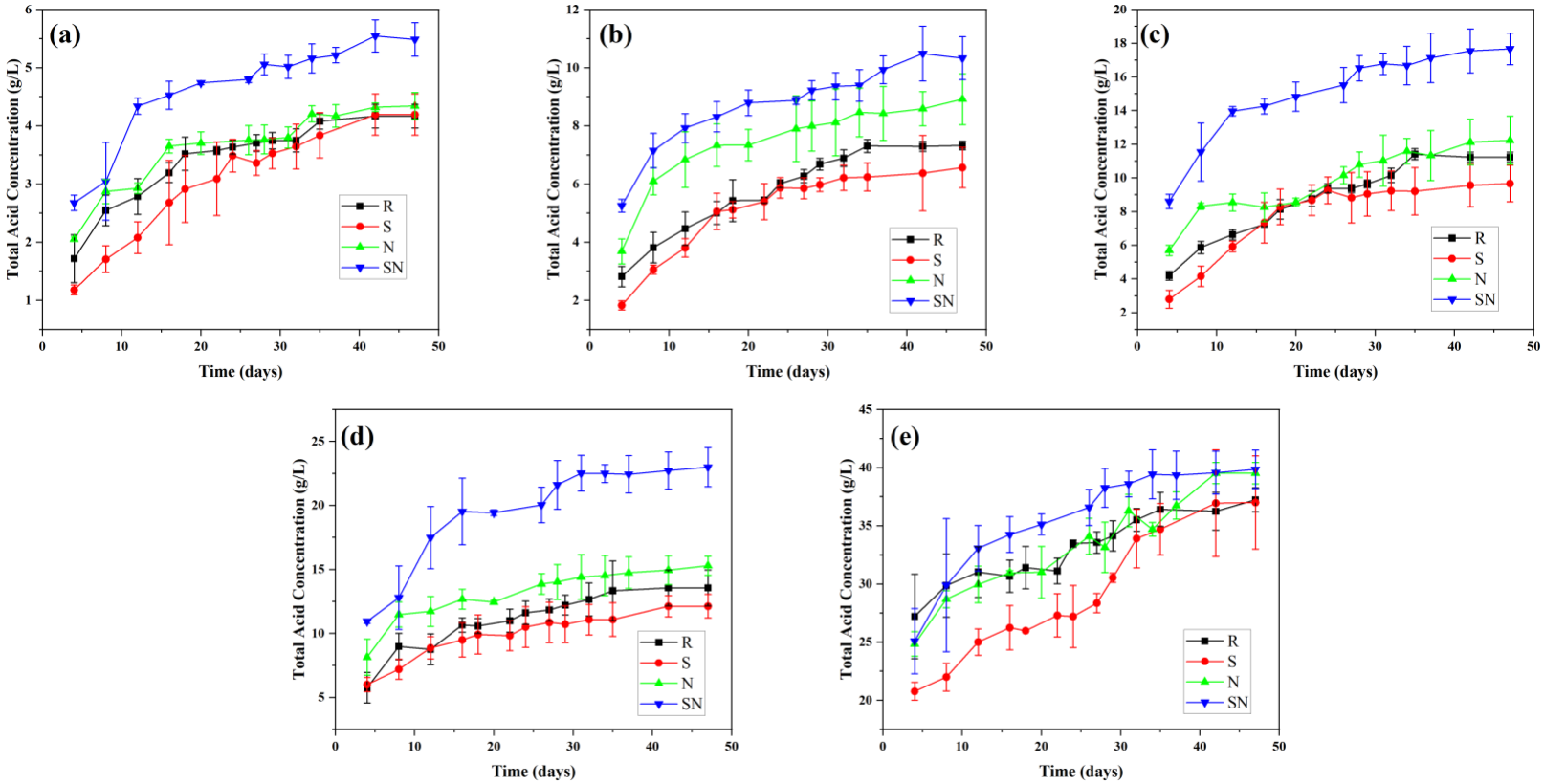

Figure 3-3. Acid concentration profile. (a) 20 g/L, (b) 40 g/L, (c) 70 g/L, (d) 100 g/L, and (e) 100+ g/L.

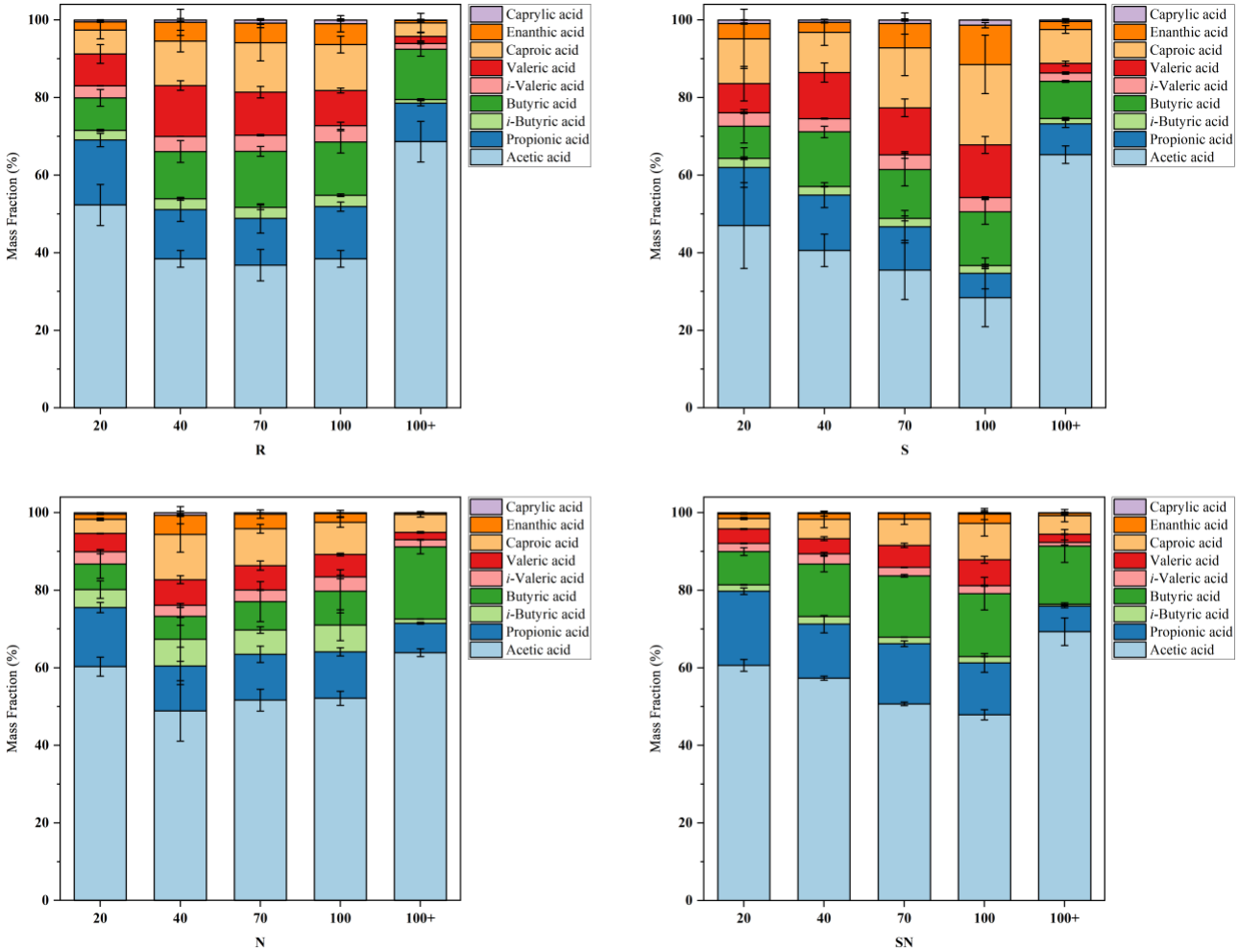

Figure 3-4. Acid composition for all batch digesters.

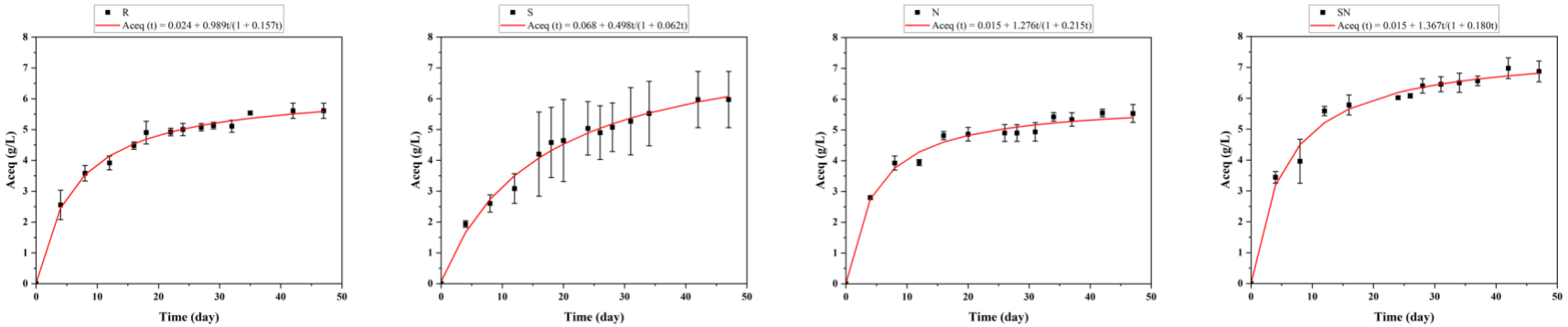

Figure 3-5. Aceq concentration profiles for each pretreatment condition based on 20 g/L initial substrate concentration.

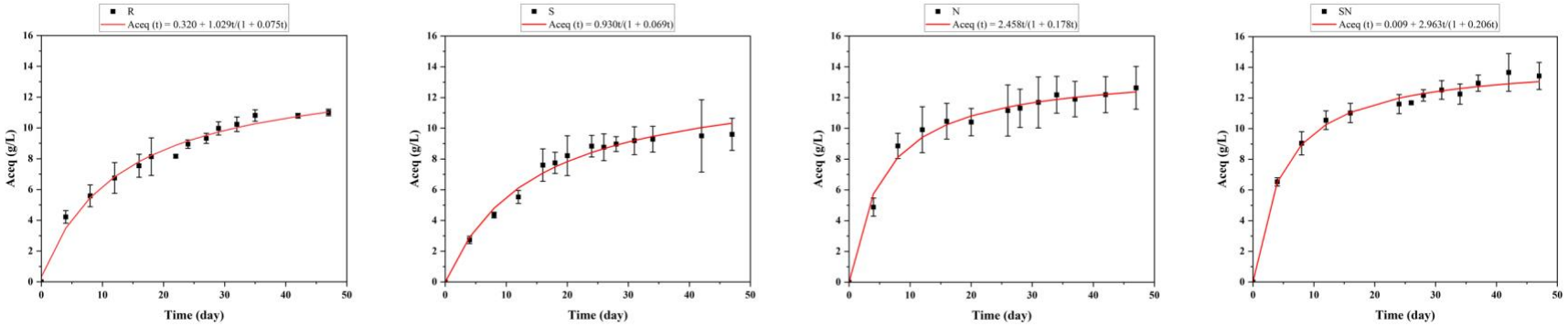

Figure 3-6. Aceq concentration profiles for each pretreatment condition based on 40 g/L initial substrate concentration.

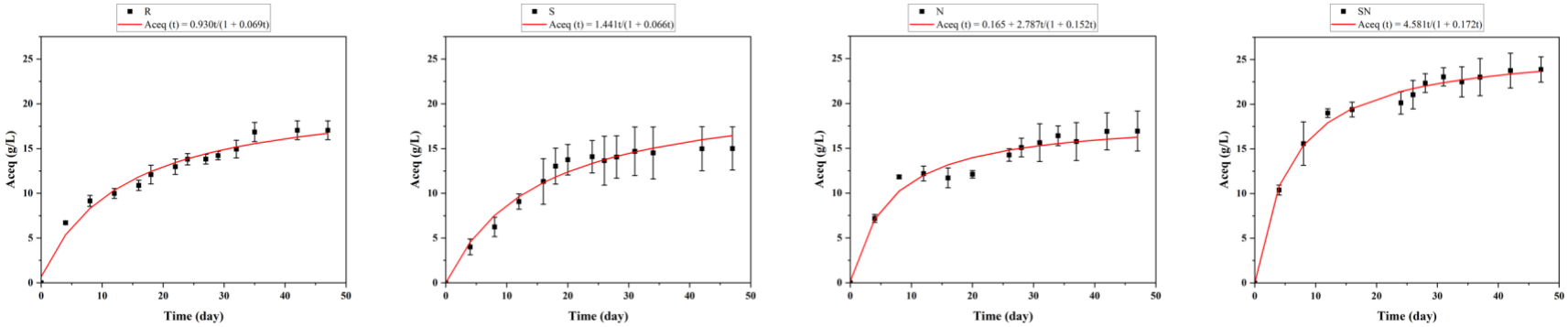

Figure 3-7. Aceq concentration profiles for each pretreatment condition based on 70 g/L initial substrate concentration.

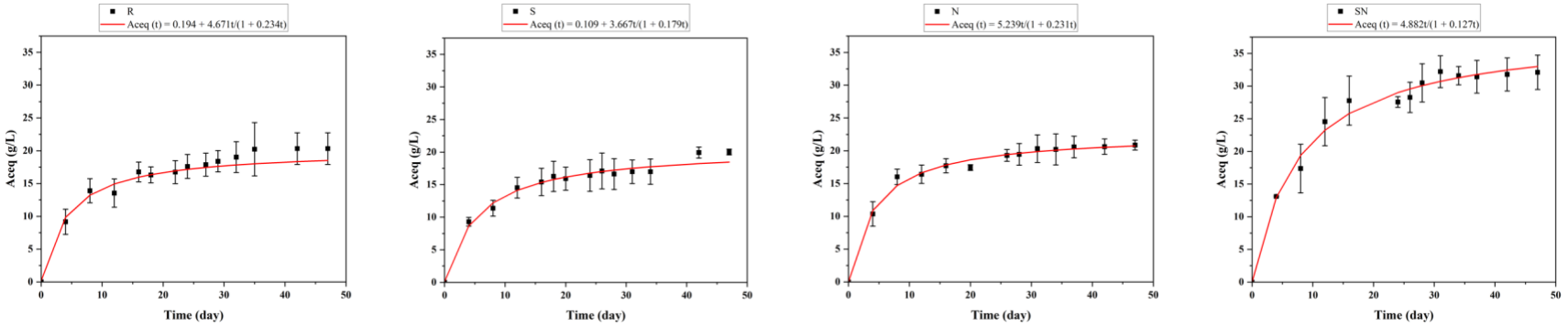

Figure 3-8. Aceq concentration profiles for each pretreatment condition based on 100 g/L initial substrate concentration.

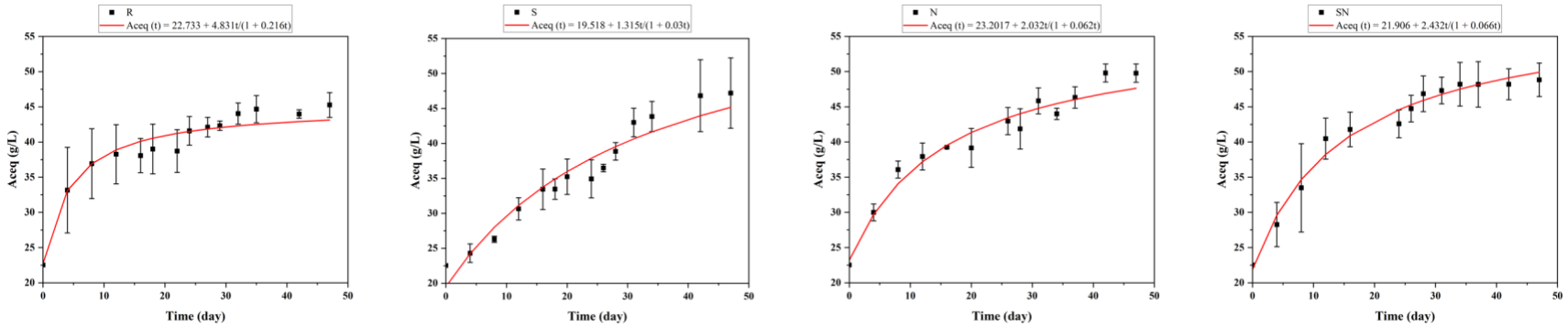

Figure 3-9. Aceq concentration profiles for each pretreatment condition based on 100+ g/L initial substrate concentration.

3.3.4. Gas Production

Although carboxylic acids are the main products observed during MAAD, carbon dioxide and hydrogen are by-products. During the first few days, up to 30% carbon dioxide and <2% hydrogen was detected. Previous studies show that H_2 production in anaerobic environments reduces when pH becomes acidic.[85] Because the digesters were buffered periodically and not continually, it is possible that the pH dropped to acidic levels thereby reducing hydrogen production. Another study has shown that H_2 production is influenced by substrate composition with lipid-rich substrates yielding high H_2 concentrations.[86] Corn stover has negligible lipid content. This is possibly the reason for the low H_2 concentrations observed in this study.

After 30 d of digestion, <0.1% hydrogen was detected. This is possibly because hydrogen, a reducing agent, is consumed in interspecies hydrogen transfer, which allows its chemical energy to be incorporated into other products like carboxylic acids.[70] Because iodoform was added to inhibit methanogenesis, no methane was detected during gas analysis. Significant nitrogen was detected because it is used to purge the digesters when opened during periodic sampling. Trace amounts of oxygen were detected, likely from imperfections during sampling.

Gas volume is a reliable measure of the microbial activity within a digester. Figure 3-10 displays the total gas volume measured from all batch MAADs during the entire batch digestion. For all feedstocks at substrate concentrations 20, 40, 70, and 100+ g/L, there is no significant difference between the total gas volumes produced during the entire batch digestion (Figure 3-10). Across the lower (<100 g/L) substrate

concentrations, microbial activity is similar. At 100 g/L, **SN** produced significantly more biogas than the other batches (Figure 3-10c). At 100+ g/L, there is no significant difference in the amount of gas produced, presumably because of product inhibition.

3.3.5. MAAD Performance Parameters

In this study, substrate concentration is based on non-acid volatile solids (NAVS) and performance is assessed using three parameters: conversion, yields and selectivity. To compare the four feedstocks, conversion, yield, and selectivity were only calculated at substrate concentration 100 g/L (Table 3-3). *Conversion* is the ratio of NAVS digested to NAVS fed, and quantifies the NAVS consumed during digestion. **N** and **SN** had significantly higher conversions than **S** and **R**. **SN** had the greatest conversion (0.45 ± 0.02 g NAVS digested/g NAVS fed), which represents a 104% improvement compared to **R** (Figure 3-11a). **S** had the lowest conversion (0.22 ± 0.05 g NAVS digested/g NAVS fed).

Yield is the ratio of total acids produced to NAVS fed, and quantifies how much of the NAVS fed is converted to useful product. **SN** had the highest yield (0.17 g acids produced/g NAVS fed), which was an increase of 45, 22, and 40% compared to **N**, **S**, and **R**, respectively (Figure 3-11b). This confirms the benefits of combining shock + alkali pretreatments. *Selectivity* is the ratio of total acids produced relative to NAVS digested, and quantifies how much of the digested NAVS is converted to desired products. Other products include cells and unmeasured liquid products (e.g., ethanol, lactic acid). **S** had the highest selectivity (0.76 ± 0.05 g total carboxylic acid produced/g

NAVS digested). Selectivity is lower when conversion is high (**SN** and **N**), but higher when conversion is low (**R** and **S**) (Figure 3-11c).

3.3.6. Continuum Particle Distribution Model Predictions

From the batch MAADs, the Aceq concentrations were used to calculate the values of *e*, *f*, *g* and *h* by performing least-square regression to fit the model governing equations (Eq. 3-16). The governing specific rate equation ($\hat{r}$) for raw corn stover (**R**), shock-only (**S**), NaOH-only (**N**), and shock + NaOH (**SN**) follow:

$$\hat{r}_R = \frac{0.045(1-x)^{7.768}}{1 + 0.01(0.712 \cdot \text{Aceq})^{0.650}} \tag{3-17}$$

$$\hat{r}_S = \frac{0.031(1-x)^{4.693}}{1 + 0.162(0.686 \cdot \text{Aceq})^{0.771}} \tag{3-18}$$

$$\hat{r}_N = \frac{0.065(1-x)^{2.885}}{1 + 0.061(0.749 \cdot \text{Aceq})^{0.934}} \tag{3-19}$$

$$\hat{r}_{SN} = \frac{0.0700(1-x)^{2.106}}{1 + 0.013(0.768 \cdot \text{Aceq})^{1.576}} \tag{3-20}$$

In countercurrent digestions (Figure 1-5), a substrate concentration of 100 g NAVS/L_{liq} is representative of semi-continuous laboratory operations where enough liquid must accumulate to be transferred every 2 d. At a substrate concentration of 100 g NAVS/L_{liq}, the above specific rate equations were used to predict conversions and total acid concentrations for four-stage countercurrent MAAD with LRT ranging from 5 to 35 d, and VSLR ranging from 2 to 12 g/(L_{liq}·d).

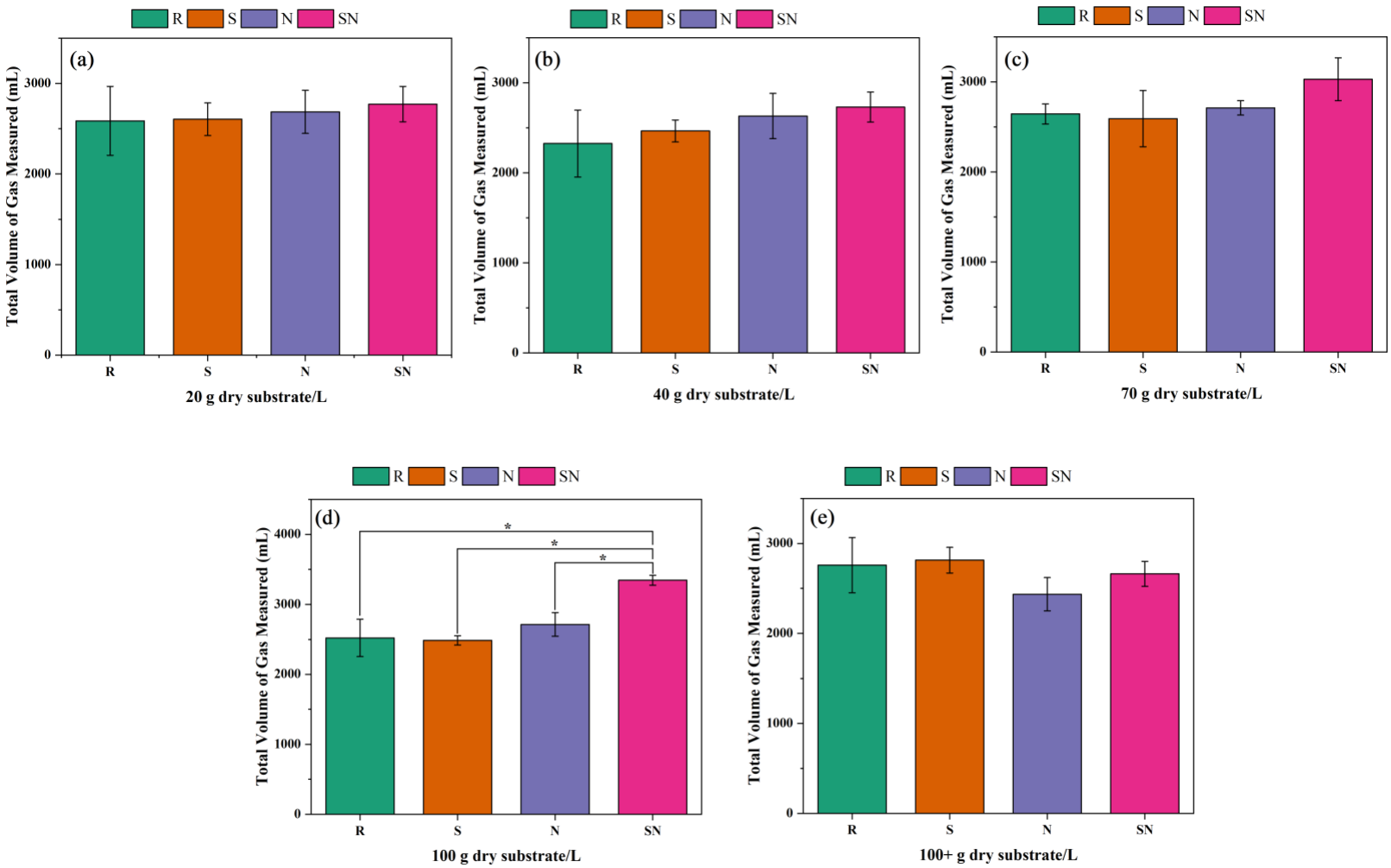

Figure 3-10. Total gas volume measured during the entire batch digestion.

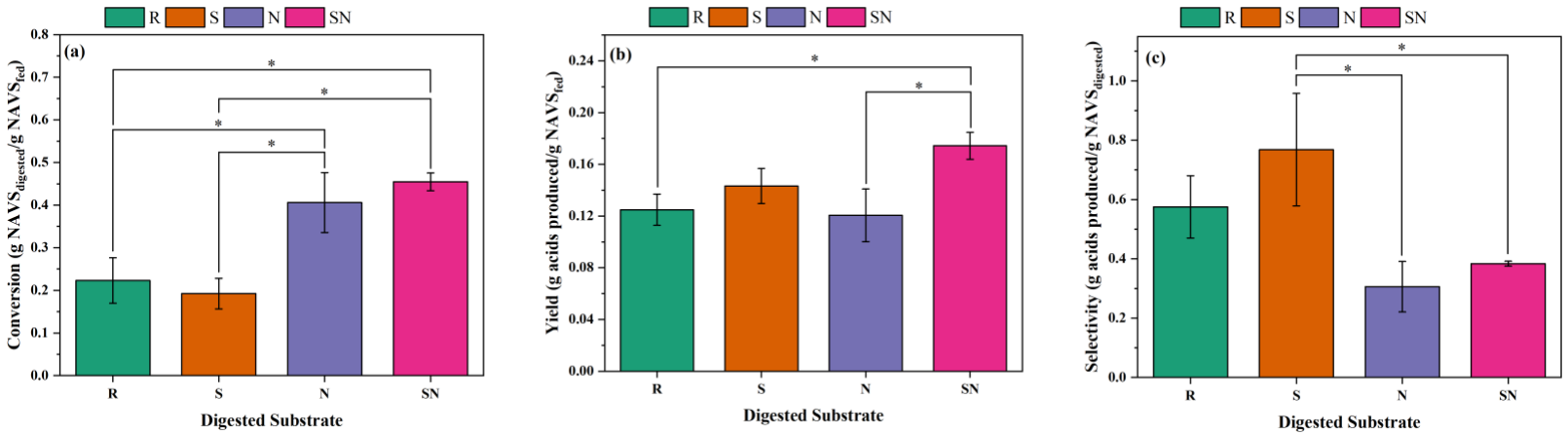

Figure 3-11. MAAD performance parameters. (a) conversion, (b) yield, and (c) selectivity.

Table 3-3. MAAD performance parameters for batch digestion at 100 g/L initial substrate concentration. Error bar represents the standard deviation of the readings from duplicate digesters.

Parameter	**R**	**S**	**N**	**SN**
Conversion (g NAVS digested/g NAVS fed)	0.22 ± 0.05	0.19 ± 0.04	0.41 ± 0.07	0.45 ± 0.02
Yield (g total carboxylic acid produced/g NAVS fed)	0.12 ± 0.01	0.14 ± 0.01	0.12 ± 0.02	0.17 ± 0.01
Selectivity (g total carboxylic acid produced/g NAVS digested)	0.58 ± 0.11	0.76 ± 0.19	0.31 ± 0.09	0.38 ± 0.01

Figure 3-12 illustrates the model predictions for the MAAD of 70 wt% of pretreated (**S**, **N**, and **SN**) or **R** with 30 wt% air-dried sewage sludge. According to the model predictions, **R** had its greatest predicted total acid concentration (21.4 g/L) at LRT of 35 d and VSLR of 8 g/(L_{liq}·d). At the same condition, **SN** had even better total acid concentration of 25.1 g/L. **S** had poorer carboxylic acid concentration of 13.5 g/L, presumably because of the soaking-and-drying procedure in laboratory-scale shock treatment.[61,71]

Compared to raw corn stover, the model predictions gradually shift towards the upper right from raw corn stover to **N**, and then to **SN**. In contrast, **S** shifts slightly lower left, which indicates reduced MAAD performance from shock-only. In contrast, **N** and **SN** improve digestion. **SN** reached its peak acid concentration (27.9 g/L) and had a conversion of 0.55 g $NAVS_{digested}$/g $NAVS_{fed}$ at LRT of 35 d and VSLR of 4 g/(L_{liq}·d).

In industrial countercurrent digestions (Figure 1-5), a substrate concentration of 300 g NAVS/L_{liq} is used as the maximum achievable concentration when liquid is transferred countercurrently in a continuous manner. Figure 3-13 displays the model predictions at 300 g NAVS/L_{liq}. At this high substrate concentration, the solid residence time is exceedingly long resulting in higher conversions and acid concentrations. At all combinations of VSLR and LRT, **SN** and **N** had similar conversions with the highest conversion 0.89 g $NAVS_{digested}$/g $NAVS_{fed}$ observed at LRT of 35 d and VSLR of 4 g/(L_{liq}·d). However, **SN** yielded slightly higher total acids than **N**. At these operating conditions, compared to **R**, **SN** improved acid concentration by 97% and biomass conversion by 128%. At this high substrate concentration and long solid residence time,

shock treatment was no longer beneficial. Presumably, this occurs because the long solid residence time allows microorganisms to completely digest the biomass, thereby rendering shock micro-fractures unnecessary. **R** and **S** performed significantly worse than **N** and **SN**. For industrial applications that seek high product concentrations and high conversions, large LRT and small VSLR are required. It should be noted that the continuum particle distribution model predictions should be experimentally verified before being implemented at industrial scale.

3.4. Conclusion

In MAAD, shock pretreatment benefitted NaOH-treated corn stover under moderate hydroxide loading (4 g OH^-/100 g dry biomass) treated at 50°C for 1 h, which corroborates results from enzymatic hydrolysis.[71] However, shock-only treatment did not benefit MAAD performance, presumably because of increased crystallinity.[38,43] The cause of increased crystallinity is unknown. Further investigations are required to determine if it results from shock itself, or the soaking-and-drying process associated with the laboratory-scale shock treatment.[71] Using 100-g/L batch MAAD, total acid concentration profiles indicated that shock + NaOH had the greatest acid concentration compared to other groups. Relative to raw corn stover, shock + NaOH improved conversion by 104% and yield by 40%. Shock-only produced the highest percentages of medium-chain fatty acids.

The continuum particle distribution model simulated four-stage countercurrent MAAD. At a substrate concentration of 100 g/L_{liq}, the model predictions showed that shock enhanced NaOH treatment. At a substrate concentration of 300 g/L_{liq}, the model

predictions showed that shock did not enhance NaOH treatment. At 300 g/L_{liq}, the solids residence time is very long, so the presumed kinetic advantages from opening micro-fissures using shock treatment is no longer advantageous. Shock has value at shorter solid residence times and offers a way to reduce pretreatment costs without sacrificing pretreatment efficacy.

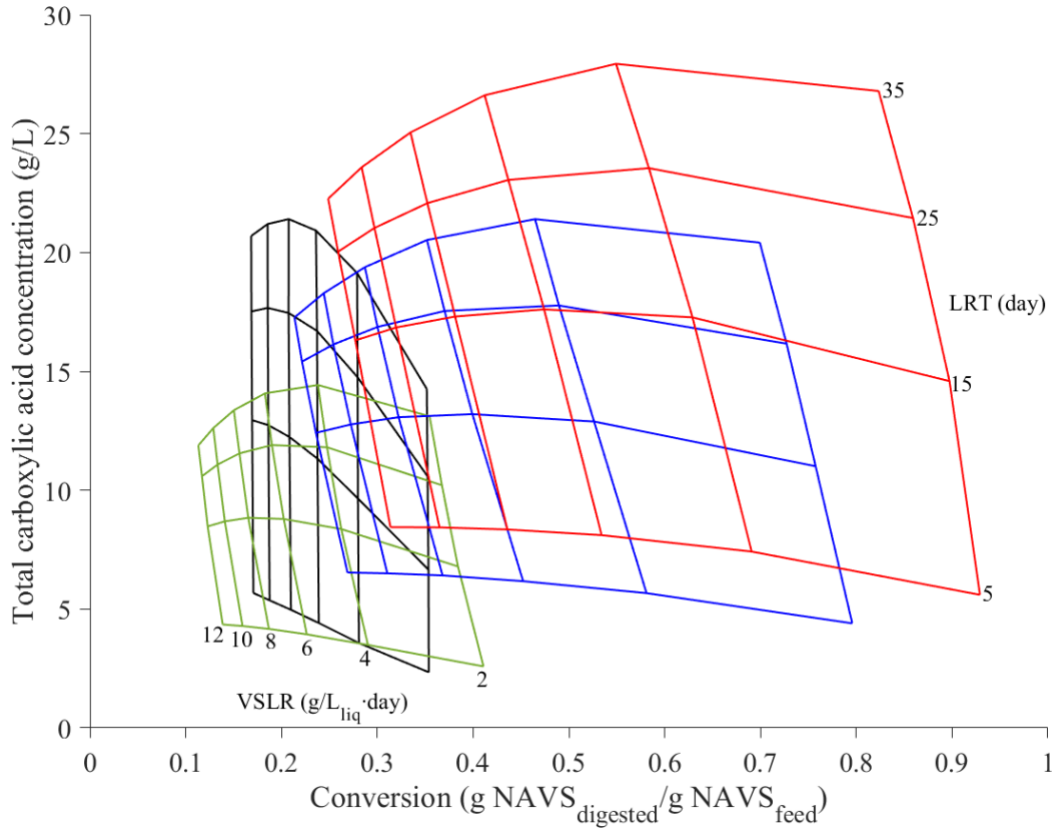

Figure 3-12. The continuum particle distribution model maps for four-stage countercurrent fermentation using 70 wt% raw or pretreated corn stover and 30 wt% air-dried sewage sludge. Substrate concentration is 100 g NAVS/Lliq. **R** (black), **S** (green), **N** (blue), **SN** (red)

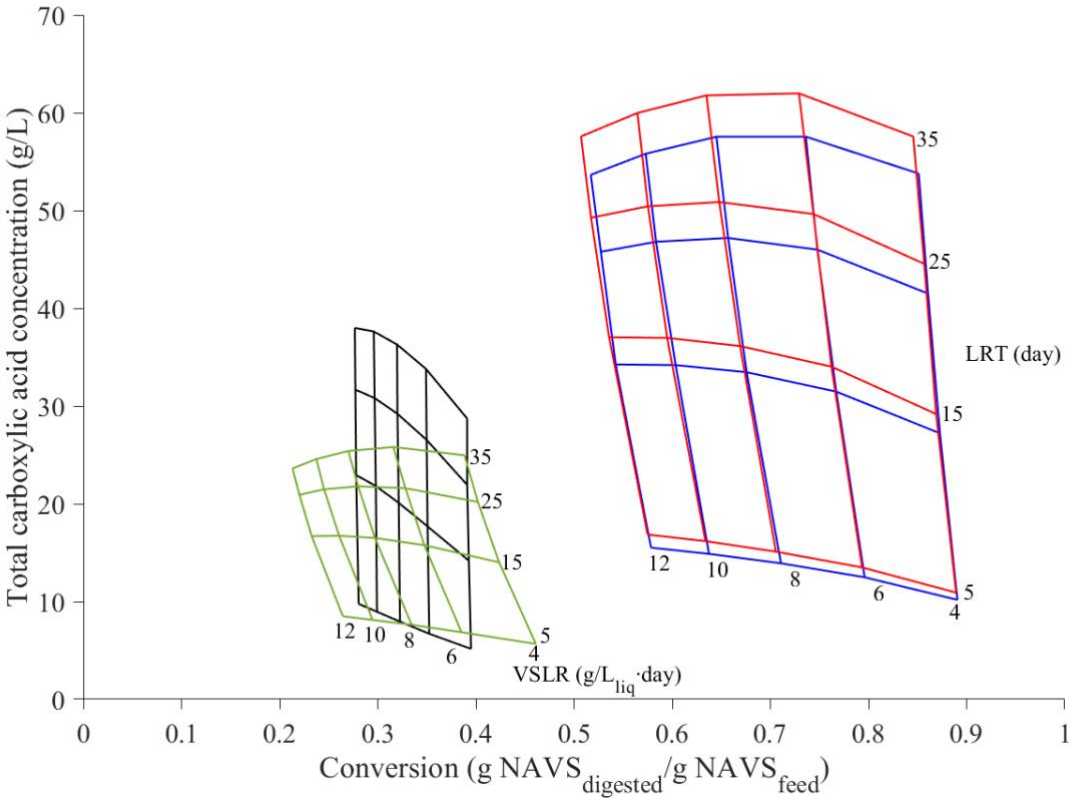

Figure 3-13. The continuum particle distribution model maps for four-stage countercurrent fermentation using 70 wt% raw or pretreated corn stover and 30 wt% air-dried sewage sludge. Substrate concentration is 300 g NAVS/Lliq. **R** (black), **S** (green), **N** (blue), **SN** (red)

4. ENHANCEMENT OF CARBOXYLIC ACID PRODUCTION FROM SEMI-CONTINUOUS MIXED-ACID FERMENTATION OF CELLULOSIC SUBSTRATES BY *IN-SITU* PRODUCT REMOVAL WITH CARBON-DIOXIDE SUSTAINED ANION-EXCHANGE RESIN ADSORPTION

4.1. Introduction

The World Meteorological Organization (WMO) shows that concentrations of the major greenhouse gases (CO_2, CH_4, and N_2O) continues to increase.[87] Replacing fossil fuels with renewable resources for the sustainable production of energy and commodities is essential to combat climate change and build circular economy. Analogues to traditional oil refinery, biorefinery is an example of cleaner production that can convert renewable biomass to fuels and chemicals in a sustainable way (Takkellapati et al., 2018). The carboxylate platform is an emerging biorefinery concept that features carboxylic acids and utilizes both biological and chemical processes for conversion of organic wastes to valuable bioproducts (Agler et al., 2011; Fernando-Foncillas and Varrone, 2021; Fu and Holtzapple, 2010).

As the largest biomass resource, lignocellulose (cellulose, hemicellulose, and lignin) from waste stream is an ideal feedstock for carboxylate platform.[88] The MixAlco™ process is a version of the carboxylate platform that can sustainably convert lignocellulosic biomass into value-added bioproducts. The process has four parts: (1) lignocellulose pretreatment to enhance digestibility, (2) biological production of mixed carboxylic acids via *methane-arrested anaerobic digestion* (MAAD) with undefined

microbial consortia, (3) recovery of carboxylic acids, and (4) downstream chemical conversion of carboxylic acids to chemicals or fuels[8,16]. In general, MAAD is considered as the most critical part for the process, because it has the following economic advantages: (1) the genetic diversity of the mixed culture ferments nearly all biomass components (except lignin and ash), (2) no external enzymes are required, and (3) sterile operating conditions are not needed. Therefore, MAAD that has a high carboxylic acid productivity with specific acid profiles can lower the downstream cost and ensure process success.

Compared to traditional anaerobic digestion MAAD shares three stages (hydrolysis, acidogenesis, acetogenesis) but arrests the fourth stage (methanogenesis) by adding an inhibitor, high organic loading rate, inoculum pretreatment, or acidic/alkaline pH.[28,89–91] In this study, methanogenesis was arrested using iodoform as methane inhibitor, thus allows for the high-rate accumulation of carboxylic acids (C2 to C8) in near-neutral pH (6.8–7.2).[92] However, accumulated carboxylic acids can upset the process, leading to system instability, low productivity, and subsequent metabolic shift towards undesired products.[93,94] Specifically, when short-chain carboxylic acids (SCCAs, C1 to C5) accumulates in an insufficient buffering digester environment, undissociated acids can permeate cell membrane and cause cytosolic pH drops, and eventually inhibit cell growth.[95,96]

In MAAD, hydrolysis of complex biopolymer (e.g., cellulose, protein, lipid) is considered the rate-limiting step.[97] Regardless of the system pH, carboxylic acid accumulation can inhibit the hydrolysis of cellulosic biomass.[98] Recent studies also

equipped carboxylate platform with *chain elongation* (CE), where SCCAs can be converted to medium-chain carboxylic acids (MCCAs, C6 to C12) for higher commercial values.[99] However, the high toxicity from MCCAs also challenges the developments of CE process.[100] Therefore, proper modification of MAAD is necessary to minimize product inhibition and maximize the process performance.

In-situ product removal (ISPR) is a type of process intensification that enhances performance by simultaneously separating inhibitory products from the digestion medium.[30] Methods for separating carboxylates from medium include precipitation, adsorption, liquid-liquid extraction, electrodialysis, nanofiltration, and reverse osmosis.[31] Compared to other techniques, the main advantages of adsorption with ion-exchange resin include the relative simplicity of implementation, the ease of the auxiliary phase removal, and the wide range of commercially available adsorbents.[31–33] Furthermore, anion-exchange resins act as a buffer by adsorbing carboxylic acids and increasing the pH of the digestion medium, thus decrease the need for buffer addition. Roy et al., 2021 shows that batch MAAD incorporated with ISPR using weak-base anion-exchange resin (Amberlite IRA-67) significantly improves acid yield by 2.2-, 1.54-, and 1.55-fold for α-cellulose, paper, and lime-pretreated corn stover, respectively. Reduced product inhibition also increased yields of valuable MCCAs.[80] Unfortunately, the desired digestion pH (~7.0) is much greater than the pK_a of carboxylic acids (~4.8). Because only a small portion of the acids are undissociated, resin adsorption capacity is greatly reduced.[33,101] This challenge can be overcome by acidifying the digestion broth with CO_2, which is abundantly produced by MAAD. Using CO_2 as an acidulant, Husson and

King (1999) demonstrated a sto step process: (1) acidifying lactate-containing digestion broth to produce lactic acid, and (2) removed lactic acid with ion exchange resin.[102]

Operating bioprocess under continuous mode can minimize process downtime and lower the production cost. Kinetics model developed for MAAD show that both high product concentration and low substrate availability negatively impact the digestion rate.[27] These limitations are overcome using multi-staged countercurrent operation (MSCO) which enhances MAAD performance by allowing solid and liquid phases to flow countercurrently through a cascade of digesters. Specifically, fresh (least-digested) biomass is added into the digester with the highest carboxylate concentration and fresh water is added into the digester containing the most-digested biomass. Because inhibition from accumulated carboxylates is minimized, both high conversion of biomass and high product concentration can be obtained.[76,103,104] Compared with batch MAAD, MSCO achieved a 225% increase in total carboxylic acid yield.[14] Thus far, no study has yet been conducted MAAD to investigate the combined effects of ISPR and MSCO, which has the potential to improve carboxylic acid productivity and increase the mass fraction of longer-chain carboxylic acids.

Unlike the previous two-step process, this study employs a one-step process where CO_2 was added during ISPR using anion-exchange resin (IRA-67). The adsorption is integrated into a four-stage semi-continuous countercurrent MAAD system operated at near-neutral pH and mesophilic conditions (40 °C). Office paper and chicken manure are co-digested to supplying carbon and nutrient sources, respectively. Digestion performance (e.g., acid concentration, profiles, yield, productivity, conversion) is

evaluated to determine the optimal resin loadings for the integrated system. Long-term resin utilization is also addressed. This study was performed with Shenchun Hsu and Haoran Wu.

4.2. Materials and Methods

4.2.1. Inoculum

The original inoculum was a mixed-culture of marine microorganisms collected from beach sediment in Galveston Island, TX. The typical composition of microorganisms has been reported elsewhere.[24] In this study, the digestion broth from a previous paper-consuming MAAD was used as the inoculum.

4.2.2. Substrates

MAAD was performed using shredded unused office paper and chicken manure as the carbon and nutrient sources, respectively. On a dry weight basis, the ratio of carbon source to nutrient source was 4:1. Fresh chicken manure was collected from the Department of Poultry Science, Texas A&M University (College Station, TX). To maintain consistency during the entire experiment, fresh chicken manure was dried in the oven at 105 °C for 48 h and stored in an airtight container at room temperature (25 °C). Urea was added as a supplemental nitrogen source to adjust the carbon-nitrogen ratio to 30 g non-acid carbon/g nitrogen. The optimal carbon-nitrogen ratio for the fermentations was found to be 20 to 40 g non-acid carbon/g nitrogen.[76] The desired products of mixed-acid fermentation are carboxylic acids. The mass of digestible biomass was quantified as non-acid volatile solids (NAVS), which excludes carboxylic acids naturally present in the feedstock:

$$\text{NAVS} = (\text{g total wet biomass})(1 - \text{MC})(1 - \text{AC}) - (\text{g carboxylic acid in biomass}) \quad (4\text{-}1)$$

where MC is the moisture content and AC is the ash content.

4.2.3. Fermentation Medium

The fermentation medium was deoxygenated water prepared by boiling de-ionized water to liberate dissolved oxygen. After cooling, 0.275 g/L cysteine hydrochloride and 0.275 g/L sodium sulfide were added to further reduce the oxygen content.[24] Deoxygenated water was used only in the initial batch period of fermentation. During continuous operation, de-ionized water was used as the liquid-phase inlet.

4.2.4. Methane Inhibitor

Methanogenesis was inhibited by using an iodoform (CHI_3) solution (20 g CHI_3/L, 200-proof ethanol). During countercurrent MAAD, 120 μL of iodoform solution was added into each fermentor every 48 h. Because iodoform is sensitive to light, high temperature, and air, the solution was kept in an amber-colored glass bottle wrapped in foil and stored in a refrigerator until use.

4.2.5. pH Control

The pH of the slurry in fermentors was measured using an Oakton (WD-35614, Vernon Hills, IL) pH meter. During the initial batch phase of the MAAD, $MgCO_3$ and CO_2 were used to buffer the fermentation broth to a near-neutral pH (6.8–7.2). To reach steady state during the countercurrent MAAD, $NaHCO_3$ and CO_2 were used as buffers. $NaHCO_3$ was preferred over $MgCO_3$ because less precipitate formed during anion-exchange resin adsorption.

4.2.6. Digester Configuration

The fermentor (Figure 4-1a) was a 1-L polypropylene centrifuge bottle capped by a rubber stopper inserted with a glass tube and two segments of 0.25-inch (6.35-mm) stainless steel pipe. These metal bars mix the digester contents as it rotated in a Wheaton Modular Cell Production Roller Incubator (Fisher Scientific, Pittsburgh, PA). The rollers rotated horizontally at 4 rpm. A rubber septum sealed the glass tube and allowed for gas sampling and release.

4.2.7. CO_2-sustained Anion-exchange Resin Adsorption Apparatus

Amberlite® IRA-67 ion-exchange resin (DuPont™, Wilmington, DE) was used as adsorbent for carboxylic acid removal. According to the product data sheet for IRA-67, IRA-67 is a weak-base anion-exchange resin with a particle size of 500–750 μm, density (ρ_r) of 1.07 g/mL wet resin, and total exchange capacity (C_r) >1.60 eq/L (free-base form).[105] For carboxylic acids produced in mixed-acid fermentation, one mole of acid equals one equivalent (eq). The tested moisture content of IRA-67 resin beads is 56 ± 0.6 g water/100 g wet resin. A prescribed amount of IRA-67 was loaded into a refillable resin cartridge (Max Water®, Concord, Canada) directly from the manufacturer package without further treatment. In this study, the loaded amount of resin in each cartridge was denoted as *wet resin loading*. Prior to adsorption, IRA-67 was pre-washed with de-ionized water to remove impurities and excess amines. The refillable resin cartridge was equipped with a fine-mesh screen (210-μm, polypropylene) to keep the resin in the cartridge and allow the fermentation broth to pass through the resin bed without blockage. A segment of 0.25-inch (6.35-mm) stainless steel pipe was inserted into the

cartridge to introduce carbon dioxide for acidification and mixing during adsorption (Figure 4-1b). (*Note:* This CO_2-sustained adsorption differs from Husson and King (1999) who added carbon dioxide prior to adsorption.)

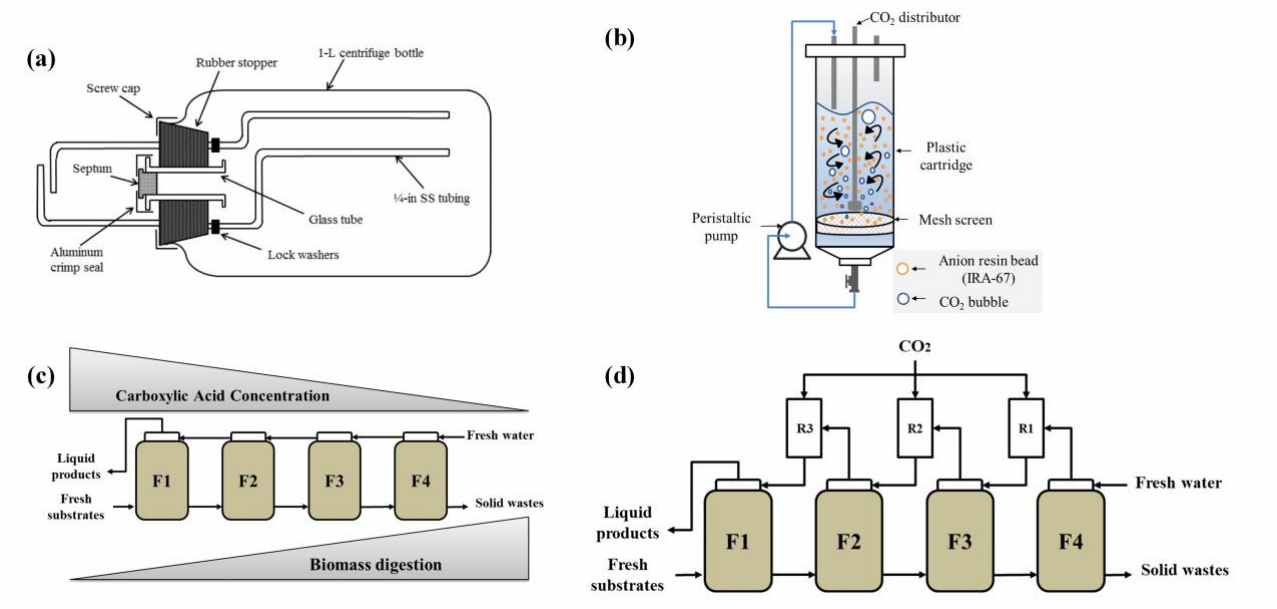

Figure 4-1. Mixed-acid fermentation process. (a) Schematic of fermentor; (b) Schematic of CO2-sustained anion-exchange resin adsorption column; (c) Diagram of four-stage countercurrent fermentations; (d) Diagram of CO2-sustained anion exchange resin adsorption.

4.2.8. MAAD Procedures

4.2.8.1. Semi-continuous Countercurrent MAAD

Four trains (T1–T4) of semi-continuous four-stage countercurrent MAAD were operated under anerobic conditions at 40 °C with the same substrate feed rate (9.71 g NAVS/T) where *T* is "transfer time" (Table 4-1). The substrate consisted of 80% paper and 20% homogenized chicken manure by dry weight. For four trains, the calculated volatile solids loading rate (VSLR) was 3.41–3.44 g NAVS/(L_{liq}·d), and liquid residence

time (LRT) was 28.2–28.6 d. To establish microbial cultures, the MAAD trains were initiated as batch digesters with a concentration of 100 g total solid/L digestion medium (deoxygenated water and inoculum). After initial batch growth, countercurrent operation was started by transferring liquids and solids in opposite directions (Figure 4-1c). Every 48 h, digesters were removed from the roller incubator, biogas samples from each digester were collected, and the gas volume was measured. The liquid and solid biomass from each digester were separated via centrifuge and weighted. Liquid samples (1.5-mL) were then collected and analyzed to monitor acid concentrations. The pH of the digestion broth was measured and recorded. Afterwards, the mass transfers were performed. The retained solid and liquid weights in each digester were controlled by solid/liquid mass setpoints, and the solid/liquid mass removed from each digester was determined by the following mass balance:

Mass remove = Initial mass + mass added from previous digester
(or fresh feed) – mass setpoint (4-2)

The liquids collected from digester F1 were defined as *liquid product*, whereas the solids collected from digester F4 were defined as *solid waste*. If the pH measured after mass transfer was out of the desired pH range (6.8–7.2), $NaHCO_3$ buffer was added. Before returning the digesters to the incubator, methane inhibitor was added, and then they were purged with nitrogen and properly resealed to create an anaerobic environment.

The first steady-state region for countercurrent operation served as the *control* and was achieved after three months. Then, digestion data were collected for over two

months to determine average carboxylic acid concentrations, biomass conversion, total carboxylic acids yield, selectivity, and productivity. The following definitions were used throughout this study:

$$\text{LRT} = \text{TLV}/F_{out} \tag{4-3}$$

$$\text{VSLR} = \text{NAVS}_{\text{fed}}/(\text{TLV}\cdot T) \tag{4-4}$$

$$\text{Conversion } (x) = \text{NAVS}_{\text{digested}}/\text{NAVS}_{\text{fed}} \tag{4-5}$$

$$\text{Yield } (Y) = \text{Total carboxylic acids produced}/\text{NAVS}_{\text{fed}} \tag{4-6}$$

$$\text{Selectivity } (\sigma) = \text{Total carboxylic acids produced}/\text{NAVS}_{\text{digested}} = Y/x \tag{4-7}$$

$$\text{Productivity } (P) = \text{Total carboxylic acids produced}/(\text{TLV}\cdot T) \tag{4-8}$$

where

TLV is total liquid volume in one MAAD train (L),

F_{out} is the liquid flow rate out of the MAAD train (L/T),

T is the mass transfer time (T = 2 d),

NAVS_{fed} is non-acid volatile solids fed from substrate (g),

$\text{NAVS}_{\text{digested}}$ is the mass difference between NAVS from the substrate and NAVS from the waste (g).

The detailed digestion performance from four MAAD trains was averaged and reported as the *control* in Table 4-3.

4.2.8.2. Countercurrent MAAD with CO_2-sustained Fluidized-bed Anion-exchange Resin Adsorption

CO_2-sustained anion-exchange resin adsorption was applied to the established MAAD trains described in the previous section (Figure 4-1d). The theoretical amount of resin loading (L_t) needed for each countercurrent MAAD train was calculated as

$$L_t \text{ (g wet resin/}T\text{)} = (R_a \cdot \rho_r)/(M_w \cdot C_r) \quad (4\text{-}9)$$

where

R_a is the acid production rate by countercurrent MAAD (g/T),

M_w is the average molecular weight of acid products based on mass fraction (g/mol),

C_r is the total exchange capacity (1.60 eq/L, 1 eq = 1 mol),

ρ_r is resin density for IRA-67 (1.07 g/mL).

Because the adsorption mechanism is based on hydrophobic interactions of undissociated acids onto polymeric resins, the adsorption efficiency of weak-base anion-exchange resin is lowered when the adsorption pH is higher than the pK_a of the carboxylic acid (López-Garzón and Straathof, 2014; Yousuf et al., 2016).[31,106] The pK_{a1} of CO_2 is 6.37 at 25 °C. During adsorption, CO_2 can sustain the pH of digestion broth within 6.5 to 7.5; thus, the resin has 70–85% of its maximum adsorption capacity. Therefore, CO_2 was used as an acidulent during adsorption to maintain resin adsorption capacity. Seven sets of wet resin loadings were chosen to study their effects on digestion performance.

In this study, four countercurrent MAAD trains were operated initially at lower resin loadings (10, 20, 30, 40 g wet resin/*T*) using Trains T1, T2, T3, and T4, respectively. After these initial tests were completed, the tests for higher loadings (50, 60, 80 g wet resin/*T*) were operated by using Trains T2, T3, and T4, respectively. Table 4-2 lists the detailed operating parameters and normalized parameters of different resin loading steady-state regions.

For countercurrent MAAD with acid adsorption, compared to the control, the only difference in the operation method was the liquid mass transfer; therefore, the other common operation methods will not be repeated in this section. As shown in Figure 4-1d, every 48 h, when liquid sampling from each stage was completed, the effluent broth from F4, F3, and F2 was passed through the adsorption columns (R) ordered respectively as R1, R2, and R3. To be clear, only a single adsorption column was used for this adsorption process per MAAD train; R1, R2, R3 only denote the order of adsorption. To reduce the length of periodic air exposure, the operation time for unit adsorption cycle was set to 10 min. To fully use the resin adsorption capacity within the limited operation time, the CO_2 flowrate added to the adsorption column was set to 1.5 L/min to maintain the pH of adsorption system and fully fluidize the resin bed. When each adsorption cycle was completed, a liquid sample was collected from adsorption effluent before addition to the next digester stage. After adsorption, sodium bicarbonate was added into digesters to bring the pH to near-neutral (6.8–7.2) after CO_2-sustained adsorption and mass transfer.

After three adsorption cycles (R1, R2, R3), IRA-67 was regenerated with 1-N NaOH solution. The regeneration method followed suggestions by the manufacturer

(Rohm and Haas Company, 2020). One bed volume (BV) is defined as 1 m^3 solution per m^3 resin. The saturated resin was rinsed with 8 BV of NaOH solution for more than 30 min under circulation. Then, the regenerated resin column was washed with de-ionized water to remove excess NaOH solution and stored in de-ionized water until next use.

Table 4-3 lists the detailed digestion performance for the steady-state regions with resin adsorption.

4.2.9. Analytical Methods

Moisture and ash contents were determined as previously described.[24] To minimize the mass loss of volatile solids from evaporation, 30 mg $Ca(OH)_2$/(g sample) was added into the liquid sample before placing into the oven. Samples were dried in a 105 °C oven for at least 24 h, and subsequent combustion in a 575 °C furnace for at least 24 h. The volatile solid (VS) was determined as the difference between the oven dry weight and the ash weight.

Liquid samples were collected every 48 h for acid analysis. The concentrations of carboxylic acids were measured by using a gas chromatograph (Agilent 6890 Series, Santa Clara, CA) equipped with an automatic liquid sampler, a flame ionization detector (FID), and a DB-FFAP capillary column (30 mm × 0.320 mm). The details for acid analysis and sample processing are previously described.[107]

The biogas volume was measured by displacing liquid in an inverted glass graduated cylinder apparatus that was filled with a 300-g/L $CaCl_2$ solution at 25°C at 1 atm abs.[28] Biogas composition was determined as previously described.[24]

Table 4-1. Operating parameters for countercurrent mixed-acid fermentations. Values in normalized section represent the mean of the steady-state values ± CI (95% CI).

	Train	T1	T2	T3	T4
Controlled	Solid and liquid transfer frequency, *T* (h)	48	48	48	48
	NAVS feed rate (g NAVS/*T*)	9.71	9.71	9.71	9.71
	Paper (g/*T*)	10.2	10.2	10.2	10.2
	Chicken manure (g/*T*)	2.4	2.4	2.4	2.4
	Urea added (g/*T*)	0.2	0.2	0.2	0.2
	C-N ratio (g OC_{NA}/g N)	30.3	30.3	30.3	30.3
	Liquid feed rate (mL/*T*)	120	120	120	120
	Centrifuge solid retained in F1–F4 setpoint (g)	200 (250 for F4)	200 (250 for F4)	200 (250 for F4)	200 (250 for F4)
	Centrifuge liquid retained in F1–F4 setpoint (g)	200	200	200	200
	Temperature (°C)	40	40	40	40
	Methane inhibitor (μL/(*T*·fermentor))	120	120	120	120
	Wet resin loading (g/*T*)	10	20	30	40
Normalized	VSLR (g NAVS/(L_{liq}·d))	3.41 ± 0.01	3.41 ± 0.02	3.44 ± 0.02	3.42 ± 0.02
	LRT (d)	28.4 ± 0.75	28.2 ± 0.54	28.6 ± 0.61	28.2 ± 0.47
	TLV (L)	1.42 ± 0.01	1.42 ± 0.01	1.41 ± 0.01	1.42 ± 0.01

Table 4-2. Operating parameters for countercurrent mixed-acid fermentations with CO2-sustained anion exchange resin adsorption. Values in normalized section represent the mean of the steady-state values ± CI (95% CI).

	Train[a]	T1-10	T2-20	T3-30	T4-40	T2-50	T3-60	T4-80
Controlled	Solid and liquid transfer frequency, *T* (h)	48	48	48	48	48	48	48
	NAVS feed rate (gNAVS/*T*)	9.71	9.71	9.71	9.71	9.71	9.71	9.71
	Paper (g/*T*)	10.2	10.2	10.2	10.2	10.2	10.2	10.2
	Chicken manure (g/*T*)	2.4	2.4	2.4	2.4	2.4	2.4	2.4
	Urea added (g/*T*)	0.2	0.2	0.2	0.2	0.2	0.2	0.2
	C-N ratio (g OC_{NA}/g N)	30.3	30.3	30.3	30.3	30.3	30.3	30.3
	Liquid feed rate (mL/*T*)	120	120	120	120	120	120	120
	Centrifuge solid retained in F1–F4 setpoint (g)	200 (250 for F4)	200 (250 for F4)	200 (250 for F4)	200 (250 for F4)	200 (250 for F4)	200 (250 for F4)	200 (250 for F4)
	Centrifuge liquid retained in F1–F4 setpoint (g)	200	200	200	200	200	200	200
	Temperature (°C)	40	40	40	40	40	40	40
	Methane inhibitor (μL/(*T*·fermentor))	120	120	120	120	120	120	120
	Wet resin loading (g/*T*)	10	20	30	40	50	60	80
Normalized	VSLR (g NAVS/(L_{liq}·d))	3.48 ± 0.05	3.48 ± 0.02	3.52 ± 0.02	3.54 ± 0.02	3.62± 0.03	3.64 ± 0.02	3.61 ± 0.04
	LRT (d)	29.5 ± 0.60	29.7 ± 0.61	30.2 ± 1.08	30.3 ± 0.54	33.0 ± 1.03	32.1 ± 1.55	33.7 ± 1.31
	TLV (L)	1.39 ± 0.02	1.40 ± 0.01	1.38 ± 0.01	1.37 ± 0.01	1.34 ± 0.01	1.34 ± 0.01	1.34 ± 0.01
	Normalized wet resin loading (g wet resin/(L_{liq} · day))	3.58 ± 0.05	7.16 ± 0.04	10.9 ± 0.08	14.6 ± 0.07	18.6 ± 0.19	22.56 ± 0.13	29.8 ± 0.35

[a] The names of trains are designated according to the countercurrent fermentation trains (T1–T4) used and the wet resin loadings (10–80 g/*T*) applied in Section 4.3.2

Table 4-3. Fermentation performance summary for countercurrent mixed-acid fermentations with CO2-sustained anion exchange resin adsorption. Values represent the mean of the steady-state values ± CI (95% CI).

Train	*Control*	T1-10	T2-20	T3-30	T4-40	T2-50	T3-60	T4-80
Total carboxylic acid concentration (g/L)	17.5 ± 1.12	15.2 ± 0.74	14.2 ± 0.70	14.7 ± 0.72	13.2 ± 0.46	14.3 ± 0.83	13.7 ± 0.43	13.1 ± 0.25
Acetic acid (wt.%)	43.1 ± 3.39	40.7 ± 2.28	39.4 ± 2.50	38.5 ± 2.91	39.5 ± 0.79	40.1 ± 1.07	42.4 ± 0.83	40.8 ± 1.27
Propionic acid (wt.%)	31.1 ± 2.54	37.6 ± 1.61	36.7 ± 1.54	40.4 ± 3.23	35.2 ± 2.18	31.6 ± 1.73	36.4 ± 1.95	29.6 ± 1.49
Isobutyric acid (wt.%)	0.72 ± 0.29	1.22 ± 0.18	1.24 ± 0.19	1.59 ± 0.24	0.92 ± 0.16	1.01 ± 0.16	1.00 ± 0.26	0.71 ± 0.22
Butyric acid (wt.%)	22.1 ± 2.07	16.3 ± 0.77	16.4 ± 0.60	14.3 ± 0.99	16.1 ± 1.04	17.2 ± 1.17	14.5 ± 1.48	18.7 ± 0.63
Isovaleric acid (wt.%)	0.33 ± 0.11	0.55 ± 0.07	0.46 ± 0.07	0.52 ± 0.06	0.49 ± 0.12	0.59 ± 0.08	0.36 ± 0.03	0.42 ± 0.04
Valeric acid (wt.%)	1.21 ± 1.10	1.88 ± 0.34	3.69 ± 0.58	2.49 ± 0.52	5.18 ± 1.29	5.69 ± 0.86	3.60 ± 1.01	6.02 ± 1.34
Caproic acid (wt.%)	1.00 ± 0.49	1.48 ± 0.50	1.67 ± 0.32	1.35 ± 0.42	2.51 ± 0.80	3.44 ± 0.80	1.62 ± 0.50	3.55 ± 0.90
Enanthic acid (wt.%)	0.28 ± 0.22	0.24 ± 0.28	0.37 ± 0.46	0.87 ± 0.67	0.06 ± 0.03	0.20 ± 0.08	0.06 ± 0.01	0.12 ± 0.02
Caprylic acid (wt.%)	0.13 ± 0.23	0.00 ± 0.00	0.05 ± 0.02	0.06 ± 0.03	0.05 ± 0.03	0.12 ± 0.02	0.06 ± 0.01	0.05 ± 0.01
Acids in liquid product, P_{Liq} (g/(L_{liq}·d))	0.39 ± 0.02	0.34 ± 0.03	0.34 ± 0.03	0.36 ± 0.04	0.34 ± 0.03	0.32 ± 0.04	0.32 ± 0.04	0.30 ± 0.03
Acids in liquid product, P_{ad} (g/(L_{liq}·d))	–	0.26 ± 0.03	0.36 ± 0.06	0.41 ± 0.05	0.50 ± 0.02	0.48 ± 0.02	0.50 ± 0.03	0.48 ± 0.06
Resin utilization	–	70.4 ± 7.90	46.2 ± 6.79	34.2 ± 3.66	31.4 ± 1.25	24.4 ± 0.73	20.7 ± 0.69	14.5 ± 1.09

Biogas productivity ($L/(L_{liq} \cdot d)$)	0.30 ± 0.01	0.41 ± 0.01	0.44 ± 0.02	0.44 ± 0.02	0.45 ± 0.01	0.45 ± 0.01	0.47 ± 0.01	0.45 ± 0.03
Conversion, x (g $NAVS_{digested}$/g $NAVS_{fed}$)	0.18 ± 0.00	0.23 ± 0.02	0.30 ± 0.02	0.41 ± 0.03	0.40 ± 0.02	0.32 ± 0.02	0.31 ± 0.01	0.36 ± 0.05
Yield, Y (g acid produced/g $NAVS_{fed}$)	0.11 ± 0.01	0.17 ± 0.00	0.20 ± 0.00	0.22 ± 0.00	0.23± 0.00	0.22 ± 0.00	0.22 ± 0.00	0.21 ± 0.01
Selectivity, σ (g acid produced/g $NAVS_{consumed}$)	0.65 ± 0.05	0.75 ± 0.06	0.66 ± 0.04	0.54 ± 0.04	0.58± 0.02	0.67± 0.04	0.72 ± 0.03	0.59 ± 0.08
Total acid productivity, P (g /($L_{liq} \cdot d$))	0.39 ± 0.02	0.60 ± 0.05	0.69 ± 0.08	0.77 ± 0.07	0.84 ± 0.04	0.80 ± 0.05	0.82 ± 0.05	0.78 ± 0.08

4.2.10. Statistical Analysis

For countercurrent MAAD, the steady-state region is defined as the period during which the total acid concentration in liquid product (F1) does not vary by more than ±2.2 standard deviations from the average for a period of at least one liquid residence time. For each MAAD train, Table 4-1 lists the steady-state regions. The means and standard deviations of the total acid concentration, non-acid volatile solids (NAVS) in and out were determined from steady-state data. Using the Slope Method, these values were then used to calculate digestion performance, such as acid productivity (P), selectivity (σ), yield (Y), and conversion (x).[108] Student's two-sample t-test (two-tailed, type 3) was used to compute p values. All error bars are reported as 95% confidence interval.

4.3. Results and Discussion

4.3.1. Biogas Production

Although MAAD aims to produce carboxylic acids as the main product, biogas is a by-product. During a 48-h operation cycle, countercurrent MAAD (*control*) had an average biogas productivity at 0.3 $L/L_{liq}\cdot day$. When resin adsorption was applied, productivity increased to 0.41–0.47 $L/L_{liq}\cdot day$. It was noticed that as the wet resin loading increased from 0 to 20 g per transfer, the gas productivity increased from 0.3 to 0.44 $L/L_{liq}\cdot day$. At loadings greater than 20 g per transfer, biogas productivity stabilized around 0.45 $L/L_{liq}\cdot day$. Because iodoform was added as a methane inhibitor, no methane was detected in any digester during each steady-state region, and main component of biogas is CO_2.

4.3.2. Carboxylic Acid Production

Figure 4-2 shows the total carboxylic acid concentration with operation time for each MAAD train. For all digesters, concentrations were maintained in a narrow range during each steady state. By applying resin adsorption, new steady states were readily achieved for each resin loading. Tables 4-1 and 4-2 list the normalized operating conditions during each steady state. The application of resin adsorption decreased the TLV, which increased the LRT of the MAAD trains. Based on the steady-state data, Figure 4-3 shows the correlation between wet resin loading and total carboxylic acid concentrations in each stage (F1 to F4) of countercurrent MAAD trains. Figure 4-4 shows the carboxylic acid composition profiles in the liquid product under various wet resin loadings.

4.3.2.1. Carboxylic Acid Production in Stand-alone Countercurrent MAAD (control)

For countercurrent MAAD without resin adsorption (*control*), four trains were operated under identical conditions. All trains achieved similar acid production results, indicating the high reproducibility of countercurrent MAADs with undefined microbial consortia. The average total acid concentration in liquid product (F1) was 17.54 ± 1.12 g/L, with total acid productivity of 0.39 ± 0.02 g/L_{liq}·day. As shown in Figure 4, acetic (43 wt.%), propionic (31 wt.%), and butyric (22 wt.%) acids were the primary components in the liquid product. Furthermore, in each train, the pH of digestion broth prior to resin adsorption increased from F1 (6.00 ± 0.05) to F4 (6.85 ± 0.21), indicating the availability of digestible substrate playing an important role in acid production.

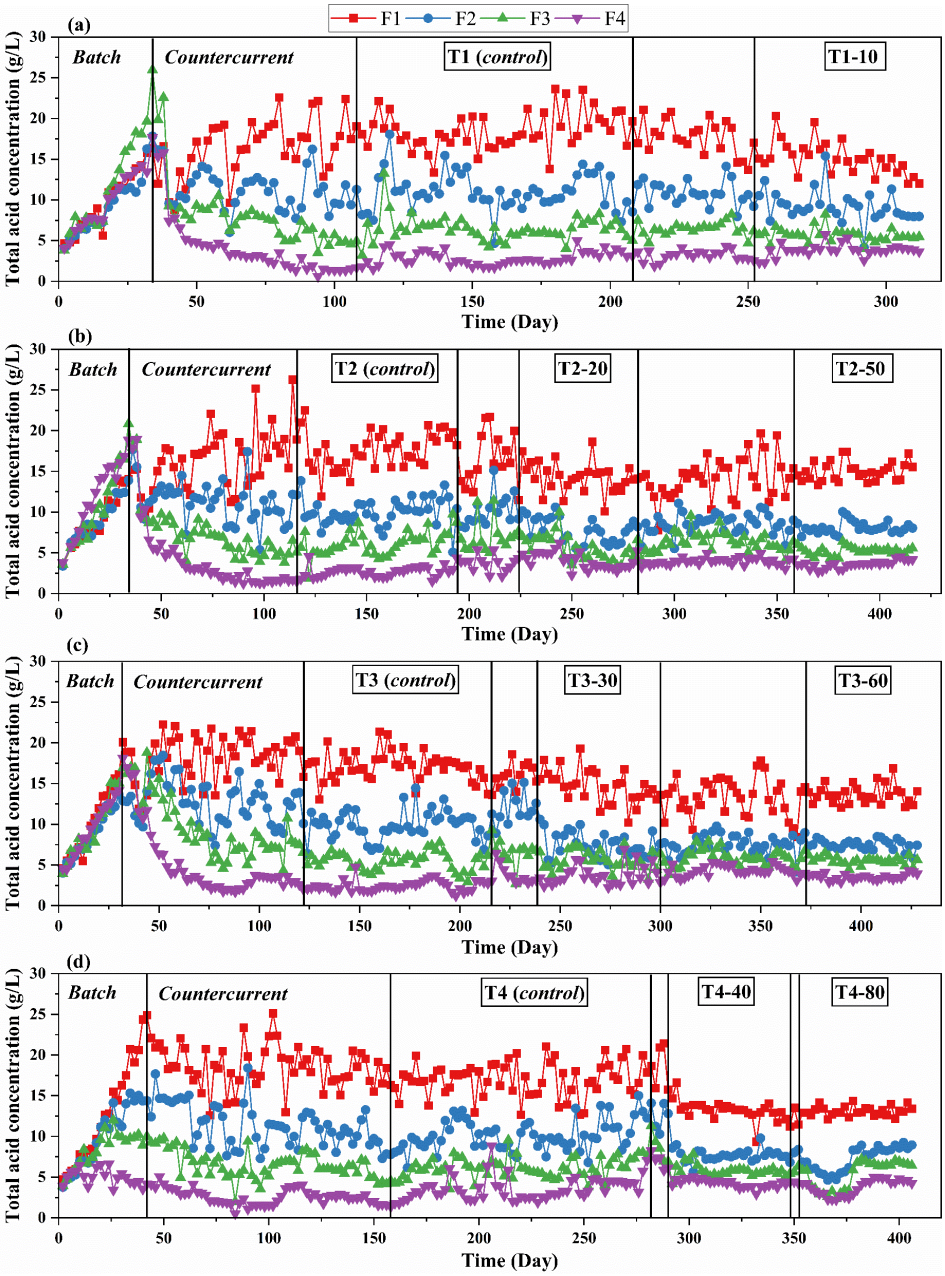

Figure 4-2. Total carboxylic acid concentrations with operation time for MAAD trains. (a) Train 1; (b) Train 2; (c) Train 3; (d) Train 4.

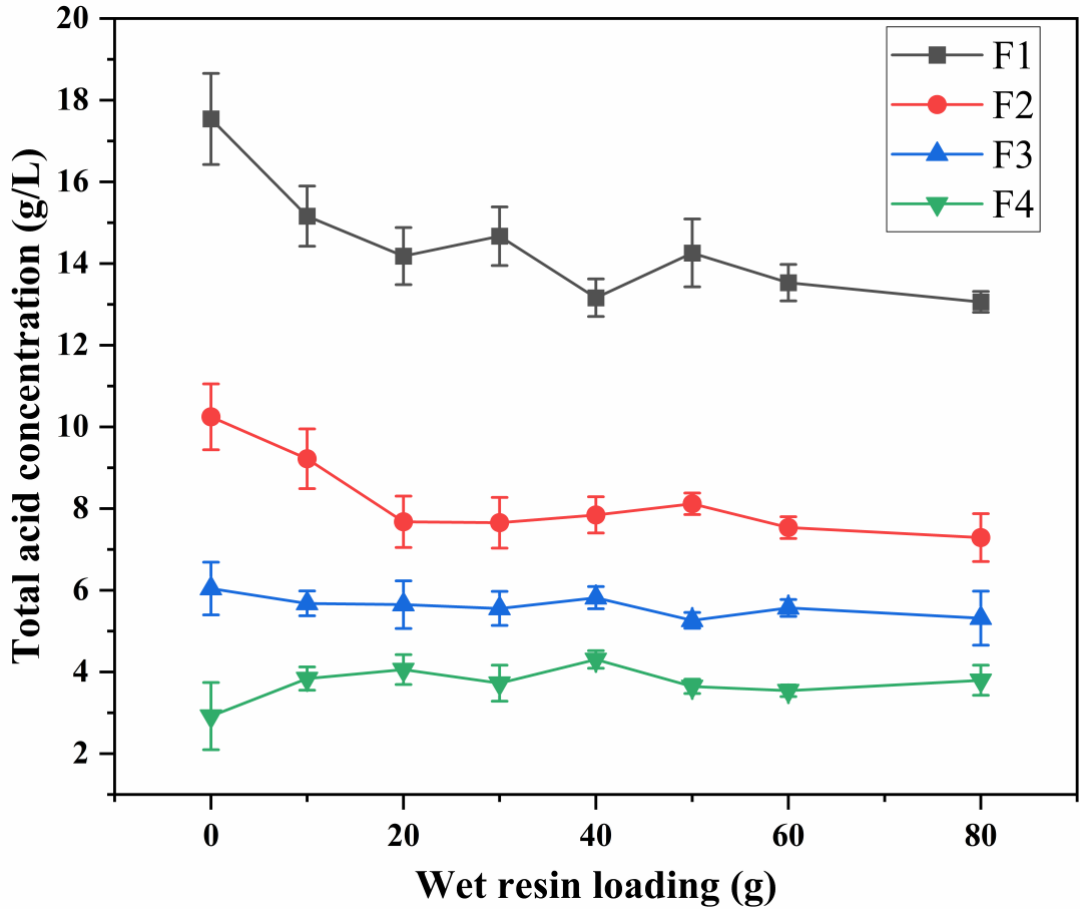

Figure 4-3. Correlation between wet resin loadings and total acid concentration in each stage of countercurrent MAAD trains. Error bars represent the 95% confidence interval of acid concentrations during the steady-state periods.

Previous study co-digesting paper and chicken manure shows Firmicutes and Actinobacteria helped degrade the cellulose portion, whereas Prevotella and Actinobaculum- and Arcanobacterium-like bacteria were responsible for the degradation of the non-cellulose portion of feedstocks.[104]

4.3.2.2. Effect of *In-situ* Acid Separation on Carboxylic Acid Production

To study the effect of acid removal on countercurrent MAAD, different wet resin loadings were applied to each MAAD trains. Figure 4-3 shows that as the loadings increased from 0 to 20 g per transfer, total acid concentrations decreased in F1, F2, and F3, but increased in F4. At loadings greater than 20 g per transfer, acid concentration fluctuated around 13.7, 7.7, 5.5 and 3.8 g/L in F1, F2, F3 and F4, respectively. Compared to the control group, incorporating anion-exchange resin did not change the primary carboxylic acid components (C2, C3, C4) in the liquid product (F1) (Table 4-3). Figure 4-4 also indicates that the mass fractions of longer chain carboxylic acids (C5 and C6) in liquid products increased with resin adsorption, which agreed with the results achieved by Roy et al., 2021 for batch MAAD with IRA-67 resin adsorption.[80] Therefore, mitigating the product inhibition through *in-situ* acid separation should be considered as alternative for CE process.

Total acid production consists of acids contained within the liquid product (P_{Liq}) and acids adsorbed onto the resin (P_{Ad}). The amount of total acids adsorbed per adsorption (m_{ad}) was calculated through mass balance as

$$m_{ad}\,(\mathrm{g}) = V_i \cdot C_i - V_f \cdot C_f \qquad (4\text{-}10)$$

where V_i and V_f are the measured volumes of the liquid stream before and after resin adsorption and C_i and C_f are the measured total acid concentrations of the liquid stream before and after resin adsorption.

Although resin adsorption decreases the total acid concentration in the liquid product, Figure 4-5a shows that countercurrent MAAD with *in-situ* acid separation

significantly increased total acid productivity by at least 1.54-fold ($p < 0.05$). Increasing the resin loading from 0 to 40 g per transfer amplified acid productivity. At 40 g wet resin loading, the system reached the highest acid productivity (0.84 ± 0.04 g/L_{liq}·day), of which the acid productivity was 2.15-fold higher than the *control*, and nearly 60% acids produced were adsorbed by the resin (0.50 ± 0.02 g/L_{liq}·day). When higher wet resin loadings were applied (40 to 80 g per transfer), there was no significant additional gain in total acid productivity. It is possible that high resin loadings disturbed the integrity of the microbial community in the digestion broth, and thus offset the benefit from *in-situ* acid separation. However, if the aim of MAAD is for longer-chain carboxylic acids (e.g., C5, C6) production, it is still beneficial to use higher resin loading for *in-situ* acid separation.

The obtained results prove that the combined benefits from ISPR and MSCO can greatly promote the carboxylic acid productivity of MAAD using cellulosic biomass. Recently, MAAD were also used for other feedstocks (e.g., food waste, municipal waste, industrial wastewater) with higher portion of easily degradable molecules.[109,110] Rughoonundun and Holtzapple, 2017 co-digested sewage sludge and lime-pretreated sugarcane bagasse via countercurrent MAAD and achieved highest total acid concentration at 60.8 g/L with acid productivity at 2.31 g/L_{liq}·day.[14] Therefore, by supplying different substrates, it is promising to achieve greater acid production performance for the ISPR and MSCO integrated MAAD system.

4.3.3. Resin Utilization

During *in-situ* acid separation, the same IRA-67 resin beads were used throughout the operation time for one specific MAAD train. As mentioned in Section 4.3.2, resin was regenerated using 1-N NaOH solution when adsorption was completed. The regeneration process captured most of the carboxylic acids adsorbed on the resin column. *Resin utilization* is defined as the ratio of the actual acid adsorption amount (A_a) to the theoretical acid adsorption amount (A_t). It was used to evaluate the performance of the resin adsorption column under different wet resin loadings. For each IRA-67 resin loading, A_a and A_t are determined as follows:

$$A_t \text{ (mol/}T\text{)} = (L_a \cdot C_r)/\rho_r \quad (4\text{-}11)$$

$$A_a \text{ (mol/}T\text{)} = m_c/M_w \quad (4\text{-}12)$$

where

L_a is the actual wet resin loading in one adsorption column (g wet resin/T),

C_r is 1.60 eq/L, one mole of acid equals one equivalent (eq) for carboxylic acid,

ρ_r is 1.07 g/mL wet resin,

m_c is the amount of acid adsorbed onto resin column per transfer time in one MAAD train (g/T),

M_w is the average molecular weight of acid products based on mass fraction (g/mol).

Figure 4-5b illustrates that when the resin loading increased from 10 g to 80 g per transfer, the resin utilization dropped from around 70 to 14%. Lower resin utilization occurred because there were insufficient acids produced to occupy fully the active

adsorption sites of the packed resin column. Meanwhile, study shows that repeated adsorption/desorption cycle with biological effluents (e.g., municipal wastewater) can cause resin fouling, and eventually decrease adsorption efficiency and increase the volume of the desorption concentrate.[111] Therefore, during industrial application with longer operation time, it is necessary to keep checking on the resin actual adsorption capacity and replacing resin column when the number falls under the threshold value.

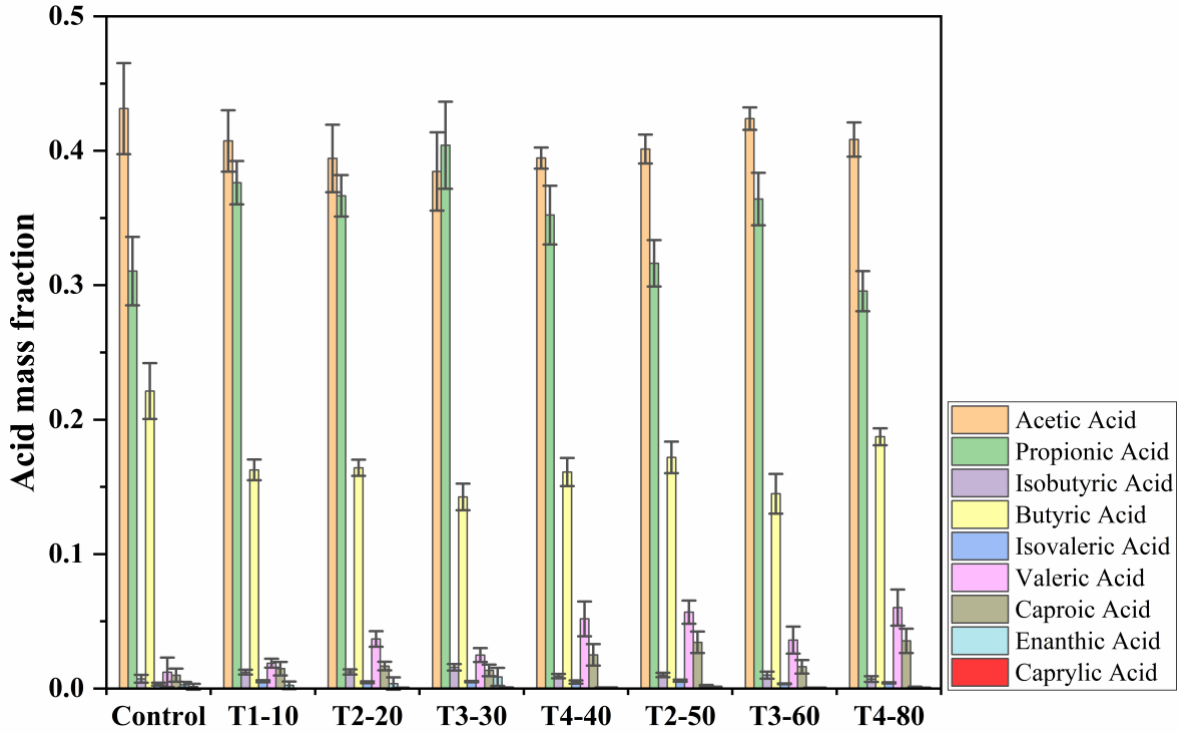

Figure 4-4. Carboxylic acid composition profiles. Error bars are the 95% confidence intervals for each carboxylic acid composition during the steady-state periods.

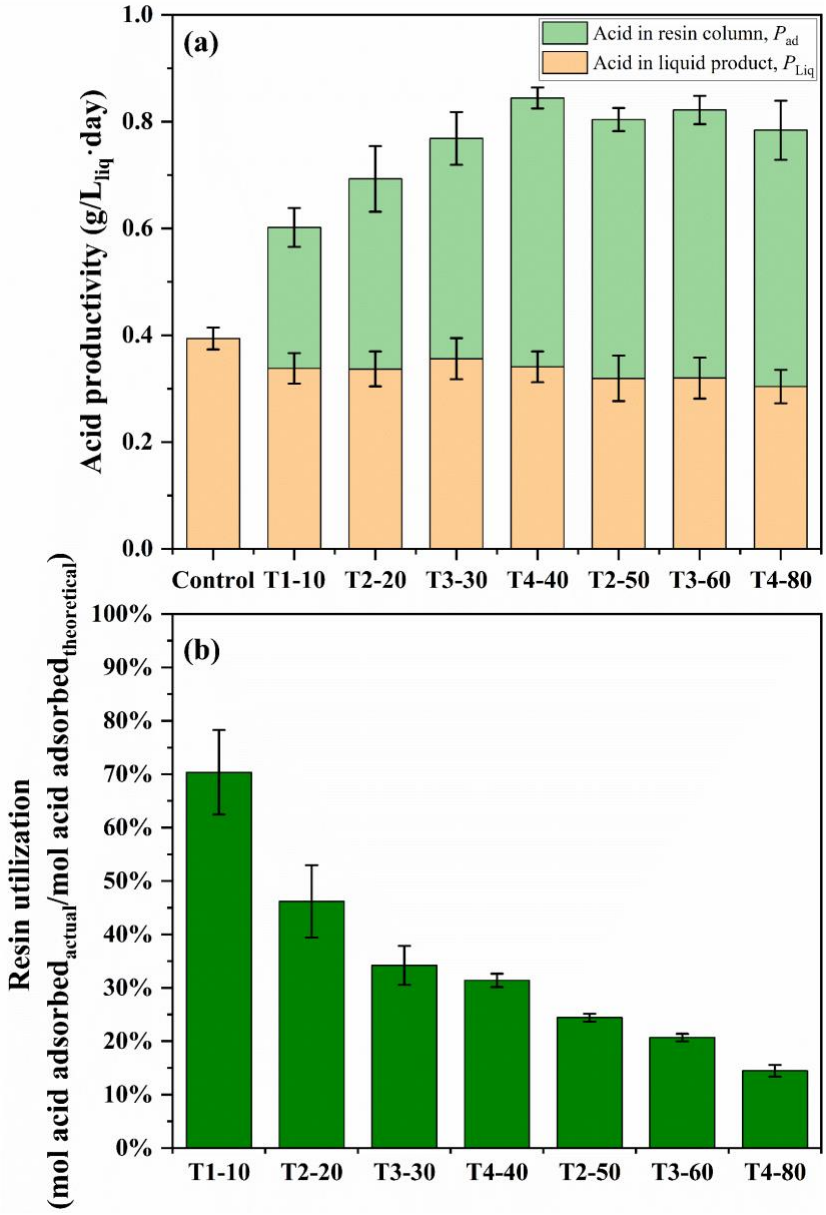

Figure 4-5. Resin performance evaluation. (a) Correlation between wet resin loadings and total acid productivities distribution; (b) Resin utilizations. Error bars are the 95% confidence intervals for each calculated data during the steady-state periods.

4.3.4. Digestion Performance

For countercurrent MAAD, the Slope Method was used to measure the digestion performance. For each steady state in all MAAD trains, Figures 4-6 and 4-7 show the accumulations of the $NAVS_{feed}$, $NAVS_{exit}$, and total acid exit. The slopes of these lines were obtained through linear regression, and were used to calculate biomass conversion, total acid yield, and selectivity.

For the *control*, four countercurrent MAAD trains achieved similar conversion (0.18 ± 0.00 g $NAVS_{digested}$/g $NAVS_{fed}$), yield (0.11 ± 0.01 g acid produced/g $NAVS_{fed}$), and selectivity (0.65 ± 0.05 g acid produced/g $NAVS_{consumed}$). These parameters were used as controls to compare with digestion performance gained from steady-state regions under various amount of wet resin loading (Table 4-2). To make these laboratory results more generally applicable, Figure 4-8 shows the digestion performance with wet resin loading normalized to the TLV in each MAAD train. Error bars are the 95% confidence intervals for each fermentation performance calculated during the steady-state periods.

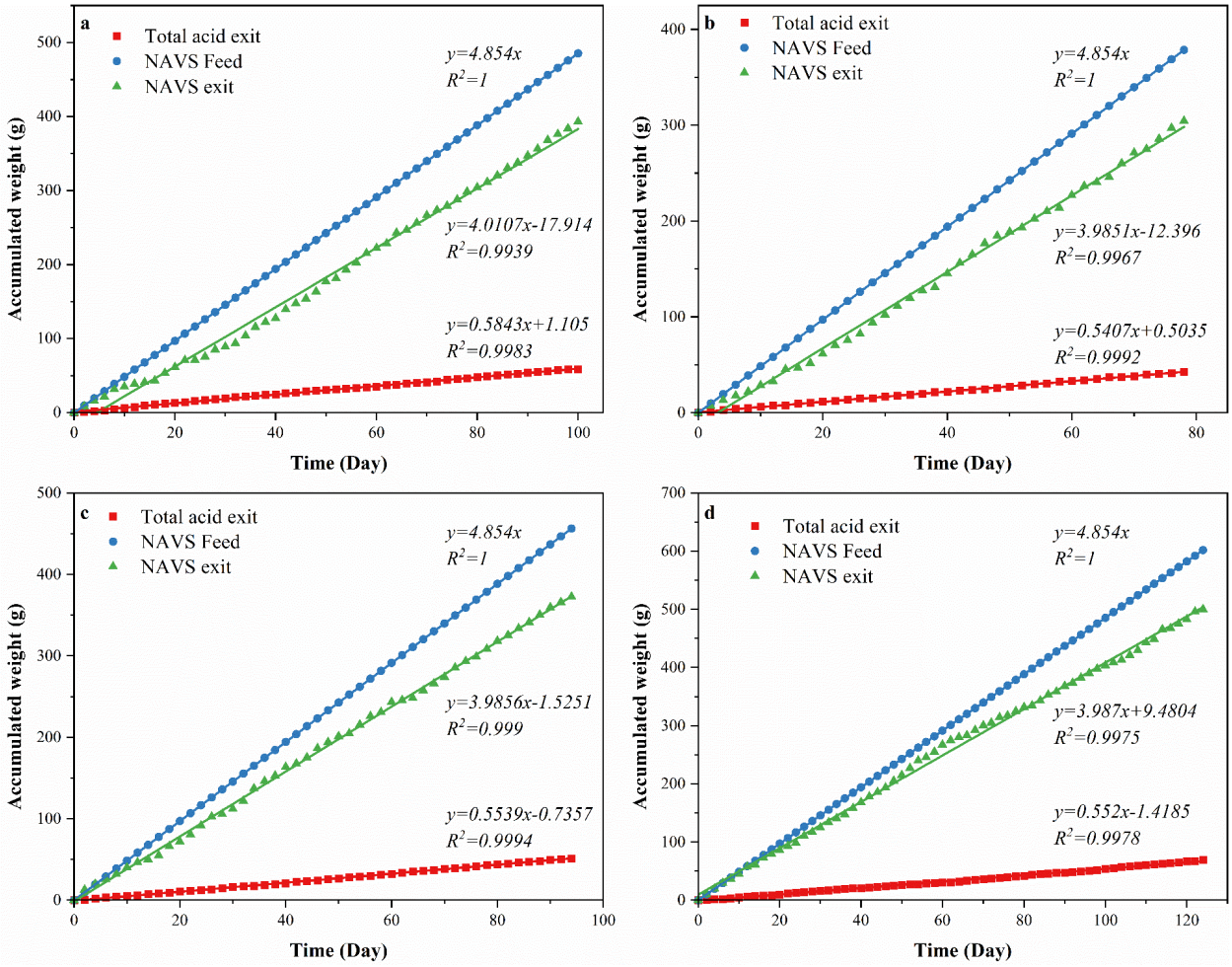

Figure 4-6. Slope method graphs for countercurrent MAAD (control). (a) T1; (b) T2; (c) T3; (d) T4.

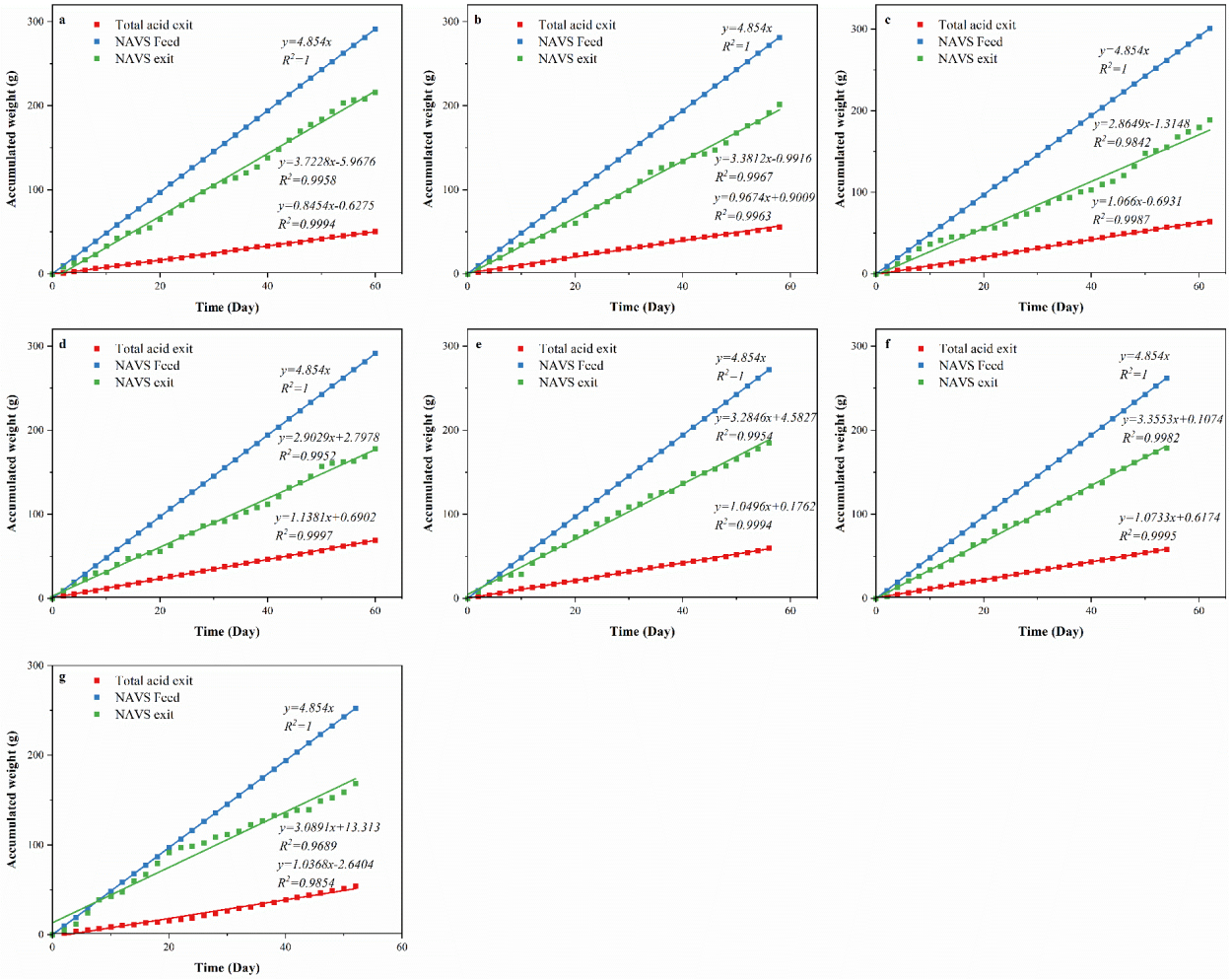

Figure 4-7. Slope method graphs for countercurrent mixed-acid fermentations with CO2-sustained anion exchange resin adsorption. (a) T1-10; (b) T2-20; (c) T3-30; (d) T4-40; (e) T2-50; (f) T3-60; (g) T4-80

Figure 4-8a shows that biomass conversion significantly increased by about 28 to 128% compared with conversion from the *control*, and reached a peak at 0.41 ± 0.03 g $NAVS_{digested}$/g $NAVS_{fed}$ with a normalized wet resin loading of 10.9 g/(L_{liq}·d) (T3-30). Statistical analysis shows that the conversion from T3-30 is significantly different from T4-40 (p = 0.001); thus, it is reasonable to conclude that the optimal normalized wet resin loading is 10.9 g/(L_{liq}·d) provided the goal is to maximize the biomass conversion.

Both Figures 4-8b and 4-8d indicate that carboxylic acid production of countercurrent MAAD significantly increased with *in-situ* acid separation through resin adsorption. Figure 4-8b shows that the acid yield reached a plateau (increased by 109%) and achieved the highest yield at 0.23 g acid produced/g $NAVS_{fed}$ with a normalized wet resin loading of 14.6 g/(L_{liq}·d) (T4-40). Provided the goal is to maximize carboxylic acid production, the optimal normalized wet resin loading is 14.6 g/(L_{liq}·d).

Carboxylic acid selectivity was determined from biomass conversion and acid yield. Figure 4-8c shows selectivity fluctuated around 0.65 g acid produced/g $NAVS_{digested}$ without obvious trends. The highest selectivity achieved was 0.75 g acid produced/g $NAVS_{digested}$ with a normalized wet resin loading of 3.6 g/(L_{liq}·d) (T1-10), whereas the lowest selectivity was 0.54 g acid produced/g $NAVS_{digested}$ with a normalized wet resin loading of 10.9 g/(L_{liq}·d) (T3-30).

Using office paper and chicken manure as model feedstocks, the overall digestion performance obtained in this study strongly shows that applying ISPR with countercurrent MAAD can largely reduce the product inhibition, and thus increase the system abilities for both biomass degradation (e.g., cellulose hydrolysis) and carboxylic acid production (e.g., acidogenesis). In the context of carboxylate platform, these improvements can help increase the platform efficiency and eventually lower the overall cost and carbon footprint. By optimizing other MAAD operating conditions (e.g., inoculum, feedstocks, temperature, LRT, VSLR), the integrated ISPR and countercurrent MAAD system will provide great support for carboxylate platform and its future industrial applications.

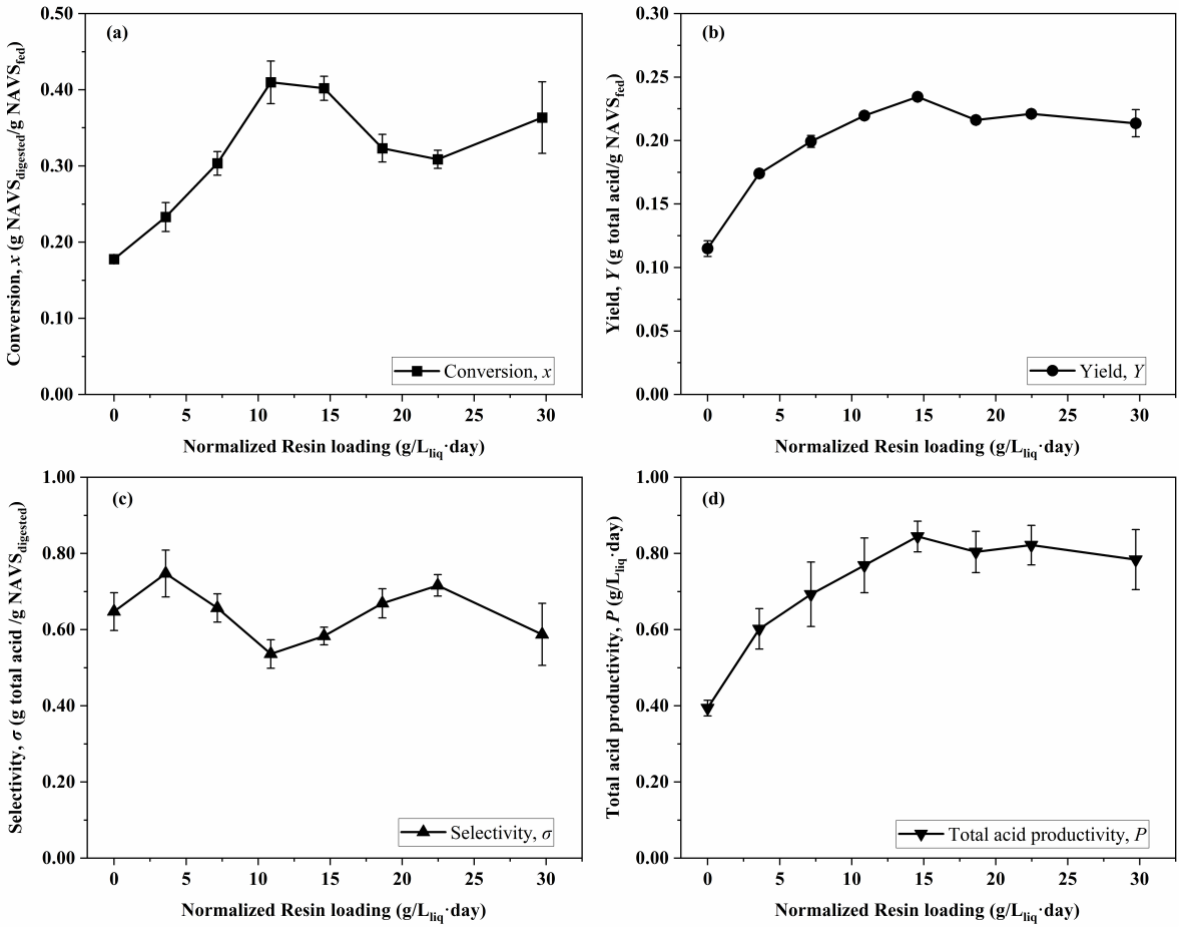

Figure 4-8. Correlation between fermentation performance and normalized resin loading. (a) Substrate conversion; (b) Total acid yield; (c) Total acid selectivity; (d) Total acid productivity.

4.4. Conclusion

The procedure for *in-situ* CO_2-sustained anion-exchange resin adsorption was developed for semi-continuous countercurrent MAAD. The results indicate that minimizing acid inhibition enhances digestion performance. The maximum increases carboxylic acid production with resin adsorption was 2.15 times. Furthermore, biomass conversion and acid yield significantly increased by 2.28 and 2.09 times, respectively. The mass fraction for longer-chain carboxylic acids in liquid products increased with

resin adsorption. For a four-stage countercurrent MAAD train, the optimal resin loading is 10.9 to 14.6 g wet resin/(L_{liq}·d). This study shows the newly developed integrated system is promising for sustainable production of carboxylic acids and its further application within carboxylate platform.

5. ASSESSMENT OF NUTRIENTS ON METHANE-ARRESTED ANAEROBIC DIGESTION IN THE CARBOXYLATE PLATFORM

5.1. Introduction

In 2020, U.S. energy consumption was 93 quadrillion Btu of which 79% was from fossil fuels.[112] Alternative sources of domestic liquid transportation fuels are necessary because of greenhouse gas emissions, unstable crude oil prices, and unreliable international oil suppliers. To address these issues, liquid biofuels are an important component of our energy future because they can be produced from a wide range of domestic carbon-neutral feedstocks (e.g., wood, straw, and food waste).[113] Currently, liquid biofuels are primarily produced by converting food crops to ethanol; unfortunately, production is limited because of competition with food. This limitation can be overcome by using the sugar platform to convert lignocellulose to sugars that are fermented to ethanol; however, this approach is hindered by high enzyme costs and mandatory sterile operating conditions.[114,115] The carboxylate platform is an alternative pathway that is more resilient and robust, and requires neither enzyme addition nor sterile operating conditions.

Using a mixed culture of marine-derived microorganisms, the carboxylate platform anaerobically digests biomass to carboxylic acids, which are recovered and chemically transformed into industrial chemicals and fuels.[14] It is an example of consolidated bioprocessing (CBP) where enzyme production, saccharification, and anaerobic digestion are integrated in a single process step and thereby reduces

processing costs and increases hydrolysis rates.[12,13] The mixed culture of microorganisms digests nearly all biomass components to carboxylic acids, which consequently contributes to high yields. The carboxylate platform provides a sustainable answer to the energy crisis and waste management struggles that plague many nations.

The MixAlco™ process is an example of the carboxylate platform developed at Texas A&M University. One version involves the following process steps: (1) alkaline pretreatment of lignocellulose removes lignin and exposes cellulose, (2) methane-arrested anaerobic digestion (MAAD) converts all biomass components (except lignin and ash) to carboxylic acids, (3) carboxylic acids are recovered and converted to ketones, (4) ketones are hydrogenated to secondary alcohols, and (5) secondary alcohols are dehydrated and oligomerized to produce hydrocarbons.

The heart of the MixAlco™ process is methane-arrested anaerobic digestion (MAAD). From various perspectives, several studies have been conducted to optimize the process and increase carboxylic acid yields, as elucidated in the following examples. Ross et al. developed countercurrent MAAD to minimize product inhibition and improve biomass conversion.[26] Fu et al. observed chain elongation at lower temperatures ($\leq$ 40°C), but little or no medium-molecular-weight acids at elevated temperatures (55°C).[72] Smith et al. determined the optimal carbon/nitrogen (CN) ratio for MAAD performance is 20 to 40 g C/g N.[76] Roy et al. showed that batch MAAD incorporated with *in-situ* product removal (ISPR) using weak-based anion-exchange resins (Amberlite IRA-67) significantly improves acid yield by 2.2-, 1.54-, and 1.55-fold for α-cellulose, paper, and lime-pretreated corn stover, respectively.[80] In every cited study, lignocellulosic biomass

was co-digested with nutrient-rich substrates such as sewage sludge and chicken manure to maintain an ideal CN ratio and improve MAAD performance.

Sewage sludge (SS) – an urban waste from wastewater treatment – is a concentrated suspension of solids largely composed of nutrient-rich organic matter. In 2019, 4.75 million dry metric tons of SS were generated in the United States, most of which was disposed in landfills, incinerated for electricity production, or applied to agricultural land.[116] Unfortunately, landfills produce the second largest amount of anthropogenic methane in the United States, and incineration releases air pollutants.[35] Sewage sludge is a nutrient-rich substrate that can be co-digested with carbon-rich lignocellulosic biomass. Rughoonundun et al. co-digested sewage sludge (20%) with sugarcane bagasse (80%) to produce a total acid concentration of 61 g/L.[117]

Chicken manure (CM) is a rural waste from both egg layers and broilers. Chicken manure is rich in nitrogen, carbon, and phosphorus, which are macro-nutrient need by microorganisms for robust growth.[35,117,118] In 2017, 11.98 million metric tons of fresh layer manure was produced in the United States, most of which was disposed in landfills, or applied to agricultural land.[119] Unfortunately, poultry and livestock manure account for about 70–90% of total ammonia emissions worldwide.[120] Smith et al. co-digested office paper and wet chicken manure achieving total acid productivity of 0.84 g $acid_{produced}$/(Lliq d).[76]

Nutrients are essential for microbial metabolism and reproduction. Lack of nutrients may result in slow reaction rates, an unstable process, and lower product yields.[121] Both CM and SS contain nutrients, but lack carbohydrates needed for

metabolic energy. Co-digestion of energy- and nutrient-rich feedstocks is a productive and economical way to adjust the carbon-nitrogen ratio and improve MAAD performance.[74]

The MixAlco™ process uses countercurrent MAAD to increase conversion and product concentration. As shown in Figure 1-5, solids are transferred from fermentors F1 to F4, and liquid transfers in the opposite direction from fermentors F4 to F1. F1 has fresh biomass, so high product concentrations are achieved. F4 has low product concentrations, so high conversion is achieved. In the laboratory, countercurrent MAAD is laborious and requires long residence times to reach steady state; therefore, it is too cumbersome for rapid tests of various substrates and microorganisms.[72] To overcome these challenges, Loescher developed the Continuum Particle Distribution Model (CPDM) to predict countercurrent MAAD performance from experimental batch MAAD data.[26,27] CPDM has been shown to have a prediction accuracy within 4–20%.[44,72,73]

This chapter describes batch MAAD performed with unused office paper (energy source) and CM or SS (nutrient sources). Because of their high moisture content, these two nutrient sources have a very short shelf-life; therefore, the effect of different preservation techniques – freezing, air-drying, and baking – was investigated. CPDM was used to predict countercurrent MAAD data from batch data, and thus compare the performance of each nutrient source preserved by various methods. This study was performed with Kejia Liu.

5.2. Material and Methods

5.2.1. Digester

MAAD was implemented in a 1-L polypropylene copolymer (PPCO) bottle (Nalgene®) capped by a rubber stopper with a septum-sealed glass tube (Figure 3-1). Plastic screw caps and aluminum crimp seals ensure airtight conditions. To ensure proper mixing as the digester rotates in the rolling incubator (Wheaton®), two 0.25-in stainless steel tubes are inserted into the rubber stopper.

5.2.2. Substrate

As feedstocks, the MAAD employed unused office paper, sewage sludge, chicken manure, and urea. The properties of the different substrates (Table 5-1) were determined at the Texas A&M Soil, Water and Forage Testing Laboratory. The energy source – unused office paper (Caliber®) – was shredded using a Fellows Powershred® W-6C. The carbon and nitrogen content were approximately 36.30 and 0.07 wt%, respectively.

Antibiotic-free chicken manure was obtained from the Poultry Science Department at Texas A&M University. In previous studies, the chicken manure was oven dried at 105ºC for 48 h and kept in airtight containers at room temperature.[118] In this study, the manure was first homogenized using a Ninja® Foodie™ food processor and then stored using three different techniques (Figure 5-1): (1) immediate freezing of fresh wet manure, (2) air drying at room temperature with a box fan for 48 h before storing in a refrigerator at 4ºC, and (3) baking at 105ºC for 48 h.

Table 5-1. Substrate contents of office paper, urea, chicken manure, and sewage sludge

	Unit	Office paper	Wet Chicken Manure	Air-dried Chicken Manure	Baked Chicken Manure	Wet Sewage Sludge	Air-dried Sewage Sludge	Urea
Moisture content	g/100 g wet sample	5.91	83.6	9.95	5.92	89.1	65.0	-
Ash content	g/100 g wet sample	14.2	23.0	24.8	28.6	20.1	30.1	-
Volatile solids	g/100 g wet sample	85.8	77.0	75.2	71.4	79.9	69.8	-
Carbon	g/100 g wet sample	36.0	35.4	35.4	35.4	42.5	42.5	19.4
Nitrogen	g/100 g wet sample	0.070	4	4	4	6.94	6.94	45.2
C/N ratio	g carbon/g nitrogen	514.7	8.85	8.85	8.85	6.12	6.12	0.43

Figure 5-1. Baked, air-dried, and fresh chicken manure.

Sewage sludge was collected from the Carter Creek Wastewater Treatment Plant (College Station, TX) and centrifuged at 4000 rpm for 10 minutes to achieve 0.109 g total solids/g wet solids (STDEV = ± 0.0108). The supernatant was disposed while the concentrated slurry was preserved using two different techniques (Figure 5-2): (1) immediate freezing of fresh wet sewage sludge, and (2) air drying at room temperature with a box fan for 48 h before storing in a refrigerator at 4ºC. (*Note:* Baking sewage sludge was not considered because results from baked chicken manure were poor.)

Figure 5-2. Air-dried and fresh sewage sludge.

To adjust the carbon-to-nitrogen ratio of the digesters, urea was added. Urea contains nitrogen and carbon contents of 19.35 and 45.16 wt%, respectively. Rughoonundun et al. concluded that the recommended C/N ratio for MAAD is 20 to 40 g C/g N, and noted that the C/N ratio impacts the composition of carboxylic acids if minimal nitrogen is provided.[74] In this study, 31.1 and 25.9 g C/g N were used and the following combination of substrates were anaerobically digested: (1) **BCM** – paper and baked chicken manure at 31.1 g C/g N, (2) **ACM** – paper and air-dried chicken manure at 31.1 g C/g N, (3) **WCM** – paper and wet chicken manure at 31.1 g C/g N, (4) **FCM** – paper and fresh wet chicken manure at 25.9 g C/g N, (5) **WSS** – paper and wet sewage sludge at 25.9 g C/g N, (6) **ADS** – paper and air-dried sewage sludge at 25.9 g C/g N.

5.2.3. Digestion Media and Conditions

Paper and nutrients were added to deoxygenated water (D.O. water), which was prepared by adding 0.275 g/L cysteine hydrochloride and 0.275 g/L sodium sulfide into boiled deionized water (D.I. water). MAAD was performed in a temperature-controlled 40^{o}C incubator equipped with rollers (Wheaton®). Nutrient source (20 wt%) and shredded office paper (80 wt%) were added as substrate into each 1-L PPCO digester. Every 48 h, the pH in the supernatant was measured after the digesters were centrifuged. Sodium bicarbonate ($NaHCO_3$, Fischer) was added to neutralize the carboxylic acids produced during MAAD. If necessary, carbon dioxide was used to lower pH below 7.0.

5.2.4. Inoculum

The original inoculum was a mixed culture of marine microorganisms found in biomass-rich beach sediment collected from Galveston Island, TX. Sediments were dug

from the bottom of multiple 0.5-m-deep shoreline pits. Samples were immediately collected in airtight plastic bottles filled with deoxygenated water, capped, and frozen at –20°C until use. Before inoculation, samples were thawed, shaken vigorously, and allowed to settle by gravity. The resulting supernatant was homogenized, and aliquots (12.5% of the initial working volume) were used as inoculum.[74] A typical composition of the bacterial community in the MAAD has been reported elsewhere.[122] Before marine microorganisms can function fully in a new environment, two to three weeks for inoculum adaptation is required. To ensure high-quality data, broth from the adapted inoculum was used to inoculate the batch MAADs.

5.2.5. Methane Inhibitor

Iodoform (CHI_3) was used to inhibit methane production. Every 48 h, 60 µL of iodoform solution (20 g CHI_3/L 200-proof ethanol) was added to 0.2 L of working volume in each digester. Because of its light, temperature, and air sensitivity, the iodoform was stored in a foil-wrapped amber-colored glass bottle at 4°C.[74]

5.2.6. Batch MAAD

To calculate the necessary empirical constants needed by CPDM, batch MAADs were performed. The substrate concentrations were 20, 40, 70, 100, and 100+ g dry substrate/L liquid; each substrate loading was performed in triplicate.[44] The 100 and 100+ digesters had the same substrate concentration, but 20 g carboxylic acids/L liquid was added to the deoxygenated water in the 100+ group. The added carboxylic acid composition was 16 g acetic acid/L, 1 g propionic acid/L, and 3 g butyric acid/L. This study employed a mixture of 80 wt% carbon source and 20 wt% nutrient sources, which

was recommended by Rapier.[123] Prior to starting the batch MAAD, specific amounts of substrate, inoculum, and MAAD media were specified for each loading (Tables 5-1, 5-2, and 5-3).

Chicken manure employed 31.1 and 25.9 g carbon/g nitrogen. Sewage sludge employed 25.9 g carbon/g nitrogen. Nutrient source (i.e., chicken manure or sewage sludge), office paper, deoxygenated water inoculum, urea (if applicable), methane inhibitor, and buffer (if applicable) were added and completely mixed in the digester. Before start-up, the 1-L PCCO digesters were autoclaved. To initiate each batch MAAD, specific amounts of substrate, inoculum, and digestion media were added (Tables 5-1, 5-2, and 5-3). After loading the components, digesters were purged with nitrogen and placed in the incubator.

The concentration of carboxylic acids produced during anaerobic digestion was quantified as "acetate equivalents" (α) for use in CPDM.

$$\alpha\left(\frac{\text{mol}}{\text{L}}\right) = 1.00 \times (\text{acetic})(\text{mol/L}) + 1.75 \times (\text{propionic})(\text{mol/L}) + 2.50 \times (\text{butyric})(\text{mol/L}) + 3.25 \times (\text{valeric})(\text{mol/L}) + 4.00 \times (\text{caproic})(\text{mol/L}) + 4.75 \times (\text{heptanoic})(\text{mol/L}) + 5.5 \times (\text{octanoic})(\text{mol/L}) \quad (5\text{-}1)$$

The acetate equivalent was converted to a mass basis.

$$\text{Aceq} = 60.05\ (\text{g/mol}) \times \alpha(\text{mol/L}) \quad (5\text{-}2)$$

After 46 days, the digestion was stopped because substantial batch experiment data had been generated to predict the CPDM maps and because the observed total acids concentration showed little signs of increasing.

5.2.7. Analytical Methods

5.2.7.1. Biogas Analysis

Biogas – predominantly carbon dioxide – was continuously formed as a byproduct of MAAD. Every 48 h, because the digester can only tolerate pressures under 2 atm absolute, biogas was vented to prevent explosion. By inserting a needle through the rubber septum on top of the digester, biogas was vented into a graduated column filled with 300 g/L $CaCl_2$ solution, which prevents CO_2 adsorption and microbial growth. The amount of produced biogas was measured by the displaced volume. For composition analysis, a 30-mL biogas sample was injected into the gas chromatograph (GC, Agilent 6890 Series) with a thermal conductivity detector (TCD).

5.2.7.2. Carboxylic Acids Concentration Determination

To measure the concentration of carboxylic acids, the digester contents were centrifuged (4000 rpm, 10 min) and 1-mL liquid samples were taken. Samples were stored in the freezer until analysis. To prepare samples for analysis, they were thawed, vortexed, and centrifuged to separate liquid from solids (Beckman Coulter Microfuge® 16, 13,300 rpm, 10 min). To ensure non-volatile carboxylate salts are converted to volatile carboxylic acids for GC analysis, phosphoric acid was added. In addition, an internal standard was added. Finally, the prepared supernatants were analyzed in a gas chromatograph (Agilent 6890 series) equipped with a flame ionization detector (FID) and autosampler (Agilent 7683 series).

Table 5-2. Initial loadings to start fermentation using chicken manure at 31.1 C/N ratio.

Code	Label	Substrate conc. (g/L)	Working volume (mL)	Inoculum (mL)	Dry office paper (g)	Dry chicken manure (g)	Carboxylic acids (g/L)	Total water volume (mL)
WCM (wet chicken manure)	20-WCM	20	200	25	3.2	0.8	0	175
	40-WCM	40	200	25	6.4	1.6	0	175
	70-WCM	70	200	25	11.2	2.8	0	175
	100-WCM	100	200	25	16	4	0	175
	100^{+}-WCM	100	200	25	16	4	20	171
ACM (air-dried chicken manure)	20-ACM	20	200	25	3.2	1.2	0	175
	40-ACM	40	200	25	6.4	2.4	0	175
	70-ACM	70	200	25	11.2	4.2	0	175
	100-ACM	100	200	25	16	6	0	175
	100^{+}-ACM	100	200	25	16	6	20	171
BCM (baked chicken manure)	20-BCM	20	200	25	3.2	0.8	0	175
	40-BCM	40	200	25	6.4	1.6	0	175
	70-BCM	70	200	25	11.2	2.8	0	175
	100-BCM	100	200	25	16	4	0	175
	100^{+}-BCM	100	200	25	16	4	20	171

Code	Label	Wet office paper (g)	Wet chicken manure (g)	Urea (g)	Total carbon (g)	Total nitrogen (g)	Water in feed (g)	D.O. water (mL)
WCM (wet chicken manure)	20-WCM	3.4	4.87	0.027	1.45	0.056	4.27	170
	40-WCM	6.8	9.74	0.053	2.89	0.112	8.55	166
	70-WCM	11.9	17.05	0.093	5.06	0.195	15	160
	100-WCM	17	24.4	0.133	7.23	0.279	21.4	154
	100^{+}-WCM	17	24.4	0.133	7.23	0.279	21.4	150
ACM (air-dried chicken manure)	20-ACM	3.4	0.89	0.027	1.45	0.056	0.289	175
	40-ACM	6.8	1.78	0.053	2.89	0.112	0.578	174
	70-ACM	11.9	3.11	0.093	5.06	0.195	1.01	174
	100-ACM	17	4.44	0.133	7.23	0.279	1.45	174
	100^{+}-ACM	17	4.44	0.133	7.23	0.279	1.45	170
BCM (baked chicken manure)	20-BCM	3.4	0.85	0.027	1.45	0.056	0.251	175
	40-BCM	6.8	1.70	0.053	2.89	0.112	0.502	175
	70-BCM	11.9	2.98	0.093	5.06	0.195	0.879	174
	100-BCM	17	4.25	0.133	7.23	0.279	1.26	174
	100^{+}-BCM	17	4.25	0.133	7.23	0.279	1.26	170

(Note. D.O. water stands for de-oxygenated water, and the densities of acetic acid, propionic acid, and butyric are 1.05, 0.99, and 0.96 g/cm^3. For the D.O. water required for 100^{+} group. $171.1 = 200 - 25 - 0.2 \cdot \left(\frac{16}{1.05} + \frac{1}{0.99} + \frac{3}{0.96}\right)$).

Table 5-3. Initial loadings to start fermentation using sewage sludge at 25.9 C/N ratio.

Code	Label	Substrate conc. (g/L)	Working volume (mL)	Inoculum (mL)	Dry office paper (g)	Dry sewage sludge (g)	Carboxylic acids (g/L)	Total water volume (mL)
WSS (wet sewage sludge)	20-WSS	20	200	25	3.2	0.8	0	175
	40-WSS	40	200	25	6.4	1.6	0	175
	70-WSS	70	200	25	11.2	2.8	0	175
	100-WSS	100	200	25	16	4	0	175
	100^{+}-WSS	100	200	25	16	4	20	171
ADS (air-dried sewage sludge)	20-ADS	20	200	25	3.2	1.2	0	175
	40-ADS	40	200	25	6.4	2.4	0	175
	70-ADS	70	200	25	11.2	4.2	0	175
	100-ADS	100	200	25	16	6	0	175
	100^{+}-ADS	100	200	25	16	6	20	171

Code	Label	Wet office paper (g)	Wet sewage sludge (g)	Urea (g)	Total carbon (g)	Total nitrogen (g)	Water in feed (g)	D.O. water (mL)
WSS (wet sewage sludge)	20-WSS	3.4	7.34	1.49	0.058	4.97	170	170
	40-WSS	6.8	14.7	2.99	0.115	9.94	165	165
	70-WSS	11.9	25.7	5.23	0.202	17.4	158	158
	100-WSS	17	36.7	7.47	0.289	24.9	150	150
	100^{+}-WSS	17	36.7	7.47	0.289	24.9	146	146
ADS (air-dried sewage sludge)	20-ADS	3.4	2.29	1.49	0.058	1.69	173	173
	40-ADS	6.8	4.57	2.99	0.115	3.37	172	172
	70-ADS	11.9	8	5.23	0.202	5.9	169	169
	100-ADS	17	11.4	7.47	0.289	8.43	167	167
	100^{+}-ADS	17	11.4	7.47	0.289	8.43	163	163

(Note. D.O. water stands for de-oxygenated water, and the densities of acetic acid, propionic acid, and butyric are 1.05, 0.99, and 0.96 g/cm^3. For the D.O. water required for 100^{+} group. $171.1 = 200 - 25 - 0.2 \cdot \left(\frac{16}{1.05} + \frac{1}{0.99} + \frac{3}{0.96}\right)$).

Table 5-4. Initial loadings to start fermentation using chicken manure at 25.9 C/N ratio.

Code	Label	Substrate conc. (g/L)	Working volume (mL)	Inoculum (mL)	Dry office paper (g)	Dry chicken manure (g)	Carboxylic acids (g/L)	Total water volume (mL)
FCM (fresh chicken manure)	20-FCM	20	200	25	3.2	0.8	0	175
	40-FCM	40	200	25	6.4	1.6	0	175
	70-FCM	70	200	25	11.2	2.8	0	175
	100-FCM	100	200	25	16	4	0	175
	100^{+}-FCM	100	200	25	16	4	20	171

Code	Label	Wet office paper (g)	Wet sewage sludge (g)	Urea (g)	Total carbon (g)	Total nitrogen (g)	Water in feed (g)	D.O. water (mL)
FCM (fresh chicken manure)	20-FCM	3.4	4.87	0.048	1.45	0.056	4.3	171
	40-FCM	6.8	9.74	0.096	2.89	0.112	8.6	167
	70-FCM	11.9	17.1	0.168	5.06	0.195	15.0	160
	100-FCM	17	24.4	0.240	7.23	0.279	21.4	154
	100^{+}-FCM	17	24.4	0.240	7.23	0.279	21.4	150

(Note. D.O. water stands for de-oxygenated water, and the densities of acetic acid, propionic acid, and butyric are 1.05, 0.99, and 0.96 g/cm^3. For the D.O. water required for 100^{+} group. $171.1 = 200 - 25 - 0.2 \cdot \left(\frac{16}{1.05} + \frac{1}{0.99} + \frac{3}{0.96}\right)$).

5.2.7.3. Moisture and Ash Content Measurement

The moisture and ash contents were measured as previously described.[24] Moisture content (MC) is defined as the fraction of liquid evaporated from the wet sample after 24-h heating in an oven at 105°C. Calcium hydroxide ($Ca(OH)_2$) was added to liquid samples to convert all volatile acids to their deprotonated form, ensuring that acids are not evaporated in the oven and mistakenly counted as water. Volatile solids (VS) are defined as the mass loss from the dry sample after 24-h heating in the furnace at 550°C. Ash content (AC) is defined as the residue left in the crucible after 24-h combustion in the furnace. The terms defined above are measured to determine the non-acid volatile solids (NAVS):

$$\text{NAVS} = (\text{g total wet weight of sample})(1 - \text{MC})(1 - \text{AC}) - (\text{g carboxylic acid in wet sample}) \quad (5\text{-}3)$$

5.2.8. MAAD Performance Parameters

The non-acid volatile solid (NAVS) is a term that refers to the digestible portion of the biomass. Using NAVS, performance parameters can be defined and estimated to compare different substrate and digestion conditions. In the MixAlco™ process, three parameters are important: conversion, yield, and selectivity.

$$\text{Conversion} = \frac{\text{NAVS}_{\text{digested}}(\text{g})}{\text{NAVS}_{\text{fed}}(\text{g})} \quad (5\text{-}4)$$

$$\text{Yield} = \frac{\text{Total carboxylic acids produced}(\text{g})}{\text{NAVS}_{\text{fed}}(\text{g})} \quad (5\text{-}5)$$

$$\text{Selectivity} = \frac{\text{Total carboxylic acids produced}(\text{g})}{\text{NAVS}_{\text{digested}}(\text{g})} \quad (5\text{-}6)$$

$$\text{NAVS}_{\text{digested}} = \text{NAVS}_{\text{fed}} - \text{NAVS}_{\text{remaining}} \quad (5\text{-}7)$$

$$\mathrm{NAVS_{remaining}} = \mathrm{VS_{liquid}} + \mathrm{VS_{solid}} - \text{Total acid in digester} \quad (5\text{-}8)$$

$$\mathrm{NAVS_{fed}} = \mathrm{VS_{office\ paper}} + \mathrm{VS_{nutrient}} + \mathrm{VS_{urea}} - \text{Initial acids present} \quad (5\text{-}9)$$

5.2.9. Continuum Particle Distribution Method

The Continuum Particle Distribution Model (CPDM) uses a continuous conversion distribution function to model anaerobic digestion. Different from time-parameterized functions, it tracks biomass particles as they move through the MAAD train. CPDM is used for the following reasons: (1) it can simulate the performance of countercurrent MAAD using batch data with different substrate loadings, (2) it avoids laborious countercurrent MAAD under a wide range of conditions, (3) it is easy to apply even when the relationship between reactivity and residence time is not uniform, (4) it tracks particles that are contained in a closed conversion domain from 0 to 1, (5) it is robust and resilient, and (6) it can apply to both linear and nonlinear kinetics. CPDM quantitatively accounts for liquid-phase dependencies and effects of particle conversion, while allowing for generalized reaction-rate models to be used for specific reaction systems.[27]

The Continuum Particle Distribution Model (CPDM) uses a continuous conversion distribution function to model fermentation. Different from time-parameterized functions, it tracks biomass particles as they move through the fermentation train. CPDM quantitatively accounts for liquid-phase dependencies and effects of particle conversion, while allowing for generalized reaction-rate models to be used for specific reaction systems.[27]

The acetate equivalents from the five batch substrate loadings were fit to the following empirical equation.

$$\text{Aceq}\ (t) = a + \frac{bt}{1+ct} \tag{5-10}$$

where *t* is the time in days, and *a*, *b*, and *c* are empirical constants determined by the least squares method. The reaction rate was determined by differentiating Aceq (*t*) (Equation 1).

$$r = \frac{\mathrm{d}(\text{Aceq}(t))}{\mathrm{d}t} = \frac{b}{(1+ct)^2} \tag{5-11}$$

The specific reaction rate ($\hat{r}$, the reaction rate per particle) was calculated using Equation 5-12 where S_o represents the initial substrate concentration (g volatile solids/L) calculated by dividing the mass of initial substrate (g volatile solid) by the working volume of the fermentor.

$$\hat{r} = \frac{r}{S_o} \tag{5-12}$$

In the batch fermentations, conversion $x(t)$ was calculated through the following equation

$$x(t) = \frac{\text{Aceq}(t) - \text{Aceq}(0)}{S_o \cdot \sigma} \tag{5-13}$$

where σ is selectivity (g Aceq produced/g VS digested). Selectivity σ is assumed constant throughout all substrate concentrations and is derived from selectivity *s* (g total acids produced/g VS digested) and φ, the ratio of total grams of carboxylic acid produced to total grams of Aceq.

$$\sigma = \frac{s}{\varphi} \tag{5-14}$$

The measured values of conversion $x(t)$, acetate equivalence Aceq(t), and acid-to-Aceq ratio φ were fit to Equation 5-15 where e, f, g, and h are empirical constants determined by the least square's method.

$$\hat{r}_{pred} = \frac{e(1-x)^f}{1+g(\varphi \cdot Aceq)^h} \quad (5\text{-}15)$$

For each set of batch experiments, Equation 5-15 and the corresponding set of fitted empirical constants (e, f, g, and h) were used in a MATLAB program to simulate four-stage countercurrent MAAD with different volatile solids loading rates (VSLR) and liquid retention times (LRT).[44] The MATLAB program produced an array of predicted values of carboxylic acid concentration and conversion for the countercurrent MAAD at various VSLR and LRT. These values were then used to plot the CPDM "map" displaying acid concentration exiting F1 (y-axis) and conversion exiting F4 (x-axis) for various VSLR and LRT values.

5.2.10. Statistical Analysis

All statistical methods and calculations were performed using Microsoft Excel and JMP. Microsoft Excel was used to calculate averages, standard deviations, and confidence intervals. Using JMP, Tukey's mean separation test was performed to estimate significant difference between treatments. Statically significant difference was indicated using letters (a, b, c, ab, etc.) located above or beside data points. Treatments that share a common letter are statistically similar. Treatments not sharing a common letter are significantly different. The "Solver" tool in Microsoft Excel was used to calculate the empirical constants a, b, c, e, f, g, and h. The least squares method was performed by minimizing the sum of the residuals squared, where the residual is the

difference between the experimental and predicted values. A confidence interval of 95% was used for all reported carboxylic acid concentrations.

5.3. Results and Discussion

5.3.1. Total Acid Production

Figure 5-3 displays the total acids produced from all batch MAADs. At 20 g dry substrate/L, there is a clear difference in acids produced from wet and dry feedstocks. At this substrate concentration, WCM and FCM produced 62.5% more acids than BCM and ADS, whereas WSS produced 33% more acids than ADS. At substrate concentrations of 20 and 40 g/L, BCM and ADS produce similar amounts of acids. However, at 70 and 100 g/L, BCM produced the smallest quantity of acids. In fact, at substrate concentrations of 40, 70, and 100 g/L, WCM produced ~100% more acids than BCM. Therefore, baking chicken manure significantly reduced the total acids produced during anaerobic digestion.

At lower substrate concentrations (20 g/L), the difference was not as pronounced possibly because of lower product inhibition. However, at higher substrate concentrations, the negative impact of drying was revealed. Another notable observation is ACM vs. BCM. At lower substrate concentrations (20 and 40 g/L), ACM produced slightly more acids than BCM. However, compared to BCM at 70 and 100 g dry substrate/L, ACM produces ~75% and ~46% more acids, respectively. At lower substrate concentrations, WSS outperformed ADS but both performed similarly at high substrate concentrations. This is possibly because ADS, despite being air-dried like ACM, had a substantial moisture content of 65 g/100 g wet sample, which was several

times higher than BCM and ACM. In fact, ADS was not as dry as BCM and ACM. At 100+ g dry substrate/L, product inhibition affects all the groups resulting in statistically similar total acids produced.

5.3.2. Acid Composition

Figure 5-4 compares the acid composition of all groups. Acetic, propionic, and butyric acids are the major fractions of total acid production. Similarly Chen et al. discovered that acetic acid is the chief component among the total volatile fatty acids produced in anaerobic digesters that produce biogas (methane + carbon dioxide).[124] The acid composition profile is similar for BCM, ACM, and WCM, all of which were operated at a 31.1 C/N ratio. These profiles had very little proportions of medium-molecular-weight acids (C5–C8). FCM, WSS, and ADS, which were operated at a 25.9 C/N ratio, yielded significant amounts of medium-molecular-weight acids. This corroborates the results obtained by Rughoonundun et al. in which an increase in the percentage of medium-molecular-weight acids was observed as the C/N ratio was decreased.[74]

According to Golub et al., medium-molecular-weight acids are produced when the digesters are not exposed to air.[104] However, in this study, all digesters were handled similarly. Nonetheless, at substrate concentrations of 70 and 100 g/L, WSS and ADS produced significantly more medium-molecular-weight acids than FCM. Medium-molecular-weight acids are mainly associated with the fermentation of proteins or chain-elongation of other acids via *reverse β-oxidation*.[124,125] Using sewage sludge benefited production of medium-molecular-weight acids probably because of a higher protein

content in the sewage sludge or a higher amount of reduced species that facilitate chain elongation reactions.

5.3.3. Acetate Equivalent

Figures 5-5–5-9 display the Aceq concentrations obtained from all the batch MAAD. The Aceq values are fit to Equation 5-15 and used to estimate the CPDM statistical parameters. The batch MAAD were run for 45 days. After 34 days, Aceq yields tended to stabilize. Yield is defined as *exit yield*, which quantifies the total acid exiting the MAAD, including product removed during sampling. Generally, higher substrate concentrations result in greater Aceq yields; however, because of extra product inhibition in the 100+ groups, yield grows more slowly than the other groups. Among all the chicken manure samples at 31.1 C/N ratio, WCM has the highest Aceq concentration and performed the best.

This result suggests that air- and oven-dried nutrients sources had poorer results because drying killed a desirable portion of the microbial community, and/or some essential components were damaged or volatilized. Golub studied the effect of sterilizing, drying, and freezing on chicken manure and found that the best-performing MAAD were run with chicken manure that was wet and never frozen; the worst-performing MAAD used chicken manure that was oven-dried and previously frozen.[24] WSS and ADS had similar Aceq yields. It should be noted that although ADS sludge was air dried, it still contained 65.0% moisture.

5.3.4. Gas Composition and Yields

During the experiment, biogas was randomly sampled from two digesters and was analyzed in the gas chromatograph (Agilent 6890 series). The biogas consists of carbon dioxide and nitrogen (from purging during sampling). In some samples, some oxygen (< 1%) was detected. Likely, this occurs because of insufficient purging of the digesters. At the beginning, up to 31% carbon dioxide was detected. No methane was detected; thus, iodoform blocked methanogens. Figure 5-10 shows the total gas produced from all batch MAADs. At 20 g/L substrate concentration, chicken manure batches produced more gas than sewage sludge batches. For all substrate combinations, similar volumes of gas are produced at every other substrate concentration.

5.3.5. MAAD Performance Parameters

Batch MAAD performance was characterized using conversion, yield, and selectivity. The performance parameters are listed in Table 5-5 and displayed in Figure 5-11. Only the parameters at 100 g dry substrate/L are reported because high substrate concentrations are more ideal for comparison with previous studies, and for industrial applications.

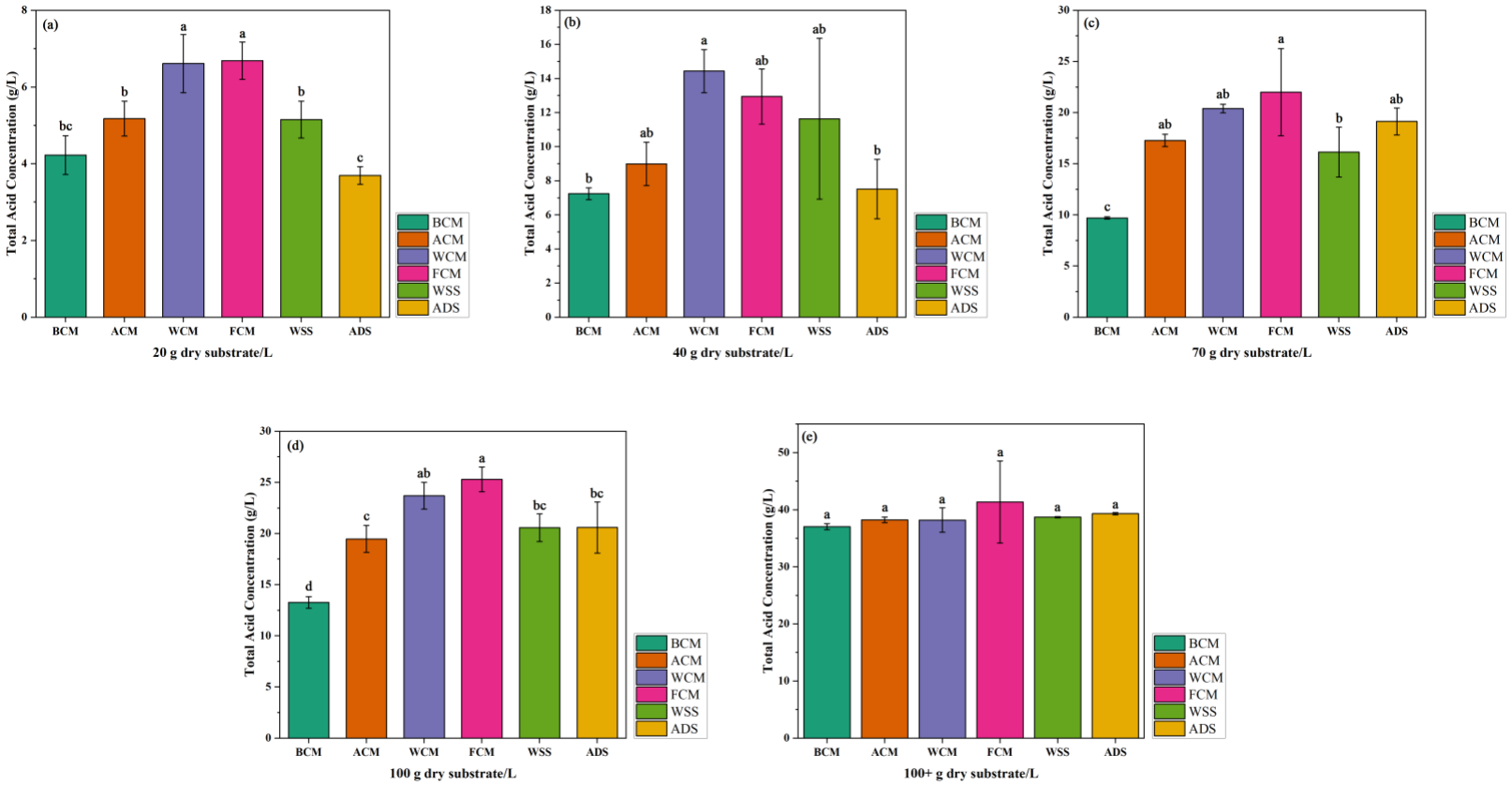

Figure 5-3. Total acids produced.

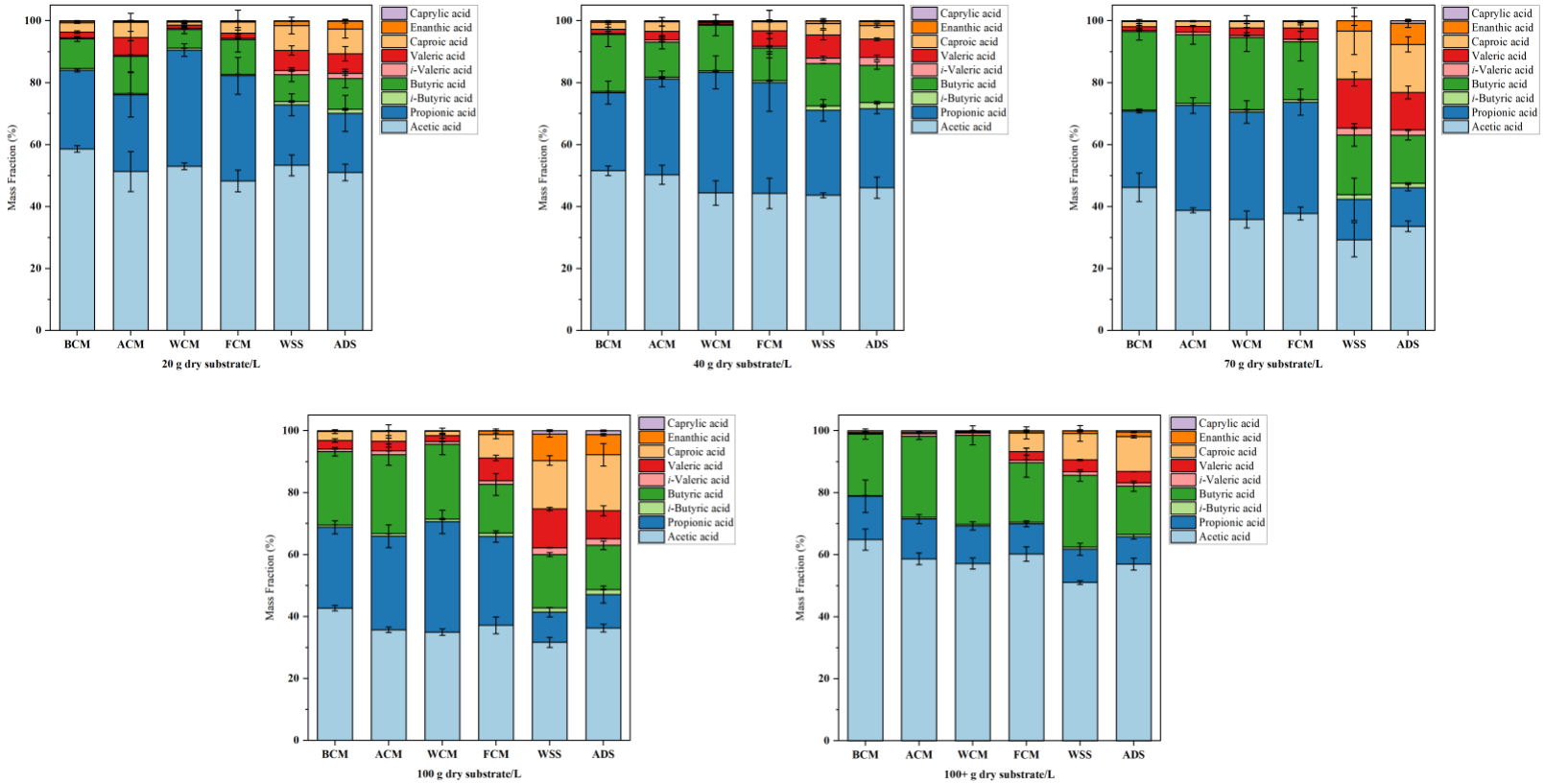

Figure 5-4. Final carboxylic acid composition.

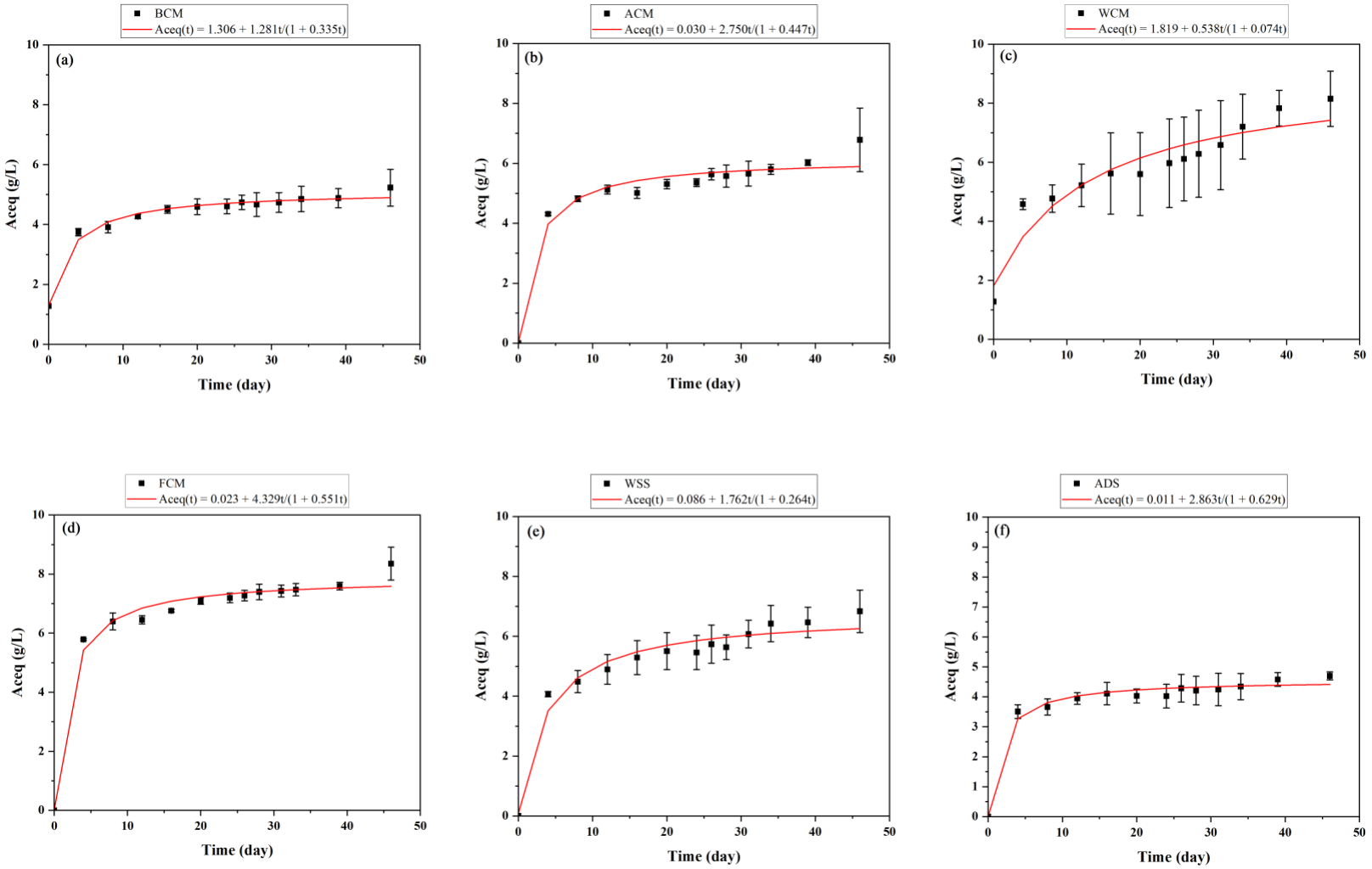

Figure 5-5. Aceq concentration profiles for each feedstock based on 20 g/L substrate concentration.

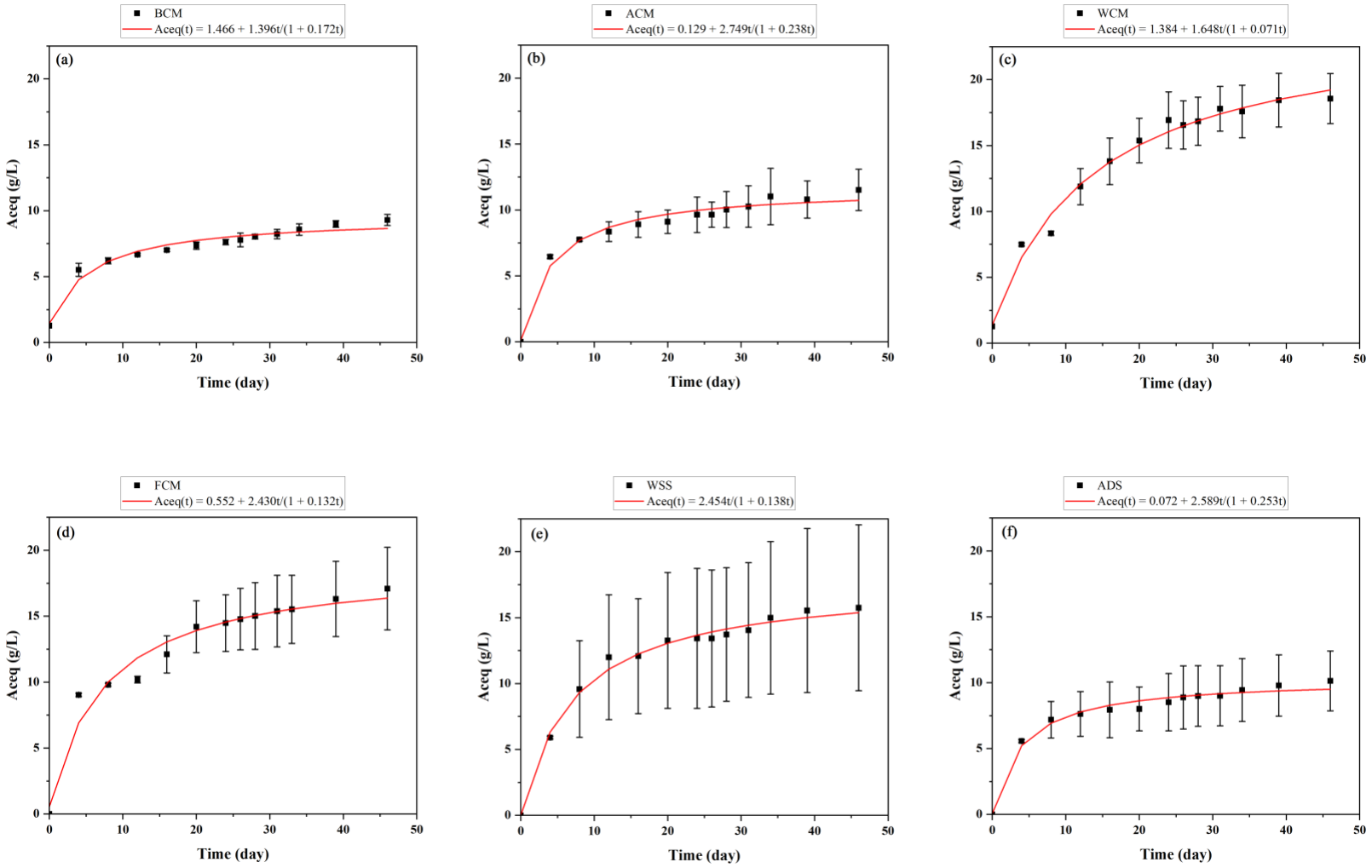

Figure 5-6. Aceq concentration profiles for each feedstock based on 40 g/L substrate concentration.

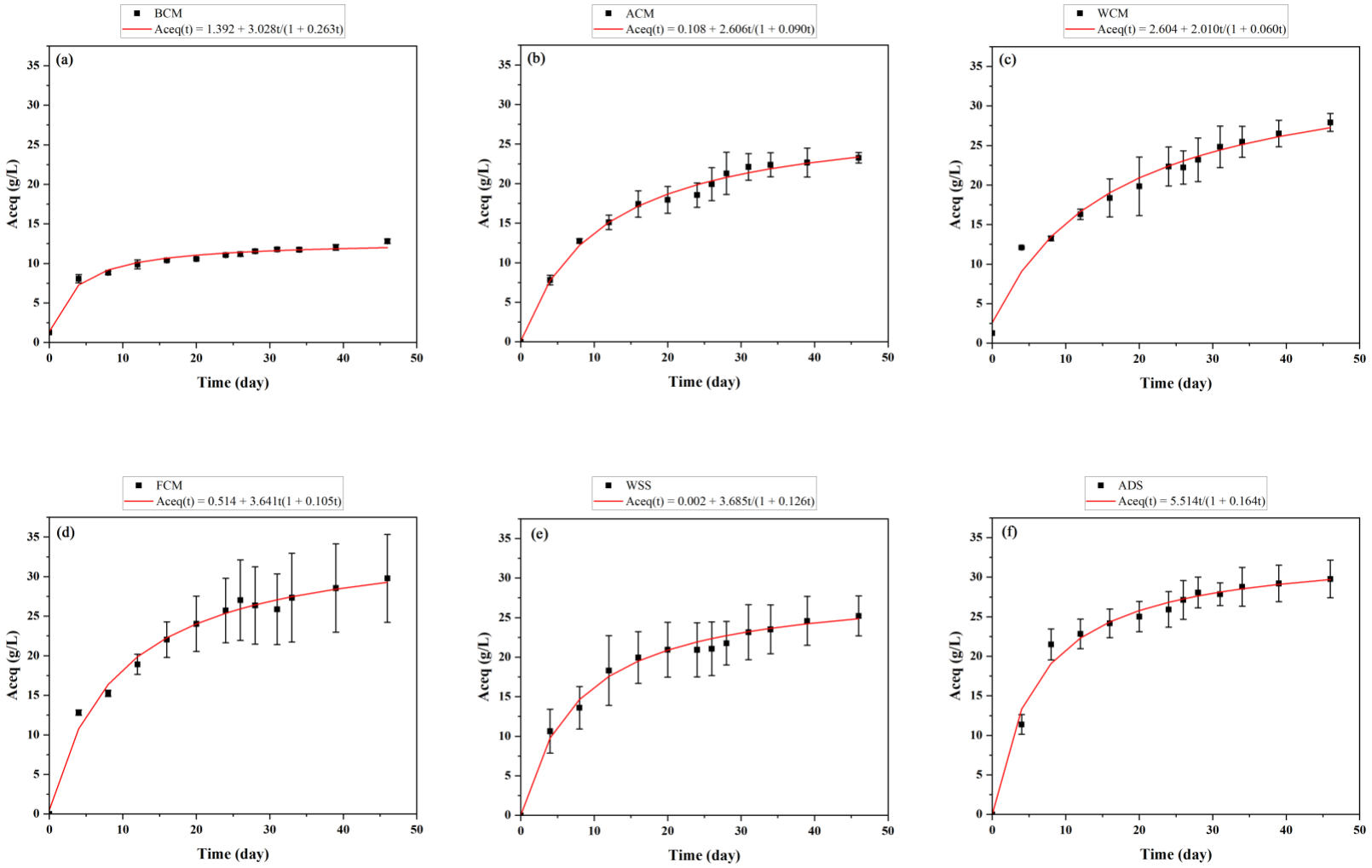

Figure 5-7. Aceq concentration profiles for each feedstock based on 70 g/L substrate concentration.

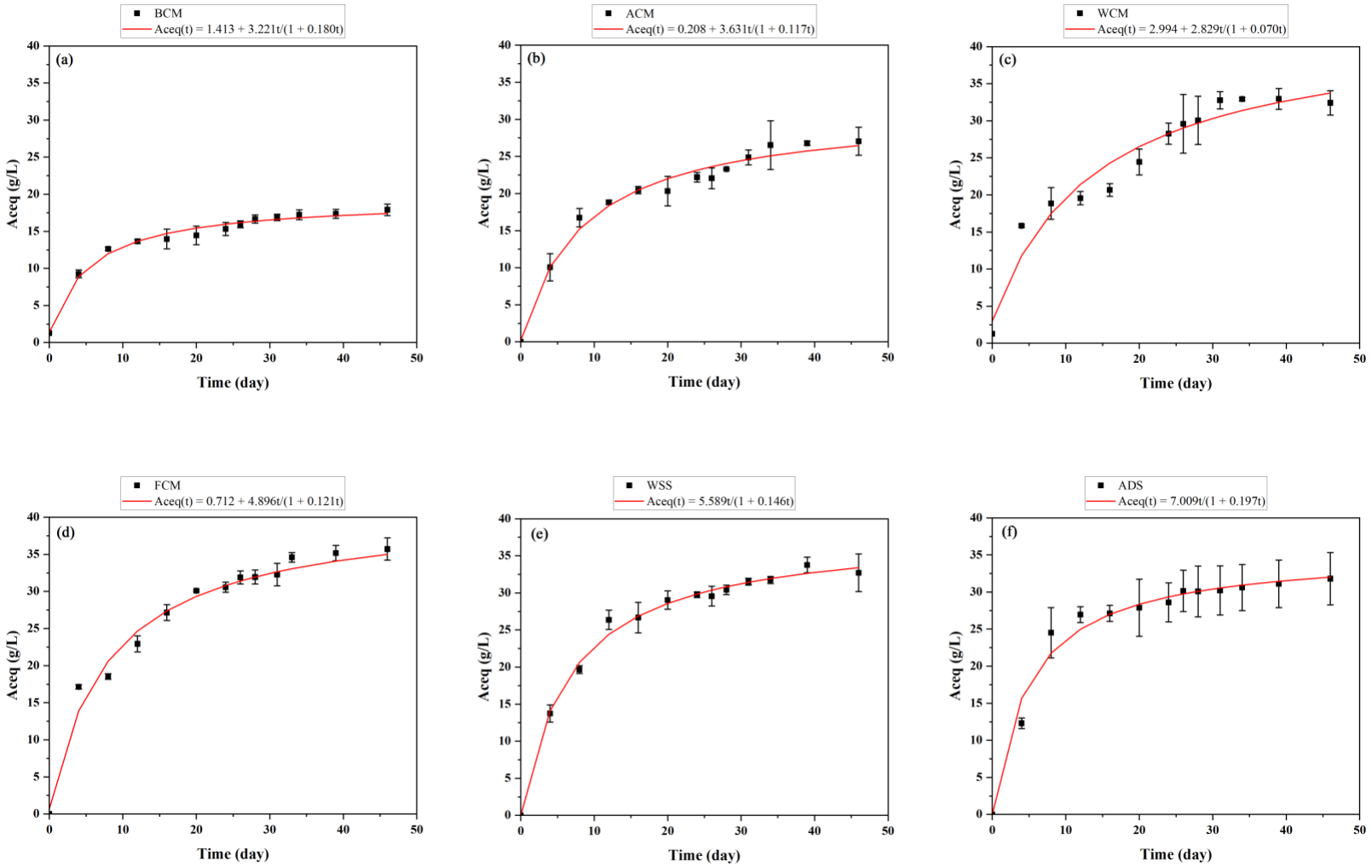

Figure 5-8. Aceq concentration profiles for each feedstock based on 100 g/L substrate concentration.

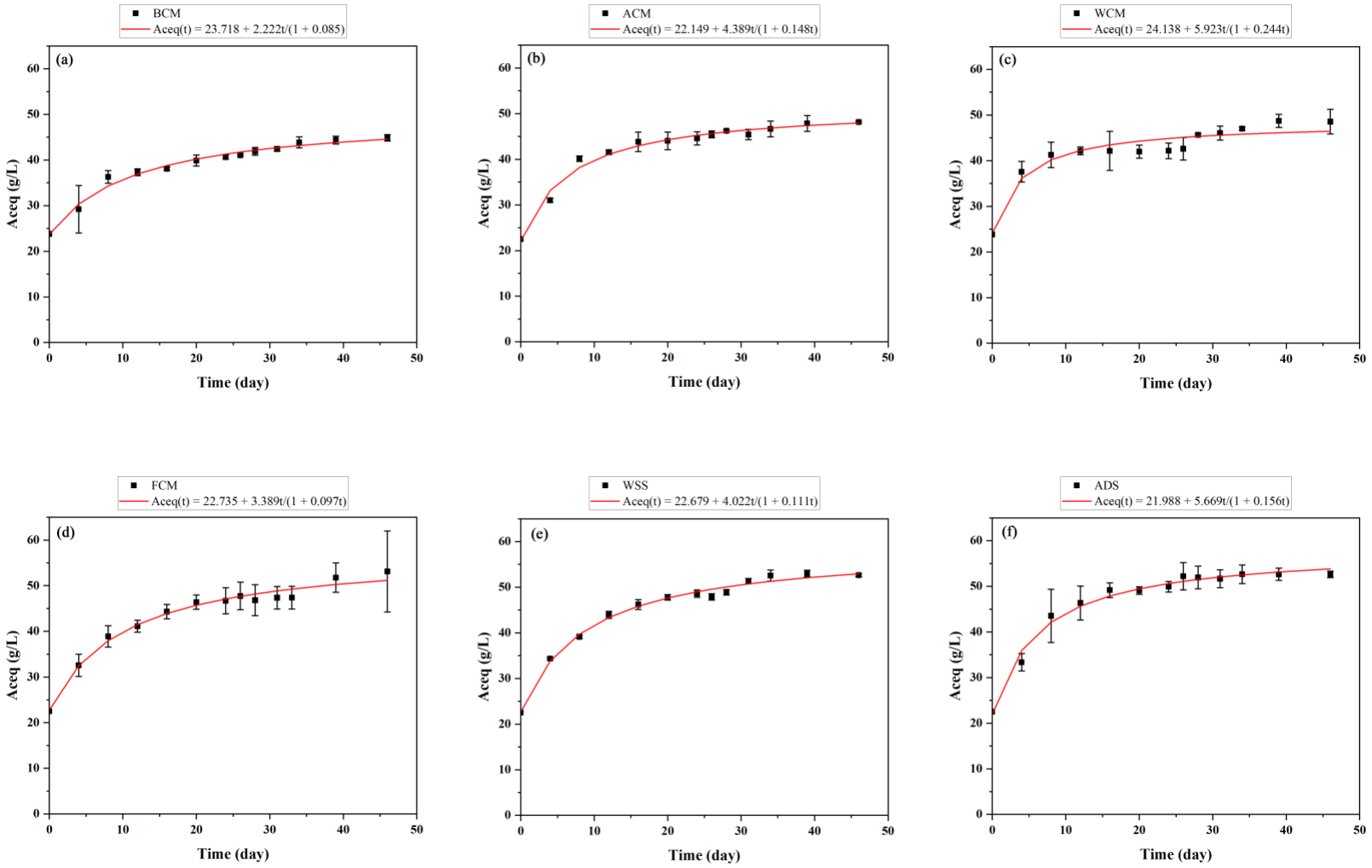

Figure 5-9. Aceq concentration profiles for each feedstock based on 100+ g/L substrate concentration.

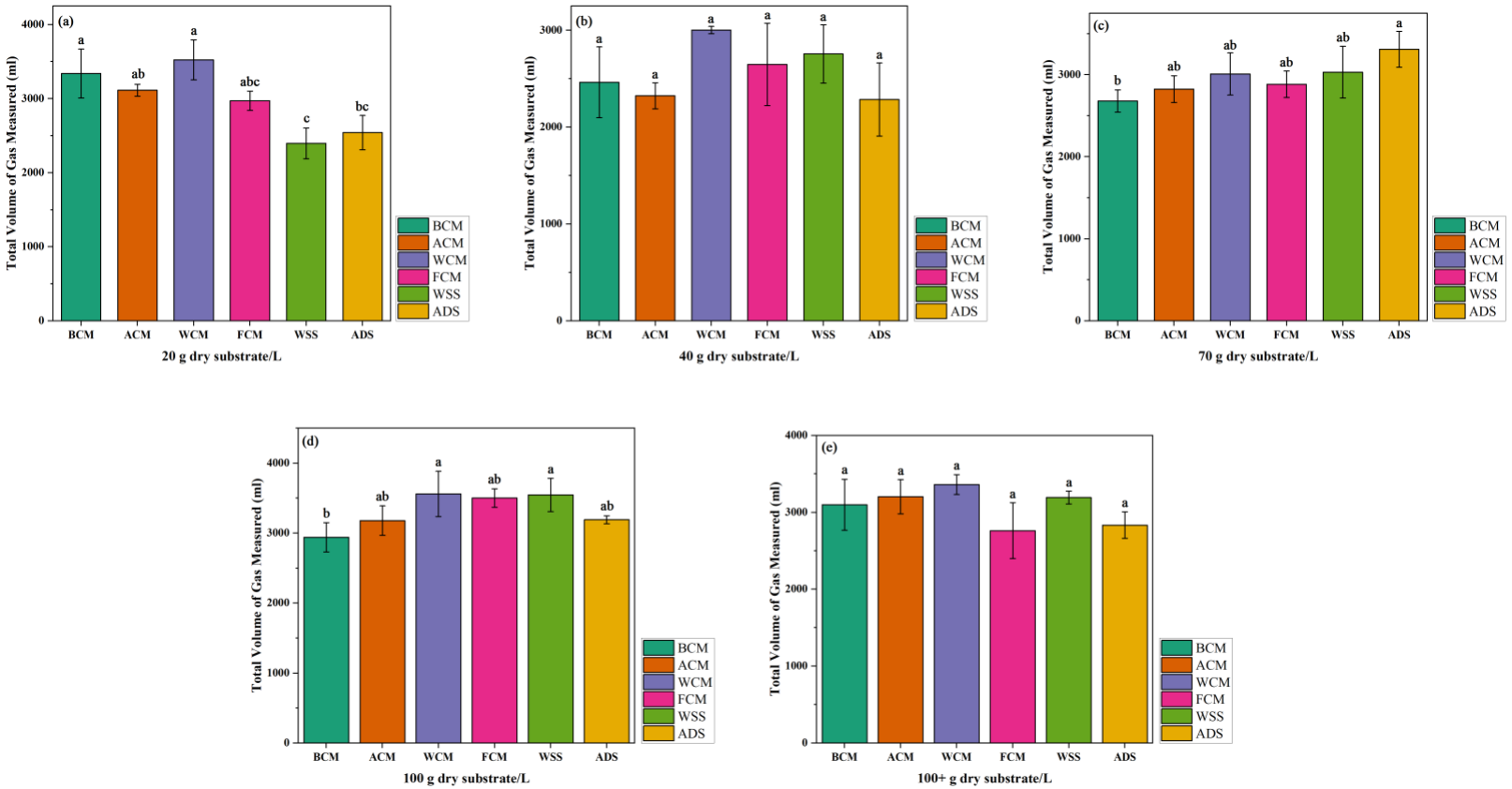

Figure 5-10. Total gas volume measured.

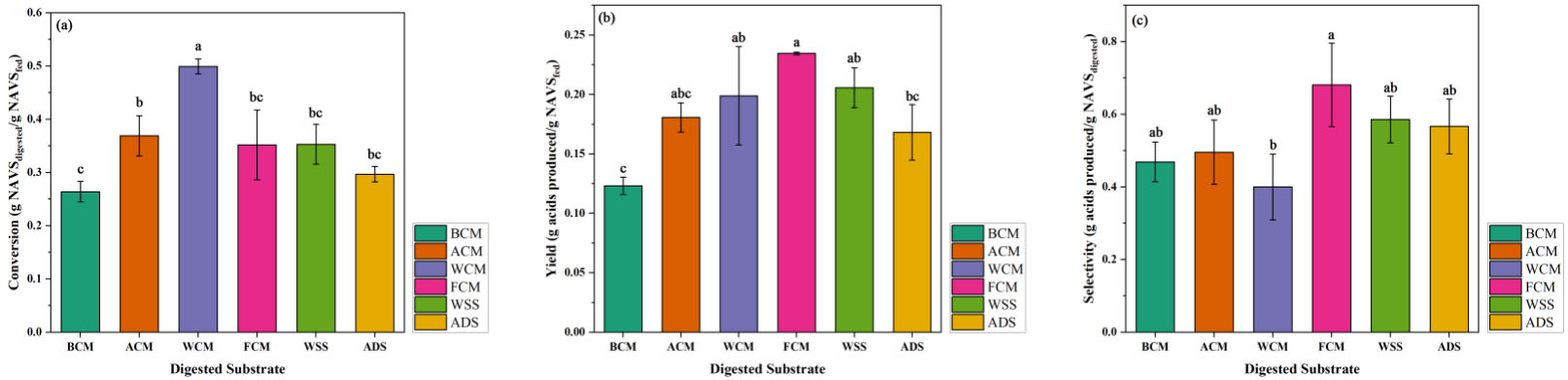

Figure 5-11. MAAD performance parameters for all feedstocks at substrate concentration of 100 g dry substrate/L.

Table 5-5. MAAD performance parameters for all feedstocks at substrate concentration of 100 g dry substrate/L.

Parameter	BCM	ACM	WCM	FCM	WSS	ADS
Conversion (g NAVS digested/g NAVS fed)	0.26 ± 0.02	0.37 ± 0.04	0.50 ± 0.01	0.35 ± 0.07	0.35 ± 0.04	0.30 ± 0.01
Yield (g total carboxylic acid produced/g NAVS fed)	0.12 ± 0.01	0.18 ± 0.01	0.20 ± 0.04	0.23 ± 0.00	0.21 ± 0.02	0.17 ± 0.02
Selectivity (g total carboxylic acid produced/g NAVS digested)	0.47 ± 0.05	0.50 ± 0.09	0.40 ± 0.09	0.68 ± 0.11	0.59 ± 0.06	0.57 ± 0.08

5.3.5.1. Conversion

Conversion is a measure of the amount of substrate consumed during anaerobic digestion. At 25.9 C/N ratio, conversion shows a high sensitivity to the kind of chicken manure used. WCM improved conversion by 35% compared to ACM and 92% compared to BCM. WCM had a 43% increase in conversion compared to FCM. The higher C/N ratio used in WCM seems to have increased the consumption of volatile solids (VS) present in the feed.

The above results corroborate previous studies which revealed that within an optimal C/N ratio range, conversion increases as C/N ratio increases.[74] In anaerobic digesters, microbial metabolic activity is significantly affected by the C/N ratio because microorganisms utilize carbon 25–30 times faster than nitrogen.[126] At 25.9 C/N ratio, there is no significant difference in conversion. FCM and WSS had the exact same conversion of 0.35 g NAVS digested/g NAVS fed. Despite air-drying of sewage sludge, ADS still performs almost as well as WSS.

5.3.5.2. Yield

Yield is a measure of the quantity of acids produced from the fed substrate. At 25.9 C/N ratio, FCM produced the highest yield among all the batches. FCM and WSS produced similar yields. ADS performed slightly below WSS. Regardless of the C/N ratio, every fresh substrate (WCM, FCM, WSS) performed significantly better than BCM. BCM produced the lowest yield 50, 67, 92, 75, and 42% lower than ACM, WCM, FCM, WSS, and ADS, respectively.

The above results further prove that baking the chicken manure has a detrimental impact on MAAD performance. According to a previous study, when proteins in dairy products were heated, they lost their solubility and functionality.[127] Perhaps the proteins in the chicken manure were rendered unusable by the baking process. However, air-drying chicken manure and sewage sludge did not have as much of a detrimental effect as baking. Because air-drying was performed at room temperatures, most of the nutrient content was not denatured or destroyed, which explains why ACM and ADS performed better than BCM.

Fresh chicken manure and fresh sewage sludge performed the best possibly because of readily available soluble nutrients and the impact of microbial activity on MAAD performance. According to studies by Nodar et al. and Nascimento et al., both fresh chicken manure and wet sewage sludge possess a high density and diversity of microorganisms.[128,129] When this dense and diverse microbial community interacts with the adapted inoculum fed into each digester, a more robust mixed-culture could form. Possibly, this new mixed culture can more efficiently utilize the substrate thereby leading to better MAAD performance.

5.3.5.3. Selectivity

Selectivity is a measure of the amount of digested substrate used to produce acids. Low selectivity (< 0.5) values signifies that most of the substrate was utilized for cell growth and multiplication. High selectivity (> 0.5) values implies that a larger portion of the substrate was converted to carboxylic acids. According to Figure 5-11(c), selectivity values were similar for most batches implying that selectivity is mildly

sensitive to the choice of feedstock. Selectivity of experiments at 25.9 C/N ratio was greater than at 31.1 C/N ratio. FCM had a significantly higher selectivity than WCM.

5.3.6. CPDM map

As previously described, using data from batch MAAD, empirical constants *e, f, g,* and *h* (Equation 5-15) were calculated by minimizing the sum of square errors between the experimental and predicted Aceq values. For ADS and WCM, to obtain a better fit, the inhibitor term (*h*) was set within a suggested range ($0.3 < h < 5$). Selectivity (σ) and ratio of carboxylic acids to Aceq (φ) were assumed to be constant. The specific rate ($\hat{r}$) models are listed below:

$$\hat{r}_{ACM} = \frac{0.0819(1-x)^{4.6842}}{1+0.0808(0.7587\cdot\text{Aceq})^{0.6500}} \quad (5\text{-}16)$$

$$\hat{r}_{BCM} = \frac{0.0602(1-x)^{7.6939}}{1+0.1202(0.7808\cdot\text{Aceq})^{0.6730}} \quad (5\text{-}17)$$

$$\hat{r}_{WCM} = \frac{0.0435(1-x)^{2.1645}}{1+0.001(0.7669\cdot\text{Aceq})^{1.7600}} \quad (5\text{-}18)$$

$$\hat{r}_{FCM} = \frac{0.1112(1-x)^{4.1429}}{1+0.009(0.7501\cdot\text{Aceq})^{1.8100}} \quad (5\text{-}19)$$

$$\hat{r}_{ADS} = \frac{0.1104(1-x)^{6.5190}}{1+0.1677(0.7017\cdot\text{Aceq})^{0.4000}} \quad (5\text{-}20)$$

$$\hat{r}_{WSS} = \frac{0.075(1-x)^{3.6381}}{1+0.0690(0.6990\cdot\text{Aceq})^{1.0000}} \quad (5\text{-}21)$$

Based on the above specific rate ($\hat{r}$) models, the CPDM maps were subsequently created to predict total acid concentrations and conversions for four-stage countercurrent MAAD with VSLR from 2 to 12 g/(L·day) and LRT from 5 to 35 days. As VSLR increases, the dominant impact is a decline in conversion. Similarly, as LRT increases, the dominant impact is an increase in acid concentration. Industry desires both high

conversion and high acid concentration, so the preferred location is the upper right of the CPDM map.

The CPDM maps simultaneously discussed in the next three sections all correspond to 100 g NAVS/L liquid, which is a typical solid loading in laboratory digesters where 48 h of liquid accumulates and then is moved through the MAAD train. In the fourth section, the solids loading increases to 300 g NAVS/L liquid, which is representative of an industrial digester that continuously withdraws liquid and moves it countercurrently through the digester train.

5.3.6.1. Chicken Manure at 31.1 C/N Ratio

Figure 5-12 shows predicted total acid concentrations and conversion at different VSLR and LRT using 80 wt% office paper and 20 wt% chicken manure with different treatments. In general, the CPDM map shifted towards the upper right from BCM to ACM, and then from ACM to WCM. These results are consistent with the batch data and show that drying negatively affects substrate digestibility, particularly when the nutrient source is oven baked. At each condition, BCM has the worst performance. At high VSLR, the difference between ACM and WCM is not clear; however, WCM has higher acid concentration and conversion at low VSLR of 2 g/(L·day). When WCM serves as a nutrient source, the highest acid concentration (32.3 g/L) is acquired at VSLR of 4 g/(L·day) and LRT of 35 days, whereas the highest conversion (0.82 g $NAVS_{digested}$/g $NAVS_{feed}$) is acquired at VSLR of 2 g/(L·day) and LRT of 5 days.

Figure 5-12. CPDM map for countercurrent fermentation at 100 g NAVS/L liquid using 80 wt% office paper and 20 wt% chicken manure at 31.1 g carbon/g nitrogen. (*Note:* The *y*-axis is actual acid concentration, not Aceq.)

5.3.6.2. Chicken Manure at 31.1 C/N Ratio vs. Chicken Manure at 25.9 C/N Ratio

As shown in Figure 5-13, even though two experiments were conducted within the recommended range of C/N ratio, there are still differences in acid concentration and conversion. At VSLR of 6 g/(L·day) and LRT of 35 days, FCM has its peak acid concentration of 29.3 g/L and conversion of 0.41 g $NAVS_{digested}$/g $NAVS_{feed}$. By increasing the C/N ratio to 31.1 g carbon/g nitrogen, the highest acid concentration reached 32.3 g/L. Rughoonundun et al. [74] investigated the influence of carbon-to-nitrogen ratio. She showed that even though acid concentration fluctuates when C/N

ratio falls within the recommended range, it is relatively constant. In her study, yield was mostly affected at extreme C/N ratio (C/N > 31.8 and C/N ratio < 13.2).

Figure 5-13. CPDM map for countercurrent fermentation at 100 g NAVS/L liquid using 80 wt% office paper and 20 wt% wet chicken manure at 25.9 and 31.1 g carbon/g nitrogen. (*Note:* The *y*-axis is actual acid concentration, not Aceq.)

5.3.6.3. Chicken Manure at 25.9 C/N Ratio vs. Sewage Sludge at 25.9 C/N Ratio

Figure 5-14 shows the CPDM maps for four-stage countercurrent MAAD for ADS, WSS, and FCM, all of which have the same C/N ratio. For all groups, total acid concentration is relatively constant at each LRT. When MAADs were performed using air-dried sewage sludge at VSLR of 8 g/(L·day) and LRT of 35 days, the highest acid concentration was achieved (29.6 g/L). Compared to ADS, WSS has greater changes in

conversion with respect to VSLR, which is from 0.22 to 0.66 g $NAVS_{digested}$/g $NAVS_{feed}$. For FCM and WSS, the CPDM map is generally shifted to the upper right, from WSS to FCM. At each VSLR and LRT, MAAD is predicted to have better performance using wet chicken manure than wet sewage sludge. Highest conversion (0.67 g $NAVS_{digested}$/g $NAVS_{feed}$) appears when wet chicken manure serves as nutrients and VSLR and LRT are set at 6 g/(L·day) and 5 days.

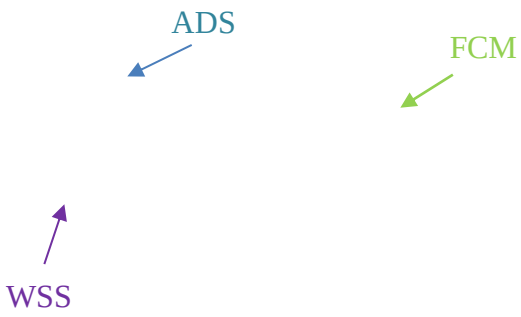

Figure 5-14. CPDM map for countercurrent fermentation at 100 g NAVS/L liquid using 80 wt% office paper and 20 wt% wet chicken manure or sewage sludge at 25.9 g carbon/g nitrogen. (*Note:* The *y*-axis is actual acid concentration, not Aceq.)

5.3.6.4. CPDM Map using Chicken Manure or Sludge as Nutrients at 300 g NAVS/L liquid

Figures 5-15, 5-16, and 5-17 show CPDM maps for 300 g NAVS/L liquid, which represents the highest substrate concentration that could be employed in industrial-scale operations. The model does not work at VSLR of 2 g/(L·day). This occurs because the consumption rate is faster than the daily loading rate, which fails to maintain the amount of retained solids required to maintain the substrate concentration. At each condition, because solid retention time increases at low VSLR, conversion and acid concentration improve. In Figure 5-16, when using WCM as nutrients, the highest conversion (0.89 g $NAVS_{digested}$/g $NAVS_{feed}$) and acid concentration (52.8 g/L) are acquired. In Figure 5-17, although FCM and WCM were both conducted within the recommended C/N range, because of increasing substrate concentration, differences in acid concentration and conversion become more prominent. In Figure 5-17, WSS has higher acid concentration than FCM, which is different from the results in laboratory-scale operations. At VSLR of 12 g/(L·day) and LRT of 35 days, ADS has the highest acid concentration (52.4 g/L). Compared to WSS and FCM, ADS has a narrow conversion range.

In all cases, predictions from CPDM maps must be verified using continuous countercurrent MAAD.

Figure 5-15. CPDM map for countercurrent fermentation at 300 g NAVS/L liquid using 80 wt% office paper and 20 wt% wet chicken manure at 31.1 g carbon/g nitrogen. (*Note:* The *y*-axis is actual acid concentration, not Aceq.)

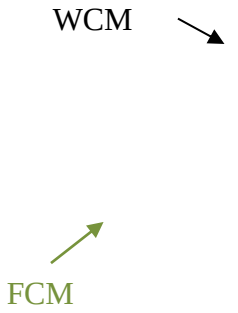

Figure 5-16. CPDM map for countercurrent fermentation at 300 g NAVS/L liquid using 80 wt% office paper and 20 wt% wet chicken manure at 25.9 and 31.1 g carbon/g nitrogen. (*Note:* The *y*-axis is actual acid concentration, not Aceq.)

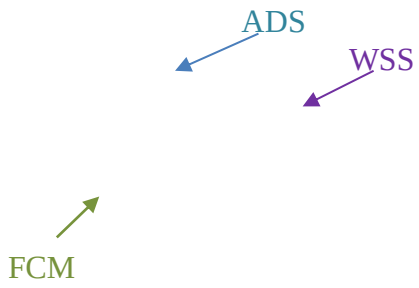

Figure 5-17. CPDM map for countercurrent fermentation at 300 g NAVS/L liquid using 80 wt% office paper and 20 wt% wet chicken manure or sewage sludge at 25.9 g carbon/g nitrogen. (*Note:* The *y*-axis is actual acid concentration, not Aceq.)

5.4. Conclusion

Both chicken manure (without antibiotics) and sewage sludge are valuable nutrients for MAAD. For fresh wet nutrients preserved by freezing, the CPDM maps for chicken manure and sewage sludge were similar. In general, compared to dried nutrients, fresh nutrients yield higher conversions, product yields, and acid concentrations. An exception is air-dried sewage sludge, which has higher product concentrations at high VSLR; however, low conversions make this an unattractive operating regime. Considering that wet nutrients are difficult to transport, it may be acceptable to air-dry sewage sludge and accept a slight reduction in performance. Another option is to utilize wet nutrients at their point of production. This will involve the construction of anaerobic digesters at farms and wastewater treatment plants.

6. METHANE-ARRESTED ANAEROBIC DIGESTION OF PRICKLY PEAR CLADODES

6.1. Introduction

In a globalized economy, affordable transportation is crucial. Most imports and exports are transported using cargo ships or planes. These heavy-duty vehicles require energy-dense fuels, such as diesel and jet fuel. Therefore, to reduce the carbon footprint of heavy-duty vehicles, liquid biofuels are a more suitable replacement than renewable electricity (solar and wind). First-generation liquid biofuels are produced primarily from food crops such as corn, sugarcane, and oil seeds; however, they have high production costs and compete for land and water used for food production.[4,71] Second-generation biofuels are produced from lignocellulosic non-food biomass such as corn stover, cereal straw, sugarcane bagasse, switchgrass, agricultural residue, and municipal solid wastes.[4]

Lignocellulosic biomass is the world's fourth largest energy source behind oil, coal, and gas, respectively.[71] Lignocellulose is converted to biofuels using three platforms: thermochemical platform, sugar platform, and carboxylate platform. The thermochemical platform, which involves the gasification or pyrolysis of biomass, has low conversion efficiency, and produces the lowest yields.[130] The sugar platform biochemically breaks down complex sugars to simple sugars, then ferments the simple sugars into ethanol, or other products. Even though it has high yields, it is expensive because of the use of genetically modified microorganisms, mono-culture fermentation, and expensive specialty enzymes.[130] The carboxylate platform biochemically converts

biodegradable biomass (sugars, fats, and proteins) into volatile fatty acids (VFAs), which can be processed into specialty chemicals or liquid fuels. It has the highest product yields of the three and the lowest costs because it uses methane-arrested anaerobic digestion to produce thermodynamically favored products under non-aseptic conditions.[130]

A proven example of the carboxylate platform is the MixAlco™ process. In one version of the process (1) alkaline pretreatment removes lignin and exposes the biodegradable cellulose components, (2) methane-arrested anaerobic digestion (MAAD) ferments all biodegradable biomass components into carboxylic acids, (3) carboxylate acids are concentrated and thermochemically converted to ketones, (4) ketones are distilled and hydrogenated to mixed alcohols, (5) mixed alcohols are dehydrated and oligomerized to produce hydrocarbons.[17,114,130,131] Using one version of the MixAlco™ process, Vasquez et al. successfully produced 100 L of jet fuel and 100 L of gasoline from shredded office paper and chicken manure.[131]

Because of its structural characteristics, the enzymatic digestibility of lignocellulosic biomass is typically low (<20% yield).[18] Lignocellulose is a heterogeneous complex of carbohydrate polymers (cellulose and hemicellulose) and lignin. It is composed of 40–50% cellulose (glucose polymer), 25–35% hemicellulose (sugar heteropolymer), 15–20% lignin (non-fermentable phenyl-propene compound), extractives, and several inorganic materials.[15,19] Cellulose contains tightly packed polymer chains making it highly crystalline, insoluble in water, and resistant to depolymerization. Hemicellulose forms hydrogen-bonds with cellulose, thereby

providing the structural backbone for the plant cell wall. Lignin provides further structural strength and provides resistance against chemicals, diseases, pests, and microbes.[18,19] In the MixAlco™ process, cellulose and hemicellulose are sources of fermentable sugars; however, lignin hinders digestion of biomass to carboxylic acids.

Pretreatment, the first step in the MixAlco™ process, makes lignocellulose more digestible by altering the biomass structure. Pretreatment increases accessible biomass surface area, reduces lignin content, and reduces cellulose crystallinity.[19,21,22] Despite recent advances in pretreatment technologies, most effective pretreatment techniques are energy-intensive and require expensive chemicals. Pretreatment is one of the most expensive processing steps in lignocellulose-to-biofuel conversion.[18] The only avenue to reduce or eliminate pretreatment costs is to utilize biomass feedstocks with low resistance to biochemical degradation.

Prickly pear cactus (*Opuntia ficus-indica*) produces nutritious fruits, which are used to produce edible food products like candy, juice, jams, etc.[132] The cladodes (stems) are generally not consumed; however, the tender stems (nopalitos) are used as a vegetable in some parts of South America.[133] Because of their structural characteristics, prickly pear plants survive in arid and semiarid climates in which few other crops can survive. They produce high yields (Table 6-1), protect against soil erosion, inhibit desertification, and protect wildlife.[132,134,135]

Table 6-1. Yields of prickly pear at different farming conditions.

	Yield (ton dry matter/(hectare·yr))	Yield (ton dry matter/(acre·yr))
Brazil, rain-fed, intense fertilization, close planting.[134]	50	22
Brazil, rain-fed, low fertilization.[134]	20	9
Texas, Brownsville, rain-fed, row planting.[135]	13.5	6
Texas, Brownsville, rain-fed, row planting.[135]	29	12.8

Table 6-2 displays the chemical composition of prickly pear stem pads (cladodes) on a dry matter basis and fresh weight basis.[136–144] Cladode composition varies depending on the harvest season, the age of the plants, and the soil factors at the cultivation site.[136–138] Cladodes typical contain a hydrocolloid known as *mucilage*, which can absorb and retain large amounts of water.[145] Mucilages are complex polymeric substances comprised of carbohydrates with a highly branched structure.[146] The average sugar composition of cladode mucilage is 24.6–42% arabinose, 22–22.2% xylose, 21–40.1% galactose, 8–12.7% galacturonic acid, and 7–13.1% rhamnose, respectively.[147,148] Potassium, calcium, and magnesium are the main minerals, amounting to ~80% of the total ash content in cladodes.[136,149,150] Prickly pear cladodes can serve as a nutritious feedstock for the MixAlco™ process. The low lignin content, high sugar content, drought resistance, and high productivity make it a potential solution for eliminating expensive chemical pretreatments.

Table 6-2. Average chemical composition of prickly pear cladodes.

	Dry matter basis (g/100 g)	Fresh weight basis (g/100 g)
Water	–	88–95
Carbohydrates	64–71	3–7
Ash	19–23	1–2
Fibers	18	1–2
Protein	4–10	0.5–1
Lipids	1–4	0.2
Lignin	3.6–3.9	0–0.2

This research study was performed to investigate the potential of prickly pear cladodes as a feedstock for the MixAlco™ process. In previous studies, prickly pear was used as a feedstock for bioethanol and biogas production.[151–154] However, very few studies have been performed for the sole purpose of producing VFAs from prickly pear. MAAD is the heart of the MixAlco™ process and the VFA producing step. MAAD employs the first three steps of anaerobic digestion: hydrolysis, acidogenesis, and acetogenesis.[23] The fourth step – methanogenesis – is inhibited; thus, high-value carboxylic acids accumulate in the reactor instead of low-value methane. MAAD performs optimally at near-neutral pH, so the acids are present predominantly as their neutral carboxylate salts.

As batch MAAD progresses, product inhibition and low biomass reactivity reduces digestion performance. Countercurrent MAAD was developed to reduce product

inhibition and increase biomass reactivity resulting in higher biomass conversion and higher product yields.[24] However, countercurrent MAAD typically requires 3 to 5 months to achieve a single steady-state condition. In contrast, batch MAAD reaches completion in less than 60 days. To reap the benefits of countercurrent MAAD without its laborious consequences, the Continuum Particle Distribution Model (CPDM) was developed. CPDM uses batch data to predict continuous countercurrent with an accuracy within 4–20%.[44,72,73] This study describes batch MAAD performed with prickly pear cladodes as the feedstock. Performance parameters are estimated and compared with previous studies using the MixAlco™ process. CPDM is used to predict "maps," which served as a comparison tool with previous CPDM maps from other feedstocks.

6.2. Materials and Methods

6.2.1. Substrate

Mature prickly pear cladodes of the spineless variety were harvested around Fall 2020. The cladodes were chopped into small cubes using a kitchen knife, then blended into a pulp using a Ninja® Foodie™ food processor. The pulp was stored in a freezer until needed. The mineral composition of the pulp (Table 6-3) was determined at the Texas A&M Soil, Water and Forage Testing Laboratory (College Station, TX) based on a high-temperature combustion method using an Elementar Vario Max CN element analyzer. The carbon-to-nitrogen (C-N ratio) was reported as 22.15 g carbon/g nitrogen, which lies within the optimal C-N ratio recommended by Smith et al.[76] Therefore, the cladode pulp was not co-digested with any other substrates.

6.2.2. Digester

Batch MAAD was implemented in 1-L polypropylene copolymer (PPCO) plastic bottles capped by a rubber stopper with a septum-covered glass tube as previously described.[155] To ensure air-tight conditions, plastic screw caps and aluminum crimp seals were used. Digesters were horizontally placed in the rolling incubator (Wheaton®) maintained at 40ºC to ensure proper mixing at 4 rpm.

Table 6-3. Composition of prickly pear cladode pulp.

	Unit	Prickly Pear
Moisture	g/100g wet sample	92.01
Ash	g/100g dry sample	23.35
Volatile solids (dry basis)	g/100g dry sample	76.65
Total Carbon	g/100g dry sample	31.90
Nitrogen	g/100g dry sample	1.44
Calcium	g/100g dry sample	7.21
Potassium	g/100g dry sample	3.27
Magnesium	g/100g dry sample	1.30
Phosphorus	g/100g dry sample	0.11
Sodium	g/100g dry sample	0.02

6.2.3. Digestion Media

The digestion media – deoxygenated water – was prepared by adding 0.275 g/L cysteine hydrochloride and 0.275 g/L sodium sulfide into boiled deionized water as previously described.[24] Cladode pulp was added to deoxygenated water in each 1-L

PPCO digester. Iodoform (CHI_3) was used to inhibit methanogenesis in all batch MAADs. It was prepared by dissolving 20 g of iodoform in 1 L of 190-proof ethanol. A fixed amount (120 μL) of iodoform solution (20 g CHI_3/L 190-proof ethanol) was added to each digester every 48 h. Because of its light sensitivity, the solution was stored in amber-colored glass bottles to prevent degradation caused by light. To keep the pH neutral, $NaHCO_3$ was added to the fermentors as needed.

6.2.4. Inoculum

Inoculum was a mixed culture of marine microorganisms obtained from 1-m-deep shoreline pits at Galveston Beach, Texas as previously described.[24] The inoculum was adapted to prickly pear by performing a batch fermentation of cladode pulp for 3 weeks. Broth from the inoculum adaptation was used to inoculate all the batch MAADs in this research study. Inoculum accounted for 12.5% of the digester liquid volume.

6.2.5. Batch MAAD

Batch experiments were performed to obtain data for the CPDM and to determine experimental reproducibility. Varying initial substrate concentrations (10, 20, 40, 70, and 70 + g dry substrate/L liquid) were used. Each substrate concentration was performed in triplicate. The 70 and 70+ digesters had the same initial substrate concentrations, but the 70+ digester contained a medium with a mixture of carboxylate salts with a total concentration of 20 g carboxylic acids/L liquid. The composition of the mixture was 16 g acetic acid/L, 1 g propionic acid/L, and 3 g butyric acid/L. The 70+ g dry substrate/L was performed to observe the effects of product inhibition on MAAD performance. Previous studies using CPDM utilized batch data with initial substrate

concentrations ranging from 20–100 g dry substrate/L liquid.[44,72,73] However, because of the high moisture content of the cladode pulp, it was not possible to obtain a substrate concentration of 100 g dry substrate/L liquid without drying or evaporation. Provided a broad enough range of initial substrate concentrations are evaluated, this difference in initial substrate concentration range does not affect the accuracy of the mathematical model.[26,27]

To start each batch MAAD, the 1-L PPCO bottles and the rubber stoppers were sterilized in an autoclave. After the digesters cooled to room temperature, specific amounts of substrate, inoculum, deoxygenated water, and methane inhibitor was added to each digester (Table 6-4). The bottles were then purged with nitrogen, capped, and placed in the rolling incubator (Wheaton®) maintained at 40°C. Every 48 h, the digesters were removed from the incubator and a 30-mL gas sample was taken from each digester for analysis in a gas chromatograph. The volume of the gas in the headspace was measured, as described later. Then, the digesters were centrifuged (4000 rpm, 10 min) and 1.5-mL liquid samples were taken from the supernatant. The supernatant pH was also adjusted to neutrality by (1) adding $NaHCO_3$ to neutralize acidic broth or (2) adding pressurized CO_2 to acidify alkaline broth. Finally, iodoform solution (120 μL) was added to each digester followed by purging with nitrogen, capping, vigorous shaking for homogenization, and placing in the rolling incubator. Anaerobic digestion was terminated once total acid concentration appeared stable across all digesters. Solid and liquid samples were obtained from the terminated batches to calculate moisture content, ash content, and MAAD performance parameters.

Table 6-4. Initial loadings to start methane-arrested anaerobic digestions.

Initial Substrate Concentration (g dry substrate/L liquid)	Working Volume (mL)	Inoculum (mL)	Cladode Pulp Dry Basis (g)	Cladode Pulp Wet Basis (g)	Water in feed (g)	Carboxylic acids (g/L)	D.O. water (mL)
10	400	50	4	50.1	46.1	0	303.9
20	400	50	8	100.2	92.2	0	257.8
40	400	50	16	200.3	184.3	0	165.7
70	400	50	28	350.5	322.5	0	27.5
70^{+}	400	50	28	350.5	322.5	20	19.7

(Note. D.O. water stands for deoxygenated water.)

6.2.6. Analytical Methods

6.2.6.1. Biogas Analysis

As anaerobic digestion occurs, gases are formed as a byproduct. The plastic bottles used as digesters can only tolerate pressures under 2 atm absolute. If the digester is over-pressurized, the plastic cap and rubber stopper can leak. To avoid this, the digesters were vented every 48 h. To vent the biogas, a needle was inserted through the rubber septum on top of the digester. The needle was connected to an inverted graduated column filled with 300 g/L $CaCl_2$ solution, which prevents microbial activity and carbon dioxide absorption, as previously described.[24] The volume of displaced water is equivalent to the volume of gas in the headspace of the digester. Occasionally, 30-mL biogas samples were obtained from the fermenters using a syringe and a needle. The sample composition (N_2, CO_2, CH_4, and H_2) was measured by manually injecting the gas sample into an Agilent 6890 series chromatograph with a thermal conductivity detector (TCD). A 4.6-m stainless steel packed column with 2.1-mm ID (60/80 Carboxen 100,

Supelco 1-2390) was used. The inlet temperature was 230°C, the detector temperature was 200°C, and the oven temperature was 200°C. The total run time was 20 minutes, and helium was the carrier gas.

6.2.6.2. Digester Broth Analysis

Every 2 d, liquid samples (1.5-mL) were obtained from the supernatant of each digester. The samples were stored in the freezer immediately until analysis. To analyze, the samples were first thawed and centrifuged to separate liquid from solids (Beckman Coulter Microfuge® 13,300 rpm, 1 h). Because supernatant is viscous, the centrifuged samples were diluted with HPLC-grade water. The diluted samples were vortexed (Fisher Vortex Genie 2™) for 10 s, centrifuged (13,300 rpm, 10 min), and filtered through 0.2-μm nylon filters (Millex®). Volatile fatty acids (VFAs), lactic acid (LA), and ethanol concentrations were analyzed using high performance liquid chromatography (HPLC). The subset of VFAs analyzed using the HPLC were formic (C1), acetic (C2), propionic (C3), isobutyric (IC4), butyric (C4), isovaleric (IC5), valeric (C5), and caproic (C6). The HPLC method was adapted from a previous study.[156] The analysis was performed using HPLC (1260 Infinity II HPLC Agilent) equipped with a guard column (PL Hi-Plex H, 50 × 7.7 mm, Agilent), an analysis column (Hi-Plex H, 300 × 7.7 mm, Agilent) at a flow rate of 0.6 mL/min, and column temperature of 60°C. The HPLC was equipped with a refractive index detector and a diode array detector set to 210 nm.

Gas chromatography was performed to determine the concentrations of enanthic acid (C7) and caprylic acid (C8). Supernatant from dilute samples (0.5 mL), 3-M

phosphoric acid (H_3PO_4, 0.5 mL), and internal standard solution (4-methyl-*n*-valeric acid, 1.16 g/L, 0.5 mL) were mixed in a vial as the intermediate. To ensure high quality data, the intermediate was centrifuged again (13,300 rpm, 10 min), filtered using a 0.2-μm nylon syringe filters (Millipore Sigma, Burlington, MA), and then transferred to glass vials for GC analysis. The GC system employs an automatic liquid sampler (Agilent 7683 series), a flame ionization detector (FID), and a 30-m fused-silica capillary column (J&W Scientific, Model # 123-3232). The column head pressure was maintained at 2 atm abs. For each sample injected, the GC program raised the temperature from 40 to 200°C at 20°C/min. The temperature was subsequently maintained at 200°C for 2 min. Each sample was run for 11 min. Helium was used as carrier gas.[24] The external standard used was a mixture of carboxylic acids prepared in the laboratory.

6.2.6.3. Moisture and Ash Content

Moisture and ash contents were calculated as described previously.[24] Moisture content (MC) is defined as the amount of moisture that evaporates from a wet sample after baking at 105^{o}C for 24 h. Ash content (AC) is defined as the amount of a dry sample that remains after heating in a furnace at 550^{o}C for 12 h. Calcium hydroxide (30 mg $Ca(OH)_2$/g sample) was added to liquid samples before MC analysis to ensure all volatile acids were converted to salts thereby increasing data accuracy.

6.2.7. MAAD Performance Parameters

In the MixAlco™ process, batch performance is measured using three parameters: conversion, yield, and selectivity. However, these parameters depend on the

amount of non-acid volatile solids (NAVS) present at the start and finish of the experiment. The NAVS refers to the digestible portion of the substrate. It was calculated as the difference between the volatile solids (VS) and acids present in the sample. Volatile solids (VS) are defined as the mass of dry solid material that is combusted at 550°C after 12 h. NAVS was calculated using the following equation:

$$\text{NAVS} = (\text{g total wet weight of sample})(1 - \text{MC})(1 - \text{AC}) - (\text{g carboxylic acid in wet sample}) \quad (6\text{-}1)$$

where MC is the fraction of moisture in the wet biomass and AC is the fraction of ash in the dry biomass. The MAAD performance parameters were estimated using the following equations:

$$\text{Conversion} = \frac{\text{NAVS}_{\text{digested}}(\text{g})}{\text{NAVS}_{\text{fed}}(\text{g})} \quad (6\text{-}2)$$

$$\text{Yield} = \frac{\text{Total carboxylic acids produced (g)}}{\text{NAVS}_{\text{fed}}(\text{g})} \quad (6\text{-}3)$$

$$\text{Selectivity} = \frac{\text{Total carboxylic acids produced (g)}}{\text{NAVS}_{\text{digested}}(\text{g})} \quad (6\text{-}4)$$

$$\text{NAVS}_{\text{digested}} = \text{NAVS}_{\text{fed}} - \text{NAVS}_{\text{remaining}} \quad (6\text{-}5)$$

$$\text{NAVS}_{\text{remaining}} = \text{VS}_{\text{liquid}} + \text{VS}_{\text{solid}} - \text{Total acid in digester} \quad (6\text{-}6)$$

$$\text{NAVS}_{\text{fed}} = \text{VS}_{\text{office paper}} + \text{VS}_{\text{nutrient}} + \text{VS}_{\text{urea}} - \text{Initial acids present} \quad (6\text{-}7)$$

6.2.8. Continuum Particle Distribution Model (CPDM)

The Continuum Particle Distribution Model (CPDM) uses a continuous conversion distribution function to model the kinetics of anaerobic digestion. In CPDM, a *continuum particle* is defined as one gram of volatile solids in the initial unreacted state. As a conversion-parameterized model, CPDM tracks biomass

particles as they move through the anaerobic digestion train. The CPDM estimates reaction rates by tracking continuum particles using constant model parameters obtained from batch MAADs.[26,27]

To simplify CPDM calculations, the carboxylic acid concentrations detected by chromatography were converted into one single acid concentration (Aceq). Aceq signifies the amount of acetic acid that would have been produced if all carboxylic acids were acetic acid.[27,81] Carboxylic acid concentrations from each batch were converted to Aceq using Equations 6-8 and 6-9. The coefficients in Equation 6-8 are based on the reducing power of the carboxylic acids estimated using disproportionation reactions.[27] For each initial substrate loading, the average and standard deviations of the Aceq values are estimated.

$$\alpha\ (\mathrm{mol/L}) = 1.00 \times \mathrm{acetic}\ (\mathrm{mol/L}) + 1.75 \times \mathrm{propionic}\ (\mathrm{mol/L}) + 2.50 \times \mathrm{butyric}\ (\mathrm{mol/L}) + 3.25 \times \mathrm{valeric}\ (\mathrm{mol/L}) + 4.00 \times \mathrm{caproic}\ (\mathrm{mol/L}) + 4.75 \times \mathrm{heptanoic}\ (\mathrm{mol/L}) + 5.50 \times \mathrm{octanoic}\ (\mathrm{mol/L}) \quad (6\text{-}8)$$

$$\mathrm{Aceq}\left(\frac{\mathrm{g}}{\mathrm{L}}\right) = 60.05\left(\frac{\mathrm{g}}{\mathrm{mol}}\right) \times \alpha\left(\frac{\mathrm{mol}}{\mathrm{L}}\right) \quad (6\text{-}9)$$

The concentrations of Aceq(*t*) for each batch group was estimated using Equation 6-10, where *a*, *b*, and *c* are constants fit by least squares regression, and *t* is time in days. Aceq(*t*) is a calculated value that depends on experimental Aceq values. Constants *a*, *b*, and *c* were calculated by minimizing the residuals – the difference between experimental and calculated Aceq values – using Excel Solver.

$$\mathrm{Aceq}(t) = a + \frac{bt}{1+ct} \quad (6\text{-}10)$$

$$\text{Residuals} = \sum_{\text{data}}\left(\text{Aceq}_{\text{exp}} - \text{Aceq}_{\text{calculated}}\right)^2 \quad (6\text{-}11)$$

The reaction rate r for the MAAD was calculated by differentiating the $\text{Aceq}(t)$.

$$r = \frac{d(\text{Aceq})}{dt} = \frac{b}{(1+ct)^2} \quad (6\text{-}12)$$

The specific reaction rate $\hat{r}$ was defined as the reaction rate by particle and calculated by dividing the reaction rate with the initial substrate concentration (S_o).

$$\hat{r} = \frac{r}{S_o} \quad (6\text{-}13)$$

The initial substrate concentration (S_o, g VS/L) was defined by dividing the initial mass of volatile solids by the total liquid volume in each batch group. The biomass conversion *x* was calculated for each batch group using Equation 6-14.

$$x(t) = \frac{\text{Aceq}(t) - \text{Aceq}(0)}{S_o \cdot \sigma} \quad (6\text{-}14)$$

where σ is the selectivity (g Aceq produced/g VS digested). To simplify calculations, the selectivity σ was assumed to be constant and was calculated from the average value of selectivity *s* (g total acid produced/g VS digested) determined from the batch experiments.

$$\sigma = \frac{s}{\phi} \quad (6\text{-}15)$$

The $\text{Aceq}(t)$ and conversion *x* values were fit to Equation 6-16, the governing equation of the CPDM method.

$$\hat{r}_{pred} = \frac{e(1-x)^f}{1+g(\phi \cdot Aceq)^h} \quad (6\text{-}16)$$

where

x = fractional conversion of volatile solids

e, *f*, *g*, and *h* = empirical constants

ϕ = the ratio of total grams of carboxylic acid to total grams of acetic acid equivalents

The numerator shows that as conversion increases, the reaction rate decreases. The denominator accounts for product inhibition of the microorganisms, which decreases reaction rate. For all substrate concentrations, Equation 6-16 was fit to the specific reaction rate $\hat{r}$. Empirical constants *e*, *f*, *g*, and *h* were estimated by minimizing the residuals of the specific reaction rate using Excel Solver. Afterwards, the constants were used in a MATLAB program to simulate four-stage countercurrent MAAD with varying volatile solids loading rates (VSLR) and liquid retention times (LRT).[72] The program outputs an array of Aceq concentration and biomass conversion values at varying VSLRs and LRTs. This array was used to plot the CPDM "maps" displaying total acid concentration (*y*-axis) and biomass conversion (*x*-axis) at various VSLRs and LRTs.

6.2.9. Statistical Analysis

Least square regressions for CPDM were performed using Solver in Microsoft Excel. All average values and standard deviations were calculated using Excel. Error bars were used to denote the standard deviations of total acid concentrations. Using JMP® software, t-tests and Tukey's mean separation tests were performed to estimate significant difference at the 0.05 level. Statistically significant difference between data points were indicated using letters (a, b, c, ab, etc.)

6.3. Results

6.3.1. Volatile Fatty Acid Production

Figure 6-1 displays the total volatile fatty acids (C1–C8) concentration profile for all batch MAADs. At Day 0, the total VFA concentration is 21.57 g/L for 70+ g/L – which was augmented with acids – and 1.57 g/L for the other substrate concentrations. Generally, higher substrate concentrations produce greater total acids. At substrate concentration 10 g/L, the total acid concentration reached 5.2 g/L in only 6 d. This rapid digestion can be explained by the low lignin content, the low substrate concentration in the digester, and the presence of soluble sugars in the biomass, as previously mentioned. In contrast, lignocellulosic biomass sources used in the carboxylate platform have a high lignin content that must be remediated through expensive pretreatment. Furthermore, lignocellulose contains sugar polymers (e.g., cellulose, hemicellulose) that must be hydrolyzed before acid production (acetogenesis and acidogenesis) can begin. The simple sugars in prickly pear are readily metabolized to carboxylic acids. When an adapted mixed culture of microorganisms accessed this easily digestible substrate at a low substrate concentration, it is consumed quickly and converted to products.

For all substrate concentrations, the total acid concentration increases rapidly during the first 8 d. After 40 d, the total acid concentration plateaued because of increased product inhibition and decreased biomass reactivity. (*Note:* For the 10 g/L digester, it is likely that the acid concentration plateaued only because of decreased biomass reactivity. At such a low product concentration, it is very unlikely that product inhibition played much of a role.) Implementing a fed-batch or countercurrent system

equipped with periodic product removal and substrate addition has proved to address product inhibition and reduced biomass reactivity.[24] However, this study is limited to batch MAAD to test the efficacy of prickly pear cladodes as a feedstock for the carboxylate platform.

6.3.2. Carboxylic Acids and Ethanol Composition

Previous studies have shown that the products of primary fermentation of glucose are formic acid, acetic acid, propionic acid, lactic acid, and ethanol.[125] During secondary fermentation, these metabolites are further reacted to form longer chain VFAs. In the *reverse β-oxidation pathway*, a VFA of chain length x is elongated by reacting with acetyl-CoA in a condensation reaction to produce a VFA of chain length $x + 2$.[125] Therefore, in most chain elongation reactions, formic acid is elongated to propionic or valeric acid whereas acetic acid is elongated to butyric or hexanoic acid.

Figure 6-2 shows lactic acid, ethanol, total VFAs, and total carboxylic acid concentration profiles. *Total carboxylic acid concentration* is defined as the sum of total VFA and lactic acid concentrations. As performed in this study, MAAD the proportions of catabolic products depends on two factors: (1) the microbial community, which affects metabolic activities and (2) the presence of electron donors and acceptors, which influence the kinetics and thermodynamics of the biochemical reactions.[125] Previous studies have shown that lactic acid and ethanol are promising electron donors for VFA chain elongation through the *reverse β-oxidation pathway*. Some studies supplement the feedstock with lactate to produce caproic acid (C6).[91] Sagar et al. showed that adding ethanol to a MAAD increases the production of medium-chain fatty acids (e.g., C6) from

lignocellulosic biomass.[107] With acetic acid as the electron acceptor, lactic acid and ethanol are consumed to produce longer acids like C4, C6, and C8.

In this study, the only substrate used was prickly pear cladode pulp. During primary fermentation – which occurred in the first few days – simple sugars were quickly converted to acetic acid, ethanol, and lactic acid. However, ethanol and lactic acid are chain elongators that produce longer chain carboxylic acids. Figure 6-2 shows that for all substrate concentrations, lactic acid increased rapidly within the first 2 d and then decreased to zero after 6 d. As lactic acid concentration increased and then decreased, the total VFAs produced increased sharply.

Figure 6-2 shows that lactic acid, a product of primary fermentations, is produced initially and later converted to longer chain VFAs. Using free sugars as substrate at pH 5 or lower, lactic acid formers outperform acidogens, which directly ferment glucose to acetic or propionic acid in primary fermentations.[91,125] In this study, the digesters were buffered periodically rather than continuously. The pH of each digester was ~4.85, ~6.53, and ~6.61 on Days 2, 4, and 6, respectively. So, during the first 2 d, the pH dropped low enough to benefit lactic acid formers. However, chain elongation – a secondary fermentation between lactic acid and acetic or propionic acids – is thermodynamically favored. Given enough time, higher acids are made.

At substrate concentration of 10 g/L, ethanol behaved similarly to lactic acid (Figure 6-2). The ethanol concentration increased and peaked at Day 12 before rapidly decreasing to zero by Day 20. At substrate concentration of 20 g/L, the ethanol concentration decreased to zero by Day 36.

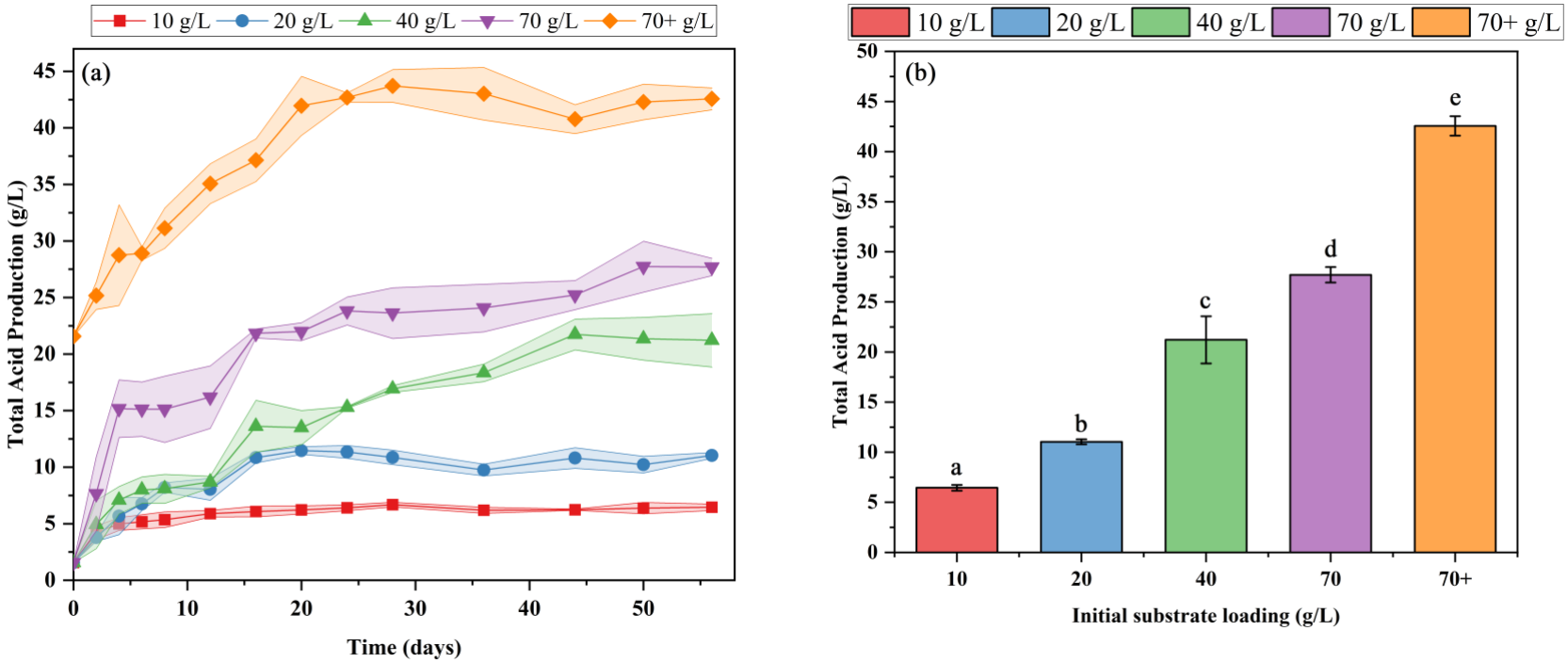

Figure 6-1. (a) Volatile fatty acid concentration profile and (b) Total volatile fatty acids produced after 56 d.

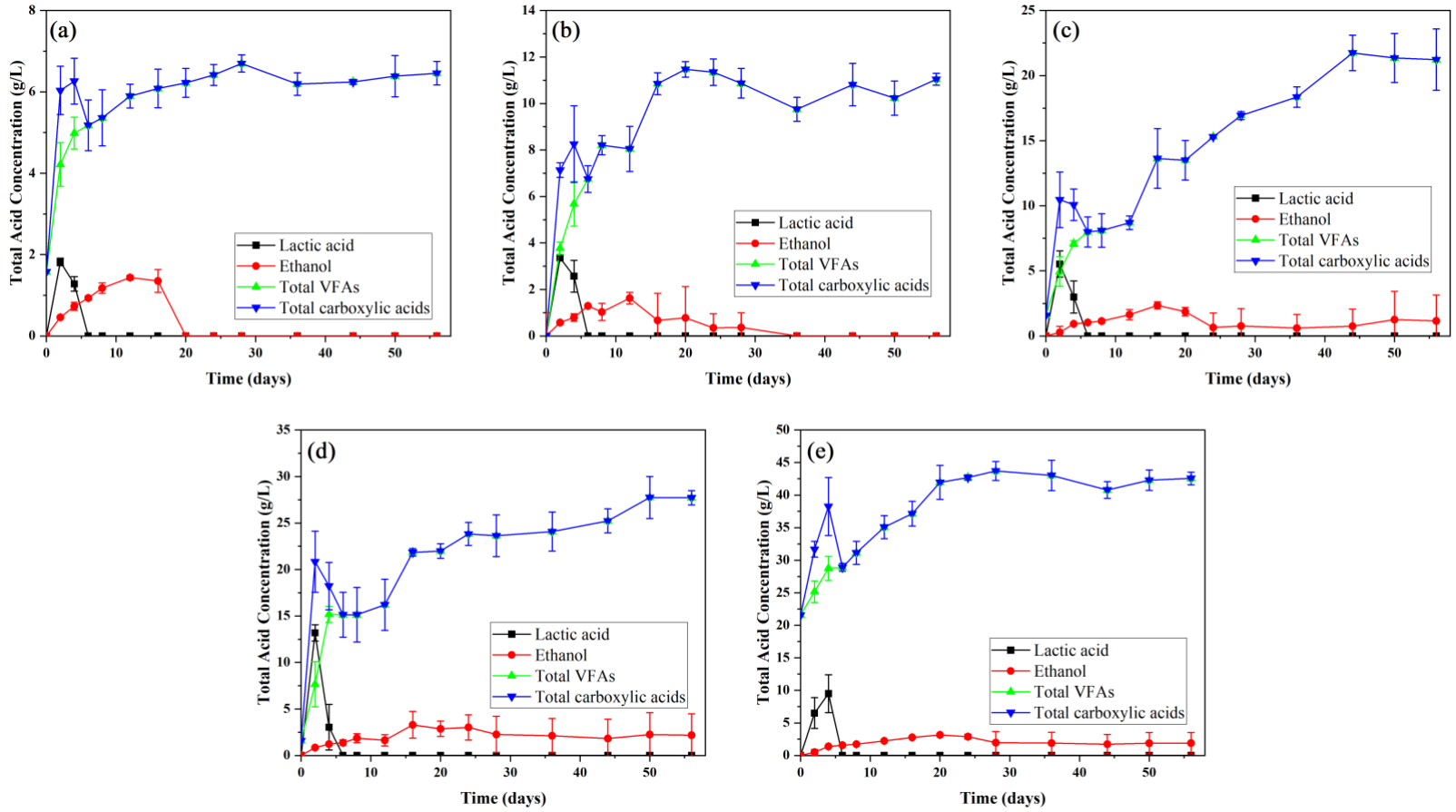

Figure 6-2. Concentration profiles of lactic acid, ethanol, total volatile fatty acids, and total carboxylic acids. (a) 10 g/L, (b) 20 g/L, (c) 40 g/L, (d) 70 g/L, (e) 70+ g/L.

However, at substrate concentrations of 40, 70, and 70+ g/L, the ethanol concentration increased, decreased, and finally plateaued at Day 24. It is possible that some of the ethanol was consumed for chain elongation. However, the presence of ethanol after Day 56 implies that product inhibition made the environment less suitable for bacteria to perform chain elongation.

Figure 6-3 displays the mass fraction of carboxylic acids and ethanol produced at different substrate concentrations during the MAAD. For all substrate concentrations, the mass fractions of lactic acid and ethanol decrease as the mass fractions of butyric acid and caproic acid increase. The mass fractions of acetic or butyric acid tend to decrease slightly when caproic acid increases. It is possible that some of the acetic acid or butyric acid is converted to caproic acid via chain elongation. At all substrate concentrations, the mass fraction of formic acid is lowest on Day 56. It is possible that formic acid is converted to propionic acid, valeric acid, or used in a different chain elongation metabolic pathway.

When the digestion was stopped, the predominant carboxylic acids were acetic, butyric, and caproic acids. This further proves that lactic acid and ethanol served as electron donors in the chain elongation of the even-numbered chains. At substrate concentration of 10 g/L, the prominent carboxylic acid was caproic acid (31%). The mass fraction of caproic acid present on Day 56 decreases with increasing substrate concentration. In fact, at 70+ g/L, only 4% of caproic acid is observed. This further shows that chain elongation was negatively impacted by high carboxylic acid concentrations.

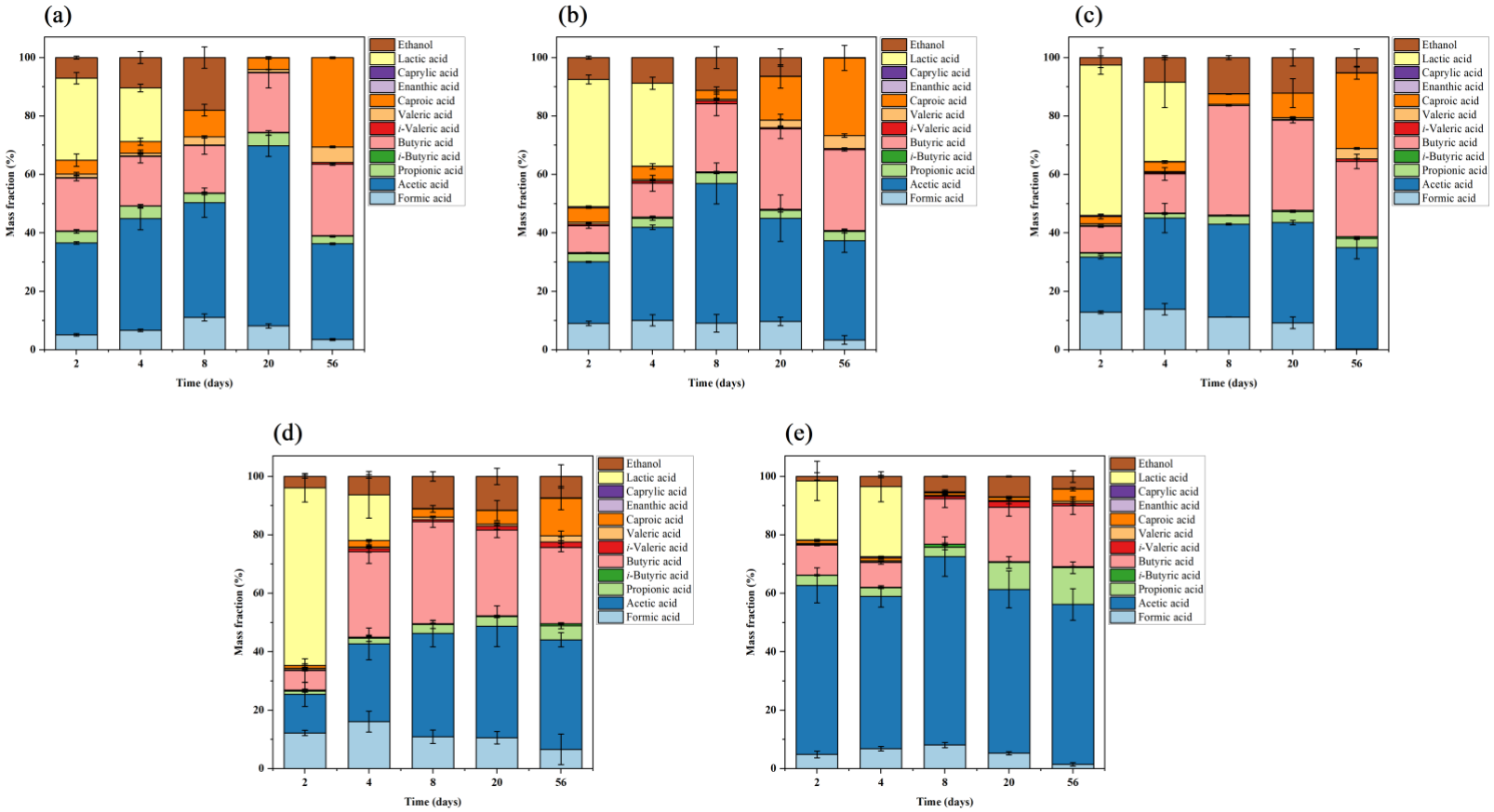

Figure 6-3. Total carboxylic acids and ethanol composition of batch digesters at the following initial substrate loadings: (a) 10 g/L, (b) 20 g/L, (c) 40 g/L, (d) 70 g/L, and (e) 70+ g/L.

6.3.3. Acetate Equivalent

Figure 6-4 illustrates the Aceq concentration profile for all batch MAADs. Just like total acid concentration, higher substrate concentrations produce greater Aceq. The changes in individual acid compositions are incorporated into the Aceq term. On Day 0, Aceq is 24.59 g/L for 70+ g/L and 2.06 g/L for all other substrate concentrations. The longer the VFA chain, the higher the acetate equivalent. At substrate concentration of 10 g/L, the final Aceq is 9.88 g/L. This value is only possible because of the high mass fraction of caproic acid (31%) at this substrate concentration. The empirical constants, *a*, *b*, and *c* were estimated by minimizing the sum of squared errors between the experimental Aceq values and the predicted Aceq values (Equation 6-10).

6.3.4. Biogas Production and Composition

Figure 6-5 shows the volume of biogas produced from all digesters. Biogas production indicates microbial growth and metabolic activity. As with VFA production, higher substrate concentrations produce greater biogas volumes. Because of lower product inhibition, the 70 g/L digesters produced 11% more biogas than the 70+ g/L digesters. Nonetheless, despite product inhibition, the 70+ g/L digesters outperformed all other batches except the 70 g/L digesters.

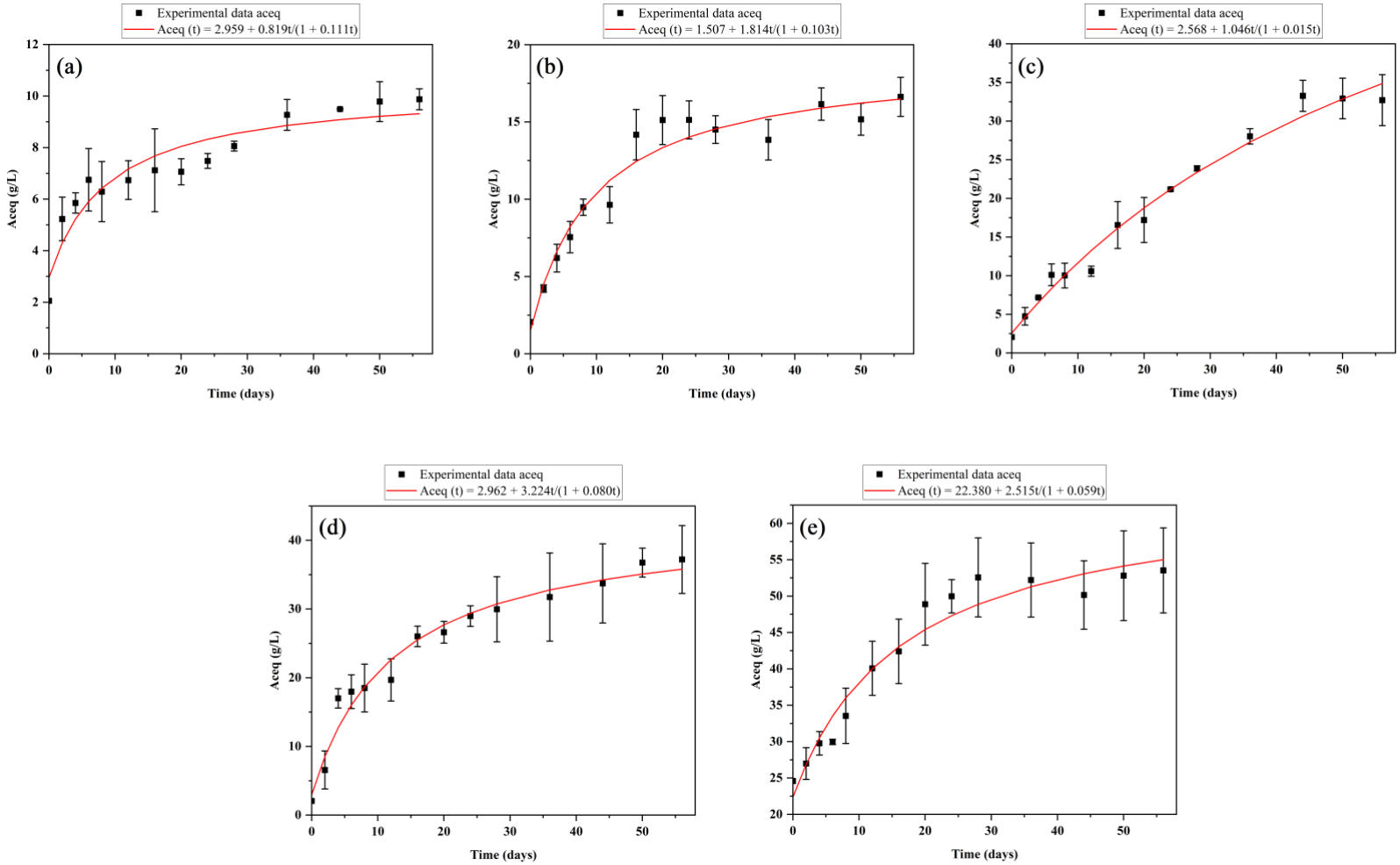

Figure 6-4. Aceq concentration profiles for each initial substrate loading. (a) 10 g/L, (b) 20 g/L, (c) 40 g/L, (d) 70 g/L, (e) 70+ g/L.

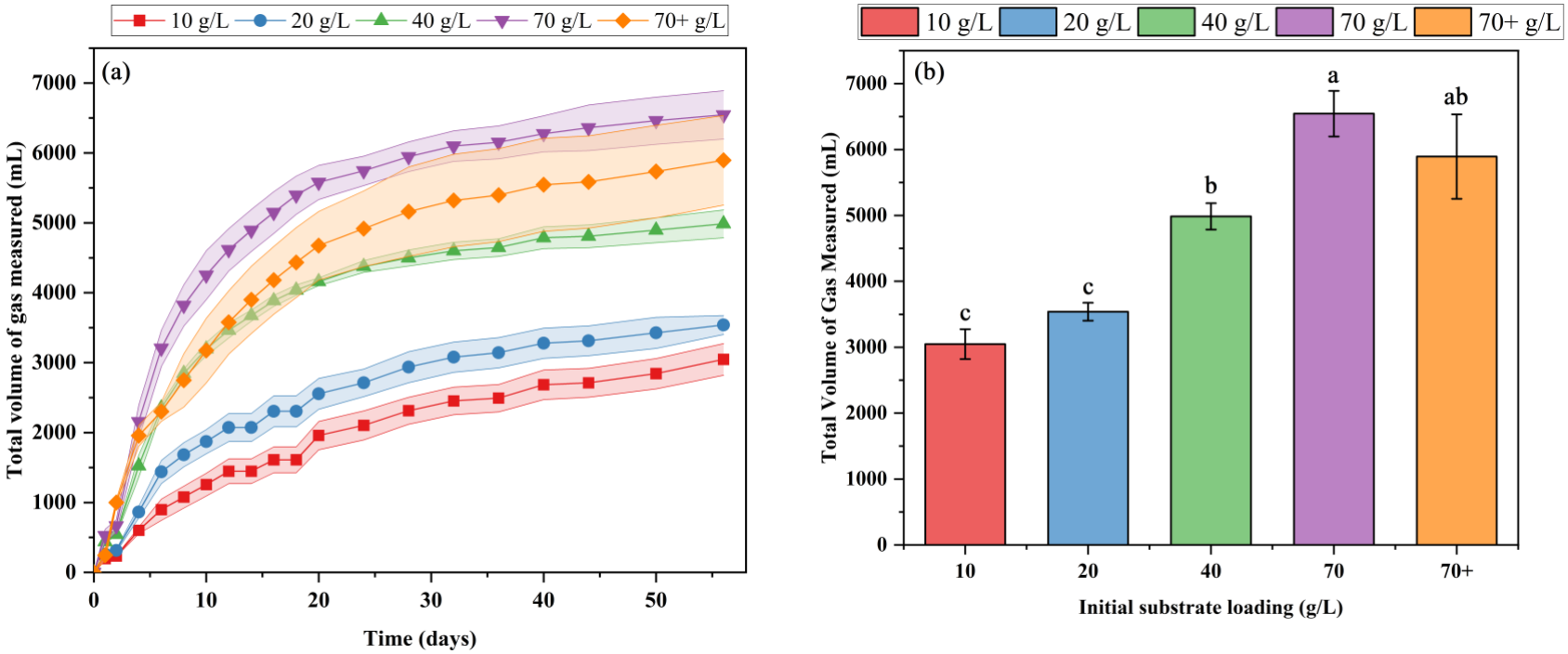

Figure 6-5. (a) Cumulative volume of gas produced and (b) Total volume of gas measured.

In the 70+ g/L digesters, even though chain elongation was hindered by product inhibition, acidogens where still active. This activity can be ascribed to cell growth or acid production. The biogas produced from all digesters consisted of carbon dioxide, nitrogen (from purging), and <1% of oxygen. No methane was detected, which verifies that methanogenesis was inhibited. At the beginning of digestion, up to 50% carbon dioxide was observed. The percentage of carbon dioxide produced decreased as the digestion progressed until <5% of carbon dioxide was observed signifying the decrease in metabolic activity and plateauing of MAAD products.

6.3.5. MAAD Performance Parameters

The performance of each digester was determined by measuring non-acid volatile solids (NAVS). Performance parameters such as conversion, yield, and selectivity were estimated for each substrate concentration. The Aceq yield and Aceq selectivity use acetate equivalents instead of total acids produced. Figure 6-6 displays the conversion, yield, and selectivity for each digester. Because the separation of the liquid phase and solid phase by centrifugation is more accurate for higher solid contents, conversion and selectivity were only estimated for the highest substrate concentration. In contrast, yield and Aceq yield were estimated for all substrate concentrations.

Conversion is the ratio of NAVS digested to NAVS fed. The NAVS digested is estimated using the moisture content and ash content of the digester contents before and after MAAD. Prickly pear achieved a conversion of 0.71 g $NAVS_{digested}$/g $NAVS_{fed}$ at 70 g/L and 0.85 g $NAVS_{digested}$/g $NAVS_{fed}$ at 70+ g/L. These conversions are remarkably high compared to previous batch digester studies. Roy et al. utilized *in-situ* product

removal during the digestion of lime-pretreated corn stover and dried chicken manure to achieve 0.65 g $NAVS_{digested}$/g $NAVS_{fed}$.[80] However, prickly pear attained higher conversion without any *in-situ* product removal or chemical pretreatment.

Yield is the ratio of VFAs produced to NAVS fed. It is also termed *exit yield* because it accounts for the acids in product liquid, waste solids, and liquid samples. At substrate concentration 10, 20, and 40 g/L, the yield is statistically similar with the highest yield, 0.65 g total acid produced/g $NAVS_{fed}$, occurring at 10 g/L. Because of the negative impact of product inhibition, the lowest yield, 0.25 g total acid produced/g $NAVS_{fed}$, occurred in the 70+ g dry substrate/L digester. It is worth noting that the lowest yield obtained in this study, 0.25 g total acid produced/g $NAVS_{fed}$, is slightly greater than the yields obtained from the enzymatic digestion of most lignocellulosic biomass (<20%).[18] At 70 g dry substrate/L, the digester yielded 0.48 g total acid produced/g $NAVS_{fed}$. The Aceq yield follows a similar trend to the yield. At 70 g dry substrate/L, the Aceq yield was 0.61 g acetate equivalent/g $NAVS_{fed}$. In a batch MAAD using lime-pretreated corn stover (80%) and baked chicken manure (20%) with *in-situ* product removal, Roy et al. obtained a yield of 0.37 g total acid produced/g $NAVS_{fed}$ and an Aceq yield of 0.54 g acetate equivalent/g $NAVS_{fed}$.[80] Moreover, prickly pear attained greater yields without co-treatment or pretreatment.

Selectivity is the ratio of total acids produced to NAVS digested. It measures how efficiently the microbial community produces VFAs from the consumed substrate. Low selectivity (< 0.5) implies that most of the substrate was utilized for cell growth whereas high selectivity (> 0.5) implies that most of the substrate was utilized for acid

production. At substrate concentration of 70 g/L, the selectivity was high at 0.68 g total acids produced/g $NAVS_{digested}$. Moreover, product inhibition caused the selectivity of 70+ g/L to be low at 0.30 g total acids produced/g $NAVS_{digested}$. This implies that the high product concentration reduced the acid producing capacity of the microorganisms present in this digester. At substrate concentrations of 70 and 70+ g/L, the Aceq selectivity was 0.86 g Aceq produced/g $NAVS_{digested}$ and 0.41 g Aceq/g $NAVS_{digested}$, respectively. From cellulose or starch, the maximum theoretical Aceq selectivity is 1.11 g Aceq/g $NAVS_{digested}$, which accounts for the water of hydrolysis. Prickly pear cladodes produced higher yields, conversions, and selectivity than most previous studies on the MixAlco™ process (Table 6-5).

6.3.6. CPDM Predictions

Using Aceq values and the specific reaction rate, empirical constants *e*, *f*, *g*, and *h* (Equation 6-16) were calculated by minimizing the sum of square errors between the specific reaction rate and the predicted reaction rate. The CPDM governing equation obtained from the batch MAAD is shown below:

$$\hat{r}_{pred} = \frac{0.1344(1-x)^{1.800}}{1+0.0002(0.7041 \cdot Aceq)^{0.6500}} \quad (6\text{-}17)$$

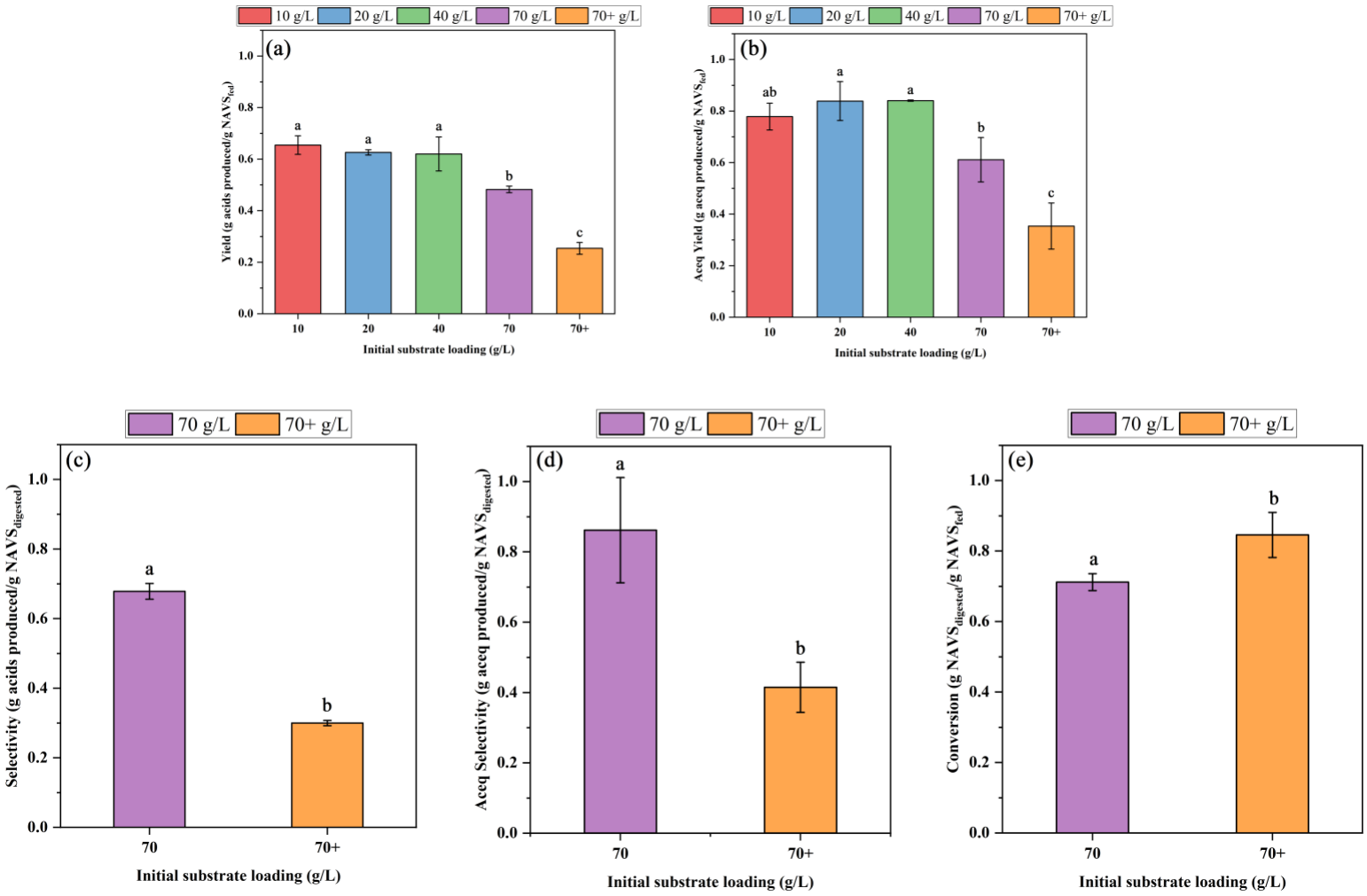

Figure 6-6. MAAD performance parameters. (a) yield, (b) Aceq yield, (c) selectivity, (d) Aceq selectivity, (e) conversion.

Table 6-5. Comparison of performance parameters achieved in this study to previous studies reported in the MixAlco™ process.

Study	Substrate	Experimental procedure	Conversion	Yield	Selectivity
This study	Prickly pear cladode pulp	Batch digestion of 70 g dry substrate/L performed at 40℃ for 56 days.	0.71 ± 0.02	0.48 ± 0.01	0.68 ± 0.02
Roy et al.[80]	Lime-pretreated corn stover (80%) and chicken manure (20%)	Batch digestion of 100 g dry substrate/L with *in-situ* product removal performed at 40℃ for 28 days.	0.65 ± 0.03	0.31 ± 0.01	0.53 ± 0.02
Forrest et al.[83]	Sugar molasses (80%) and chicken manure (20%)	Batch digestion of 100 g dry substrate/L performed at 55℃ for 24 days.	0.82 ± 0.07	0.17 ± 0.02	0.21 ± 0.01
	Wood molasses (80%) and chicken manure (20%)		0.42 ± 0.16	0.22 ± 0.01	0.58 ± 0.23
Rughoonundun et al.[117]	Sewage sludge (80%) and lime-pretreated bagasse (20%)	Batch digestion of 100 g dry substrate/L performed at 55℃ for 28 days.	0.52 ± 0.00	0.23 ± 0.01	0.45 ± 0.02
Smith et al.[76]	Office paper (93%) and wet chicken manure (7%)	Batch fermentation at 40℃ for 32 days.	0.44 ± 0.05	0.24 ± 0.03	0.50 ± 0.08

The empirical constants and governing equation were used to plot the CPDM "map." Figure 6-7 illustrates the predicted CPDM "map" at a substrate concentration of 100 g NAVS/L_{liq}, which is the typical solids concentration of a semi-continuous laboratory-scale digester. The VSLR ranged from 6 to 12 g/(L_{liq}·d) and the LRT ranged from 5 to 35 d. The map predicted a high total acids concentration of about 93 g/L and conversion of about 0.93 g $NAVS_{digested}$/g $NAVS_{fed}$ at a VSLR of 6 g/(L_{liq}·day) and LRT of 35 d.

Figure 6-8 displays the CPDM "map" at a substrate concentration of 300 g NAVS/L_{liq}, a typical solids concentration for industrial operations. (*Note:* This high substrate concentration could only occur if the prickly pear cactus were dried before being added to the digesters.) This concentration was chosen because it is the maximum achievable solids concentration where liquid can be transferred continuously from one digester to the next. The map predicts a high total acid concentration of about 175 g/L and conversion of about 0.89 g $NAVS_{digested}$/$NAVS_{fed}$ at a VSLR of 20 g/(L_{liq}·day) and LRT of 27 d. These predictions are by far the highest ever recorded using the CPDM in the MixAlco™ process. However, CPDM predictions must be experimentally verified before process scale-up.

6.4. Conclusion

In MAAD, prickly pear cladodes produced high yields, conversion, and selectivity without needing process improvements, like chemical pretreatment or *in-situ* product removal. They performed better than previous studies using the MixAlco™ process. Prickly pear cladodes are highly digestible feedstocks that could potentially improve

MixAlco™ process yields and reduce costs. This biomass warrants further investigation using the carboxylate platform and other biomass-to-biofuel technologies.

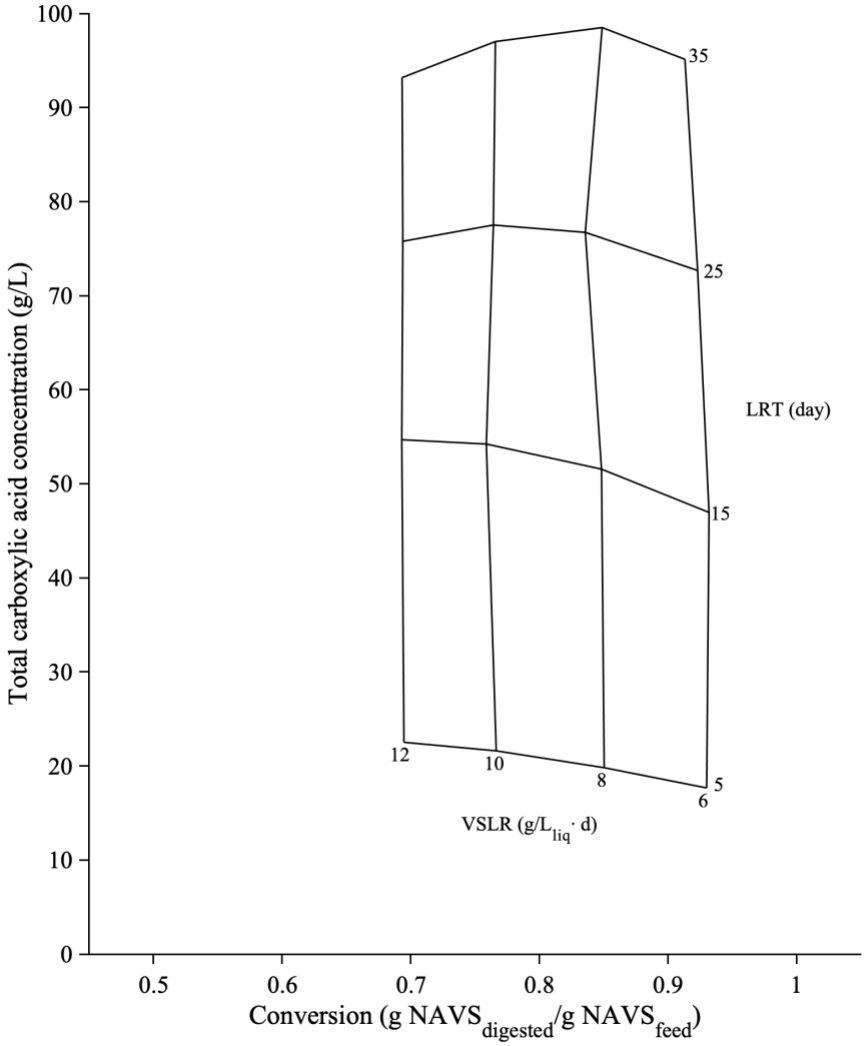

Figure 6-7. The continuum particle distribution model maps for four-stage countercurrent anaerobic digestion using prickly pear cladode pulp. Substrate concentration is 100 g NAVS/L_{liq}.

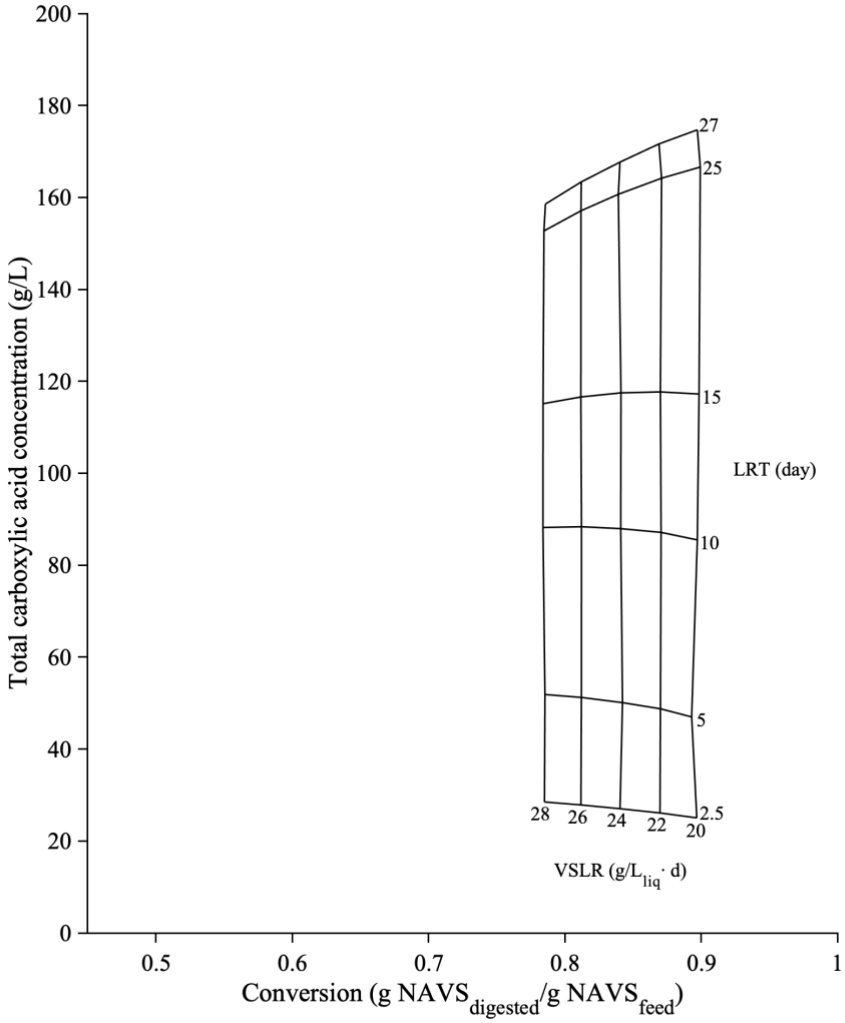

Figure 6-8. The continuum particle distribution model maps for four-stage countercurrent anaerobic digestion using prickly pear cladode pulp. Substrate concentration is 300 g NAVS/L_{liq}.

7. CO-TREATMENT OF LIGNOCELLULOSIC BIOMASS

7.1. Introduction

Lignocellulose can provide energy-rich components for industrial production of biofuels and other chemicals.[18] To enhance biological conversion processes, numerous physical and chemical pretreatments have been studied. Although physical pretreatments have been considered, they are often disregarded because of concerns regarding energy costs, equipment costs, and low digestibility.[157] Therefore, researchers have predominantly pursued chemical pretreatments.

Most chemical pretreatments have a common objective: the removal of lignin to increase access to digestible structural polysaccharides (e.g., cellulose and hemicellulose). Lignin is the phenylpropanoid-based polymer that binds polysaccharides together, and imparts structural strength and biochemical resistance in plants.[71,158] Chemical pretreatments typically use aggressive chemicals (e.g., sodium hydroxide, sulfuric acid, ammonia, and ionic liquids) at elevated temperatures and pressures. The intense process conditions and chemical toxicity require chemically resistant construction materials, advanced engineering designs, sophisticated waste stream management, and development of robust operational protocols to ensure worker safety.[158]

Other than cost, physical pretreatments do not have many challenges such as those listed above. Previous studies have suggested combining chemical and physical pretreatments to benefit from the size reduction of physical pretreatment and lignin

removal of chemical pretreatment.[71,158,159] Such combinations have the potential to achieve economic feasibility. Another option for reducing costs and maximizing biomass digestibility is to combine physical pretreatment with anaerobic digestion, which is naturally observed in ruminant animals.

Ruminants have a very efficient natural cellulose-degrading system.[160] For millennia, ruminants have served mankind with their ability to convert cellulosic biomass into milk, meat, wool, and hides.[160] By observing ruminal digestion, which is an evolutionary and commercial success, improvements can be made to engineered consolidated bioprocesses.[160] Among domestic and wild ruminant animals, cattle stand out because of their high muzzle width ratio, which prevents selective eating of highly digestible forage.[161] However, cattle possess a unique dentition pattern that grinds and tears forage fiber, resulting in a higher fiber consumption than other ruminants. Using their ruminal digestive system, cattle can digest a predominantly fibrous diet.

In cattle, the biomass is first chewed, a form of physical pretreatment. The diet of cattle is mostly composed of fibrous grass and hay. The forage is chewed, swallowed, regurgitated, chewed again, and finally swallowed. The process of regurgitating previously swallowed food is termed *chewing the cud*. Applying this process to the carboxylate platform, the substrate would be digested, ground, and digested some more. During mastication, cattle apply a shearing force. To properly simulate this, the biomass must be put through a grinder that applies a shearing force.

As a mechanical "co-treatment," this study employs a double-disc attrition mill during methane-arrested anaerobic digestion (MAAD) of corn stover. The synergistic

effects of mechanical shear and MAAD are expected to disrupt the biomass structure and enhance yields of carboxylic acids. Co-treatment substitutes for typical chemical pretreatment processes, such as those that use various acids and bases to treat the substrate.[20] Co-treatment has no chemical inputs and requires only shaft power for the attrition mill. It is best implemented after the microorganisms have had a chance to digest as much raw biomass as possible. Microbial digestion weakens the biomass structure via natural enzymes produced by microorganisms and reduces the amount of mass that must pass through the attrition mill. These combined effects should reduce the energy expenditure compared to solely mechanical attrition of raw biomass, which is practiced conventionally. To investigate the impact of co-treatment, batch MAAD using corn stover (80%) and chicken manure (20%) were performed at varying levels of co-treatment.

7.2. Materials and Methods

7.2.1. Substrate

The substrate used was corn stover (80%) and baked chicken manure (20%) at 100 g dry substrate/L. The corn stover was previously described in Section 3.2.1. The chicken manure was collected from the Texas A&M Poultry Science Center and baked at 105^{o}C for 48 h before storing in Ziploc bags. The carbon-to-nitrogen ratio (C-N ratio) was measured by Soil, Water and Forage Testing Laboratory, Texas A&M University (College Station, Texas). The test was based on a combustion method using an Elementa Variomax CN.[75] The C-N ratio for corn stover was reported as 69.2 g carbon/g nitrogen (41.5 wt% total carbon and 0.6 wt% total nitrogen). The C-N ratio for baked chicken

manure was reported as 8.85 g carbon/g nitrogen (35.4 wt% total carbon and 4 wt% total nitrogen). When combined, the C-N ratio was 25.0 g carbon/g nitrogen, which is within the recommended CN ratio for anaerobic digestion.[76]

7.2.2. Fermentation Media and Inoculum

Fermentation media was deoxygenated water prepared by boiling distilled water. Then, after it cooled to room temperature, 0.275 g/L of cysteine hydroxide and 0.275 g/L of sodium sulfide were added and mixed until total dissolution. Sodium bicarbonate was added as a buffer to keep the digesters at near-neutral conditions. The original inoculum was sourced from Galveston Beach, Texas. The inoculum underwent similar treatments and inoculum adaptation as described in Section 3.2.4. Each fermentor was inoculated with 12.5% of its working volume. Iodoform solution (20 g CHI_3/L 200-proof ethanol) was used to prevent methanogenesis in all fermenters. Every 48 h, 120 µL of iodoform solutions was added to each batch fermentor.

7.2.3. Co-treatment Procedure

Six digesters were filled with the substrate, fermentation media, and inoculum. Three bottles served as the control whereas the other three bottles served as the experimental intervention. Digesters were placed in the incubator at 40°C. Every 48 h, digesters were removed from the incubator, vented, and centrifuged. Then, liquid from the three control bottles was mixed at 500 rpm for 5 min. To ensure homogeneity when buffering and sampling, this was also repeated for the experimental batch. By mixing the contents of the three bottles, the liquid volume was increased to 1.2 L. A larger liquid volume was implemented to minimize the effects of mass loss on digestion performance.

A cast iron manual-crank grain mill (Figure 7-1) was used to grind the solids from each experimental batch.[162] The grain mill is equipped with a double-disc attrition mill. The grinder was securely fastened to a wooden table via the attached screw clamp. Upon being secured to the table, each component was assembled following the manufacturer's instructions. To ensure adequate shear stress was applied to the feedstock, the burrs of the grinder were tightened until a significant amount of torque was required to operate the grinder. To catch the ground solids, a rectangular plastic box with adequate height was placed under the burrs of the grinder.

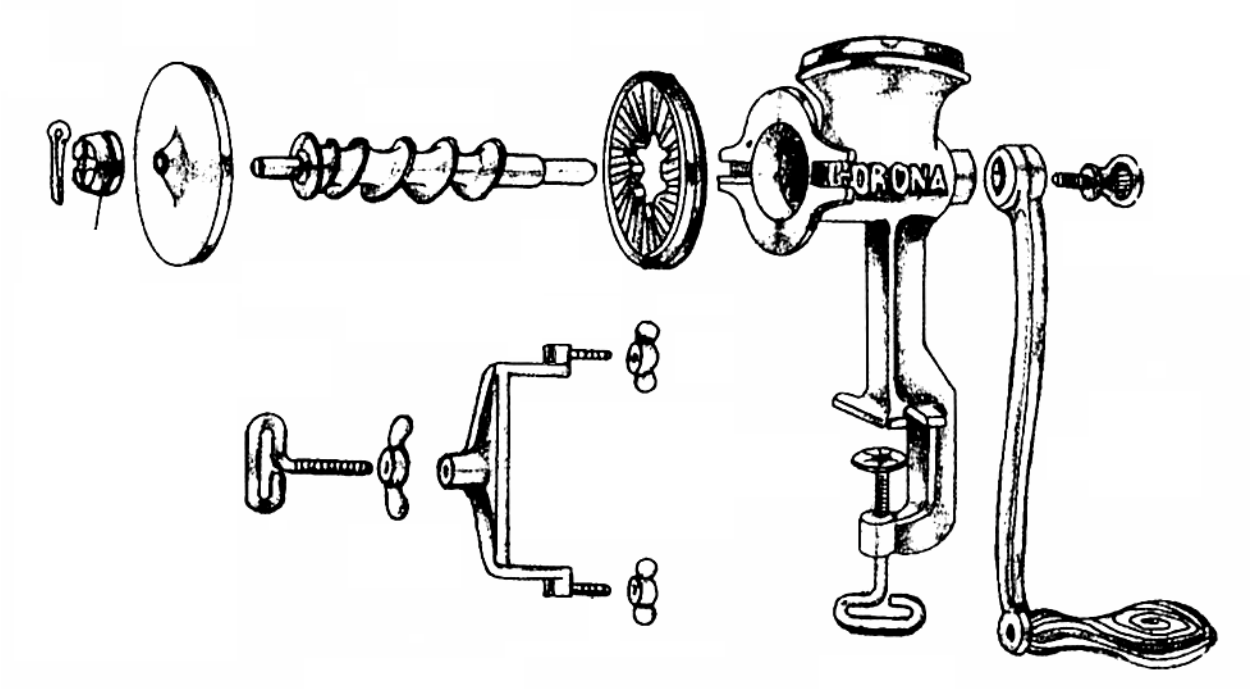

Figure 7-1. Schematic diagram of the cast iron manual crank grain mill.

Using a spatula, solids from each of the experimental bottles was incrementally added to the mill hopper until all the experimental batch solids were ground. To reduce the effects of confounding variables on the experiment, the control batch solids were incrementally emptied into a similar plastic container to simulate the grinding environment. After all the experimental batch solids were ground, the solids were mixed in their holding container until visually uniform. Next, the grinder was carefully disassembled. All the parts were cleaned using spatulas and toothpicks to remove solids stuck in the burr blades and auger. Once the residual solids were recovered, solids were weighed and equally distributed into the three experimental digesters. Similarly, the control batch solids were weighed and equally distributed into the three control bottles. Liquid was added back to the fermentors, then each bottle was purged with nitrogen, capped, and placed back into the incubator until the next sampling period. MAAD was performed for 78 days to ensure maximum utilization of biomass components. During the 78 days, the solid content of the experimental batch was ground numerous times. As shown in Table 7-1, three experimental batches were performed with equivalent control batches. To account for the effects of air exposure, an equivalent control was implemented for each number of grinds. AGR was ground on Day 10 only, BGR was ground on Days 10 and 14, and CGR was ground on Days 10, 14, and 18.

Table 7-1. Labels for co-treatment batches.

	Label		
	One Grind	Two Grinds	Three Grinds
Experiment	AGR	BGR	CGR
Control	C-AGR	C-BGR	C-CGR

7.2.4. Co-treatment Grinding Torque Analysis

Undergraduate student Drew Marks attached an object of known mass to the grinder arm and applied torque that was just shy of producing movement (stall). Figure 7-2 shows the coordinate system in which the *x*-direction aligns with the radius of the grinder arm and the *y*-direction is the tangent to the circle defined by the rotating grinder arm. The known mass applied a gravity force F_g to the grinder arm. This gravity force F_g was resolved into two components $F_{g,x}$ and $F_{g,y}$. The *y*-component $F_{g,y}$ is the tangential force that applies torque at radius *r*, which was measured as

$\tau = 65.7\ \text{in}\cdot\text{lb}_\text{f} = 7.5\ \text{N}\cdot\text{m}$

$\sigma = 4.7\ \text{in}\cdot\text{lb}_\text{f} = 0.53\ \text{N}\cdot\text{m}$

where τ is the average torque and σ is the standard deviation.

Figure 7-2 Coordinate system for grinding torque analysis.

7.2.5. Co-treatment Grinding Energy Analysis

At a rotation rate of 60 rev/min, the laboratory process produces 43 wet g/min. At a moisture content of 80%, this is equivalent to 8.6 dry g/min, or 0.14 dry g/rev.

The cost to grind the corn stover at industrial scales can be estimated based on the following assumptions:

- The torque analysis accurately describes the torque requirement for grinding the corn stover at early stages of fermentation
- Torque applied is constant for the duration of the grinding process
- The motor used for grinding the corn stover has an efficiency $\eta = 0.92$
- The grid price of electricity is \$0.05/kWh

$$\frac{\dot{W}}{\dot{m}} = \frac{2\pi\tau\dot{n}}{m_{rev}\dot{n}} = \frac{2\pi\tau}{m_{rev}} = \frac{2\pi\left(7.5\ \text{N·m}\right)}{0.14\ \text{g}} \times \frac{10^6\ \text{g}}{\text{tonne}} \times \frac{\text{kWh}}{3.6\times10^6\ \text{N·m}} = 94\frac{\text{kWh}}{\text{tonne}}$$

$$\text{Cost} = \frac{1}{0.92} \times \frac{\$0.05}{\text{kWh}} \times 94\frac{\text{kWh}}{\text{tonne}} = \frac{\$5.11}{\text{tonne}}$$

Assuming that on average, half the biomass flows through the grinder 4 times, the cost would be ~\$10/ton of raw biomass.

7.2.6. Analytical methods

Biogas volume, biogas composition, carboxylic acid concentration, moisture content, and ash content were measured as previously described in Section 5.2.7.

7.3. Results and Discussion

7.3.1. Carboxylic Acid Composition

Figure 7-3 displays the mass fraction of carboxylic acids produced after 78 d of anaerobic digestion. The predominant products were acetic, propionic, butyric, valeric, and caproic acids. In all batches, a similar amount of caproic acid was produced. **CGR** and **C-CGR** produced the lowest mass fractions of butyric acid. However, these two batches produced the most enanthic and caprylic acids. It is possible that some of the butyric acid was consumed in chain elongation reactions to produce enanthic and caprylic acid. When compared to one another, despite the number of co-treatments, there is very little observable difference in the mass fraction of each batch.

7.3.2. Carboxylic Acid Production

Figure 7-4 displays the total carboxylic acids produced from each batch. After 24 d of digestion, there is a clear observable temporary increase in acid production for **AGR** and **BGR**; however, co-treatment had no effect on **CGR**. After 78 d of digestion, there was no observable increase in acid production from co-treatment. In fact, total acid production decreased when air exposure was increased. **BGR** was exposed to air for prolonged periods twice, whereas **CGR** was exposed thrice. Both produced ~46% less acids than **AGR**.

Co-treatment is based on the concept of combining physical pretreatment with MAAD. Based on the observable process of rumination, co-treatment should have provided a substantial increase in total acids production; however, these results do not confirm this expectation. Further research must be performed to fully understand how to implement rumination into bioreactor design.

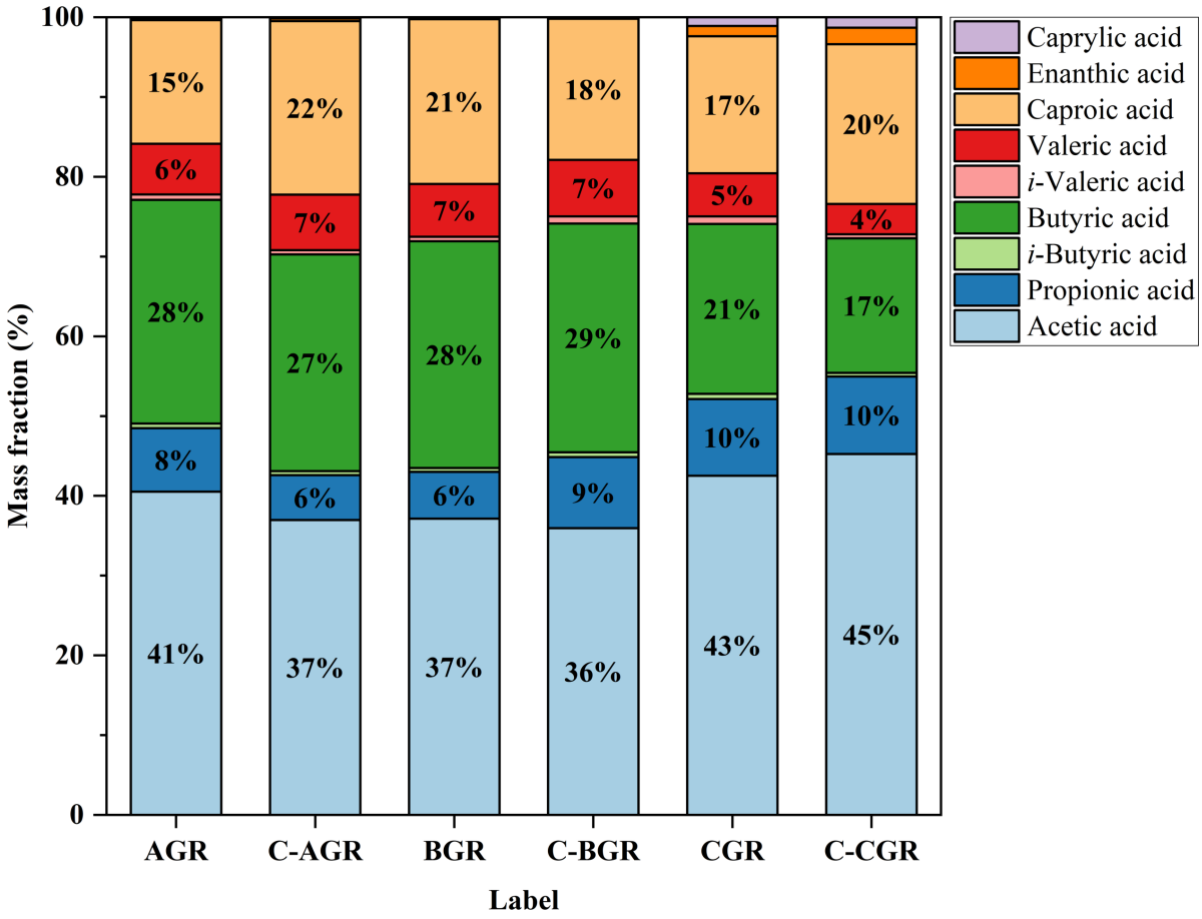

Figure 7-3. Carboxylic acid composition of co-treatment batches after 78 days of digestion.

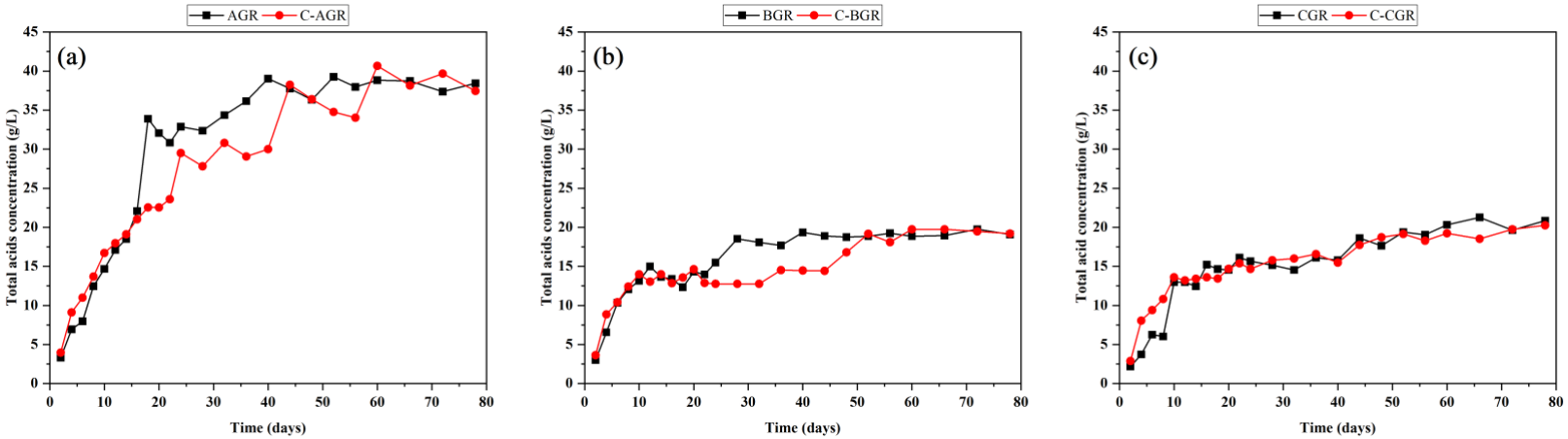

Figure 7-4. Total acid concentration profiles.

One possible reason for these results might be the feedstock. The corn stover used for this study had already been milled into ~1 cm particles before use. It is possible that the particles were already so small, that further milling during MAAD had no effect on performance. Future studies should minimize the implementation of size-reduction processes on the feedstock and minimize the exposure of digester contents to air. This might ensure that there is significant benefit from the milling aspect of co-treatment during MAAD. Although baking provides a convenient and reproducible nutrient source, it is known to damage the nutritional value as established in Section 5.3. In future studies, the nutrient source should not be baked. Preferably, it should be fresh or frozen.

7.4. Conclusion

Co-treatment is a new concept that requires further research before it can be properly applied to bioreactor designs and fermentation engineering. Future work should focus on less digestible biomass consisting of larger particle sizes with a smaller amount of exposed surface area. Bioreactor designs that have an in-built grinding system should be considered to reduce exposure to air.

8. METHANE-ARRESTED ANAEROBIC DIGESTION (MAAD) OF ALGAE

8.1. Introduction

After coal, petroleum, and natural gas, lignocellulose is the fourth largest energy source.[71] Despite its abundance, the presence of lignin increases processing costs and reduces yield in biological conversion processes. An alternative is to utilize lignin-free biomass sources, such as algae. Before anaerobic digestion, algae require minimal pretreatment. It predominantly consists of fatty acids, proteins, and sugar polymers, which are easily digestible.[163]

Typically, algae are used to produce triglycerides that are chemically converted to biofuels. However, after triglyceride extraction, residue biomass must be disposed. To minimize waste, the residue from extraction must be used in another process. Given its ability to utilize all the digestible components of a wet biomass source, the carboxylate platform is an obvious choice.

To create large percentages of oil in algae, nutrients (e.g., nitrogen, phosphorous) must be restricted. This reduces growth rates and makes the selected algae strain less competitive with contaminants. These challenges can be overcome by processing the entire algae cell, not just the extraction residue. This approach introduces an additional degree of freedom and allows the selection of algae strains that grow rapidly and thereby out-compete contaminants.

This study was performed to investigate the suitability of algae as a feedstock for the carboxylate platform.

8.2. Materials and Methods

ExxonMobil supplied the Holtzapple laboratory with three algae samples: (1) dried algae residue from oil extraction (**AR**), (2) triglyceride induced algae (**TI**), and (3) non-triglyceride induced algae (**NTI**). The specific details of these algal samples were proprietary; however, from multiple discussions with ExxonMobil, a few details were disclosed. **AR** was obtained after extracting triglycerides from algae in an aggressive manner suitable for quantitative laboratory analysis, not industrial production. After extraction, the residue was dried in an oven, which previous studies (Chapter 5) have shown to damage nutrients. **TI** was an algae strain induced to produce triglycerides, and was supplied as a frozen wet sample. **NTI** was an algae strain that was not induced to produce oil, and was supplied as a frozen wet sample.

The properties of the algae samples (Table 8-1) were determined at Texas A&M Soil, Water, and Forage Testing Laboratory (College Station, Texas). Previous studies show that algae are rich in nitrogen and can serve as a nutrient source for co-digestion.[164] Unused office paper (Caliber®) served as the energy source for some digesters. In this study, the following combination of substrates were anaerobically digested: (1) **TIP** – triglyceride induced algae and paper, (2) **NTIP** – non-triglyceride induced algae and paper, (3) **ARP** – algae residue and paper, (4) **TI** – triglyceride induced algae, (5) **NTI** – non-triglyceride induced algae, and (6) **AR** – algae residue. These combinations allowed the assessment of methane-arrested anaerobic digestion (MAAD) performance with algae serving either as the only substrate or as a nutrient supplement.

Table 8-1. Substrate content of office paper and algae samples.

	Unit	Office paper	TI	NTI	AR
Moisture	g/100g wet sample	5.9	86.4	85.3	7.20
Ash	g/100g dry sample	14.2	28.1	37.1	17.9
Volatile solids	g/100g dry sample	85.8	71.9	63.0	82.1
Carbon	g/100g dry sample	36.0	35.3	31.5	52.0
Nitrogen	g/100g dry sample	0.07	1.42	4.36	1.41
CN ratio	g carbon/g nitrogen	514.7	24.9	7.21	36.9

During co-digestion, 80% paper and 20% algae were combined at an initial dry substrate concentration of 100 g/L. For all digesters, urea was used to adjust the CN ratio to 24.9 g C/g N. Digester configuration, digestion medium, inoculum, analytical methods, and MAAD performance parameters were previously described in Section 5.2.

8.3. Results and Discussion

8.3.1. Gas Production and Composition

Figure 8-1a displays the gas produced from each digester. **TIP** and **NTIP** produced the highest gas volume. **AR** produced the lowest gas volume. Figure 8-1b displays the average composition of gas samples obtained during digestion. In all samples, nitrogen was the predominant gas because each digester was purged with nitrogen every 2 d. Even though **TIP** and **NTIP** produced the highest gas volumes, **TI** and **NTI** produced the highest fraction of carbon dioxide, a by-product of carboxylic acid production. This implies that microbial activity was strong in **TIP**, **NTIP**, **TI**, and

NTI digesters. **ARP** and **AR** produced the lowest gas volumes and the lowest mass fraction of carbon dioxide. Low carbon dioxide production implies low microbial activity; therefore, dried algae residue performed poorly.

8.3.2. Total Acid Produced

Figure 8-2a displays the total acids produced from each digester. For all digesters, acid production plateaued after 46 d. **NTI** produced the highest total acids at ~23 g/L after 66 d. By Day 20, ~21 g/L of total acids were produced, implying a production of ~1 g total acid/(L·d) for the first 20 days. **NTI** produced ~30% more acids than **TI**. This implies that inducing algae for oil production made it less digestible by mixed cultures. **NTIP** and **TIP** performed similarly. This is likely because algae comprised only 20% of the substrate, thereby reducing the impact of highly digestible non-triglyceride induced algae. **ARP** produced more acids than **AR**. This observation is the direct opposite of other algae samples, which produced more acids than their algae + paper counterparts. **AR** was highly undigestible producing only ~3.7 g/L total acids after 66 d.

Co-digesting dried algae residue improved acid production by ~116% likely because of digestible carbohydrates supplied from paper. It is possible that the extraction and drying process for producing **AR** (1) introduced compounds that are harmful to mixed cultures, (2) removed the most digestible biomass components, and (3) rendered the digestible components inaccessible to microbes. According to Kulkarni and Nikolov, the solubility of algal proteins after heat-drying was reduced 5–6 fold compared to wet biomass.[165] ExxonMobil did not reveal the details of the extraction or drying process. It

is inferred that the poor performance of **AR** is because of a combination of multiple negative repercussions of intense extraction/drying techniques on algal biomass.

8.3.3. Carboxylic Acid Composition

Figure 8-2b displays the mass fraction of carboxylic acids produced after 66 d of anaerobic digestion. For **TIP**, **NTIP**, and **ARP**, the predominant products were acetic, butyric, and caproic acids. In fact, algae + paper digesters produced >40% of caproic acid (C6), significantly more than algae-only digesters. Co-digesting algae with paper caused a change in the mass fraction of acids produced. This is probably because different substrate components favor different metabolic pathways.

TI and **NTI** produced >30% of butyric acid (C4). **TI** produced ~30% of C6 and small amounts of propionic (C3), isobutyric (IC4), isovaleric (IC5), and valeric (C5) acids. **NTI** produced ~9, ~4, ~8, and ~5% of C3, IC4, IC5, and C5, respectively. Compared to any other digester, **NTI** produced a higher mass fraction of these acids. However, it produced the lowest percentage of caproic acid. **NTI** likely possessed a component that encouraged the production of odd-numbered carboxylic acids and isomers of carboxylic acids. **AR** produced ~54% of C6 and 22% of C4. It recorded the highest mass fraction of C4 and C6. Despite the poor performance of **AR**, chain elongation reactions still occurred to produce significant amounts of C4 and C6.

8.3.4. MAAD Performance Parameters

In this study, non-acid volatile solid (NAVS) was used to quantify substrate concentration needed to assess MAAD performance. Figure 8-3 displays the conversion, yield, and selectivity for each digester.

Conversion is the ratio of NAVS digested to NAVS fed; it quantifies the NAVS consumed during digestion. **NTI** had the greatest conversion (0.59 g $NAVS_{digested}$/g $NAVS_{fed}$), which was an increase of 129, 105, 196, 80, and 293% compared to **TIP**, **NTIP**, **ARP**, **TI**, and **AR**, respectively.

Yield is the ratio of total acids produced to NAVS fed; it quantifies how much of the NAVS fed is converted to acids. **NTI** had the highest yield (0.33 g acid produced/g $NAVS_{fed}$) which was an increase of 129, 115, 277, 58, and 719% compared to **TIP**, **NTIP**, **ARP**, **TI**, and **AR** respectively. **AR** had the lowest yield (0.04 g acid/g $NAVS_{fed}$).

Selectivity is a ratio of total acids produced relative to NAVS digested; it quantifies how much of the digested NAVS is converted to carboxylic acids. Selectivity greater than 0.5 implies that most of the digested substrate was used to produce acids. Selectivity less than 0.5 implies that most of the digested substrate was used for other purposes other than acid production, such as cell growth. **AR** had the lowest selectivity (0.27 g acid/$NAVS_{digested}$). Such a low selectivity implies that drying likely damaged the nutrients; therefore, a large portion of the digested substrate was utilized for cell growth and reproduction instead of acid production.

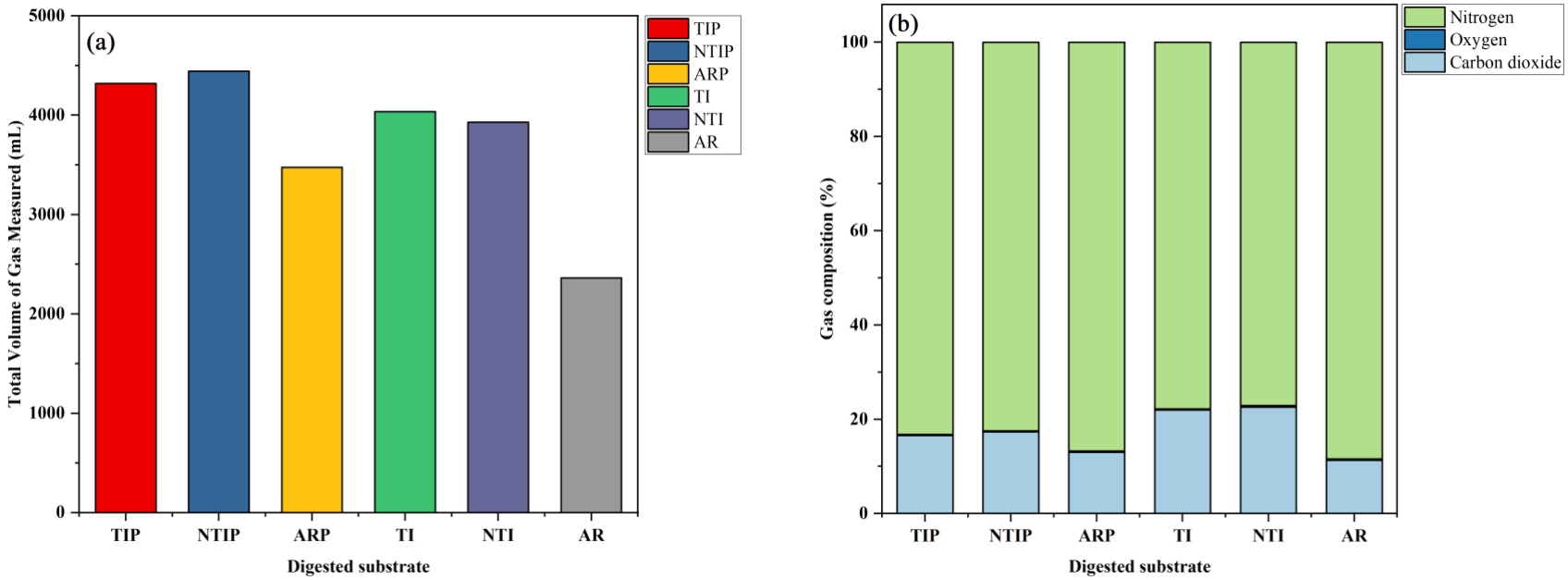

Figure 8-1. (a) Total volume of gas measured in all digesters and (b) average composition of gas samples from all digesters.

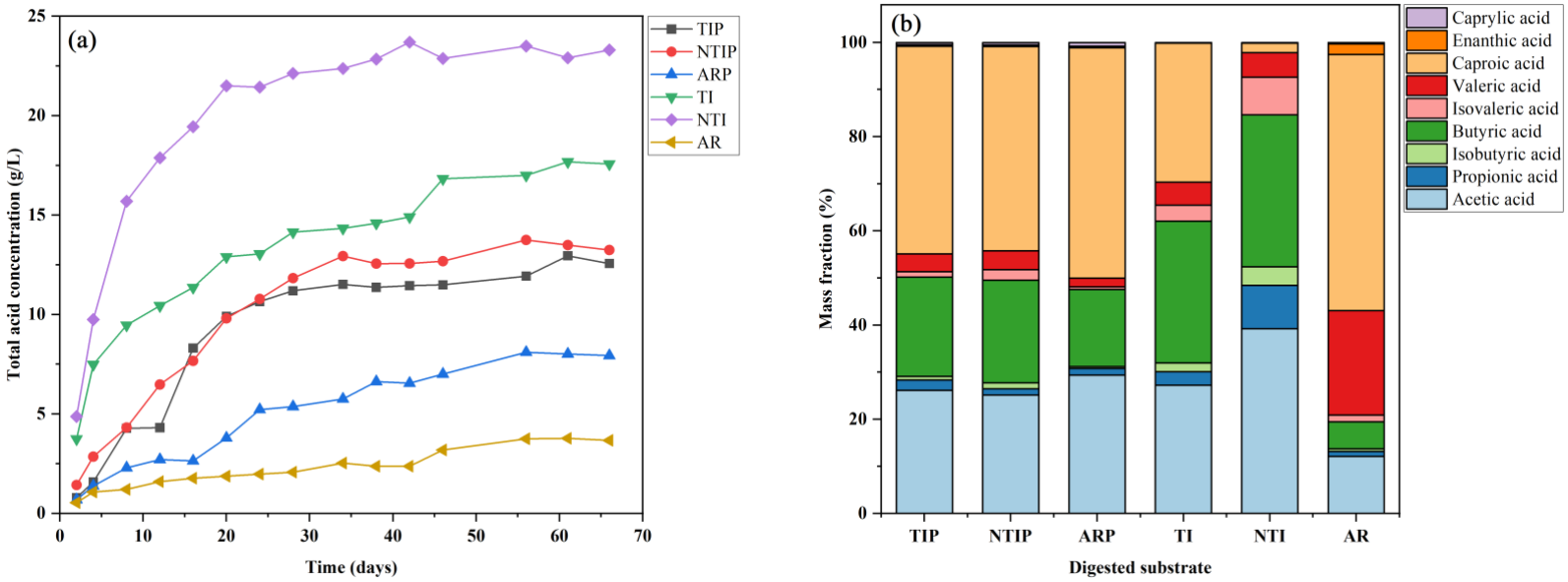

Figure 8-2. (a) Total carboxylic acid concentration profile and (b) carboxylic acid composition after 66 d.

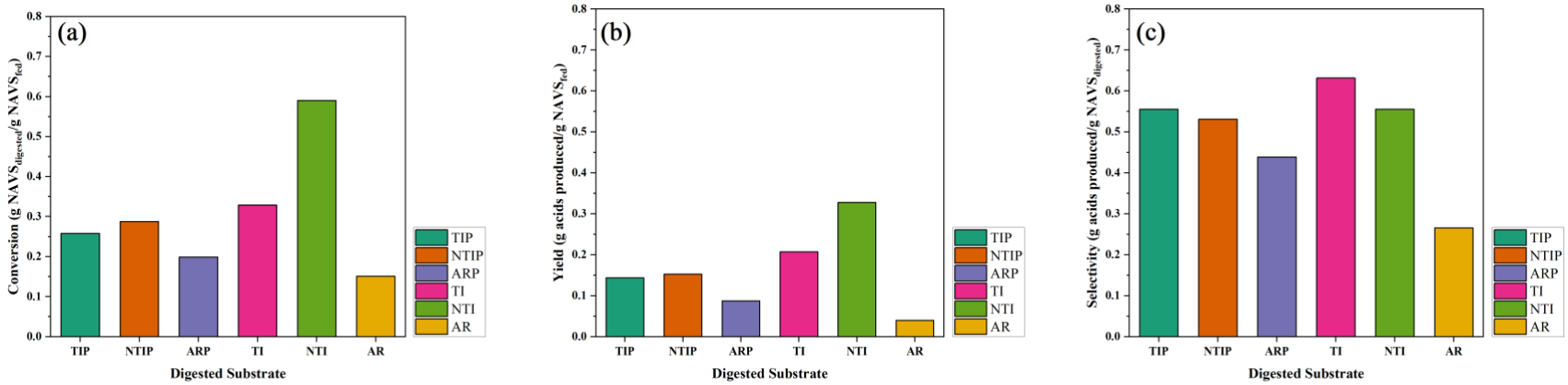

Figure 8-3. MAAD performance parameters for all algae feedstocks. (a) Conversion, (b) yield, and (c) selectivity.

8.4. Conclusion

Algae is a highly digestible feedstock for MAAD performing similarly to many other substrates previously used in the carboxylate platform; however, digestibility greatly reduced after triglyceride extraction and drying processes. Most studies on the carboxylate platform have focused on carbohydrate-rich substrates; however, anaerobic digestion of proteins and fatty acids in algae produce odd-numbered and iso-carboxylic acids. Future studies should investigate the impact of protein- and oil-rich substrates on carboxylic acid composition. Continuum particle distribution model (CPDM) should be performed to predict the performance of algae in countercurrent experiments.

9. CONCLUSIONS AND FUTURE WORK

The research studies reported in this dissertation can be divided into three main categories: (1) pretreatment, (2) methane-arrested anerobic digestion (MAAD), and (3) *in-situ* product removal (ISPR).

9.1. Pretreatment

Shock pretreatment of lignocellulosic biomass amplified alkaline pretreatment by opening the biomass structure to improve diffusion of alkali into the biomass structure. Compared to alkali-only treatment, shock + alkali treatment had an increase in yield of 15% (assessed with enzymatic hydrolysis) and 45% (assessed with anaerobic digestion). Compared to enzymatic hydrolysis, MAAD was a more robust method for analyzing the impact of pretreatment techniques on the digestibility of biomass when used in the carboxylate platform. Soaking and drying lignocellulosic biomass increases crystallinity. As historically practiced in the laboratory, soaking and drying is a key step in shock treatment that allows for easy product storage and mass balances. However, in an industrial setting, the drying step can be eliminated, which should reduce the negative impact from higher crystallinity. Future studies should focus on understanding the microscopic structure of the lignocellulose matrix, understanding the impact of soaking and drying, and completely demystifying the mechanics of shock treatment.

Because alkaline treatment can be costly from the use of expensive chemicals and high temperatures, “co-treatment” – a process that mimics rumination – was investigated. In this study, co-treatment did not yield a significant improvement in

MAAD performance. Future work should focus on less digestible biomass consisting of larger particle sizes with a smaller amount of exposed surface area. Bioreactor designs that have a built-in grinding system should be considered to reduce exposure to air.

9.2. Methane-Arrested Anaerobic Digestion

The impacts of nutrient sources and preservation techniques were investigated. Both chicken manure (without antibiotics) and sewage sludge contain valuable nutrients for MAAD. In general, compared to dried nutrients, fresh nutrients yield higher conversions, yields, and acid concentrations. Considering that wet nutrients are difficult to transport, it may be acceptable to air-dry sewage sludge and accept a slight reduction in performance. Another option is to utilize wet nutrients sources at their point of production. This will involve the construction of anaerobic digesters at farms and wastewater treatment plants. Future research should investigate the impact of moisture content on digestion performance. It is possible that there is an optimal range for the moisture content of feedstocks used in the carboxylate platform.

Because pretreatment is one of the most expensive processing steps in lignocellulose-to-biofuel conversion, the only avenue to reduce or eliminate pretreatment costs is to utilize biomass feedstocks with low resistance to biochemical degradation. In this regard, this study considered two feedstocks: prickly pear cladodes and algae. In MAAD, prickly pear cladodes produced high yields, conversion, and selectivity without needing process improvements, such as chemical pretreatment or *in-situ* product removal. They performed significantly better than previous feedstocks studied using the MixAlco™ process. Prickly pear cladodes are highly digestible feedstocks that could

potentially improve MixAlco™ process yields and reduce costs. This biomass warrants further investigation using the carboxylate platform and other biomass-to-biofuel technologies.

Algae is a highly digestible feedstock for MAAD; however, digestibility greatly reduced after aggressive triglyceride extraction and drying using laboratory processes that quantify the composition. Most studies on the carboxylate platform have focused on carbohydrate-rich substrates; however, anaerobic digestion of proteins and fatty acids in algae has the potential to produce odd-numbered and iso-carboxylic acids. Future studies should be performed to investigate the impact of substrate composition on carboxylic acid composition.

Within all digesters in this study, enanthic (C7) and caprylic (C8) acid were produced in very small quantities. However, C7 and C8 have a water solubility of only 0.02 g/L and 0.01 g/L, respectively. With such low solubilities, it is possible that these neutralized acids precipitate onto the solid residue at the base of the digester. Because the digesters were first centrifuged before sampling, very little C7 or C8 was detected. Future studies should investigate the solid residue in digesters after anaerobic digestion is complete.

9.3. *In-situ* Product Removal

The procedure for *in-situ* CO_2-sustained anion-exchange resin adsorption was developed for semi-continuous countercurrent MAAD. The results indicate that minimizing acid inhibition enhances digestion performance. *In-situ* product removal significantly increased biomass conversion and product yield by 228 and 209%,

respectively. The mass fraction of longer-chain carboxylic acids also increased with resin adsorption. This study shows that *in-situ* product removal is a promising approach for improving digestion performance. Future studies should investigate extraction techniques like liquid-liquid extraction, electrodialysis, etc.

REFERENCES

(1) Total Energy Annual Data - U.S. Energy Information Administration (EIA) https://www.eia.gov/totalenergy/data/annual/index.php (accessed 2021 -04 -21).

(2) Houghton, J. T.; Meira Filho, L. G.; Bruce, J. P.; Lee, H.; Callander, B. A.; Haites, E. F. *Climate Change 1994: Radiative Forcing of Climate Change and an Evaluation of the IPCC 1992 IS92 Emission Scenarios*; Cambridge University Press, 1995.

(3) Kim, S.; Dale, B. E. Life Cycle Assessment of Various Cropping Systems Utilized for Producing Biofuels: Bioethanol and Biodiesel. *Biomass and Bioenergy* **2005**, *29* (6), 426–439. https://doi.org/10.1016/j.biombioe.2005.06.004.

(4) Sims, R. E. H.; Mabee, W.; Saddler, J. N.; Taylor, M. An Overview of Second Generation Biofuel Technologies. *Bioresource Technology* **2010**, *101* (6), 1570–1580. https://doi.org/10.1016/j.biortech.2009.11.046.

(5) Limayem, A.; Ricke, S. C. Lignocellulosic Biomass for Bioethanol Production: Current Perspectives, Potential Issues and Future Prospects. *Progress in Energy and Combustion Science* **2012**, *38* (4), 449–467. https://doi.org/10.1016/j.pecs.2012.03.002.

(6) Wyman, C. E. BIOMASS ETHANOL: Technical Progress, Opportunities, and Commercial Challenges. *Annu. Rev. Energy. Environ.* **1999**, *24* (1), 189–226. https://doi.org/10.1146/annurev.energy.24.1.189.

(7) Kim, S. Lime Pretreatment and Enzymatic Hydrolysis of Corn Stover. Doctoral Dissertation. Texas A&M University, College Station. Doctoral dissertation, Texas A&M University, 2003.

(8) Holtzapple, M. T.; Granda, C. B. Carboxylate Platform: The MixAlco Process Part 1: Comparison of Three Biomass Conversion Platforms. *Appl. Biochem. Biotechnol.* **2009**, *156* (1–3), 95–106. https://doi.org/10.1007/s12010-008-8466-y.

(9) Wright, M. M.; Brown, R. C. Comparative Economics of Biorefineries Based on the Biochemical and Thermochemical Platforms. *Biofuels, Bioproducts and Biorefining* **2007**, *1* (1), 49–56. https://doi.org/10.1002/bbb.8.

(10) Agler, M. T.; Wrenn, B. A.; Zinder, S. H.; Angenent, L. T. Waste to Bioproduct Conversion with Undefined Mixed Cultures: The Carboxylate Platform. *Trends in Biotechnology* **2011**, *29* (2), 70–78. https://doi.org/10.1016/j.tibtech.2010.11.006.

(11) Darvekar, P.; Holtzapple, M. T. Assessment of Shock Pretreatment of Corn Stover Using the Carboxylate Platform. *Appl Biochem Biotechnol* **2016**, *178* (6), 1081–1094. https://doi.org/10.1007/s12010-015-1930-6.

(12) Minty, J. J.; Lin, X. N. Chapter 18 - Engineering Synthetic Microbial Consortia for Consolidated Bioprocessing of Ligonocellulosic Biomass into Valuable Fuels and Chemicals. In *Direct Microbial Conversion of Biomass to Advanced Biofuels*; Himmel, M. E., Ed.; Elsevier: Amsterdam, 2015; pp 365–381. https://doi.org/10.1016/B978-0-444-59592-8.00018-X.

(13) Lynd, L. R.; Zyl, W. H. van; McBride, J. E.; Laser, M. Consolidated Bioprocessing of Cellulosic Biomass: An Update. *Current Opinion in Biotechnology* **2005**, *16* (5), 577–583. https://doi.org/10.1016/j.copbio.2005.08.009.

(14) Rughoonundun, H.; Holtzapple, M. T. Converting Wastewater Sludge and Lime-Treated Sugarcane Bagasse to Mixed Carboxylic Acids – a Potential Pathway to Ethanol Biofuel Production. *Biomass and Bioenergy* **2017**, *105*, 73–82. https://doi.org/10.1016/j.biombioe.2017.06.007.

(15) Holtzapple, M. T. Chapters Cellulose, Hemicelluloses, and Lignin. *Macrae R., Robinson RK, SadlerM. J.(Eds.), Encyclopedia of Food Science, Food Technology, and Nutrition. Academic Press, London* **1993**, 758–768.

(16) Holtzapple, M.; Lonkar, S.; Granda, C. Producing Biofuels via the Carboxylate Platform. *Chemical Engineering Progress* **2015**, *111* (3), 52–57.

(17) Pham, V.; Holtzapple, M.; El-Halwagi, M. Techno-Economic Analysis of Biomass to Fuel Conversion via the MixAlco Process. *Journal of Industrial Microbiology and Biotechnology* **2010**, *37* (11), 1157–1168. https://doi.org/10.1007/s10295-010-0763-0.

(18) Mosier, N. Features of Promising Technologies for Pretreatment of Lignocellulosic Biomass. *Bioresource Technology* **2005**, *96* (6), 673–686. https://doi.org/10.1016/j.biortech.2004.06.025.

(19) Taherzadeh, M. J.; Karimi, K. Pretreatment of Lignocellulosic Wastes to Improve Ethanol and Biogas Production: A Review. *International Journal of Molecular Sciences* **2008**, *9* (9), 1621–1651. https://doi.org/10.3390/ijms9091621.

(20) Kumar, P.; Barrett, D. M.; Delwiche, M. J.; Stroeve, P. Methods for Pretreatment of Lignocellulosic Biomass for Efficient Hydrolysis and Biofuel Production. *Ind. Eng. Chem. Res.* **2009**, *48* (8), 3713–3729. https://doi.org/10.1021/ie801542g.

(21) Zhu, L.; O'Dwyer, J. P.; Chang, V. S.; Granda, C. B.; Holtzapple, M. T. Structural Features Affecting Biomass Enzymatic Digestibility. *Bioresour. Technol.* **2008**, *99* (9), 3817–3828. https://doi.org/10.1016/j.biortech.2007.07.033.

(22) Kumar, R.; Wyman, C. E. Does Change in Accessibility with Conversion Depend on Both the Substrate and Pretreatment Technology? *Bioresource Technology* **2009**, *100* (18), 4193–4202. https://doi.org/10.1016/j.biortech.2008.11.058.

(23) Appels, L.; Baeyens, J.; Degrève, J.; Dewil, R. Principles and Potential of the Anaerobic Digestion of Waste-Activated Sludge. *Progress in Energy and Combustion Science* **2008**, *34* (6), 755–781. https://doi.org/10.1016/j.pecs.2008.06.002.

(24) Golub, K. W. Effect of Bioreactor Mode of Operation on Mixed-Acid Fermentations. Doctoral Dissertation. Texas A&M University, College Station, 2012.

(25) Aiello-Mazzarri, C.; Coward-Kelly, G.; Agbogbo, F. K.; Holtzapple, M. T. Conversion of Municipal Solid Waste into Carboxylic Acids by Anaerobic

Countercurrent Fermentation. *Appl Biochem Biotechnol* **2005**, *127* (2), 79–93. https://doi.org/10.1385/ABAB:127:2:079.

(26) Ross, M. K. Production of Acetic Acid from Waste Biomass. Doctoral Dissertation. Texas A&M University, College Station. Texas A&M University, College Station. Doctoral dissertation, Texas A&M University, United States -- Texas, 1998.

(27) Loescher, M. E. Volatile Fatty Acid Fermentation of Biomass and Kinetic Modeling Using the CPDM Method. Doctoral Dissertation. Texas A&M University, College Station. Doctoral dissertation, Texas A & M University, United States -- Texas, 1996.

(28) Fu, Z.; Holtzapple, M. T. Anaerobic Mixed-Culture Fermentation of Aqueous Ammonia-Treated Sugarcane Bagasse in Consolidated Bioprocessing. *Biotechnology and Bioengineering* **2010**, *106* (2), 216–227. https://doi.org/10.1002/bit.22679.

(29) Freeman, A.; Woodley, J. M.; Lilly, M. D. In Situ Product Removal as a Tool for Bioprocessing. *Nat Biotechnol* **1993**, *11* (9), 1007–1012. https://doi.org/10.1038/nbt0993-1007.

(30) Dafoe, J. T.; Daugulis, A. J. In Situ Product Removal in Fermentation Systems: Improved Process Performance and Rational Extractant Selection. *Biotechnology Letters* **2014**, *36* (3), 443–460. https://doi.org/10.1007/s10529-013-1380-6.

(31) López-Garzón, C. S.; Straathof, A. J. J. Recovery of Carboxylic Acids Produced by Fermentation. *Biotechnology Advances* **2014**, *32* (5), 873–904. https://doi.org/10.1016/j.biotechadv.2014.04.002.

(32) Moldes, A. B.; Alonso, J. L.; Parajó, J. C. Recovery of Lactic Acid from Simultaneous Saccharification and Fermentation Media Using Anion Exchange Resins. *Bioprocess Biosyst Eng* **2003**, *25* (6), 357–363. https://doi.org/10.1007/s00449-002-0316-7.

(33) Pradhan, N.; Rene, E.; Lens, P.; Dipasquale, L.; D'Ippolito, G.; Fontana, A.; Panico, A.; Esposito, G. Adsorption Behaviour of Lactic Acid on Granular Activated Carbon and Anionic Resins: Thermodynamics, Isotherms and Kinetic Studies. *Energies* **2017**, *10* (5), 665. https://doi.org/10.3390/en10050665.

(34) Garrett, B. G.; Srinivas, K.; Ahring, B. K. Performance and Stability of Amberlite™ IRA-67 Ion Exchange Resin for Product Extraction and PH Control during Homolactic Fermentation of Corn Stover Sugars. *Biochemical Engineering Journal* **2015**, *94*, 1–8. https://doi.org/10.1016/j.bej.2014.11.004.

(35) Roy, S. Effect of Extraction Using Ion-Exchange Resins on Batch Mixed-Acid Fermentations. Master's Thesis. Texas A&M University, College Station. Thesis, 2014.

(36) McMillan, J. D. Pretreatment of Lignocellulosic Biomass. In *Enzymatic Conversion of Biomass for Fuels Production*; ACS Symposium Series; American Chemical Society, 1994; Vol. 566, pp 292–324. https://doi.org/10.1021/bk-1994-0566.ch015.

(37) Tao, L.; Aden, A.; Elander, R. T.; Pallapolu, V. R.; Lee, Y. Y.; Garlock, R. J.; Balan, V.; Dale, B. E.; Kim, Y.; Mosier, N. S.; Ladisch, M. R.; Falls, M.; Holtzapple, M. T.; Sierra, R.; Shi, J.; Ebrik, M. A.; Redmond, T.; Yang, B.; Wyman, C. E.; Hames, B.; Thomas, S.; Warner, R. E. Process and Technoeconomic Analysis of Leading Pretreatment Technologies for Lignocellulosic Ethanol Production Using Switchgrass. *Bioresource Technology* **2011**, *102* (24), 11105–11114. https://doi.org/10.1016/j.biortech.2011.07.051.

(38) Falls, M.; Meysing, D.; Liang, C.; Karim, M. N.; Carstens, G.; Tedeschi, L. O.; Holtzapple, M. T. Development of Highly Digestible Animal Feed from Lignocellulosic Biomass Part 2: Oxidative Lime Pretreatment (OLP) and Shock Treatment of Corn Stover1. *Translational Animal Science* **2017**, *1* (2), 215–220. https://doi.org/10.2527/tas2017.0025.

(39) Liang, C.; Lonkar, S.; Darvekar, P.; Bond, A.; Zentay, A. N.; Holtzapple, M. T.; Karim, M. N. Countercurrent Enzymatic Saccharification of Pretreated Corn Stover Part 2: Lime + Shock Pretreated Corn Stover and Commercial Approach. *Biomass and Bioenergy* **2017**, *97*, 43–52. https://doi.org/10.1016/j.biombioe.2016.12.003.

(40) Bond, A. E. Making Bombs for Peaceful Purposes: How Explosive Processes Render Lignocellulosic Biomass More Amenable to Biological Digestion. Doctoral Dissertation. Texas A&M University, College Station. Doctoral dissertation, 2016.

(41) Holtzapple, M.; Wales, M.; Fu, Z.; Rughoonundun, H.; Bond, A.; Darvekar, P.; Zentay, N.; Mann, T. *Novel Mechanical Pretreatment for Lignocellulosic Feedstocks*; DOE Project# DE-EE0005005. 000; Texas A&M University, 2014.

(42) Bond, A.; Rughoonundun, H.; Petersen, E.; Holtzapple, C.; Holtzapple, M. Shock Treatment of Corn Stover. *Biotechnol Progress* **2017**, *33* (3), 815–823. https://doi.org/10.1002/btpr.2437.

(43) Falls, M.; Madison, M.; Liang, C.; Karim, M. N.; Sierra-Ramirez, R.; Holtzapple, M. T. Mechanical Pretreatment of Biomass – Part II: Shock Treatment. *Biomass and Bioenergy* **2019**, *126*, 47–56. https://doi.org/10.1016/j.biombioe.2019.04.016.

(44) Darvekar, P. Assessment of Shock Pretreatment of Corn Stover Using the Carboxylate Platform. Doctoral Dissertation. Texas A&M University, College Station. Thesis, 2016.

(45) MacDonald, D. G.; Bakhshi, N. N.; Mathews, J. F.; Roychowdhury, A.; Bajpai, P.; Moo-Young, M. Alkali Treatment of Corn Stover to Improve Sugar Production by Enzymatic Hydrolysis. *Biotechnology and Bioengineering* **1983**, *25* (8), 2067–2076. https://doi.org/10.1002/bit.260250815.

(46) McDonough, T. J. Oxygen Delignification. *IPC Technical Paper Series* **1989**, *318*.

(47) Council, N. R.; Resources, B. on A. and N.; Nutrition, C. on A.; Nutrition, S. on D. C. *Nutrient Requirements of Dairy Cattle: Seventh Revised Edition, 2001*; National Academies Press, 2001.

(48) Tedeschi, L. O.; Fox, D. G. *The Ruminant Nutrition System: An Applied Model for Predicting Nutrient Requirements and Feed Utilization in Ruminants*; XanEdu, 2020.

(49) Falls, M. D. Development of Oxidative Lime Pretreatment and Shock Treatment to Produce Highly Digestible Lignocellulose for Biofuel and Ruminant Feed Applications. Doctoral Dissertation. Texas A&M University, College Station. Ph.D. Dissertation, 2011.

(50) Falls, M.; Meysing, D.; Lonkar, S.; Liang, C.; Karim, M. N.; Carstens, G.; Tedeschi, L. O.; Holtzapple, M. T. Development of Highly Digestible Animal Feed from Lignocellulosic Biomass Part 1: Oxidative Lime Pretreatment (OLP) and Ball Milling of Forage Sorghum1. *Translational Animal Science* **2017**, *1* (2), 208–214. https://doi.org/10.2527/tas2017.0024.

(51) Selig, M.; Weiss, N.; Ji, Y. Enzymatic Saccharification of Lignocellulosic Biomass. National Renewable Energy Laboratory NREL. **2008**.

(52) Sluiter, A.; Hames, B.; Ruiz, R.; Scarlata, C.; Sluiter, J.; Templeton, D.; Crocker, D. Determination of Structural Carbohydrates and Lignin in Biomass. *Laboratory analytical procedure* **2008**, *1617*, 1–16.

(53) Hsu, S.-C. Effects of Product Removal Using Ion-Exchange Resin and Sodium Hydroxide Pretreatment in Mixed-Culture Fermentation. Master's Thesis. Texas A&M University, College Station. Thesis, 2019.

(54) Lonkar, S.; Liang, C.; Bond, A.; Darvekar, P.; Brooks, H.; Derner, J.; Yang, R.; Wilson, E.; Garcia, S.; Nazmul Karim, M.; Holtzapple, M. Countercurrent

Saccharification of Lime-Pretreated Corn Stover – Part 1. *Biomass and Bioenergy* **2017**, *96*, 28–37. https://doi.org/10.1016/j.biombioe.2016.10.013.

(55) Liang, C. Batch Enzymatic Hydrolysis of Pretreated Corn Stover and Improvements with Countercurrent Saccharification. Master's Thesis. Texas A&M University, College Station. Thesis, 2015.

(56) Novozymes Cellic® CTec3 https://www.novozymes.com/-/media/Project/Novozymes/Website/website/advance-your-business/05_L2_Bioenergy/Benefit-sheets/Cellic-CTec3-HS-application-sheet-NA.pdf (accessed 2020 -05 -06).

(57) Novozymes Cellic® HTec3 https://www.yumpu.com/en/document/read/30214569/novozymes-cellicar-htec3 (accessed 2020 -05 -06).

(58) US Patent Application for PROCESSES FOR CONVERTING BIOMASS INTO HIGH-VALUE PRODUCTS Patent Application (Application #20210002603 issued January 7, 2021) - Justia Patents Search https://patents.justia.com/patent/20210002603 (accessed 2021 -08 -26).

(59) Ahmadi, F.; Rad, A. R.; Holtzapple, M. T.; Zamiri, M. J. Short-Term Oxidative Lime Pretreatment of Palm Pruning Waste for Use as Animal Feedstuff. *Journal of the Science of Food and Agriculture* **2013**, *93* (8), 2061–2070. https://doi.org/10.1002/jsfa.5963.

(60) Podgorbunskikh, E. M.; Bychkov, A. L.; Lomovsky, O. I. Determination of Surface Accessibility of the Cellulose Substrate According to Enzyme Sorption. *Polymers* **2019**, *11* (7), 1201. https://doi.org/10.3390/polym11071201.

(61) Weimer, P. J.; Hackney, J. M.; French, A. D. Effects of Chemical Treatments and Heating on the Crystallinity of Celluloses and Their Implications for Evaluating the Effect of Crystallinity on Cellulose Biodegradation. *Biotechnology and Bioengineering* **1995**, *48* (2), 169–178. https://doi.org/10.1002/bit.260480211.

(62) Data Explorer | Climate Watch https://www.climatewatchdata.org/data-explorer/historical-emissions?historical-emissions-data-sources=cait&historical-emissions-end_year=2018&historical-emissions-gases=all-ghg&historical-emissions-regions=All%20Selected&historical-emissions-sectors=total-including-lucf&page=1 (accessed 2021 -04 -29).

(63) Klass, D. L. *Biomass for Renewable Energy, Fuels, and Chemicals*; Elsevier, 1998.

(64) Perlack, R. D. *Biomass as Feedstock for a Bioenergy and Bioproducts Industry: The Technical Feasibility of a Billion-Ton Annual Supply*; Oak Ridge National Laboratory, 2005.

(65) Langholtz, M. H.; Stokes, B. J.; Eaton, L. M. 2016 Billion-Ton Report: Advancing Domestic Resources for a Thriving Bioeconomy, Volume 1: Economic Availability of Feedstock. *Oak Ridge National Laboratory, Oak Ridge, Tennessee, managed by UT-Battelle, LLC for the US Department of Energy* **2016**, *2016*, 1–411.

(66) Kim, S.; Holtzapple, M. T. Lime Pretreatment and Enzymatic Hydrolysis of Corn Stover. *Bioresource Technology* **2005**, *96* (18), 1994–2006. https://doi.org/10.1016/j.biortech.2005.01.014.

(67) Kaar, W. E.; Holtzapple, M. T. Using Lime Pretreatment to Facilitate the Enzymic Hydrolysis of Corn Stover. *Biomass and Bioenergy* **2000**, 11.

(68) Holtzapple, M. T.; Jun, J.-H.; Ashok, G.; Patibandla, S. L.; Dale, B. E. The Ammonia Freeze Explosion (AFEX) Process. *Appl Biochem Biotechnol* **1991**, *28* (1), 59–74. https://doi.org/10.1007/BF02922589.

(69) Wyman, C. E.; Dale, B. E.; Elander, R. T.; Holtzapple, M.; Ladisch, M. R.; Lee, Y. Y. Coordinated Development of Leading Biomass Pretreatment Technologies. *Bioresource Technology* **2005**, *96* (18), 1959–1966. https://doi.org/10.1016/j.biortech.2005.01.010.

(70) Darvekar, P.; Liang, C.; Karim, M. N.; Holtzapple, M. T. Effect of Headspace Gas Composition on Carboxylates Production in Open-Culture Fermentation of Corn Stover. *Biomass and Bioenergy* **2019**, *126*, 57–61. https://doi.org/10.1016/j.biombioe.2019.04.019.

(71) Olokede, O.; Hsu, S.; Schiele, S.; Ju, H.; Holtzapple, M. Assessment of Shock Pretreatment and Alkali Pretreatment on Corn Stover Using Enzymatic Hydrolysis. *Biotechnology Progress* **2022**, *38* (1), e3217. https://doi.org/10.1002/btpr.3217.

(72) Fu, Z. *Conversion of Sugarcane Bagasse to Carboxylic Acids under Thermophilic Conditions*; 2009.

(73) Domke, S. B.; Aiello-Mazzarri, C.; Holtzapple, M. T. Mixed Acid Fermentation of Paper Fines and Industrial Biosludge. *Bioresource Technology* **2004**, *91* (1), 41–51. https://doi.org/10.1016/S0960-8524(03)00156-1.

(74) Rughoonundun, H.; Mohee, R.; Holtzapple, M. T. Influence of Carbon-to-Nitrogen Ratio on the Mixed-Acid Fermentation of Wastewater Sludge and Pretreated Bagasse. *Bioresource Technology* **2012**, *112*, 91–97. https://doi.org/10.1016/j.biortech.2012.02.081.

(75) McGeehan, S. L.; Naylor, D. V. Automated Instrumental Analysis of Carbon and Nitrogen in Plant and Soil Samples. *Communications in Soil Science and Plant Analysis* **1988**, *19* (4), 493–505.

(76) Smith, A. D.; Holtzapple, M. T. Investigation of the Optimal Carbon–Nitrogen Ratio and Carbohydrate–Nutrient Blend for Mixed-Acid Batch Fermentations. *Bioresource Technology* **2011**, *102* (10), 5976–5987. https://doi.org/10.1016/j.biortech.2011.02.024.

(77) *2013 Peer Review Report - U.S. Department of Energy*.

(78) Industry Product Pricing http://www.westlake.com/industry-product-pricing (accessed 2022 -02 -08).

(79) Domke, S. B. Fermentation of Industrial Biosludge, Paper Fines, Bagasse, and Chicken Manure to Carboxylate Salts. Doctoral Dissertation. Texas A&M University, College Station. Ph.D., Texas A&M University, United States -- Texas.

(80) Roy, S.; Olokede, O.; Wu, H.; Holtzapple, M. In-Situ Carboxylic Acid Separation from Mixed-Acid Fermentation of Cellulosic Substrates in Batch Culture. *Biomass and Bioenergy* **2021**, *151*, 106165. https://doi.org/10.1016/j.biombioe.2021.106165.

(81) Datta, R. Acidogenic Fermentation of Corn Stover. *Biotechnology and Bioengineering* **1981**, *23* (1), 61–77. https://doi.org/10.1002/bit.260230106.

(82) Chan, W. N.; Fu, Z.; Holtzapple, M. T. Co-Digestion of Swine Manure and Corn Stover for Bioenergy Production in MixAlco™ Consolidated Bioprocessing. *Biomass and Bioenergy* **2011**, *35* (10), 4134–4144. https://doi.org/10.1016/j.biombioe.2011.06.053.

(83) Forrest, A. K. Effects of Feedstocks and Inoculum Sources on Mixed-Acid and Hydrogen Fermentations. Doctoral Dissertation. Texas A&M University, College Station, 2011.

(84) Fan, L.; Gharpuray, M. M.; Lee, Y.-H. Enzymatic Hydrolysis. In *Cellulose Hydrolysis*; Fan, L., Gharpuray, M. M., Lee, Y.-H., Eds.; Biotechnology Monographs; Springer: Berlin, Heidelberg, 1987; pp 21–119. https://doi.org/10.1007/978-3-642-72575-3_3.

(85) Kapdan, I. K.; Kargi, F. Bio-Hydrogen Production from Waste Materials. *Enzyme and Microbial Technology* **2006**, *38* (5), 569–582. https://doi.org/10.1016/j.enzmictec.2005.09.015.

(86) Daly, S. E.; Usack, J. G.; Harroff, L. A.; Booth, J. G.; Keleman, M. P.; Angenent, L. T. Systematic Analysis of Factors That Affect Food-Waste Storage: Toward

Maximizing Lactate Accumulation for Resource Recovery. *ACS Sustainable Chem. Eng.* **2020**, *8* (37), 13934–13944. https://doi.org/10.1021/acssuschemeng.0c03161.

(87) Organization (WMO), W. M.; World Meteorological Organization (WMO). *WMO Provisional Report on the State of the Global Climate 2020*; WMO; WMO: Geneva, 2020.

(88) Lange, J.-P. Lignocellulose Conversion: An Introduction to Chemistry, Process and Economics. *Biofuels, Bioproducts and Biorefining* **2007**, *1* (1), 39–48. https://doi.org/10.1002/bbb.7.

(89) Bastidas-Oyanedel, J.-R.; Bonk, F.; Thomsen, M. H.; Schmidt, J. E. Dark Fermentation Biorefinery in the Present and Future (Bio)Chemical Industry. *Rev Environ Sci Biotechnol* **2015**, *14* (3), 473–498. https://doi.org/10.1007/s11157-015-9369-3.

(90) Hao, L.; Lü, F.; Li, L.; Shao, L.; He, P. Response of Anaerobes to Methyl Fluoride, 2-Bromoethanesulfonate and Hydrogen during Acetate Degradation. *Journal of Environmental Sciences* **2013**, *25* (5), 857–864. https://doi.org/10.1016/S1001-0742(12)60203-4.

(91) Wu, H.; Dalke, R.; Mai, J.; Holtzapple, M.; Urgun-Demirtas, M. Arrested Methanogenesis Digestion of High-Strength Cheese Whey and Brewery Wastewater with Carboxylic Acid Production. *Bioresource Technology* **2021**, *332*, 125044. https://doi.org/10.1016/j.biortech.2021.125044.

(92) Holtzapple, M. T.; Davison, R. R.; Ross, M. K.; Aldrett-Lee, S.; Nagwani, M.; Lee, C.-M.; Lee, C.; Adelson, S.; Kaar, W.; Gaskin, D.; Shirage, H.; Chang, N.-S.; Chang, V. S.; Loescher, M. E. Biomass Conversion to Mixed Alcohol Fuels Using the MixAlco Process. *Appl Biochem Biotechnol* **1999**, *79* (1), 609–631. https://doi.org/10.1385/ABAB:79:1-3:609.

(93) Murali, N.; Srinivas, K.; Ahring, B. K. Biochemical Production and Separation of Carboxylic Acids for Biorefinery Applications. *Fermentation* **2017**, *3* (2), 22. https://doi.org/10.3390/fermentation3020022.

(94) Pind, P. F.; Angelidaki, I.; Ahring, B. K. Dynamics of the Anaerobic Process: Effects of Volatile Fatty Acids. *Biotechnology and Bioengineering* **2003**, *82* (7), 791–801. https://doi.org/10.1002/bit.10628.

(95) Gottwald, M.; Gottschalk, G. The Internal PH of Clostridium Acetobutylicum and Its Effect on the Shift from Acid to Solvent Formation. *Archives of Microbiology* **1985**, *143* (1), 42–46. https://doi.org/10.1007/BF00414766.

(96) Mills, T. Y.; Sandoval, N. R.; Gill, R. T. Cellulosic Hydrolysate Toxicity and Tolerance Mechanisms in Escherichia Coli. *Biotechnology for Biofuels* **2009**, *2* (1), 26. https://doi.org/10.1186/1754-6834-2-26.

(97) Yin, J.; Yu, X.; Wang, K.; Shen, D. Acidogenic Fermentation of the Main Substrates of Food Waste to Produce Volatile Fatty Acids. *International Journal of Hydrogen Energy* **2016**, *41* (46), 21713–21720. https://doi.org/10.1016/j.ijhydene.2016.07.094.

(98) Siegert, I.; Banks, C. The Effect of Volatile Fatty Acid Additions on the Anaerobic Digestion of Cellulose and Glucose in Batch Reactors. *Process Biochemistry* **2005**, *40* (11), 3412–3418. https://doi.org/10.1016/j.procbio.2005.01.025.

(99) Angenent, L. T.; Richter, H.; Buckel, W.; Spirito, C. M.; Steinbusch, K. J. J.; Plugge, C. M.; Strik, D. P. B. T. B.; Grootscholten, T. I. M.; Buisman, C. J. N.; Hamelers, H. V. M. Chain Elongation with Reactor Microbiomes: Open-Culture Biotechnology To Produce Biochemicals. *Environ. Sci. Technol.* **2016**, *50* (6), 2796–2810. https://doi.org/10.1021/acs.est.5b04847.

(100) Wu, Q.; Bao, X.; Guo, W.; Wang, B.; Li, Y.; Luo, H.; Wang, H.; Ren, N. Medium Chain Carboxylic Acids Production from Waste Biomass: Current Advances and Perspectives. *Biotechnology Advances* **2019**, *37* (5), 599–615. https://doi.org/10.1016/j.biotechadv.2019.03.003.

(101) Wu, H.; Valentino, L.; Riggio, S.; Holtzapple, M.; Urgun-Demirtas, M. Performance Characterization of Nanofiltration, Reverse Osmosis, and Ion Exchange Technologies for Acetic Acid Separation. *Separation and Purification Technology* **2021**, *265*, 118108. https://doi.org/10.1016/j.seppur.2020.118108.

(102) Husson, S. M.; King, C. J. Carbon Dioxide-Sustained Adsorption of Lactic Acid at PH > p K_a of the Acid. *Ind. Eng. Chem. Res.* **1999**, *38* (4), 1625–1632. https://doi.org/10.1021/ie980428v.

(103) Agbogbo, F. K. Anaerobic Fermentation of Rice Straw and Chicken Manure to Carboxylic Acids. Doctoral Dissertation. Texas A&M University, College Station. Book, Texas A&M University, 2005.

(104) Golub, K. W.; Smith, A. D.; Hollister, E. B.; Gentry, T. J.; Holtzapple, M. T. Investigation of Intermittent Air Exposure on Four-Stage and One-Stage Anaerobic Semi-Continuous Mixed-Acid Fermentations. *Bioresource Technology* **2011**, *102* (8), 5066–5075. https://doi.org/10.1016/j.biortech.2011.02.011.

(105) Rohm and Haas Company, 2020. Product data sheet of AMBERLITE IRA-67 https://www.lenntech.com/Data-sheets/Rohm-&-Haas-Amberlite-IRA-67-L.pdf.

(106) Yousuf, A.; Bonk, F.; Bastidas-Oyanedel, J.-R.; Schmidt, J. E. Recovery of Carboxylic Acids Produced during Dark Fermentation of Food Waste by Adsorption on Amberlite IRA-67 and Activated Carbon. *Bioresource Technology* **2016**, *217*, 137–140. https://doi.org/10.1016/j.biortech.2016.02.035.

(107) Lonkar, S.; Fu, Z.; Holtzapple, M. Optimum Alcohol Concentration for Chain Elongation in Mixed-Culture Fermentation of Cellulosic Substrate: Optimum Alcohol Concentration for Chain Elongation. *Biotechnology and Bioengineering* **2016**, *113* (12), 2597–2604. https://doi.org/10.1002/bit.26024.

(108) Smith, A. D.; Holtzapple, M. T. The Slope Method: A Tool for Analyzing Semi-Continuous Data. *Appl Biochem Biotechnol* **2011**, *163* (7), 826–835. https://doi.org/10.1007/s12010-010-9086-x.

(109) Njokweni, S. G.; Steyn, A.; Botes, M.; Viljoen-Bloom, M.; van Zyl, W. H. Potential Valorization of Organic Waste Streams to Valuable Organic Acids through Microbial Conversion: A South African Case Study. *Catalysts* **2021**, *11* (8), 964. https://doi.org/10.3390/catal11080964.

(110) Zhou, M.; Yan, B.; Wong, J. W. C.; Zhang, Y. Enhanced Volatile Fatty Acids Production from Anaerobic Fermentation of Food Waste: A Mini-Review Focusing on Acidogenic Metabolic Pathways. *Bioresource Technology* **2018**, *248*, 68–78. https://doi.org/10.1016/j.biortech.2017.06.121.

(111) Li, H.; Li, A.; Shuang, C.; Zhou, Q.; Li, W. Fouling of Anion Exchange Resin by Fluorescence Analysis in Advanced Treatment of Municipal Wastewaters. *Water Research* **2014**, *66*, 233–241. https://doi.org/10.1016/j.watres.2014.08.027.

(112) U.S. Energy Facts Explained https://www.eia.gov/energyexplained/us-energy-facts/ (accessed 2021 -03 -02).

(113) Ragauskas, A. J.; Williams, C. K.; Davison, B. H.; Britovsek, G.; Cairney, J.; Eckert, C. A.; Frederick, W. J.; Hallett, J. P.; Leak, D. J.; Liotta, C. L.; Mielenz, J. R.; Murphy, R.; Templer, R.; Tschaplinski, T. The Path Forward for Biofuels and Biomaterials. *Science* **2006**, *311*, 484–489.

(114) Granda, C. B.; Holtzapple, M. T.; Luce, G.; Searcy, K.; Mamrosh, D. L. Carboxylate Platform: The MixAlco Process Part 2: Process Economics. *Appl Biochem Biotechnol* **2009**, *156* (1), 107–124. https://doi.org/10.1007/s12010-008-8481-z.

(115) Schmer, M. R.; Vogel, K. P.; Mitchell, R. B.; Perrin, R. K. Net Energy of Cellulosic Ethanol from Switchgrass. *PNAS* **2008**, *105* (2), 464–469. https://doi.org/10.1073/pnas.0704767105.

(116) US EPA, O. Basic Information about Biosolids https://www.epa.gov/biosolids/basic-information-about-biosolids (accessed 2020 -10 -13).

(117) Rughoonundun, H.; Granda, C.; Mohee, R.; Holtzapple, M. T. Effect of Thermochemical Pretreatment on Sewage Sludge and Its Impact on Carboxylic Acids Production. *Waste Management* **2010**, *30* (8), 1614–1621. https://doi.org/10.1016/j.wasman.2010.03.017.

(118) Wu, H. Effect of Carbon Dioxide-Sustained Adsorption Using Ion Exchange Resin on Mixed-Acid Fermentation. Master's Thesis. Texas A&M University, College Station. Thesis, 2018.

(119) Hoover, N. L.; Law, J. Y.; Long, L. A. M.; Kanwar, R. S.; Soupir, M. L. Long-Term Impact of Poultry Manure on Crop Yield, Soil and Water Quality, and Crop Revenue. *Journal of Environmental Management* **2019**, *252*, 109582. https://doi.org/10.1016/j.jenvman.2019.109582.

(120) Poultry Litter: Issues and Opportunities https://www.thepoultrysite.com/articles/poultry-litter-issues-and-opportunities (accessed 2021 -03 -02).

(121) Kayhanian, M.; Rich, D. Pilot-Scale High Solids Thermophilic Anaerobic Digestion of Municipal Solid Waste with an Emphasis on Nutrient

Requirements. *Biomass and Bioenergy* **1995**, *8* (6), 433–444. https://doi.org/10.1016/0961-9534(95)00043-7.

(122) Hollister, E. B.; Forrest, A. K.; Wilkinson, H. H.; Ebbole, D. J.; Malfatti, S. A.; Tringe, S. G.; Holtzapple, M. T.; Gentry, T. J. Structure and Dynamics of the Microbial Communities Underlying the Carboxylate Platform for Biofuel Production. *Appl Microbiol Biotechnol* **2010**, *88* (1), 389–399. https://doi.org/10.1007/s00253-010-2789-7.

(123) Rapier, C. R. Volatile Fatty Acid Fermentation of Lime-Treated Biomass by Rumen Microorganisms. Master's Thesis. Texas A&M University, College Station. Thesis, Texas A&M University, 1995.

(124) Chen, Y.; Jiang, S.; Yuan, H.; Zhou, Q.; Gu, G. Hydrolysis and Acidification of Waste Activated Sludge at Different PHs. *Water Research* **2007**, *41* (3), 683–689. https://doi.org/10.1016/j.watres.2006.07.030.

(125) Holtzapple, M. T.; Wu, H.; Weimer, P. J.; Dalke, R.; Granda, C. B.; Mai, J.; Urgun-Demirtas, M. Microbial Communities for Valorizing Biomass Using the Carboxylate Platform to Produce Volatile Fatty Acids: A Review. *Bioresource Technology* **2021**, 126253. https://doi.org/10.1016/j.biortech.2021.126253.

(126) Kalil, M. S.; Alshiyab, H. S.; Yusoff, W. M. W. Effect of Nitrogen Source and Carbon to Nitrogen Ratio on Hydrogen Production Using C. Acetobutylicum. *American Journal of Biochemistry and Biotechnology* **2009**, *4* (4), 393–401. https://doi.org/10.3844/ajbbsp.2008.393.401.

(127) Morr, C. V. Functionality of Heated Milk Proteins in Dairy and Related Foods. *Journal of Dairy Science* **1985**, *68* (10), 2773–2781. https://doi.org/10.3168/jds.S0022-0302(85)81165-6.

(128) Microbial Composition of Poultry Excreta. *Biological Wastes* **1990**, *33* (2), 95–105. https://doi.org/10.1016/0269-7483(90)90150-Q.

(129) Nascimento, A. L.; Souza, A. J.; Andrade, P. A. M.; Andreote, F. D.; Coscione, A. R.; Oliveira, F. C.; Regitano, J. B. Sewage Sludge Microbial Structures and Relations to Their Sources, Treatments, and Chemical Attributes. *Frontiers in Microbiology* **2018**, *9*, 1462. https://doi.org/10.3389/fmicb.2018.01462.

(130) Holtzapple, M. T.; Granda, C. B. Carboxylate Platform: The MixAlco Process Part 1: Comparison of Three Biomass Conversion Platforms. *Appl Biochem Biotechnol* **2009**, *156* (1–3), 95–106. https://doi.org/10.1007/s12010-008-8466-y.

(131) Taco Vasquez, S.; Dunkleman, J.; Chaudhuri, S. K.; Bond, A.; Holtzapple, M. T. Biomass Conversion to Hydrocarbon Fuels Using the MixAlco^{TM} Process at a Pilot-Plant Scale. *Biomass and Bioenergy* **2014**, *62*, 138–148. https://doi.org/10.1016/j.biombioe.2014.01.005.

(132) Cota-Sánchez, J. H. Chapter 28 - Nutritional Composition of the Prickly Pear (Opuntia Ficus-Indica) Fruit. In *Nutritional Composition of Fruit Cultivars*; Simmonds, M. S. J., Preedy, V. R., Eds.; Academic Press: San Diego, 2016; pp 691–712. https://doi.org/10.1016/B978-0-12-408117-8.00028-3.

(133) Sáenz, C.; Sepúlveda, E.; Matsuhiro, B. Opuntia Spp Mucilage's: A Functional Component with Industrial Perspectives. *Journal of arid environments* **2004**, *57* (3), 275–290.

(134) Nations, F. A. O. U. *Crop Ecology, Cultivation and Uses of Cactus Pear*; Food and Agriculture Organization of the United Nations, 2018.

(135) Griffiths, D. *Yields of Native Prickly Pear in Southern Texas*; U.S. Department of Agriculture, 1915.

(136) Batista, A. M.; Mustafa, A. F.; McAllister, T.; Wang, Y.; Soita, H.; McKinnon, J. J. Effects of Variety on Chemical Composition, in Situ Nutrient Disappearance and in Vitro Gas Production of Spineless Cacti. *Journal of the Science of Food and Agriculture* **2003**, *83* (5), 440–445. https://doi.org/10.1002/jsfa.1393.

(137) Retamal, N.; Durán, J. M.; Fernández, J. Seasonal Variations of Chemical Composition in Prickly Pear (Opuntia Ficus-Indica (L.) Miller). *Journal of the Science of Food and Agriculture* **1987**, *38* (4), 303–311. https://doi.org/10.1002/jsfa.2740380403.

(138) Rodriguez-Felix, A.; Cantwell, M. Developmental Changes in Composition and Quality of Prickly Pear Cactus Cladodes (Nopalitos). *Plant foods for Human nutrition* **1988**, *38* (1), 83–93.

(139) Mohamed–Yasseen, Y.; Barringer, S. A.; Splittstoesser, W. E. A Note on the Uses OfOpuntiaspp. in Central/North America. *Journal of Arid Environments* **1996**, *32* (3), 347–353.

(140) Mizrahi, Y.; Nerd, A.; Nobel, P. S. Cacti as Crops. *Hort. Rev* **1997**, *18*, 291–320.

(141) Malainine, M. E.; Dufresne, A.; Dupeyre, D.; Vignon, M. R.; Mahrouz, M. First Evidence for the Presence of Weddellite Crystallites in Opuntia Ficus Indica Parenchyma. *Zeitschrift für Naturforschung C* **2003**, *58* (11–12), 812–816.

(142) Retamal, N.; Durán, J. M.; Fernández, J. Ethanol Production by Fermentation of Fruits and Cladodes of Prickly Pear Cactus [Opuntia Ficus-indica (L.) Miller]. *Journal of the Science of Food and Agriculture* **1987**, *40* (3), 213–218.

(143) Ben, T. A. Nutritional Value of Several Opuntia Species. Thesis, Oregon State University, 1987.

(144) Stintzing, F. C.; Carle, R. Cactus Stems (Opuntia Spp.): A Review on Their Chemistry, Technology, and Uses. *Molecular nutrition & food research* **2005**, *49* (2), 175–194.

(145) Saag, L. M. K.; Sanderson, G. R.; Moyna, P.; Ramos, G. Cactaceae Mucilage Composition. *Journal of the Science of Food and Agriculture* **1975**, *26* (7), 993–1000.

(146) Matsuhiro, B.; Lillo, L. E.; Sáenz, C.; Urzúa, C. C.; Zárate, O. Chemical Characterization of the Mucilage from Fruits of Opuntia Ficus Indica. *Carbohydrate polymers* **2006**, *63* (2), 263–267.

(147) Nobel, P. S.; Cavelier, J.; Andrade, J. L. Mucilage in Cacti: Its Apoplastic Capacitance, Associated Solutes, and Influence on Tissue 5. *Journal of Experimental Botany* **1992**, *43* (5), 641–648.

(148) Trachtenberg, S.; Mayer, A. M. Composition and Properties of Opuntia Ficus-Indica Mucilage. *Phytochemistry* **1981**, *20* (12), 2665–2668.

(149) McConn, M. M.; Nakata, P. A. Oxalate Reduces Calcium Availability in the Pads of the Prickly Pear Cactus through Formation of Calcium Oxalate Crystals. *Journal of agricultural and food chemistry* **2004**, *52* (5), 1371–1374.

(150) de Chávez, M. M.; Chávez, A.; Valles, V.; Roldán, J. A. The Nopal: A Plant of Manifold Qualities. *Plants in Human Nutrition* **1995**, *77*, 109–134.

(151) do Nascimento Santos, T.; Dutra, E. D.; do Prado, A. G.; Leite, F. C. B.; de Souza, R. de F. R.; dos Santos, D. C.; de Abreu, C. A. M.; Simões, D. A.; de Morais Jr, M. A.; Menezes, R. S. C. Potential for Biofuels from the Biomass of Prickly Pear Cladodes: Challenges for Bioethanol and Biogas Production in Dry Areas. *Biomass and Bioenergy* **2016**, *85*, 215–222.

(152) Calabrò, P. S.; Catalán, E.; Folino, A.; Sánchez, A.; Komilis, D. Effect of Three Pretreatment Techniques on the Chemical Composition and on the Methane Yields of Opuntia Ficus-Indica (Prickly Pear) Biomass. *Waste Management & Research* **2018**, *36* (1), 17–29.

(153) Blair, B. B.; Yim, W. C.; Cushman, J. C. Characterization of a Microbial Consortium with Potential for Biological Degradation of Cactus Pear Biomass for Biofuel Production. *Heliyon* **2021**, *7* (8), e07854.

(154) Jamai, L.; Ettayebi, M. OPTIMIZATION OF BIOETHANOL PRODUCTION FROM PRICKLY PEAR OF Opuntia Ficus-Indica AT HIGH TEMPERATURES. *Environmental Engineering & Management Journal (EEMJ)* **2021**, *20* (6).

(155) Thanakoses, P.; Black, A. S.; Holtzapple, M. T. Fermentation of Corn Stover to Carboxylic Acids. *Biotechnology and Bioengineering* **2003**, *83* (2), 191–200. https://doi.org/10.1002/bit.10663.

(156) de Sá, L. R. V.; de Oliveira, M. A. L.; Cammarota, M. C.; Matos, A.; Ferreira-Leitão, V. S. Simultaneous Analysis of Carbohydrates and Volatile Fatty Acids by HPLC for Monitoring Fermentative Biohydrogen Production. *International Journal of Hydrogen Energy* **2011**, *36* (23), 15177–15186. https://doi.org/10.1016/j.ijhydene.2011.08.056.

(157) Kumar, A. K.; Sharma, S. Recent Updates on Different Methods of Pretreatment of Lignocellulosic Feedstocks: A Review. *Bioresources and Bioprocessing* **2017**, *4* (1), 7. https://doi.org/10.1186/s40643-017-0137-9.

(158) Weimer, P. J.; Hall, M. B. The Potential for Biomimetic Application of Rumination to Bioreactor Design. *Biomass and Bioenergy* **2020**, *143*, 105822. https://doi.org/10.1016/j.biombioe.2020.105822.

(159) Barakat, A.; de Vries, H.; Rouau, X. Dry Fractionation Process as an Important Step in Current and Future Lignocellulose Biorefineries: A Review. *Bioresource Technology* **2013**, *134*, 362–373. https://doi.org/10.1016/j.biortech.2013.01.169.

(160) Weimer, P. J.; Russell, J. B.; Muck, R. E. Lessons from the Cow: What the Ruminant Animal Can Teach Us about Consolidated Bioprocessing of Cellulosic Biomass. *Bioresource Technology* **2009**, *100* (21), 5323–5331. https://doi.org/10.1016/j.biortech.2009.04.075.

(161) Van Soest, P. J. *Nutritional Ecology of the Ruminant*; Cornell university press, 1994.

(162) Corona® Hand Mill Parts Breakdown https://coronamill.com/corona-parts.shtm (accessed 2021 -07 -22).

(163) Magdalena, J. A.; González-Fernández, C. Microalgae Biomass as a Potential Feedstock for the Carboxylate Platform. *Molecules* **2019**, *24* (23), 4404. https://doi.org/10.3390/molecules24234404.

(164) Xia, A.; Jacob, A.; Tabassum, M. R.; Herrmann, C.; Murphy, J. D. Production of Hydrogen, Ethanol and Volatile Fatty Acids through Co-Fermentation of Macro- and Micro-Algae. *Bioresource Technology* **2016**, *205*, 118–125. https://doi.org/10.1016/j.biortech.2016.01.025.

(165) Kulkarni, S.; Nikolov, Z. Process for Selective Extraction of Pigments and Functional Proteins from Chlorella Vulgaris. *Algal Research* **2018**, *35*, 185–193. https://doi.org/10.1016/j.algal.2018.08.024.

APPENDIX A

SHOCK TREATMENT PROCEDURES

A-1 Pre-operational Check

1. Gather equipment for the experiment: biomass, sieve, impact wrench, 2-L graduated cylinder, 1-gal bucket, and 1-L HDPE Nalgene® sample bottle.
2. Upon arrival at the pilot plant, empty the shock-gun, check gas cylinders for leaks, connect water hose, measure biomass weight needed based on pre-estimated moisture content, and check if the pressure transducer is properly connected and greased.
3. Turn on water pipeline, oxygen cylinders, hydrogen cylinders, and air compressor.
4. Connect the impact wrench to the pressurized air pipeline.

A-2 Loading Shock-gun

1. Mix weighed biomass with tap water to reach desired working volume. (In this study, it was 2 L. Add water to biomass until 1.8 L and use remaining 0.2 L to wash the residual biomass on the wall.)
2. Pour the biomass slurry into the shock-gun reactor and mix until homogenized.
3. Place gasket on upper flange of test section and lower the barrel on top.
4. Use impact wrench to tighten the flange.
5. Close the doors for both shock-gun reactor and control room.

A-3 Shock Treatment

1. Retreat all personnel to the control room.
2. Turn on the LabView control program (Manual Control).

3. Click “start” → click “upper exhaust” to close the exhaust → click “oxygen.”
4. Fill up the shock-gun with 6.53 bar (abs) (100 psia) oxygen and click “oxygen” again to stop the addition.
5. Click “upper exhaust” to open the exhaust to vent out gas.
6. To ensure an oxygen-rich environment, repeat Steps 3 to Step 5 for 3 times to purge out remaining nitrogen in the shock-gun.
7. Turn on “Main Control” file → click “start.”
8. Input file name and enter required pressure of fuel (hydrogen) and oxygen prior to the program starts.
9. Press “start”, then press “fill sequence.” Wait for 20 min.
10. Press “easy” bottom to ignite shock-gun.
11. From ignition to actual explosion may take approximately 20 seconds.
12. Once shock explosion completed unlock the flange with an impact wrench.

A-4 Product Collection

1. Turn on the water and prepare the 1-gal bucket to collect the pretreated biomass.
2. One person tilts the shock-gun and pours out the biomass slurry into the bucket, and the other person holds the bucket and washes out remaining biomass.
3. Filter pretreated biomass with 80-mesh sieve.
4. Wring out the excess water by hand, then store it in the sample bottle.

A-5 Cleaning Procedures

1. Turn off the water pipe and the power of air compressor.
2. Switch off the pressurized air and disconnect the impact wrench.

3. Close valves of hydrogen and oxygen cylinders.
4. Click “Manual Control” → “start” → click “upper exhaust” → click “oxygen” to vent out the remaining oxygen in the pipeline.
5. Click “hydrogen” to vent out remaining hydrogen in the pipeline.
6. Check gauge to see if the pressure has lowered to atmosphere.
7. Shut down computer and close the door of the control room.

APPENDIX B

ALKALI TREATMENT PROCEDURES

1. Record the empty weight of a clean and dry Petri dish.
2. Weigh ~5g of untreated biomass and placed on a petri dish. Transfer Petri dish to oven (105℃) for 4 h.
3. Pre-heat the shaker and water bath at 50℃.
4. Record post oven weight and calculate the moisture content (MC) of the sample.
5. Add pretreated biomass in dry weight basis into the reactor. W_{Biomass} stands for the actual biomass weight used for experiment, and W_{dry} stands for biomass in dry weight basis.

$$W_{\text{biomass}}(\text{g BM}) = \frac{W_{\text{dry}}\ (\text{g BM})}{1 - \text{MC}}$$

6. Calculate $V_{\text{caustic solution}}$ using the equation below. NaOH loading was calculated using Equation 3-1. In this study, $c_{caustic} = 20$ g NaOH/L solution was used.

$$V_{\text{caustic solution}}\left(\frac{\text{L}}{100\ \text{g dry BM}}\right) = \frac{W\left(\frac{\text{g caustic}}{100\ \text{g dry BM}}\right)}{c_{\text{caustic}}\left(\frac{\text{g caustic}}{\text{L}}\right)}$$

7. Measure D.I. water until the slurry reaches 10 wt% total reaction weight. In this experiment, assume the 20 g/L NaOH solution has the same density as water, so that $V_{\text{caustic solution}}$ can be approximated as its weight (W_{caustic}), and W_{water} is the weight of D.I. water:

$$10\ \text{wt\%} = \frac{W_{\text{biomass}}\ (\text{g BM})}{W_{\text{water}}\ (\text{g}) + W_{\text{caustic}}(\text{g}) + W_{\text{biomass}}(\text{g})}$$

8. Mix W_{water}, W_{caustic}, and W_{biomass} into a reactor (1-L PCCO Nalgene® bottle).
9. Place reactors in water bath at 50℃ for 10 min.
10. Transfer reactors into pre-heated shaker for the stipulated duration.
11. Remove the reactors from pre-heated shaker and place in cold water for 5–10 min to terminate the reaction.
12. If the reactor contents are to be used for enzymatic hydrolysis, open the reactor, and use hydrochloric acid to neutralize the slurry.
13. Separate liquid phase from solid phase using a sieve.
14. Perform moisture content analysis on liquid and solids.
15. Begin preparations for enzymatic hydrolysis.
16. If reactor contents are to be used for anaerobic digestion, open the reactor, and use carbon dioxide to neutralize the slurry.
17. Connect the inlet of a gas distributor with a carbon dioxide (CO_2) pipeline, sealing the joint with Parafilm.
18. Insert gas distributor into the pretreatment slurry in the reactor.
19. Turn on the CO_2 at the flow rate 0.5 L/min, then gradually increases to 1.0 L/min.
20. Turn off the CO_2 as soon as the bubble starts to form, then check the pH.
21. Terminate the neutralization if the pH is 6.5–7.0. The pretreated biomass is ready for methane-arrested anaerobic digestion.

APPENDIX C

ENZYME DILUTION

1. Fill 50-mL volumetric flask with approximately 20-25 mL of D.I.water.
2. Take enzyme (CTec3 or HTec3) out of refrigerator and shake vigorously.
3. Measure 5 mL enzyme solution with an adjustable auto pipette.
4. Clean off enzyme residue that sticks to the outside of pipette tip using lab wipes.
5. Empty pipette tip into 50-mL volumetric flask. To ensure accuracy, measure 5 mL of distilled water with the same pipette tip and empty into volumetric flask.
6. Add distilled water to the flask to 50-mL mark and shake vigorously.
7. Store diluted enzyme solution in 50-mL centrifuge tubes kept in the refrigerator.

APPENDIX D

CITRIC BUFFER PREPARATION

1. Fill a 1-L volumetric flask with about 750 mL of distilled water.
2. Add 8.4 g citric acid monohydrate and 17.65 g trisodium citrate dihydrate to volumetric flask. Stir until complete dissolved.
3. Fill flask with water to the 1-L mark and shake vigorously.
4. Measure the pH; it should be within 4.78–4.82.
5. Store at 4℃ in refrigerator.

APPENDIX E

ANTIBIOTICS PREPARATION

1. Weigh 1 g of tetracycline hydrochloride then pour into a 100-mL volumetric flask.
2. Add 70 mL of 190-proof ethanol to the same flask.
3. Add distilled water to 100-mL mark and shake well.
4. Use up the solution immediately because tetracycline will precipitate over time. Always make the exact amount required per time.
5. Repeat the same process using 1 g of cycloheximide. However, do not use ethanol. Use only distilled water as solvent.

APPENDIX F

BATCH ENZYMATIC HYDROLYSIS

For each sample one 1-L Nalgene bottles is used as enzyme reactor.

1. Determine dry mass *m* of each of your biomass samples using moisture content analysis.
2. Calculate volume of slurry on a 5% biomass per volume ratio.

$$V = \frac{m}{0.05}$$

3. Calculate volume of citrate buffer. The slurry is buffered with 0.05-M citrate buffer. Half of volume *V* is therefore 0.1-M citrate buffer.

$$V_{\text{buffer}} = 0.5 \cdot V$$

4. Perform Steps 1–3 for every sample and sum up the buffer volumes and add 5%.

$$V'_{\text{buffer}} = 1.05 \cdot \sum V_{\text{buffer}}$$

5. Use 2 mg HTec3/g dry biomass and 2 mg CTec3/g dry biomass. HTec3 stock has 243 g enzyme/L while CTec3 stock has 326 g enzyme/L. Dilute both enzyme stocks 1:10 in water. The dilute enzyme solutions have 24.3 g/L (HTec3) and 32.6 g/L (CTec3). To achieve 2 mg/g dry biomass enzyme loading, calculate required volume of dilute enzyme solution needed.

$$V_{\text{HTec3}} = V'_{\text{buffer}} \cdot 0.00824 \frac{\text{mL enzyme solution}}{\text{mL buffer}}$$

$$V_{\text{CTec3}} = V'_{\text{buffer}} \cdot 0.00614 \frac{\text{mL enzyme solution}}{\text{mL buffer}}$$

6. Calculate volume of tetracycline solution and cycloheximide solution needed.

$$V_{\text{Tetracycline}} = V'_{\text{buffer}} \cdot 0.0160 \frac{\text{mL solution}}{\text{mL buffer}}$$

$$V_{\text{Cyclohexamide}} = V'_{\text{buffer}} \cdot 0.0120 \frac{\text{mL solution}}{\text{mL buffer}}$$

7. Measure out and mix calculated volumes of buffer, enzymes, tetracycline, and cycloheximide for each batch. This is the "reactive buffer."
8. Add D.I. water to your batches to reach the calculated volume in Step 2.

$$V_{water} = V - V_{buffer} - V_{Cyclohexamide} - V_{Tetracycline} - V_{CTec3} - V_{HTec3} - m_{BM,wet}$$

$m_{BM,wet}$ is the mass of water in biomass.

9. For samples with liquid only, use the same reactive buffer (same concentrations) and add it in a 1:1 ratio to the liquids. Ensure liquids have a pH within 5–6 before adding reactive buffer.
10. Close bottles and place them in incubator (50°C, 120 rpm). Leave for 5 days.
11. After 5 days take the samples out of incubator. Put them into an 80°C water bath for at least 10 min to deactivate enzymes.
12. Measure sugar concentrations with HPLC.

APPENDIX G

DE-OXYGENATED WATER PREPARATION

1. Fill a large glass flask (~ 4L) with distilled water.
2. Place flask on a hot plate and boil for 10 min.
3. Seal the flask with aluminum foil and cool down to room temperature.
4. Based on water volume, add 0.275 g/L cysteine hydrochloride and 0.275 g/L sodium sulfide to the flask.
5. Stir the solution until both chemicals are completely dissolved.
6. Pour solution into de-oxygenated water storage tank.

APPENDIX H

IODOFORM SOLUTION PREPARATION PROCEDURE

1. Measure 500 mL of ethanol in graduated cylinder and pour into a 1-L beaker.
2. Weigh 10 g of iodoform and pour into 1-L beaker.
3. Mix solution until complete dissolution, then pour it into a storage jar.
4. Wrap up jar with aluminum foil and store it in refrigerator.

APPENDIX I

INOCULUM ADAPTATION PROCEDURE

1. Prepare enough deoxygenated (D.O.) water.
2. Autoclave digester bottles and rubber stoppers (with glass tube and septum).
3. Weigh 50 g/L dry solids of substrate into an autoclaved bottle. In this study, 400 mL is the working volume of the digester, thus 20 g dry solid is required.
4. Add 350 mL of D.O. water, 50 mL of fresh Galveston inoculum, and 120 μL iodoform to each bottle.
5. Purge bottle with nitrogen, cap with rubber stopper, and place in incubator.
6. Every 2 d, remove bottles from incubator.
7. Take a 30-mL gas sample with a syringe and analyze gas composition using gas chromatography.
8. Replace rubber stopper with a plastic cap.
9. Centrifuge each bottle for 10 min at 4000 rpm.
10. Decant supernatant into beaker.
11. Adjust pH using desired buffer. Return supernatant to bottle.
12. Add 120 μL iodoform. Purge with nitrogen, cap with rubber stopper, and place in incubator.
13. After 2 wk, store supernatant in refrigerator for use as inoculum in future batch experiments.

APPENDIX J

MOISTURE AND ASH CONTENT DETERMINATION

1. Remove empty crucibles from oven and place in desiccator using only tongs.
2. After crucibles are cooled to room temperature, record weight of each crucible (W1)
3. Add approximately 0.1 g of $Ca(OH)_2$ if sample is a liquid containing volatile acids. Record weight of crucible + lime (W_1').
4. Weigh approximately 3 g of sample into crucible. Record weight of crucible + lime + sample (W_2).
5. Dry crucible at 105°C for 24 h in oven. In a desiccator, allow to cool to room temperature before weighing. Record post oven weight (W_3).
6. Ash crucible at 550 °C for at least 12 h. Remove and allow sample to cool to room temperature in a desiccator. Record post furnace weight (W_4).
7. Moisture content (MC) of sample is calculated as:

$$\text{MC (No lime added)} = \frac{W_2 - W_3}{W_2 - W_1}$$

$$\text{MC (Lime added)} = \frac{W_2 - W_3}{W_2 - W_1'}$$

8. Ash content (AC) of sample is calculated as:

$$\text{AC (No lime added)} = \frac{W_4 - W_1}{W_3 - W_1}$$

$$\text{AC (Lime added)} = \frac{W_4 - W_1}{W_3 - W_1'}$$

9. Remove ash from crucibles. Wash and place in oven to dry.

APPENDIX K

COUNTERCURRENT ANAEROBIC DIGESTION

1. Remove digesters from incubator and allow to cool to room temperature. Record digester weight.
2. Take a 30-mL gas sample for gas composition analysis using a syringe and needle.
3. Measure gas volume in digester headspace using vacuum gas release system.
4. Remove digester caps. Using a nitrogen line, blow down residual solids adhered to stopper and metal bars.
5. Cap digester with a regular plastic cap.
6. Centrifuge each digester to separate solid and liquid phases. Centrifuge for 10 min at 4000 rpm and brake level of 5.
7. Pour supernatant into pre-weighted beakers and record weight.
8. Take a 1.5 mL sample from liquid phase of each digester. Store sample in freezer for further analysis. Record pre-transfer pH.
9. Weigh each digester bottle containing solids and compare with target weight. To achieve steady state, a constant wet cake weight must be maintained in each digester. Remove the difference and add to the next digester. For F1, weight of fresh biomass should also be taken into consideration.
10. Add fresh biomass (10.2 g paper, 2.4 g chicken manure) to F1.

11. Compare the liquid weight with target liquid weight (assume the density is 1 g/mL), remove the difference and add to the next digester. For F1, remove liquid product. Weight of fresh liquid added to F4 should be taken into consideration.
12. Add 120 mL deionized water to beaker containing liquid broth from F4.
13. Balance after-transfer pH of liquid in F1–F4 beakers. If pH > 7.2, add carbon dioxide. If pH < 6.8, add sodium bicarbonate.
14. Return liquids back to digesters.
15. Add 0.2 g urea to F4.
16. Add 120 mL iodoform solution to each digester.
17. Purge each digester with nitrogen and replace digester caps.
18. Weigh and return digesters to incubator.

APPENDIX L

ION-EXCHANGE RESIN ADSORPTION APPARATUS ASSEMBLY

1. Cut wire mesh into the same shape as mesh holder. Place mesh on the holder and use a foil sticker to connect both along the edge.
2. Place mesh holder inside cartridge. Ensure it is well secured with wire mesh facing upwards.
3. Connect a ¼-in female pipe taper (FTP) fitting for outlet of the cartridge. Attach a rubber tube to the other end of the FTP. Connect the rubber tube to a stopcock for control flow.
4. Connect outlet of the stopcock to inlet of a peristaltic pump.
5. Connect outlet of the pump to inlet of the cartridge.
6. Insert a stainless tube into cartridge. Connect other end of tube to a CO_2 flowmeter for regulating the flowrate of carbon dioxide.

APPENDIX M

CO_2-SUSTAINED ION-EXCHANGE RESIN ADSORPTION PROCEDURE

1. Select four graduated cylinders that will be reused for this process until the experiment is over. Wash, dry and record their weights.
2. Ensure digesters have been centrifuged and liquid phase has been separated from wet cake.
3. Ensure weight of liquid to be transferred has been calculated for each transfer. This calculated weight will be referred to as transfer-liquid going forward.
4. Assemble cartridge and mesh. The cartridge and mesh will be referred to as the column going forward.
5. Weigh resin beads and place them in column. Use D.I. water to ensure all beads leave weigh boat. Rinse resin beads twice with 250 mL of deionized water. Use a vacuum pump to remove any excess water.
6. Rinse peristaltic pump with 300 mL of D.I. water. Remove excess water with a vacuum pump.
7. Pour calculated amount of transfer-liquid (F4 to F3) into the dried graduated cylinders and record the volume.
8. Adjust carbon dioxide flow rate to 1.5 L/min. Ensure CO_2 bubbles contacts the bottom of the column.

9. Pour transfer-liquid from graduated cylinder into column. Ensure that the pump outlet is connected to the column inlet. Switch on pump and start timer. Let circulation run for 10 min.
10. During circulation, weigh the empty graduated cylinder to account for loss of liquid during the process.
11. After 10 min, close valve at the bottom of the column and disconnect it from pump.
12. Transfer the liquid back to the same graduated cylinder and record weight.
13. Get a clean filtration flask of known weight. For 30 seconds, use a vacuum pump to remove remaining liquid from column into the filtration flask. Ensure filtration flask is airtight during this process. Calculate the weight of liquid in the flask.
14. Take a 1.5-mL sample of liquid that underwent adsorption.
15. Pour liquid from graduated cylinder and filtration flask into beaker containing liquid for F3.
16. Record weight of graduated cylinder and filtration flask for mass loss calculations.
17. Repeat steps 6–15 using the liquid to be transferred from F3 to F2 and F2 to F1.

APPENDIX N

ION-EXCHANGE RESIN REGENERATION PROCEDURE

1. Turn off carbon dioxide flow. Close valve of carbon dioxide tank.
2. Remove stainless-steel tube to ensure that no carbon dioxide is in the system. While removing tube, use some D.I. water to wash resin beads back into column.
3. The saturated resin must be rinsed with 8 bed volume (BV) of 1-N NaOH solution for more than 30 min under circulation. One bed volume (BV) is defined as 1 m^3 solution per m^3 resin. Based on this, calculate the required volume of 1-N NaOH solution for regeneration.
4. Measure desired amount of 1-N NaOH solution into a pre-weighed conical flask.
5. Connect resin column outlet and peristaltic pump inlet to conical flask.
6. Open valve at the base of resin column and switch on peristaltic pump. Run for 30 min.
7. Once regeneration is complete, recover NaOH solution by draining the column and vacuum pumping into flask.
8. Record flask weight. Collect 1.5-mL sample from recovered NaOH.
9. Wash resin beads in column with 250 mL of deionized water twice.
10. Fill column with 100 mL of D.I. water for storage.

APPENDIX O

GAS CHROMATOGRAPH MANUAL

O-1 Sample preparation

1. Remove frozen sample and allow to thaw to room temperature.
2. Centrifuge liquid sample for 10 min at 13,300 rpm.
3. Pipette 0.5 mL of supernatant into a 2.0-mL microcentrifuge tube.
4. Pipette 0.5 mL internal standard (4-methyl-valeric acid 1.162 g/L, ISTD) and 0.5 mL 3-M phosphoric acid into the same tube.
5. Cap and vortex tube for a few seconds.
6. Centrifuge tube (ISTD + 3-M H_3PO_4 + supernatant) for 10 min at 13,300 rpm.
7. Pipette 1.0 mL supernatant into a glass vial and cap it properly. Transfer vial to gas chromatograph (GC).

O-2 Running the gas chromatograph

8. Input the list of samples in the sequence on the computer.
9. Before starting GC, check gas supply cylinders (compressed helium, air, and hydrogen) to ensure there is enough gas in each cylinder.
10. Check solvent and waste bottles on the injection tower. Fill up solvent vials with new methanol. Dispose waste methanol.
11. Replace septum beneath the injection tower.
12. Place samples in autosampler racks. Include at least one vial with external standard (a mixture of acids of known concentration).

13. Check the setting conditions in the method.
    a) Inlet conditions:
        i. Temperature: 230 °C
        ii. Pressure: 15 psig
        iii. Flow rate: 185 mL/min
    b) Detector conditions:
        i. Temperature: 230 °C
        ii. Air flow rate: 400 mL/min
        iii. H_2 flow rate: 40 mL/min
        iv. The (makeup) flow rate: 45 mL/min
    c) Oven conditions:
        i. Initial temperature: 40 °C
        ii. Initial hold time: 2 min
        iii. Ramp rate: 20 °C/min
        iv. Final temperature: 200 °C
        v. Final hold time: 1 min
        vi. Total run time per vial: 20 min
14. Start the GC on the computer program (on-line mode) by selecting the method with the conditions listed above. Load the sample sequence. At the end of the sequence table, set the GC to standby mode to save gas.
15. To ensure proper analysis, run the external standard every 15–25 samples.

APPENDIX P

HIGH PERFORMANCE LIQUID CHROMATOGRAPH MANUAL

P-1 Standard preparation

1. Standards for sugars should be prepared individually. Sugars should never be mixed. Standards for formic, acetic, propionic, isobutyric, butyric, isovaleric, valeric acid can be mixed to form a standard acid mixture. Standards for caproic acid and ethanol should be prepared individually.
2. Dilute standards to desired dilution levels. Ensure dilution levels are broad enough to account for both low and high concentrations. Do not dilute with D.I. water. Dilute with HPLC-grade water.
3. Store all standards in 50-mL tubes in refrigerator. Use Parafilm to wrap the cover of each tube to prevent evaporation.

P-2 HPLC calibration

4. Prepare HPLC mobile phase (0.005 mol H_2SO_4/L water) using 99% sulfuric acid and HPLC-grade water.
5. Ensure HPLC has enough mobile phase (at least 2 L). Check the bottle fillings section of the quaternary pump. Adjust the volume of the bottle fillings if necessary. Note that pump will shut down if the mobile phase is below a set minimum value.
6. Use 1-mL syringes and 0.2-μm filters to filter standards into glass vials. Ensure that each vial contains at least 0.5 mL of liquid.

7. Develop the conditions for “analysis method,” which is used for analyzing samples. The “rest method” is for conserving mobile phase. Here is an example of the “analysis method” conditions used in this study.

   a) Quaternary pump

      i. Flow rate: 0.6 mL/min

      ii. Stop time: 75 min (each sample run takes 75 min)

      iii. Post time: off

      iv. Minimum stroke: automatic

      v. Compressibility: $100 \times 10^{-6}/\text{bar}$

      vi. Maximum flow gradient: 100 mL/min^2

   b) Multicolumn thermostat (MCT)

      i. Temperature: 60^{o}C (both left and right)

      ii. Valve position: position 1

      iii. Stop time: as pump/injector

      iv. Post time: off

      v. Enable analysis: when temperature is within ± 0.8^{o}C

   c) Diode array detector (DAD)

      i. Signals: Signal A, wavelength 210 nm, bandwidth 4 nm.

      ii. Peak width: > 0.1 min (2-s response time) (2.5 Hz)

      iii. Stop time: as pump/injector

      iv. Post time: off

      v. Auto balance: pre run

vi. Lamps on required for acquisition: UV lamp

d) Refractive index detector (RID)

i. Optical unit temperature: 40°C

ii. Peak width: > 0.1 min (2-s response time) (4.63 Hz)

iii. Stop time: as pump/injector

iv. Post time: off

v. Signal polarity: positive

vi. Automatic zero before analysis: on

vii. Automatic purge: on (purge time is 1.5 min, wait time is 0 min)

e) Sampler

i. Injection volume: 30 μL

ii. Needle wash: enabled (every 3 s)

iii. Stop time: as pump/injector

iv. Post time: off

v. Draw speed: 100 μL/min

vi. Eject speed: 400 μL/min

vii. Wait time after draw: 1.2 s

viii. Needle height offset: 0.0 mm

8. Develop a "rest method" which reduces the pump flow rate to 0.25 mL/min. Always include a line at the end of the sequence with "rest method."

9. Set HPLC to "analysis method" and run standards through HPLC once conditions are steady and equipment is ready. Quat pump pressure should be 40–46 bar.

10. If pressure is above 46 bar, call Agilent for technical support. The needle might be blocked. Or the guard column might need to be replaced.
11. If pressure is ideal, arrange the samples in sample tray. Create a new sequence file and type in your sample names.
12. Insert two blank runs at the beginning of the sequence. This improves the quality of the analysis.
13. Insert a blank run at the end of the sequence. Change method for last run to "rest method."
14. Save sequence. Run sequence. The sequence can be edited at any time during the run.
15. After sample run, turn off the MCT, DAD, and RID.
16. Create methods in the data analysis software and type in compound names, calibration levels and retention times.
17. Reprocess results to ensure that a good calibration table was generated.
18. Save the newly edited methods to the "master method." This ensures that method exists outside the current data set and can be used to analyze other runs.

P-3 Sample analysis

1. Remove sample from freezer and allow to thaw to room temperature.
2. Centrifuge liquid sample for 10 min at 13,300 rpm.
3. Use 1-mL syringes and 0.2-μm filters to filter sample into glass vial. Ensure vial contains at least 0.5 mL of liquid.

4. Arrange vial in autosampler tray. Ensure there are two designated vials with HPLC grade water. One vial is for needle wash while the other is for blank sample runs.
5. Obtain a single standard solution from refrigerator. Filter and include it in the analysis. This will serve as a quality control check to ensure retention time of each analyte stays consistent over time.
6. Set HPLC to “analysis method.” Switch on MCT, DAD, and RID in the software.
7. Open RID purge valve for 15 min. Close purge valve.
8. Wait for pump pressure to be below 46 bar.
9. Record pressure and temperatures in HPLC logbook.
10. Prepare sequence table following the same format as before. Ensure the last run is a blank sample with “rest method.” Run sequence.

APPENDIX Q

CPDM MATLAB CODE FOR SIMULATION OF A FOUR-STAGE COUNTERCURRENT FERMENTATION

Matlab code for CPDM prediction

```
%MATLAB Code for CPDM Prediction
%This code is for a standard four-stage countercurrent fermentation
%Program predicts acid concentrations and conversion at varying VSLR
and LRT.
%Department of Chemical Engineering, Texas A&M University, College St,
TX
clc
clear all
close all
global so taus e1 f1 g1 h1
global holdup moist ratio stages loading tauloverall
global acid nnot factr1
global x_1 nhat_1 x_2 nhat_2 x_3 nhat_3 x_4 nhat_4

%Start Simulation
disp(['Program starts at: ', datestr(now)]);
tic;

VSLR_data= [2,4,6,8,10,12]';
LRT_data= [5,15,25,35]';
ACID = [];
CONVERSION = [];
VSLR_loop=2; %loop is for varying VSLR.
%To make map, set to lowest VSLR, otherwise, set to specific VSLR
while VSLR_loop<12.1 % if want loop, set to highest VSLR (volatile
solid loading rate)
    LRT_loop=5; %loop is for varying LRT (liquid residence time).
    %To make map, set to lowest LRT, otherwise set to specific LRT
    while LRT_loop<35.1 %if want loop, set to highest VSLR

        %%Basic parameters for Fermentation
        stages=4; %Fermentor stages
        so=0.843; %Aeq selectivity (gAEQ/g VS digested)
        %Please note that in older versions of the code (i.e.
Loescher's)
        %this term referred to a VS selectivity of g VS/g total solids
and
        %was carried over in the differiental equations in Ross and Fu.
        holdup =2.0; %ratio of liq to solid in wet cake (g liq/gVS
cake)
        %Note: holdup is the liq in the solid cake NOT the lig of the
        %total slurry
        moist =.07; %ratio of liquid to solid in feed (g liq/gVS cake)
```

```
        SQ =1.0;
        ratio=0.7; %phi ratio of g total acid to g AEQ
        loading = VSLR_loop;
        tauloverall = LRT_loop;
        vol=[0.48,0.28,0.28,0.28]'; %Liquid volume in each fermentor
        totvol=sum(vol);
        liquidfeed = totvol/tauloverall;
        nnotreal = [300,300,300,300]'; %VS concentration gVS/L (?in
each fermentor?)
        solidfeed = loading*totvol; %Solid Feed (g dry weight)
        Convrsn = [.1,.2,.3,.4]'; %Initial value for conversion
        nnot = nnotreal./(1-Convrsn);
        taus = nnot.*vol/solidfeed;
        L =0.1*ones(stages+1,1); %L initial value for liquid flow rate
in every reactor
        taul = tauloverall/stages*ones(stages,1);

        e1=0.075; f1=3.64; g1=0.069; h1=1.00; % CPDM parameters
%         e1=0.103; f1=2.404; g1=3.76e-4; h1=1.725; %CPDM parameters
        %acd=22.3; % acd need to trfer into the Function M file
        rmodel = @(x1,acid) e1.*(1-x1).^f1./(1+g1.*(acid.*ratio).^h1);
        syms x1 acid
        drmodel_1 = diff(e1.*(1-x1).^f1./(1+g1.*(acid.*ratio).^h1),x1);
        drmodel = @(x2,acid2) subs(drmodel_1,{x1,acid},{x2,acid2});

        done = 0; %The index used to trace whether the condtion is
satisfied
        liqtoler = 0.05; %tolerance for Liquid flowrate 0.005
        acidtoler = 0.1; %tolerance for acid concentration  0.02
        nnottoler = 1; %tolerance for nnot

        %Initial values for acid, acidold
        %ans=ones(stages,1); % dont use ans it is a matlab variable.
        acid=[35,30,28,25]';
        acidold=ones(stages,1);
        taulnew = 1000*ones(stages,1);  %column vector
        nhatzero =100*ones(stages,1);  %CP concentration
        creation = ones(stages,1);
        destruction = ones(stages,1);
        tauloverallnew = 20;

        disp('Calculation is in progress.......');

        while done < 0.50
            taulnew = 1000*ones(stages,1);  %Obtain Flowrate for each
fermentor
            taulover_error = 0.001;
            while abs(tauloverall-tauloverallnew) > taulover_error
                liquidfeed = liquidfeed*(1+(tauloverallnew-
tauloverall)/tauloverall*0.5);
                L(5) = liquidfeed;
                L(4) = L(5) + solidfeed/1000*holdup*(Convrsn(4)-
Convrsn(3));
```

```
                L(3) = L(4) + solidfeed/1000*holdup*(Convrsn(3)-
Convrsn(2));
                L(2) = L(3) + solidfeed/1000*holdup*(Convrsn(2)-
Convrsn(1));
                L(1) = moist*solidfeed/1000 + L(2) -
solidfeed/1000*holdup*(1.0-Convrsn(1));
                tauloverallnew = totvol/L(1);
            end

            taul = vol./L(1:stages);  %vol 4*1, L 5*1
            nnot = nnotreal./(1-Convrsn);
            taus = nnot.*vol/solidfeed;
            scale = ones(stages,1);

            disp([' nnot= ',num2str(nnot','%15.5f')]);

            %parameters for ODE45
            options = odeset('RelTol',1e-3,'AbsTol', 1e-3);
            x_low=0; x_high=0.99;

            %Reactor 1

            i=1;
            while abs(taulnew(i) - taul(i))> liqtoler  %liqtoler = 0.05
                nhat0 =nhatzero(i);
                [x,nhat]= ode15s(@Chan1,[x_low,x_high],nhat0,options);
                x_1=x;  nhat_1 = nhat;
                F_1 = @(x_1)interp1(x,nhat,x_1);
                factr1 = nnot(i)/quad(F_1,x_low,x_high);  %calculate
factor
                F_11 = @(x_1)
factr1*interp1(x,nhat,x_1).*rmodel(x_1,acid(i));
                robs = quad(F_11,x_low,x_high);
                F_12 = @(x_1) interp1(x,nhat,x_1).*x_1;
                Convrsn(i) = quad(F_12,x_low,x_high)/nnot(i)*factr1;
                taulnew(i) = (L(i)*acid(i) + solidfeed/1000*(1-
Convrsn(i))*holdup*acid(i)-L(i+1)*acid(i+1))/(L(i)*robs);
                acid(i) = acid(i) + (taul(i)*robs-
(L(i)*acid(i)+solidfeed/1000*(1-Convrsn(i))*holdup*acid(i)-
L(i+1)*acid(i+1))/L(i))*.4;  %why 0.4 here?
            end
            disp(['  acid(',num2str(i),')=',num2str(acid(i),'%15.5f'),'
taulnew(',num2str(i),')=',num2str(taulnew(i),'%15.5f'),'  robs=',
num2str( robs, '%15.5f')]);

            %Reactor 2

            i=2;
            nnottoler = nnot(i)/50;
            while abs(taulnew(i)-taul(i))>liqtoler;
                ndone = 0;
                while ndone <0.50
```

```
                    nhat0=nhatzero(i);
                    options = odeset('RelTol',1e-3,'AbsTol',1e-3);
                    [x,nhat] =
ode15s(@Chan2,[x_low,x_high],nhat0,options);
                    x_2=x;  nhat_2=nhat;
                    F_2 = @(x_2)interp1(x,nhat,x_2);
                    nhattot=quad(F_2,x_low,x_high);
                    disp(['  nhatzero= ',num2str(nhatzero(i),
'%15.5f'),';  nhattot= ',num2str(nhattot, '%15.5f'),';
nnot(',num2str(i),')= ',num2str(nnot(i), '%15.5f')]);
                    if abs(nhattot - nnot(i))<nnottoler;
                        ndone = 1;
                    end
                    if (nhatzero(i) + (nnot(i) - nhattot)*1.0)>0
                        nhatzero(i)= nhatzero(i) + (nnot(i) -
nhattot)*0.7;
                    else
                        nhatzero(i)= nhatzero(i) + (nnot(i) -
nhattot)*0.2;
                    end
                end

                F_22 = @(x_2)interp1(x,nhat,x_2).*x_2;
                Convrsn(i)= quad(F_22,x_low,x_high)/nnot(i);
                robs = solidfeed*so/vol(i)*(Convrsn(i)-Convrsn(i-1));

                taulnew(i) = (L(i)*acid(i) + solidfeed/1000*(1-
Convrsn(i))*holdup*acid(i)-L(i+1)*acid(i+1))/(L(i)*robs);
                acid(i) = acid(i) + (taul(i)*robs-
(L(i)*acid(i)+solidfeed/1000*(1-Convrsn(i))*holdup*acid(i)-
L(i+1)*acid(i+1))/L(i))*.5;
                disp(['  taulnew(',num2str(i),')=',num2str(taulnew(i),
'%15.5f'),'  taul(',num2str(i),')=',num2str(taul(i),'%15.5f'),]);
            end
            disp(['  acid(',num2str(i),')=',num2str(acid(i),'%15.5f'),'
taulnew(',num2str(i),')=',num2str(taulnew(i),'%15.5f'),'  robs=',
num2str( robs, '%15.5f')]);

            %Reactor 3

            i=3;
            nnottoler = nnot(i)/100;
            while abs(taulnew(i)-taul(i))>liqtoler;
                ndone = 0;
                while ndone <0.50
                    nhat0 =nhatzero(i);
                    options = odeset('RelTol',1e-3,'AbsTol',1e-3);
                    [x,nhat] =
ode15s(@Chan3,[x_low,x_high],nhat0,options); %was chan3
                    x_3=x;  nhat_3=nhat;
                    F_3 = @(x_3)interp1(x,nhat,x_3);
                    nhattot=quad(F_3,x_low,x_high);
```

```
                    disp(['  nhatzero= ',num2str(nhatzero(i),
'%15.5f'),';  nhattot= ',num2str(nhattot, '%15.5f'),';
nnot(',num2str(i),')= ',num2str(nnot(i), '%15.5f')]);
                    if abs(nhattot - nnot(i))<nnottoler;
                        ndone = 1;
                    end
                    if (nhatzero(i) + (nnot(i) - nhattot)*1.0)>0
                        nhatzero(i)= nhatzero(i) + (nnot(i) -
nhattot)*0.7;
                    else
                        nhatzero(i)= nhatzero(i) + (nnot(i) -
nhattot)*0.2;
                    end
                end

                F_32 = @(x_3)interp1(x,nhat,x_3).*x_3;
                Convrsn(i)= quad(F_32,x_low,x_high)/nnot(i);
                robs = solidfeed*so/vol(i)*(Convrsn(i)-Convrsn(i-1));

                %taulnew(i) = (L(i)*acid(i) + solidfeed/1000*(1-
Convrsn(i))*holdup*acid(i)-solidfeed/1000*(1-Convrsn(i-
1))*holdup*acid(i-1))/(L(i)*robs);
                %acid(i) = acid(i) + (taul(i)*robs-
(L(i)*acid(i)+solidfeed/1000*(1-Convrsn(i))*holdup*acid(i)-
solidfeed/1000*(1-Convrsn(i-1))*holdup*acid(i-1))/L(i))*0.5;
                taulnew(i) = (L(i)*acid(i) + solidfeed/1000*(1-
Convrsn(i))*holdup*acid(i)-L(i+1)*acid(i+1))/(L(i)*robs);
                acid(i) = acid(i) + (taul(i)*robs-
(L(i)*acid(i)+solidfeed/1000*(1-Convrsn(i))*holdup*acid(i)-
L(i+1)*acid(i+1))/L(i))*.5;
                disp(['  taulnew(',num2str(i),')=',num2str(taulnew(i),
'%15.5f'),'  taul(',num2str(i),')=',num2str(taul(i),'%15.5f'),]);
            end
            disp(['  acid(',num2str(i),')=',num2str(acid(i),'%15.5f'),'
taulnew(',num2str(i),')=',num2str(taulnew(i),'%15.5f'),'  robs=',
num2str( robs, '%15.5f')]);


            %Reactor 4

            i=4;
            nnottoler = nnot(i)/100;
            while abs(taulnew(i)-taul(i))>liqtoler;
                ndone = 0;
                while ndone <0.50
                    nhat0 =nhatzero(i);
                    options = odeset('RelTol',1e-3,'AbsTol',1e-3);
                    [x,nhat] =
ode15s(@Chan4,[x_low,x_high],nhat0,options); %was chan4
                    x_4=x;  nhat_4=nhat;
                    F_4 = @(x_4)interp1(x,nhat,x_4);
                    nhattot=quad(F_4,x_low,x_high);
```

```
                    disp(['  nhatzero= ',num2str(nhatzero(i),
'%15.5f'),';  nhattot= ',num2str(nhattot, '%15.5f'),';
nnot(',num2str(i),')= ',num2str(nnot(i), '%15.5f')]);
                    if abs(nhattot - nnot(i))<nnottoler;
                        ndone = 1;
                    end
                    if (nhatzero(i) + (nnot(i) - nhattot)*1.0)>0
                        nhatzero(i)= nhatzero(i) + (nnot(i) -
nhattot)*0.7; %25/nnot(i);
                    else
                        nhatzero(i)= nhatzero(i) + (nnot(i) -
nhattot)*0.2;
                    end
                end

                F_42 = @(x_4)interp1(x,nhat,x_4).*x_4;
                Convrsn(i)= quad(F_42,x_low,x_high)/nnot(i);
                robs = solidfeed*so/vol(i)*(Convrsn(i)-Convrsn(i-1));

                taulnew(i) = (L(i)*acid(i) + solidfeed/1000*(1-
Convrsn(i))*holdup*acid(i)-solidfeed/1000*(1-Convrsn(i-
1))*holdup*acid(i-1))/(L(i)*robs);
                acid(i) = acid(i) + (taul(i)*robs-
(L(i)*acid(i)+solidfeed/1000*(1-Convrsn(i))*holdup*acid(i)-
solidfeed/1000*(1-Convrsn(i-1))*holdup*acid(i-1))/L(i))*0.5;
                disp(['  taulnew(',num2str(i),')=',num2str(taulnew(i),
'%15.5f'),'  taul(',num2str(i),')=',num2str(taul(i),'%15.5f'),]);
            end
            disp(['  acid(',num2str(i),')=',num2str(acid(i),'%15.5f'),'
taulnew(',num2str(i),')=',num2str(taulnew(i),'%15.5f'),'  robs=',
num2str( robs, '%15.5f')]);
            disp(['  Conversion in each stage (from nhat):
',num2str(Convrsn','%13.5f')]);

            if max(abs(acid-acidold))<acidtoler
                done=1;
            end
            acidold = acid;
        end

        %Output results section

        disp('Congratulations!  The simulation is successfully
finished!')
        toc  %toc is used to check the whole time of the process

        for i3 = 1:(stages+1);
            disp(['  L(',int2str(i3),')= ',num2str(L(i3))]);
        end
        creation(1) = L(1)*acid(1) + solidfeed/1000*(1-
Convrsn(1))*holdup*acid(2)-L(2)*acid(2);
```

```
        creation(2) = L(2)/acid(2) + solidfeed/1000*(1-
Convrsn(2))*holdup*acid(3)-L(3)*acid(3)- solidfeed/1000*(1-
Convrsn(1))*holdup*acid(2);
        creation(3) = L(3)*acid(3) + solidfeed/1000*(1-
Convrsn(3))*holdup*acid(4)-L(4)*acid(4)- solidfeed/1000*(1-
Convrsn(2))*holdup*acid(3);
        creation(4) = L(4)*acid(4) - solidfeed/1000*(1-
Convrsn(3))*holdup*acid(4);
        %Calculation of Destruction
        destruction(1) = solidfeed/1000*(Convrsn(1)-0);
        for i3=2:stages;
            destruction(i3)=solidfeed/1000*(Convrsn(i3)-Convrsn(i3-1));
        end
        selectivi = creation./destruction;
        selec = L(1)*acid(1)/(solidfeed*Convrsn(4));

        %output the result and plot the result
        disp(['  Selectivity = ',num2str(selectivi','%15.5f')]);
        disp(['  Creation = ',num2str(creation','%15.5f')]);
        disp(['  Destruction = ',num2str(destruction','%15.5f')]);
        disp(['  selectivity = ',num2str(selec','%15.5f')]);
        disp(['  tauloverall = ',num2str(tauloverall,'%15.5f')]);
        disp(['  taus = ',num2str(sum(taus),'%15.5f')]);
        disp(['  acid levels = ',num2str(acid','%13.5f')]);

        disp(['  VSLR_LOOP = ',num2str(VSLR_loop),'  LRT_loop =
',num2str(LRT_loop)]);

        %Collect data for CPDM map
        ACID = [ACID;acid(1)];
        CONVERSION = [CONVERSION;Convrsn(4)];
        LRT_loop = LRT_loop + 10;
    end
    VSLR_loop = VSLR_loop + 2;
end
disp(['  acid levels = ',num2str(acid','%13.5f')]);
disp(['  convrsn levels = ',num2str(Convrsn','%13.5f')]);
 %disp(['  VSLR = ',num2str(VSLR_data','%13.5f')]);
 %disp(['  LRT = ',num2str(LRT_data','%13.5f')]);
 disp(['  Acid levels = ',num2str(ACID','%13.5f')]);
 disp(['  Conversions = ',num2str(CONVERSION','%13.5f')]);
```

Matlab code for CPDM prediction map

```
clc

VSLR=[2;2;2;2;4;4;4;4;6;6;6;6;8;8;8;8;10;10;10;10;12;12;12;12];
LRT=[5;15;25;35;5;15;25;35;5;15;25;35;5;15;25;35;5;15;25;35;5;15;25;35]
;
lw = 2;
```

```
% PLOTTING FCM
ACID =
[4.9472;13.3959;20.116;25.3483;7.8703;18.5685;25.0529;29.3202;9.7068;20
.502;26.0179;29.3409;10.8713;21.1865;25.8945;28.5591;11.6029;21.2832;25
.3567;27.6545;12.1473;21.1304;24.7066;26.7323];
CONVERSION =
[0.67400;0.64657;0.61748;0.58839;0.55617;0.50002;0.45344;0.42128;0.4755
6;0.40430;0.36209;0.33490;0.41486;0.34306;0.30647;0.28439;0.36813;0.299
34;0.26733;0.25135;0.33196;0.26811;0.24070;0.22786];

mapdata=[VSLR,LRT,CONVERSION,ACID];
VSLR_sorted=sortrows(mapdata,1);
LRT_sorted=sortrows(mapdata,2); %sort
[map_num,map_1]=size(mapdata);
VSLR_sort = sort(mapdata(:,1));
uniqueM = [diff(VSLR_sort);1] > 0;
%count = [VSLR_sort(uniqueM); diff(find([1;uniqueM]))]
VSLR_sort1 = VSLR_sort(uniqueM);
VSLR_number = diff(find([1;uniqueM]));
LRT_sort = sort(mapdata(:,2));
uniqueM = [diff(LRT_sort);1] > 0;
%count = [sortM(uniqueM) diff(find([1;uniqueM]))]
LRT_sort1 = LRT_sort(uniqueM);  %Unique LRT
LRT_number = diff(find([1;uniqueM]));
%plot for VSLR part
temp1=zeros(length(VSLR_sort1)+1,1);
for j1=1:length(VSLR_sort1)
temp1(j1+1)=temp1(j1)+VSLR_number(j1);
mapdata_1=VSLR_sorted(temp1(j1)+1:temp1(j1+1),:) ;
%for VSLR(j1)
F = @(x)interp1(mapdata_1(:,3),mapdata_1(:,4),x,'spline');
hold on;
plot(mapdata_1(:,3),F(mapdata_1(:,3)),'linewidth',lw,'color',[0.4660
0.6740 0.1880]);
if j1==1
for j3=1:length(mapdata_1(:,3))
%text(mapdata_1(j3,3),mapdata_1(j3,4), ['  ', num2str(mapdata_1(j3,2))]
,'HorizontalAlignment','left');
end
%text(mapdata_1(1,3)-0.17,mapdata_1(1,4)-3, ' VSLR (g/L-day) '
,'HorizontalAlignment','left');
end
end
%plot for LRT part
temp1=zeros(length(LRT_sort1)+1,1);
for j1=1:length(LRT_sort1)
temp1(j1+1)=temp1(j1)+LRT_number(j1);
mapdata_2=LRT_sorted(temp1(j1)+1:temp1(j1+1),:) ;
%for LRT(j1)
F2 = @(x)interp1(mapdata_2(:,3),mapdata_2(:,4),x,'spline');
hold on;
plot(mapdata_2(:,3),F2(mapdata_2(:,3)),'linewidth',lw,'color',[0.4660
0.6740 0.1880]);
```

```
if j1==1
for j3=1:length(mapdata_2(:,3))
%text(mapdata_2(j3,3)+0.005,mapdata_2(j3,4)-1.5, ['
',num2str(mapdata_2(j3,1))] ,   'HorizontalAlignment','right');
end
%text(mapdata_2(1,3)-0.025,mapdata_2(1,4)+20, 'LRT (day) '
,'HorizontalAlignment','left');
grid on
end
end
%hold off;
xlabel('Conversion (g NAVS_d_i_g_e_s_t_e_d/g NAVS_f_e_e_d)');
ylabel('Total carboxylic acid concentration (g/L)');
axis([0.15 1.00 0 80]);

% PLOTTING WCM
ACID
=[4.9826;14.0885;21.9806;28.7471;6.7225;17.7461;25.9973;32.2494;7.5063;
18.6502;26.1426;31.4647;7.8335;18.6075;25.3005;29.7938;8.008;18.2208;24
.1937;28.0839;8.0779;17.7344;23.0491;26.4226];
CONVERSION
=[0.82099;0.81089;0.80058;0.78905;0.60394;0.59022;0.57332;0.55854;0.474
48;0.45724;0.44261;0.43069;0.38658;0.37245;0.36222;0.35265;0.32847;0.31
539;0.30601;0.29974;0.28308;0.27380;0.26606;0.26183]

mapdata=[VSLR,LRT,CONVERSION,ACID];
VSLR_sorted=sortrows(mapdata,1);
LRT_sorted=sortrows(mapdata,2); %sort
[map_num,map_1]=size(mapdata);
VSLR_sort = sort(mapdata(:,1));
uniqueM = [diff(VSLR_sort);1] > 0;
%count = [VSLR_sort(uniqueM); diff(find([1;uniqueM]))]
VSLR_sort1 = VSLR_sort(uniqueM);
VSLR_number = diff(find([1;uniqueM]));
LRT_sort = sort(mapdata(:,2));
uniqueM = [diff(LRT_sort);1] > 0;
%count = [sortM(uniqueM) diff(find([1;uniqueM]))]
LRT_sort1 = LRT_sort(uniqueM);  %Unique LRT
LRT_number = diff(find([1;uniqueM]));
%plot for VSLR part
temp1=zeros(length(VSLR_sort1)+1,1);
for j1=1:length(VSLR_sort1)
temp1(j1+1)=temp1(j1)+VSLR_number(j1);
mapdata_1=VSLR_sorted(temp1(j1)+1:temp1(j1+1),:) ;
%for VSLR(j1)
F = @(x)interp1(mapdata_1(:,3),mapdata_1(:,4),x,'spline');
hold on;
plot(mapdata_1(:,3),F(mapdata_1(:,3)),'linewidth',lw,'color',[0 0 0]);
if j1==1
for j3=1:length(mapdata_1(:,3))
text(mapdata_1(j3,3),mapdata_1(j3,4)-0.5, ['  ',
num2str(mapdata_1(j3,2))] ,'HorizontalAlignment','left');
end
```

```
text(mapdata_1(1,3)-0.3,mapdata_1(1,4)-3, ' VSLR (g/L-day) '
,'HorizontalAlignment','left');
end
end
%plot for LRT part
temp1=zeros(length(LRT_sort1)+1,1);
for j1=1:length(LRT_sort1)
temp1(j1+1)=temp1(j1)+LRT_number(j1);
mapdata_2=LRT_sorted(temp1(j1)+1:temp1(j1+1),:) ;
%for LRT(j1)
F2 = @(x)interp1(mapdata_2(:,3),mapdata_2(:,4),x,'spline');
hold on;
plot(mapdata_2(:,3),F2(mapdata_2(:,3)),'linewidth',lw,'color',[0 0 0]);
if j1==1
for j3=1:length(mapdata_2(:,3))
text(mapdata_2(j3,3)+0.005,mapdata_2(j3,4)-1.5, ['
',num2str(mapdata_2(j3,1))] ,   'HorizontalAlignment','right');
end
text(mapdata_2(1,3)-0.01,mapdata_2(1,4)+27, 'LRT (day) '
,'HorizontalAlignment','left');
grid on
end
end
hold off;
xlabel('Conversion (g NAVS_d_i_g_e_s_t_e_d/g NAVS_f_e_e_d)');
ylabel('Total carboxylic acid concentration (g/L)');
axis([0.15 1.00 0 40]);
```